

Reductions in finite-dimensional quantum mechanics: from symmetries to operator algebras and beyond

by

Oleg Kabernik

B.Sc., Technion - Israel Institute of Technology, 2011

M.Math., University of Waterloo, 2014

A THESIS SUBMITTED IN PARTIAL FULFILLMENT OF
THE REQUIREMENTS FOR THE DEGREE OF

DOCTOR OF PHILOSOPHY

in

The Faculty of Graduate and Postdoctoral Studies

(Physics)

THE UNIVERSITY OF BRITISH COLUMBIA

(Vancouver)

March 2024

© Oleg Kabernik 2021

The following individuals certify that they have read, and recommend to the Faculty of Graduate and Postdoctoral Studies for acceptance, the dissertation entitled:

Reductions in finite-dimensional quantum mechanics: from symmetries to operator algebras and beyond

submitted by Oleg Kabernik in partial fulfillment of the requirements for

the degree of Doctor of Philosophy

in Physics

Examining Committee:

Robert Raussendorf, Associate Professor, Department of Physics and Astronomy, UBC
Supervisor

Ian Affleck, Professor, Department of Physics and Astronomy, UBC
Supervisory Committee Member

Gordon W. Semenoff, Professor, Department of Physics and Astronomy, UBC
University Examiner

Sven Bachmann, Associate Professor, Department of Mathematics, UBC
University Examiner

Additional Supervisory Committee Members:

Mark Van Raamsdonk, Professor, Department of Physics and Astronomy, UBC
Supervisory Committee Member

Joshua Folk, Associate Professor, Department of Physics and Astronomy, UBC
Supervisory Committee Member

Abstract

The idea that symmetries simplify or reduce the complexity of a system has been remarkably fruitful in physics, and especially in quantum mechanics. On a mathematical level, symmetry groups single out a certain structure in the Hilbert space that leads to a reduction. This structure is given by the irreducible representations of the group, and in general it can be identified with an operator algebra (a.k.a. C^* -algebra or von Neumann algebra). The primary focus of this thesis is the extension of the framework of reductions from symmetries to operator algebras, and its applications in finite-dimensional quantum mechanics.

Finding the irreducible representations structure is the principal problem when working with operator algebras. We will therefore review the representation theory of finite-dimensional operator algebras and elucidate this problem with the help of two novel concepts: minimal isometries and bipartition tables. One of the main technical results that we present is the Scattering Algorithm for analytical derivations of the irreducible representations structure of operator algebras.

For applications, we will introduce a symmetry-agnostic approach to the reduction of dynamics where we circumvent the non-trivial task of identifying symmetries, and directly reduce the dynamics generated by a Hamiltonian. We will also consider quantum state reductions that arise from operational constraints, such as the partial trace or the twirl map, and study how operational constraints lead to decoherence. Apart from our primary focus we will extend the idea of reduction beyond operator algebras to operator systems, and formulate a quantum notion of coarse-graining that so far only existed in classical probability theory. In addition, we will characterize how the uncertainty principle transitions to the classical regime under coarse-grained measurements and discuss the implications in a finite-dimensional setting.

Lay Summary

In modern physics, and especially in quantum mechanics, symmetry has been recognized as a powerful concept that explains many aspects of the physical world around us. On a mathematical level, symmetries identify a certain structure that reduces the complexity of a physical system. It turns out that such reductions are not primarily identified by symmetries, but by a rather more general mathematical concept of an operator algebra. The primary focus of this thesis is the extension of the framework of reductions from symmetries to operator algebras, and its applications in quantum mechanics. We will present an algorithm for deriving the complexity reducing structures directly from operator algebras and demonstrate its applications with problems from quantum information and quantum computing.

Preface

All the work presented in this thesis was conducted by the author as a member of the Quantum Information group lead by Robert Raussendorf at the University of British Columbia, Point Grey campus.

Some of the ideas presented in Chapters 2, 5 and 6 have been published [Kabernik O., "Quantum coarse graining, symmetries, and reducibility of dynamics", Phys. Rev. A 97 (2018)]. These include the concepts of bipartition tables, quantum coarse-graining and the reduction of Hamiltonians with symmetries. I am the sole author of that work and I was responsible for all aspects of its development.

The Scattering Algorithm presented in Chapter 3 and some of its applications described in Chapter 4 have been published [Kabernik O., Pollack J., and Singh A., "Quantum state reduction: Generalized bipartitions from algebras of observables", Phys. Rev. A 101 (2020)]. I was the lead investigator responsible for concept formation, analysis and manuscript composition. Pollack J. and Singh A. were involved in the initial formulation of these ideas and have contributed to the manuscript composition.

Chapter 7 is a modified version of the preprint [Kabernik O., "Quantifying The Uncertainty Principle and The Effects of Minimal Length From a Finite-Dimensional Perspective", arXiv:2002.01564]. I am the sole author of that work and I was responsible for all aspects of its development.

All other ideas presented in this thesis, in particular the contents of Chapter 5, were developed solely by the author and were not previously published.

Table of Contents

Abstract	iii
Lay Summary	iv
Preface	v
Table of Contents	vi
List of Figures	viii
Acknowledgments	x
1 Introduction	1
2 Operator algebras and the structure of irreducible representations	10
2.1 Notation and some mathematical facts	11
2.2 Finite-dimensional operator algebras	13
2.3 Bipartition tables and the irreps structure	21
3 Finding the irreps structure with the Scattering Algorithm	32
3.1 How the Scattering Algorithm works	33
3.1.1 Overview	33
3.1.2 Illustrative example	36
3.2 The Scattering Algorithm in detail	41
3.2.1 Scattering of projections	42
3.2.2 Establishing minimality of the reflection network	46
3.2.3 Establishing completeness of the reflection network	48
3.2.4 Constructing the bipartition table	50
3.2.5 Why the Scattering Algorithm works: putting it all together	51
4 Reduction of states	53
4.1 State reductions and decoherence due to inaccessible subsystems	54
4.2 State reductions and decoherence due to operational constraints	60

5	Reduction of dynamics	77
5.1	Reduction of Hamiltonians with symmetries	77
5.2	Symmetry-agnostic reduction of Hamiltonians	86
6	Beyond operator algebras	98
6.1	Motivating example	99
6.2	Partial bipartitions and quantum coarse-graining	103
6.2.1	Classical analogy	103
6.2.2	The formalism of partial bipartitions	105
6.2.3	The operational meaning of quantum coarse-graining	108
7	The uncertainty principle on a lattice	115
7.1	From quantum to classical regimes on a lattice	117
7.2	The implications of the uncertainty principle on a lattice	125
7.2.1	Inferring the size of the lattice	125
7.2.2	The continuum limit and lattice perturbations	125
7.2.3	Factorizing the Planck constant	126
8	Conclusion	128
	Bibliography	132
	Appendix	141

List of Figures

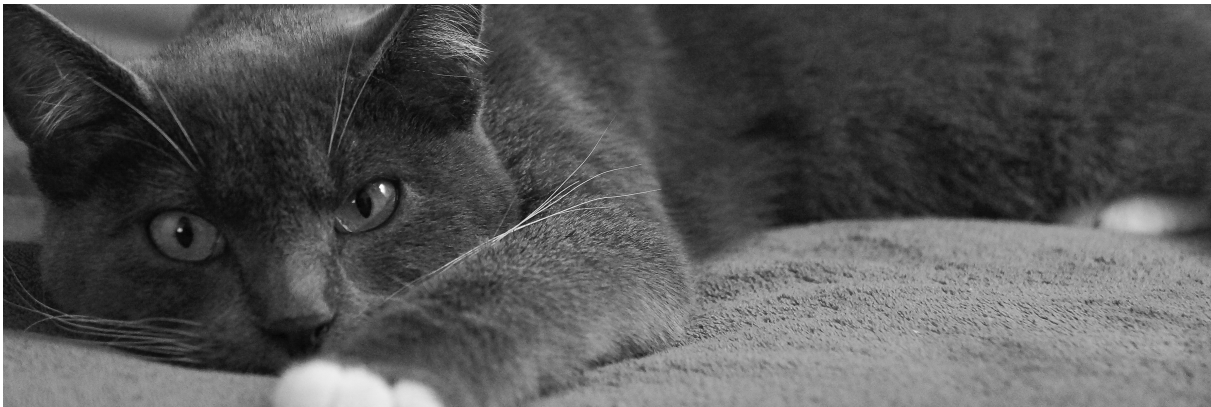
3.1	An example of the initial (improper) reflection network.	37
3.2	An example of the intermediate reflection network after one scattering. . . .	38
3.3	An example of the final (proper) reflection network after two scatterings. . . .	39
3.4	Generic update rules for the reflection relations after scattering. The red edges represent unknown reflection relations, black edges represent properly reflecting pairs, absent edges represent orthogonal pairs. Open ended edges stand for the reflection relations with the other projections in the network. In the generic case each $\Pi_{i=1,2}$ breaks into $\{\Pi_{i=1,2}^{(\lambda)}\}$ and the result is a series of properly reflecting pairs (for $\lambda = 0$ the pair is orthogonal) as described in Theorem 3.4. The open ended (external) edges are inherited from $\Pi_{i=1,2}$ by each of $\{\Pi_{i=1,2}^{(\lambda)}\}$ with the black edges being reset to red (assuming $\Pi_{i=1,2}$ did break under scattering).	44
3.5	Update rules for the reflection relations in the case where only one of the projections breaks. In this case, Π_2 may break to at most two projections (if Π_2 also does not break then the red edge of $\{\Pi_1, \Pi_2\}$ is just set to black). The difference from the generic case is that the external black edges of the unbroken projection Π_1 are not reset to red.	45
4.1	Time dependent purity of spin- $\frac{1}{2}$ coupled to spin-100.	58
4.2	Column kets of maximally polarized spin states rotate in opposite directions in the $\hat{x} - \hat{y}$ plane. The periodic brief alignments of the kets is responsible for the periodic brief revivals of coherence.	59
4.3	Generic picture of column kets on a bipartition table before (left) and after (right) unsynchronized evolution inside the columns caused by the interaction term. The diminishing overlaps between the different column kets translates into diminishing coherence terms in the reduced state.	60
4.4	The purity of the reduced state under the evolution with $H = H_{int}$	68
4.5	The column kets of the unreduced state as it evolves on the BPT. The height of each bar corresponds to the absolute value of the coefficient of the underlying BPT basis element. The distinct bar color is assigned to each column for contrast and has no numeric meaning.	69
4.6	The final reflection network for $l = \frac{1}{2}$	71

4.7	The first step reflection network for general l	74
4.8	The second step reflection network for general l	74
4.9	The final reflection network for integer l . When l is half integer the last two projections $ 0, +\rangle \langle 0, + $ and $ 0, -\rangle \langle 0, - $ do not exist.	75
5.1	Two “glued” binary trees with a symmetry breaking edge $\langle 6, 7 \rangle$. The two generators of the permutation symmetry are shown in grey using the cyclic notation (ij) . The dashed lines are the axis of reflection associated with the permutations.	82
5.2	The reflection network from the generators of the group $U(\mathcal{G})$	84
5.3	The irrep basis representation of the continuous-time quantum walk Hamiltonian over the binary trees in Fig. 5.1. In the irrep basis, the Hamiltonian decomposes into three terms that correspond to the three connected components. The connected component in the bottom row indicates the direct propagation from root 1 to root 10 that happens in a subspace exponentially smaller than the full tree. The symmetry breaking term of the Hamiltonian contributes to the dynamics in the top component, but it does not affect the dynamics in the bottom row.	86
5.4	The reflection network from the generators T_{12}, T_{23}	89
5.5	The reflection network of $\langle T_\alpha, Q \rangle$	91
5.6	The reflection network from the spectral projections of $[\vec{S}_2 \cdot \vec{S}_3]$ and $[S_{\beta=\frac{1}{2}}]$	96
7.1	(a) The continuous phase space where the cells with the area $2\pi\hbar$ represent the resolution scale associated with the uncertainty principle. (b) The discretized phase space of a lattice of integer length d . The cells with the area $\sqrt{d} \times \sqrt{d}$ arise from the scale \sqrt{d} associated with the uncertainty principle on a lattice. The Planck constant $2\pi\hbar$ can be recovered from \sqrt{d} by converting the phase space area $\sqrt{d} \times \sqrt{d}$ to proper units.	116
7.2	Periodic one dimensional lattice with d lattice sites in total, w lattice sites in each coarse-graining interval, and $k = d/w$ intervals. The lattice unit of length is δx	118
7.3	(a) The plot of the average probability $\langle p_{\text{agree}} \rangle$ that an instantaneous succession of position-momentum-position measurements will agree on both outcomes of position as a function of the resolution parameters w_x, w_p on a lattice of length d . The dotted curve $w_x w_p = d$ is the boundary that outlines the transitional scale with respect to which we distinguish the quantum and classical regimes. (b) The plot of $\langle p_{\text{agree}} \rangle$ (solid) along the diagonal $w = w_x = w_p$ with the upper and lower bounds (dashed) from Eqs. (7.11) and (7.12).	123

Acknowledgments

I acknowledge the material support of the government of Canada through the Natural Sciences and Engineering Research Council (NSERC).

I would like to express gratitude to all the people in my personal and professional lives whose support and encouragement enabled this journey. I am grateful to my research supervisor Robert Raussendorf for the stress-free environment, patient guidance, and unwavering confidence in my work. I thank my colleagues who had endured my ramblings about coarse-grainings and operator algebras, and in return offered feedback, encouragement and advice. In particular, I would like to thank Dongsheng Wang, Fumika Suzuki, Jason Pollack, Ashmeet Singh, Pedro Lopes, Michael Zurel and the members of my supervisory committee. I want to thank my parents, Felix and Svetlana Kabernik, for being so thoughtful and supportive. Most of all, I am grateful to the one person who chooses to be by my side through thick and thin; Rita, without you this journey would never begin. Finally, I must acknowledge the calming influence of a particularly talented cat who shall remain unnamed.



Chapter 1

Introduction

The main task of a theoretical physicist is to translate physical reality into mathematical models, analyze the models, and then translate the results back into predictions and explanations. The translation from physics to math, however, is far from a rigorous process and the only guiding principle, besides consistency with phenomenology, is that “Everything should be made as simple as possible, but no simpler”.¹

Any simplification in the description of a physical system can be called a *reduction*. In this thesis we will study the methods and structures associated with reductions in finite-dimensional quantum systems. Before we get into the details of what that means, we will approach the idea of reduction from a broader perspective.

The essence of reduction is to single out some significant information about the system and disregard everything else. For example, in classical mechanics we reduce the state of a rigid body that consists of some 10^{23} individual particles, to the position, momentum and angular momentum of their center of mass. Similarly, in statistical mechanics we reduce the intractable state of a many-body system to a handful of variables such as the number of particles, energy, temperature, chemical potential, volume, and pressure. The very existence of such classical descriptions of physical systems is predicated on the idea of reduction.

A very general perspective on reduction is to think of it as the result of some coarse-graining where we choose not to distinguish between every possible state of the system. One of the earliest formulations of this perspective appears in the work of Paul and Tatiana Ehrenfest [36], where they elucidate the ideas of Boltzmann, Gibbs and Einstein on statistical mechanics. Although coarse-graining is a very simple and powerful perspective, it does not translate naturally into quantum theory where the states are not fully distinguishable to begin with.

Many modern analytical methods in physics can be viewed as reductions. These include the mean-field approximation [56, 55], separation of scales and renormalization group methods [100, 55, 70], matrix product states and tensor networks [91, 80, 92]. Furthermore, the idea of *model reduction* in dynamical systems is studied on a more general level as a subject of applied mathematics [86, 44]. The landscape of all the approaches to reduction is beyond the scope of this thesis, but the notion of reduction that we will explore here is still based on the same general principle: single out some significant information about

¹This quote is commonly attributed to Albert Einstein.

the system and disregard everything else.

Which information is significant and which is not, is the principal problem of reduction. A remarkably fruitful approach to this problem traces back to the seminal work by Emmy Noether, known as Noether's theorem [76]. This theorem states that when the dynamics of a system have symmetries, there are conserved quantities that do not evolve with time. When considering time evolutions we can therefore focus on the non-conserved quantities, and disregard the conserved ones; this results in a reduction. A particle in central potential in three-dimensional space is thus reduced from having three dynamical variables of position, to one.

Today, symmetry methods are a well established staple in physics with far reaching implications and many dedicated textbooks (see for example [29, 90, 42]). The integration of symmetry methods in quantum theory traces back to a result by Eugene Wigner, known as Wigner's theorem [99, 98]. It states that in quantum mechanics symmetries are represented by a group of unitary or anti-unitary operators acting on a Hilbert space. Since anti-unitary representations are rare, especially in finite-dimensional quantum mechanics, the mathematical formalism of symmetry methods that we will focus on is that of unitary group representations.

With the advancement of finite-dimensional quantum theory driven by the development of quantum information and quantum computing, the mathematical structure given by the irreducible representations, or *irreps*, of groups has been brought into sharper focus. The irreps structure has been recognized as the principal structure in applications such as quantum error correction and fault tolerance [101, 59, 63, 14], quantum reference frames and superselection rules [11, 58], and commodification of asymmetry as a resource [67, 68, 69]. Along the way it was realized that the irreps structure is primarily defined not by the representations of groups, but by a rather more general set of transformations known as *operator algebras*.

The use of operator algebras in quantum theory was originally pioneered by John von Neumann and Francis Murray [74, 73], focusing on infinite dimensional Hilbert spaces. The use of operator algebras in finite-dimensional quantum mechanics was realized much later; see the reviews in [12] or [45], for example. These algebras are often distinguished as C^* -algebras or von Neumann algebras but in finite dimensions these distinctions are inconsequential, so we will keep calling them operator algebras. We will later formally define operator algebras; for now let us just say that these are sets of transformations, like groups, but they are not represented by unitaries and they can be composed into both products and sums.

The primary focus of this thesis is the generalization of reduction methods from symmetries to operator algebras in finite-dimensional quantum mechanics. One motivation for this generalization follows from the fact that there is no systematic way to identify symmetries, and we are mostly restricted to intuitively recognizable symmetries such as rotations

in space. By shifting the focus from symmetries to operator algebras we will develop a symmetry-agnostic approach to the reduction of dynamics.

Let us first briefly review what a reduction due to symmetries looks like in finite-dimensional quantum mechanics. We consider a group \mathcal{G} represented by the unitaries $U(\mathcal{G})$ acting on the Hilbert space \mathcal{H} of our system. We call the group \mathcal{G} a symmetry if it commutes with the Hamiltonian

$$[H, U(g)] = 0 \quad \forall g \in \mathcal{G}.$$

Without going into the details of group representation theory, the standard textbook procedure [29, 90, 42] for the reduction of dynamics due to symmetries can be summarized in the following steps:

1. Identify the smallest subspaces $\mathcal{H}_{q,i} \subset \mathcal{H}$ that are closed under the symmetry transformations $U(\mathcal{G})$. These subspaces are called *irreducible* because the action of symmetry transformations cannot be further restricted to smaller subspaces. Both indices q and i enumerate the irreducible subspaces $\mathcal{H}_{q,i}$, but with q we distinguish the subspaces with distinct representations of \mathcal{G} , and with i we distinguish the subspaces with identical representations.
2. Change to the new basis $|e_{ik}^q\rangle$ in \mathcal{H} , where q and i identify the irreducible subspace $\mathcal{H}_{q,i}$, and k enumerates the basis elements inside the subspace. Such change of basis is explicitly specified by what is known as the Clebsch-Gordan coefficients.
3. Assuming that $U(\mathcal{G})$ commutes with H , use the results of Schur's lemmas to conclude that

$$\langle e_{jl}^p | H | e_{ik}^q \rangle = \delta_{pq} \delta_{lk} \langle e_j^q | H | e_i^q \rangle, \quad (1.1)$$

where we suppress the index k on the right because the matrix elements do not depend on it.

Thus, the Hamiltonian reduces to the block-diagonal form where q and k enumerate the blocks, and i, j refer to the matrix elements inside each block. The key structure here is given by the basis $|e_{ik}^q\rangle$, that in the language of group representation theory identify the irreducible representations of $U(\mathcal{G})$.

The fact that $U(\mathcal{G})$ commutes with H is the defining property that makes $U(\mathcal{G})$ not just a group of transformations but a “symmetry”. The above procedure suggests that we can only rely on the irreps structure of symmetries in order to reduce the dynamics, otherwise Schur's lemmas cannot be invoked. One of the results that we will later show is that this is not quite the case. That is, even groups that are not symmetries can lead to a reduction of dynamics under a relaxed condition on the commutators $[H, U(g)]$.

As an alternative to groups, we will introduce the symmetry-agnostic approach where instead of asking “Which group commutes with the Hamiltonian?” we ask “Which operator

algebra contains the Hamiltonian?”. Although this may seem like two different questions, the later formulation is a generalization of the former. The idea behind the symmetry-agnostic approach is to identify an operator algebra \mathcal{A} that contains H , find the irreps structure of \mathcal{A} given by the basis $|e_{ik}^q\rangle$, and then reduce H using the irrep basis as we did in Eq. (1.1).

For example, consider the Hilbert space of three qubits $\mathcal{H}_{qubit}^{\otimes 3}$ and the Hamiltonian

$$H(\epsilon) = H_{int} + \epsilon \sigma_z \otimes I \otimes I,$$

where σ_z is a Pauli matrix acting on the first qubit and ϵ is a real parameter. The interaction term H_{int} is such that its first and only excited states are $|++0\rangle$ and $|+11\rangle$ (we use the notation $|\pm\rangle \propto |0\rangle \pm |1\rangle$), so if we normalize its energy gap to 1 it is just

$$H_{int} = |++0\rangle\langle++0| + |+11\rangle\langle+11|.$$

The terms H_{int} and $\sigma_z \otimes I \otimes I$ do not commute so we cannot simultaneously diagonalize both terms to find the spectrum of $H(\epsilon)$ as a function of ϵ . We can, however, reduce $H(\epsilon)$ and find its spectrum as a function of ϵ from the reduced Hamiltonian blocks.

In principle, there is a symmetry group that reduces $H(\epsilon)$ but it can be difficult to identify, and even then, one has to find the irrep basis that lead to the reduction. The symmetry-agnostic approach offers an alternative where we directly derive the irrep basis that lead to the reduction. The idea is to observe that $H(\epsilon)$ is a linear combination of two terms, so it is an element of the algebra

$$\mathcal{A} = \langle H_{int}, \sigma_z \otimes I \otimes I \rangle$$

generated by these terms. If we find the irrep basis of the operator algebra \mathcal{A} , we can reduce $H(\epsilon)$.

It turns out, as we will see later, that the irreps structure of \mathcal{A} is given by the basis

$$|0-0\rangle, |001\rangle, |1-0\rangle, |101\rangle, |0+0\rangle, |1+0\rangle, |011\rangle, |111\rangle$$

and when we present the Hamiltonian in these basis (in the above order) we get

$$H(\epsilon) = \begin{pmatrix} \epsilon & & & & & & & \\ & \epsilon & & & & & & \\ & & -\epsilon & & & & & \\ & & & -\epsilon & & & & \\ & & & & \frac{1}{2} + \epsilon & \frac{1}{2} & & \\ & & & & \frac{1}{2} & \frac{1}{2} - \epsilon & & \\ & & & & & & \frac{1}{2} + \epsilon & \frac{1}{2} \\ & & & & & & \frac{1}{2} & \frac{1}{2} - \epsilon \end{pmatrix}.$$

Thus, the spectrum of $H(\epsilon)$ consists of $\pm\epsilon$, and the rest is given by the eigenvalues of the 2×2 block

$$\begin{pmatrix} \frac{1}{2} + \epsilon & \frac{1}{2} \\ \frac{1}{2} & \frac{1}{2} - \epsilon \end{pmatrix}.$$

The advantage of this approach is that identifying the operator algebra that contains the Hamiltonian is trivial compared to identifying symmetries. The real challenge is in finding the irreps structure and the associated basis.

We are aware of two approaches in the literature to the problem of finding the irreps structure. First, Murota *et al.* [72] has proposed a numerical algorithm based on random sampling and motivated by problems in semidefinite programming (it was adapted in [97] for physical applications). Second, Holbrook *et al.* [47] have proposed an algorithm without sampling, but it requires the ability to find spans of sets of operators.

Ideally, just as we have a symbolic (not inherently numeric) algorithm for diagonalizing a matrix using pen and paper, we would have a symbolic algorithm for finding the irreps structure of a set of matrices. One of the main technical contributions of this thesis is the derivation of such algorithm.

The proposed algorithm is called the *Scattering Algorithm*. It is constructed around the basic operation called “scattering” that acts on pairs of projections and is symbolically represented as follows (the input is on the left, and the output is on the right):

$$\begin{array}{ccc} \Pi_1 & \searrow & \Pi_1^{(\lambda_1)}, \Pi_1^{(\lambda_2)}, \dots, \Pi_1^{(0)} \\ & \text{---} & \\ \Pi_2 & \swarrow & \Pi_2^{(\lambda_1)}, \Pi_2^{(\lambda_2)}, \dots, \Pi_2^{(0)}. \end{array}$$

The output projections $\Pi_i^{(\lambda)}$ are defined as the elements of the spectral decompositions

$$\Pi_1 \Pi_2 \Pi_1 = \sum_{\lambda \neq 0} \lambda \Pi_1^{(\lambda)} \quad \text{and} \quad \Pi_2 \Pi_1 \Pi_2 = \sum_{\lambda \neq 0} \lambda \Pi_2^{(\lambda)}.$$

From the sums of output projections we can recover the input projections as $\Pi_i = \sum_{\lambda} \Pi_i^{(\lambda)}$

(the element $\Pi_i^{(0)}$ ensures that). In this sense the scattering operation “breaks” the input projections into lower rank constituents. The main idea of the Scattering Algorithm is to start with the spectral projections of the generators of the operator algebra, break them into the minimal possible constituents, and then construct the irreps structure from these minimal projections.

One application for the Scattering Algorithm that we will demonstrate is in finding the possible qubit encodings for a given control Hamiltonian. Since different encodings have different physical characteristics, it is desirable to exhaust the possibilities of an encoding for a given Hamiltonian. Finding such encodings is not a trivial task and the symmetry of the Hamiltonian is often used to point to the possible solution. With the Scattering Algorithm we can approach this task in a more systematic manner and find solutions associated with less obvious symmetries.

In quantum dot arrays, for example, it is possible to implement the nearest neighbor Heisenberg interaction with tunable terms [66]

$$H = \epsilon_{12}\vec{S}_1 \cdot \vec{S}_2 + \epsilon_{23}\vec{S}_2 \cdot \vec{S}_3 + \epsilon_{34}\vec{S}_3 \cdot \vec{S}_4.$$

DiVincenzo *et al.* [33] and Bacon *et al.* [7] have proposed qubit encoding in such arrays based on the reduction due to the $SU(2)$ symmetry of H . By adopting the symmetry-agnostic approach and using the Scattering Algorithm we will find additional qubit encodings that cannot be revealed by the $SU(2)$ symmetry alone.

Thus, a physical application of the Scattering Algorithm is in characterizing the dynamics of Hamiltonians beyond its obvious symmetries. In particular, for the purposes of quantum information processing, the Scattering Algorithm identifies the possible qubit encodings in a systematic manner without relying on the intuition of symmetries.

So far, we have focused on reductions that follow from the dynamics of the system. There is, however, another kind of reductions that arises when we have inaccessible degrees of freedom, such as the degrees of freedom of the “environment”. In order to distinguish such reductions from the reductions of dynamics, we will refer to them as the *reductions of states*.

The prototypical state reduction is the partial trace map that reduces the state ρ_{AB} of a composite system AB into the state ρ_B of subsystem B alone. The operational meaning of the reduced state ρ_B is that it contains only the information accessible with measurements on subsystem B . In other words, the partial trace map is a map that accounts for the operational constraint that only allows measurements on subsystem B .

There are more sophisticated operational constraints that cannot be associated with a physical subsystem. A well known example of that is the operational constraint that arises from a lack of common reference frame [11]. That is, when two parties (Alice and Bob) do not share a common reference frame, any information about the quantum state that relies on this frame of reference is inaccessible to the other party. The resulting operational

constraint is a restriction to observables that are symmetric under transformations of this reference frame. The state reduction map that accounts for this constraint is called the twirl [11] and it is rooted in the irreps structure of the reference frame transformations group.

We will introduce and study the idea of state reductions due to operational constraints in the common mathematical framework of operator algebras. Within this framework state reductions are constructed directly from operational constraints, and it subsumes the specialized state reduction maps such as the partial trace or the twirl. Ideas such as noiseless subsystems [65] can also be incorporated into this framework by observing that the requirement for logical operations to commute with the operations of noise is an operational constraint. In that case, the state reduction map is a map that decodes the logical information from the physical state.

It is also interesting to consider the dynamics of reduced states. It is well known that the reduced state of a subsystem B may undergo decoherence if the composite system AB evolves in a certain way. What “certain way” means is that the Hamiltonian H of AB has an interaction term H_{int} that couples the two subsystems [17]. That is,

$$H = H_{self} + H_{int},$$

where $H_{self} = I_A \otimes H_B + H_A \otimes I_B$ and H_{int} cannot be expressed in this way. Identifying the interaction term that is responsible for decoherence is simple when we talk about subsystems. However, when considering state reduction maps associated with different operational constraints, the distinction between the “self” and “interaction” terms of the Hamiltonian is not as clear.

For example, we will consider the composite system $\underline{l} \otimes \underline{\frac{1}{2}} \otimes \underline{\frac{1}{2}}$ of two spin- $\frac{1}{2}$ ’s and an integer angular momentum l , such as the Hydrogen atom, but with the simple Hamiltonian of uniform magnetic field along the \hat{y} axis

$$H = \epsilon L_y + S_{1;y} + S_{2;y}.$$

This Hamiltonian has no interaction terms so we do not expect it to induce decoherence. This is true if we consider the reduced states of the individual spins or angular momentum, but it is not the case if different operational constraints are imposed. In particular, for the reduced states that arise due to the lack of common reference frame of directions in space, this Hamiltonian induces decoherence. We will see that under this operational constraint the “self” and the “interaction” terms of the Hamiltonian are

$$H = \underbrace{\epsilon(L_y + S_{1;y} + S_{2;y})}_{H_{self}} + (1 - \epsilon) \underbrace{(S_{1;y} + S_{2;y})}_{H_{int}}.$$

Taking a step back, let us return to the simple classical notion of reduction associated

with coarse-graining. Such notion of reduction is implicit in statistical mechanics where we choose to distinguish only between states that have different macroscopic properties. The partitioning of the micro state space into macroscopic classes of states, or macro states, is exactly what we mean by coarse-graining. The idea of coarse-graining naturally extends into probability theory where the probability for a macro state to occur is given by the probability for any micro state in the class to occur. This kind of reasoning, however, does not seem to extend naturally into quantum theory.

In the following, we will attempt to bridge this conceptual gap. In order to do that we will have to extend the mathematical framework beyond operator algebras and into *operator systems*. In the process we will end up generalizing the usual notion of a subsystem (or a *virtual* subsystem [102, 104]), to what we call a *partial* subsystem that is no longer defined by a tensor product bipartition of the Hilbert space. The main result is the definition of a state reduction map called *quantum coarse-graining*, and the derivation of its operational meaning. These ideas will be illustrated with a simple classical coarse-graining of a probability distribution, and its quantum analogue. As a motivating example we will consider the encoding (compression) of a three level system (qutrit) into a two level system (qubit) using quantum coarse-graining.

Finally, we will carry out a case study of the uncertainty principle on a lattice. Unlike previous topics, where the emphasis was on the methods, here we will focus on specific physical questions. Because a much simpler notion of coarse-graining will be used here, these analysis will be presented in a self contained manner without relying on the previously discussed mathematical framework.

It is well known that due to the uncertainty principle, the Planck constant sets a resolution boundary in phase space (see the original paper by Heisenberg [46] or [20, 22] for a modern review). It is also known that in the classical regime the outcomes of sufficiently coarse measurements of position and momentum can simultaneously be determined. If we then continuously vary the resolution of measurements, the uncertainty principle should transition between the quantum and classical regimes, but the picture of how this transition unfolds is not so clear.

In the following we will clarify this picture by studying a characteristic function that quantifies the mutual disturbance effects responsible for the uncertainty principle. Since it is also expected that the uncertainty principle is modified by the existence of minimal length in space (this is known as the generalized uncertainty principle [2]), we will conduct our investigation on a lattice.

We will see how the discontinuity of the lattice perturbs the uncertainty principle and its transition to the classical regime. We will also see that in terms of lattice units, the uncertainty principle imposes a resolution boundary given by the square root of the length of the lattice, and the Planck constant is derived from it. We will discuss the implications of these results for the existence of minimal length in space.

As a guide to the reader, we summarize the contributions of this thesis by chapters as follows:

Chapter 2 We introduce finite-dimensional operator algebras and the structure of irreducible representations in a pedagogical, self-contained manner. Here we will mostly derive previously known results but with the help of two novel concepts: minimal isometries and bipartition tables.

Chapter 3 We introduce the Scattering Algorithm for finding irreducible representations of operator algebras.

Chapter 4 We introduce the framework of state reductions due to operational constraints and integrate it with the study of decoherence.

Chapter 5 We introduce the framework of symmetry-agnostic reduction of dynamics and relax the condition for reduction with symmetries.

Chapter 6 We introduce the notions of partial subsystems and quantum coarse-graining along with their operational meaning.

Chapter 7 We study a characteristic function that quantifies how the uncertainty principle transitions between the quantum and classical regimes on a lattice.

Chapter 2

Operator algebras and the structure of irreducible representations

The irreducible representations (irreps) structure is at the core of all forms of reductions that rely on symmetries or operator algebras. In fact, identifying the irreps structure is usually one of the main technical challenges in the analysis that involve symmetries or operator algebras. Before we can begin to address this challenge we need to understand what operator algebras are, and what is the irreps structure. This is the subject of this chapter.

The abstract mathematical notion of an *algebra* and the more concrete notion of an *operator algebra* are well established fields of study in the mathematical literature. The study of operator algebras have been introduced and developed in the context of mathematical physics by John von Neumann and Francis Murray [74, 73] which is known today as the study of von Neumann algebras. In the modern physics literature another name that is commonly used is a C^* -algebra which is a slight generalization of the von Neumann algebra. Many of the subtleties in the study of operator algebras (and thus the proliferation of different names) arise from the issues associated with the infinite dimensionality of Hilbert spaces of continuous functions. Since we are only concerned with finite-dimensional Hilbert spaces, we can avoid the full mathematical treatment of this subject and restrict our attention to finite-dimensional operator algebras.

In the following we will introduce the main ideas behind finite-dimensional operator algebras in a pedagogical manner focusing on the structural aspects that are suitable for our purposes. Similar accounts of finite-dimensional operator algebras in the physics literature can be found in [12] or in the appendix of [45]. The abstract mathematical treatment of this subject appears in many textbooks (mostly focusing on the subtleties of infinite dimensional spaces), see for example [38] or the notes [50].

The central result of the representation theory of finite-dimensional operator algebras is known as the Wedderburn Decomposition which we will derive in Theorem 2.26. Even though this result is far from novel, the path that we will take there, including most of the proofs, will not follow any of the standard references. In particular, we will introduce the notions of minimal isometries and bipartition tables that anticipate the ideas behind the

Scattering Algorithm presented in Chapter 3.

In Section 2.1 we will begin by setting up the notation and stating some basic mathematical facts. In Section 2.2 we will introduce the finite-dimensional operator algebras and identify the key structural elements. The general irreps structure will be identified in Section 2.3 along with some implications and examples. The irreps structure of groups will be treated as a special case.

2.1 Notation and some mathematical facts

Unless stated otherwise, we will assume $\hbar \equiv 1$.

All Hilbert spaces are assumed to be complex and finite-dimensional. We will denote with $\mathcal{H}_1 \cong \mathcal{H}_2$ the Hilbert spaces that are isometric to each other, which means that \mathcal{H}_1 and \mathcal{H}_2 are only different in how we label their basis. All Hilbert spaces are therefore $\mathcal{H} \cong \mathbb{C}^d$ for some integer d .

We will denote with $\mathcal{L}(\mathcal{H})$ the space of linear operators on the Hilbert space \mathcal{H} . In order to avoid unnecessary notation we will not distinguish between the notions of linear operators (or simply operators) and their representations as matrices. Assuming the dimension of \mathcal{H} is d , the space $\mathcal{L}(\mathcal{H})$ is also a finite-dimensional Hilbert space of dimension d^2 .

The symbol \dagger will denote the conjugate-transpose for matrices and Hermitian adjoint for operators. We will use 0 to denote both the scalar $0 \in \mathbb{C}$ and the null operator $0 \in \mathcal{L}(\mathcal{H})$. We will often invoke the fact that $A = 0 \in \mathcal{L}(\mathcal{H})$ if and only if $AA^\dagger = 0$.

We will denote sets of element such as $\{e_{jk}^i\}$ with the convention that, unless explicitly stated otherwise, the set consists of all the elements obtained by varying the free indices (i, j, k in this case). When we explicitly state the free indices, such as $\{e_{jk}^i\}_{i=1, \dots}$, it will mean that only those indices are indeed free and the rest are a fixed constant for all elements in the set.

Projection operators are define as follows.

Definition 2.1. An operator $\Pi \in \mathcal{L}(\mathcal{H})$ is a *projection* (a.k.a. orthogonal projection) if $\Pi \neq 0$, $\Pi = \Pi^\dagger$ and $\Pi = \Pi^2$.

The following facts about projections will be used implicitly throughout this thesis.

Proposition 2.2. If $\Pi, \Pi' \in \mathcal{L}(\mathcal{H})$ are projections such that $\Pi = c\Pi'$ for some $c \in \mathbb{C}$, then $c = 1$.

Proof. Since Π and Π' are projections we have

$$c\Pi' = \Pi = \Pi^2 = (c\Pi')^2 = c^2\Pi'.$$

Since $\Pi' \neq 0$ we must have $c = 1$. □

When referring to a set of projections $\{\Pi_k\}$ as orthogonal we will always mean that in the sense of pairwise orthogonal: $\Pi_k \Pi_{k'} = \delta_{kk'} \Pi_k$ for all k, k' . The eigenspace of a projection Π is the subspace of \mathcal{H} on which Π projects all element of \mathcal{H} (Π acts as the identity on its own eigenspace). The rank of a projection Π is the number of its non-zero eigenvalues which is also its trace and it is also the dimension of its eigenspace

$$\text{rank} [\Pi] = \text{tr} [\Pi] = \text{dim} [\text{eigenspace} [\Pi]].$$

Another special type of operators that we will work with are partial isometries.

Definition 2.3. An operator $S \in \mathcal{L}(\mathcal{H})$ is a *partial isometry* if $SS^\dagger = \Pi_{fin}$ for some projection Π_{fin} .

The following facts about partial isometries will often be used implicitly.

Proposition 2.4. If S is a partial isometry then $S^\dagger S = \Pi_{in}$ is another projection with the same rank as Π_{fin} .

Proof. Clearly $\Pi_{in}^\dagger = (S^\dagger S)^\dagger = \Pi_{in}$. Note that Π_{in}^2 is a projection because $(\Pi_{in}^2)^\dagger = \Pi_{in}^2$ and

$$(\Pi_{in}^2)^2 = (S^\dagger S)^4 = S^\dagger \Pi_{fin}^3 S = S^\dagger \Pi_{fin} S = \Pi_{in}^2.$$

Since Π_{in}^2 is a projection then $\sqrt{\Pi_{in}^2} = \Pi_{in}$ is a projection. The ranks of Π_{fin} and Π_{in} are the same because

$$\text{tr} [\Pi_{fin}] = \text{tr} [SS^\dagger] = \text{tr} [S^\dagger S] = \text{tr} [\Pi_{in}].$$

□

The eigenspace of Π_{in} , that is the initial space, is isometrically mapped by S to the eigenspace of Π_{fin} , that is the final space. The partial isometry S is only supported on the eigenspace of Π_{in} and all vectors that are orthogonal to it are annihilated. Every projection Π is also a partial isometry ($\Pi_{in} = \Pi_{fin} = \Pi$), therefore we will say that S is a proper partial isometry if it is a partial isometry but it is not a projection.

Proposition 2.5. If $S \in \mathcal{L}(\mathcal{H})$ is a partial isometry with the projections Π_{in} and Π_{fin} on its initial and final spaces, then

$$S\Pi_{in} = \Pi_{fin}S = S$$

$$\Pi_{in}S^\dagger = S^\dagger\Pi_{fin} = S^\dagger$$

Proof. Note that

$$(S\Pi_{in} - S)(S\Pi_{in} - S)^\dagger = S\Pi_{in}\Pi_{in}S^\dagger - S\Pi_{in}S^\dagger - S\Pi_{in}S^\dagger + SS^\dagger \quad (2.1)$$

$$= -SS^\dagger S^\dagger + SS^\dagger = 0 \quad (2.2)$$

Therefore, $S\Pi_{in} - S = 0$ and so $S\Pi_{in} = S$. The rest follows because $S\Pi_{in} = SS^\dagger S = \Pi_{fin}S$ and $\Pi_{in}S^\dagger = (S\Pi_{in})^\dagger$. \square

Proposition 2.6. *If $S, S' \in \mathcal{L}(\mathcal{H})$ are partial isometries such that $S' = cS$ for some $c \in \mathbb{C}$, then $c = e^{i\varphi}$ with some real phase φ .*

Proof. Since both $S'S'^\dagger$ and SS^\dagger are projections such that $S'S'^\dagger = cc^*SS^\dagger$, we must have $cc^* = |c|^2 = 1$. \square

2.2 Finite-dimensional operator algebras

Since we are only concerned with finite-dimensional physical applications, our operators are always naturally represented as matrices with respect to some basis in the Hilbert space. In order to avoid an unnecessary level of abstraction and notation, we will not distinguish between operators and their defining representations as complex matrices. Therefore, the algebras that we will be dealing with are the algebras of complex matrices with the regular matrix multiplication and summation rules. From here on, by *operator algebra* we will always mean the finite-dimensional algebra of complex matrices representing physical operators (which is a special case of C^* -algebra and Von Neumann algebra).

Definition 2.7. An *operator algebra* is a subset of operators $\mathcal{A} \subseteq \mathcal{L}(\mathcal{H})$ such that:

- (1) For all $A_1, A_2 \in \mathcal{A}$ and $c_1, c_2 \in \mathbb{C}$ we have $c_1A_1 + c_2A_2 \in \mathcal{A}$.
- (2) For all $A_1, A_2 \in \mathcal{A}$ we have $A_1A_2 \in \mathcal{A}$.
- (3) For all $A \in \mathcal{A}$ we have $A^\dagger \in \mathcal{A}$.

We will say that an algebra \mathcal{A} is a *subalgebra* of $\tilde{\mathcal{A}}$ and denote it as $\mathcal{A} \subseteq \tilde{\mathcal{A}}$, if both \mathcal{A} and $\tilde{\mathcal{A}}$ are algebras and \mathcal{A} is a subset of $\tilde{\mathcal{A}}$.

Condition (1) of the definition 2.7 (with the regular matrix summation and scalar multiplication rules) implies that \mathcal{A} is a vector space. If the dimension of \mathcal{H} is d then $\mathcal{L}(\mathcal{H})$ is a d^2 dimensional vector space and $\mathcal{A} \subseteq \mathcal{L}(\mathcal{H})$ is a $D \leq d^2$ dimensional vector space. There is always a finite subset of elements $\{A_1, A_2, \dots, A_D\} \subset \mathcal{A}$ that spans the whole \mathcal{A}

$$\mathcal{A} = \text{span} \{A_1, A_2, \dots, A_D\} = \left\{ \sum_{n=1}^D c_n A_n \mid c_n \in \mathbb{C} \right\}.$$

Conditions (2) and (3) imply that \mathcal{A} is also equipped with the non-vector-space operations of matrix product and Hermitian adjoint that leave the vector space \mathcal{A} closed. It is worth noting that elements of unitary groups comply with conditions (2) and (3) but not with (1). In this sense, operator algebras generalize unitary groups by allowing linear combinations of elements in addition to products and adjoints.

Some important canonical examples of operator algebras are:

1. A trivial example is the set of all linear operators $\mathcal{L}(\mathcal{H})$ which we will refer to as the *full* or *trivial* algebra of operators acting on \mathcal{H} . All algebras that consist of operators acting on \mathcal{H} are subalgebras of $\mathcal{L}(\mathcal{H})$.
2. If the Hilbert space is composed of two (or more) subsystems $\mathcal{H} = \mathcal{H}_L \otimes \mathcal{H}_R$ then all operators acting only on one subsystem form an algebra

$$\mathcal{A} = \{A \otimes I_R \mid A \in \mathcal{L}(\mathcal{H}_L)\}.$$

3. If the Hilbert space is composed of two (or more) sectors $\mathcal{H} = \mathcal{H}_0 \oplus \mathcal{H}_1$ then all operators acting only on one sector form an algebra

$$\mathcal{A} = \{A_0 \oplus 0_1 \mid A_0 \in \mathcal{L}(\mathcal{H}_0)\}.$$

(The operator 0_1 is the null operator on \mathcal{H}_1 .)

4. All operators that are proportional to some projection Π (in particular $\Pi \equiv I$), form an one-dimensional algebra

$$\mathcal{A} = \{c\Pi \mid c \in \mathbb{C}\}.$$

5. All operators in the span of projections $\{\Pi_k\}_{k=0}^m$ that are all orthogonal to each other $\Pi_k \Pi_{k'} = \delta_{kk'}$, form an m -dimensional algebra

$$\mathcal{A} = \text{span} \{\Pi_k\}_{k=0}^m.$$

6. All operators in the span of some group \mathcal{G} represented by the unitary operators $\{U_g\}_{g \in \mathcal{G}}$ form an algebra called the *group algebra*

$$\mathcal{A} = \text{span} \{U_g\}_{g \in \mathcal{G}}.$$

7. All operators that commute with all operators in some subset $\mathcal{B} \subset \mathcal{L}(\mathcal{H})$, form an algebra called the *commutant* of \mathcal{B}

$$\mathcal{A} = \{A \mid [A, B] = 0, \forall B \in \mathcal{B}\}.$$

In particular, for every algebra $\mathcal{A} \subseteq \mathcal{L}(\mathcal{H})$ we have the commutant algebra that will be denoted by \mathcal{A}' .

Note that in examples 4 and 5 all elements of the algebra commute with each other. Such algebras are called *commutative* or *abelian*. Also note that in general, the identity operator $I \in \mathcal{L}(\mathcal{H})$ does not have to be an element of the algebra. This is clearly the case in examples 3 and 4 (with $\Pi \neq I$). Operator algebras that include an element that *acts* as the identity

on all other elements in the algebra are called *unital*. Finite-dimensional operator algebras are always unital and there is always a projection $\Pi \in \mathcal{A}$ (possibly $\Pi \equiv I$) that acts as the identity on all elements of \mathcal{A} . We will not prove this fact because in our applications we can always have the full identity operator I included in \mathcal{A} .

We will now define a common way to specify operator algebras via a finite set of generators.

Definition 2.8. The operator algebra $\mathcal{A} = \langle M_1, M_2, \dots, M_m \rangle$ is said to be *generated* by the operators M_i if it is the closure of the subset $\{M_i\}_{i=1, \dots, m} \subset \mathcal{L}(\mathcal{H})$ with respect to the conditions (1) - (3) of the Definition 2.7.

In applications, operator algebras are often specified this way. Moreover, all operator algebras can be specified via a finite set of generators. This trivially follows from the observation that the spanning set of an algebra is in particular its generating set, and all subalgebras of $\mathcal{L}(\mathcal{H})$ have finite spanning sets.

We can always assume that the generators M_i are self-adjoint operators because every non-self-adjoint operator M can be expressed as a linear combination of two self-adjoint operators

$$M = \frac{M + M^\dagger}{2} + i \frac{M - M^\dagger}{2i} = M_+ + iM_-$$

so we can always use M_+ and M_- as generators instead of M and M^\dagger . The closure with respect to the conditions (1) - (3) then means that the elements of \mathcal{A} are all the possible products of the generators and the linear combinations of these products

$$\langle M_1, \dots, M_m \rangle = \left\{ \sum_{n=1}^N c_n M_{i_{n,1}} M_{i_{n,2}} \cdots M_{i_{n,K}} \mid N, K \in \mathbb{N}; c_n \in \mathbb{C}; i_{n,k} \in \{1, \dots, m\} \right\}.$$

In principle, as with any subalgebra of $\mathcal{L}(\mathcal{H})$, the algebra $\langle M_1, \dots, M_m \rangle$ is of finite dimension $D \leq d^2$ so there is a finite spanning set $\{A_1, A_2, \dots, A_D\}$ such that

$$\langle M_1, \dots, M_m \rangle = \left\{ \sum_{n=1}^D c_n A_n \mid c_n \in \mathbb{C} \right\}.$$

In practice, given only the generators M_i , it is not a trivial task to tell the dimension of $\langle M_1, \dots, M_m \rangle$ and find a spanning set.

An important special case is the algebra $\langle M, I \rangle$ generated by a single self-adjoint operator $M = M^\dagger$ and the identity I (the identity is not really necessary here but we will include it to avoid finding the operator that acts as the identity). By definition, this algebra is the set

$$\langle M, I \rangle = \left\{ \sum_{n=0}^N c_n M^n \mid N \in \mathbb{N}, c_n \in \mathbb{C} \right\}. \quad (2.3)$$

The key fact about this algebra is that it is spanned by the spectral projections of M .

Proposition 2.9. *Let M be a self-adjoint operator with the spectral decomposition*

$$M = \sum_{k=1}^m \lambda_k \Pi_k + \lambda_0 \Pi_0$$

where $\lambda_{k=1\dots m}$ are the distinct non-zero eigenvalues, $\Pi_{k=1\dots m}$ are the projections on the corresponding eigenspaces, and Π_0 is the projection on the kernel of M ($\lambda_0 \equiv 0$). Then

$$\langle M, I \rangle = \text{span} \{ \Pi_k \}_{k=0}^m.$$

Proof. For every $k \geq 1$ the spectral projection Π_k can be expressed as

$$\Pi_k = \prod_{l \neq k} \frac{M - \lambda_l I}{\lambda_k - \lambda_l}. \quad (2.4)$$

This means that $\Pi_k \in \langle M, I \rangle$ for all $k \geq 1$. This also means that $\Pi_0 \in \langle M, I \rangle$ since

$$\Pi_0 = I - \sum_{k=1}^m \Pi_k.$$

Thus, $\text{span} \{ \Pi_k \}_{k=0}^m \subseteq \langle M, I \rangle$.

According to Eq. (2.3), every $A \in \langle M, I \rangle$ is of the form

$$A = \sum_{n=0}^N c_n M^n = c_0 I + \sum_{n=1}^N c_n \sum_{k=1}^m \lambda_k^n \Pi_k = c_0 \sum_{k=0}^m \Pi_k + \sum_{n=1}^N c_n \sum_{k=1}^m \lambda_k^n \Pi_k$$

so $A \in \text{span} \{ \Pi_k \}_{k=0}^m$. Thus, $\langle M, I \rangle \subseteq \text{span} \{ \Pi_k \}_{k=0}^m$ and so

$$\langle M, I \rangle = \text{span} \{ \Pi_k \}_{k=0}^m.$$

□

We can always say that $\langle M_i, I \rangle$ is a subalgebra of $\mathcal{A} = \langle M_1, M_2, \dots, M_m, I \rangle$ for each $i = 1, \dots, m$, so the spectral projections $\{ \Pi_{i;k} \}$ of M_i are elements of \mathcal{A} . Therefore, since the spectral projections $\{ \Pi_{i;k} \}$ span the generators M_i , we can use the projections as generators instead of M_i

$$\mathcal{A} = \langle M_1, M_2, \dots, M_m, I \rangle = \langle \{ \Pi_{1;k} \}, \{ \Pi_{2;k} \}, \dots, \{ \Pi_{m;k} \}, I \rangle.$$

This means that we can always use projections instead of self-adjoint operators to generate algebras.

We will now begin introducing the concepts that characterizes the structure of general operator algebras, starting with the simplest building blocks defined as follows.

Definition 2.10. The projection $\Pi \in \mathcal{A}$ is called *minimal projection* if for every $A \in \mathcal{A}$ we have $\Pi A \Pi = c \Pi$ for some $c \in \mathbb{C}$.

Note that rank 1 projections are of the form $\Pi = |\psi\rangle\langle\psi|$ for some $|\psi\rangle \in \mathcal{H}$ so they are always minimal

$$|\psi\rangle\langle\psi| A |\psi\rangle\langle\psi| = \langle A \rangle_\psi |\psi\rangle\langle\psi| \propto |\psi\rangle\langle\psi|.$$

The name *minimal* is chosen because of the following property.

Proposition 2.11. Let $\Pi \in \mathcal{A}$ be a minimal projection and let $\Pi' \in \mathcal{A}$ be another projection such that $\Pi \Pi' = \Pi$, then $\Pi = \Pi'$.

Proof. If $\Pi' = \Pi \Pi'$ then $\Pi' = (\Pi \Pi')^\dagger = \Pi' \Pi$ and so $\Pi' = \Pi \Pi' \Pi$. Therefore, if $\Pi' \neq \Pi$ then $\Pi' \not\propto \Pi$ and so Π is not minimal. \square

The next step in the characterization of the structure behind operator algebras is the definition of the following sets.

Definition 2.12. The set of projections $\{\Pi_k\} \subset \mathcal{A}$ is called a *maximal set of minimal projections* if all Π_k are minimal, pairwise orthogonal $\Pi_k \Pi_{k'} = \delta_{kk'} \Pi_k$, and sum to the identity $I = \sum_k \Pi_k$.

Note that a maximal set of minimal projections does not mean that these are all the minimal projections in the algebra, it just means that these are minimal projections that resolve the identity. Every algebra has at least one maximal set of minimal projections.

Lemma 2.13. Let $\mathcal{A} \in \mathcal{L}(\mathcal{H})$ be an operator algebra, then there is at least one maximal set of minimal projections $\{\Pi_k\} \subset \mathcal{A}$.

Proof. This can be shown recursively by starting with the set of just the identity $\{I\} \subset \mathcal{A}$. If I is a minimal projection in \mathcal{A} then we are done. If not then there is a minimal projection $\Pi_1 \in \mathcal{A}$ such that $\Pi_1 I = \Pi_1 \neq I$ and there is the complement projection $\Pi'_1 = I - \Pi_1 \in \mathcal{A}$. If Π'_1 is also minimal then $\{\Pi_1, \Pi'_1\}$ is a maximal set of minimal projections and we are done. If not, then there is a minimal projection Π_2 such that $\Pi_2 \Pi'_1 = \Pi_2 \neq \Pi'_1$ and there is the complement $\Pi'_2 = \Pi'_1 - \Pi_2 \in \mathcal{A}$. After k iterations we get the set $\{\Pi_1, \Pi_2, \dots, \Pi_k, \Pi'_k\}$ of pairwise orthogonal projections that sums to the identity I . The first k elements in the set are minimal projections and we are done when the last element Π'_k is also minimal. The recursion will terminate after a finite number of steps because $\text{rank}[\Pi'_k] < \text{rank}[\Pi'_{k-1}]$ and projections of rank 1 are always minimal. \square

We can partition the maximal set of minimal projections into subsets that will identify a block-diagonal form of the elements of the algebra using the following equivalence relation.

Proposition 2.14. Let $\{\Pi_k\}$ be a maximal set of minimal projections in the algebra \mathcal{A} . Then, the relation “ \sim ” where $\Pi_k \sim \Pi_l$ if and only if there is an $A \in \mathcal{A}$ such that $\Pi_k A \Pi_l \neq 0$, is an equivalence relation.

Proof. This relation is reflexive ($\Pi_k \sim \Pi_k$) since $\Pi_k \Pi_k \Pi_k \neq 0$, it is symmetric ($\Pi_k \sim \Pi_l$ implies $\Pi_l \sim \Pi_k$) since $\Pi_k A \Pi_l \neq 0$ implies $\Pi_l A^\dagger \Pi_k \neq 0$, and it is transitive ($\Pi_k \sim \Pi_l$ and $\Pi_l \sim \Pi_{k'}$ implies $\Pi_k \sim \Pi_{k'}$) since $\Pi_k A \Pi_l \neq 0$ and $\Pi_l A \Pi_{k'} \neq 0$ implies $\Pi_k A \Pi_l A \Pi_{k'} \neq 0$. \square

Using this equivalence relation we partition the maximal set of minimal projections into equivalence classes labeled by q such that $\Pi_k^q \sim \Pi_l^{q'}$ if and only if $q = q'$ (the indices k and l refer now to the distinct elements inside the equivalence classes). Thus, for every $A \in \mathcal{A}$ and $q \neq q'$ we have $\Pi_k^q A \Pi_l^{q'} = 0$ which prescribes a block-diagonal form for all the elements in the algebra. We will therefore refer to the equivalence classes q as *blocks*.

We saw that every element $A \in \langle M, I \rangle$ is spanned by the spectral projections of M

$$A = \sum_{n=0}^m c_n \Pi_k.$$

Since the spectral projections $\{\Pi_k\}_{k=0}^m$ are all orthogonal to each other we must have $\Pi_k A \Pi_l \propto \delta_{kl} \Pi_k$. Therefore, the set $\{\Pi_k\}_{k=0}^m$ is not only the spanning set of $\langle M, I \rangle$ but it is a maximal set of minimal projections in this algebra (in fact, this is the only such set). Furthermore, each spectral projection is in its own equivalence class ($\Pi_k \sim \Pi_l$ when $k \neq l$) which identifies the block diagonal structure of $\langle M, I \rangle$.

The case of $\langle M, I \rangle$ is too special to draw any general conclusions about minimal projections. In general, the set of *all* the minimal projections in an algebra $\{\Pi_\alpha\} \subset \mathcal{A}$ does not consists of pairwise orthogonal projections $\Pi_\alpha \Pi_{\alpha'} \neq 0$, and it has more than one maximal set of minimal projections. Furthermore, when dealing with algebras generated by multiple operators $\mathcal{A} = \langle M_1, M_2, \dots, M_m, I \rangle$, the spectral projections $\{\Pi_{i;k}\}$ of each generator M_i are not necessarily minimal projections in \mathcal{A} . The distillation of minimal projections from the spectral projections of the generators of the algebra is at the heart of the algorithm that we will present in Chapter 3.

In order to fully capture the structure of an operator algebra (at least in the way that is suitable for our purposes) we will need a slight generalization of the notion of minimal projections.

Definition 2.15. The partial isometry $S \in \mathcal{A}$ is called a *minimal isometry* if the projections on its initial $S^\dagger S = \Pi_{in}$ and final $SS^\dagger = \Pi_{fin}$ spaces are minimal.

Since every projection is a partial isometry $\Pi \Pi^\dagger = \Pi^\dagger \Pi = \Pi$, minimal projections are in particular minimal isometries (the converse is of course not true).

The most important property of minimal isometries is that given the initial and final spaces they are unique up to a phase factor.

Lemma 2.16. Let $S, S' \in \mathcal{A}$ be minimal isometries such that $S^\dagger S = S'^\dagger S' = \Pi_{in}$ and $SS^\dagger = S'S'^\dagger = \Pi_{fin}$, then $S' = e^{i\varphi} S$ for some real phase factor φ .

Proof. Since Π_{in} is the initial space of both S and S' and it is minimal we have

$$S^\dagger S' = \Pi_{in} S^\dagger S' \Pi_{in} = c \Pi_{in} = c S^\dagger S$$

for some $c \in \mathbb{C}$. Multiplying both sides of $S^\dagger S' = c S^\dagger S$ by S from the left and using $SS^\dagger = \Pi_{fin}$ we get

$$S' = \Pi_{fin} S' = c \Pi_{fin} S = c S.$$

Since both S and S' are partial isometries, we must have $c = e^{i\varphi}$. \square

Although minimal isometries generalize minimal projections, we can construct the former from the latter using the following Lemma.

Lemma 2.17. *Let Π_1 and Π_2 be minimal projections in \mathcal{A} , then for any $A \in \mathcal{A}$ the operator $\tilde{S} = \Pi_1 A \Pi_2$ is proportional to a minimal isometry $S \in \mathcal{A}$. In particular, when $\tilde{S} \neq 0$, we have $\text{tr} [\Pi_1] = \text{tr} [\Pi_2]$ and the minimal isometry is given by $S = c \tilde{S}$ where*

$$c = \sqrt{\frac{\text{tr} [\Pi_1]}{\text{tr} [\tilde{S} \tilde{S}^\dagger]}} \in \mathbb{R}.$$

Proof. If $\tilde{S} = 0$ then \tilde{S} is trivially proportional to all operators. If $\tilde{S} \neq 0$ then by the definition of minimal projections there is a proportionality factor a such that

$$\tilde{S} \tilde{S}^\dagger = \Pi_1 A \Pi_2 \Pi_2 A^\dagger \Pi_1 = a \Pi_1$$

We know that $a \neq 0$ (otherwise $\tilde{S} \tilde{S}^\dagger = 0$ and so $\tilde{S} = 0$), therefore

$$a = \frac{\text{tr} [\tilde{S} \tilde{S}^\dagger]}{\text{tr} [\Pi_1]}.$$

Since both $\tilde{S} \tilde{S}^\dagger \neq 0$ and $\Pi_1 \neq 0$ are non-negative self-adjoint operators, a must be a positive real. The operator $S = c \tilde{S}$ where $c = \frac{1}{\sqrt{a}}$ is then a partial isometry because $SS^\dagger = \Pi_1$ is a projection.

Similarly, we know that there is a proportionality factor $a' \neq 0$ such that

$$S^\dagger S = \frac{1}{a} \tilde{S}^\dagger \tilde{S} = \frac{1}{a} \Pi_2 A^\dagger \Pi_1 \Pi_1 A \Pi_2 = \frac{a'}{a} \Pi_2.$$

Since $S^\dagger S$ and Π_2 are projections, we must have $\frac{a'}{a} = 1$. Therefore, both $SS^\dagger = \Pi_1$ and $S^\dagger S = \Pi_2$ are minimal projections, $\text{tr} [SS^\dagger] = \text{tr} [S^\dagger S]$, and S is a minimal isometry. \square

We can now easily prove the fact that minimal projections of different ranks are orthogonal.

Corollary 2.18. Let Π_1 and Π_2 be minimal projections in \mathcal{A} such that $\text{tr} [\Pi_1] \neq \text{tr} [\Pi_2]$, then $\Pi_1 \Pi_2 = 0$.

Proof. Consider $A = I$ in Lemma 2.17. Then $\tilde{S} = \Pi_1 A \Pi_2 = \Pi_1 \Pi_2$ so if $\Pi_1 \Pi_2 \neq 0$ we must have $\text{tr} [\Pi_1] = \text{tr} [\Pi_2]$. \square

The set of operators that fully captures the structure of an operator algebra is the following special spanning set of minimal isometries.

Definition 2.19. A set of partial isometries $\{S_{kl}^q\} \subset \mathcal{A}$ is called *maximal set of minimal isometries* in \mathcal{A} if all S_{kl}^q are minimal, the set $\{S_{kl}^q\}$ spans the algebra

$$\mathcal{A} = \text{span} \{S_{kl}^q\},$$

and for all values of q, k, l we have $S_{kl}^q = S_{lk}^{q\dagger}$ and $S_{kl}^q S_{l'k'}^{q'} = \delta_{qq'} \delta_{ll'} S_{kk'}^q$.

The existence of maximal sets of minimal isometries in every algebra is guaranteed by the following theorem.

Theorem 2.20. Let $\mathcal{A} \in \mathcal{L}(\mathcal{H})$ be an operator algebra, then, there is a maximal set of minimal isometries $\{S_{kl}^q\} \subset \mathcal{A}$ that spans it.

Proof. Let $\{\Pi_k^q\}$ be a maximal set of minimal projections in \mathcal{A} provided by Lemma 2.13 and partitioned into equivalence classes q according to Proposition 2.14. By the definition of these equivalence classes, for every q, k, l there is at least one $A \in \mathcal{A}$ such that $\Pi_k^q A \Pi_l^q \neq 0$. Then, according to Lemma 2.17, for each q, k, l there is a minimal isometry $S_{kl}^q \in \mathcal{A}$ and a real positive constant c such that $S_{kl}^q = c \Pi_k^q A \Pi_l^q$ for some $A \in \mathcal{A}$. In order to get the desired properties of the Definition 2.19 we can construct the maximal set of minimal isometries with the following procedure. First, for each q, k arbitrarily choose $A \in \mathcal{A}$ such that $S_{k1}^q = c \Pi_k^q A \Pi_1^q \neq 0$ (we fixed $l = 1$ but it does not matter what value of l is fixed). Then, define $S_{1k}^q = (S_{k1}^q)^\dagger$ and $S_{kl}^q = S_{k1}^q S_{1l}^q$ which are also minimal isometries in \mathcal{A} . Thus, for all values of q, k, l we have

$$\begin{aligned} S_{kl}^q &= S_{k1}^q S_{1l}^q = (S_{1l}^q S_{1k}^q)^\dagger = S_{lk}^{q\dagger} \\ S_{kl}^q S_{l'k'}^{q'} &= S_{k1}^q S_{1l}^q S_{1l'}^{q'} S_{1k'}^{q'} = \delta_{qq'} \delta_{ll'} S_{k1}^q S_{1k'}^{q'} = \delta_{qq'} \delta_{ll'} S_{kk'}^q. \end{aligned}$$

Lemma 2.16 implies that each minimal isometry is unique in \mathcal{A} up to a phase factor. Therefore, given the set $\{S_{kl}^q\}$ as constructed above, for any $A \in \mathcal{A}$ we either have $\Pi_k^q A \Pi_l^q = 0$ or $\Pi_k^q A \Pi_l^q = \frac{e^{i\varphi}}{c} S_{kl}^q$ for some phase φ and a real c . Recalling that $\sum_{q,k} \Pi_k^q = I$, we can express any $A \in \mathcal{A}$ as

$$A = \left(\sum_{q,k} \Pi_k^q \right) A \left(\sum_{q',l} \Pi_l^{q'} \right) = \sum_{q,k,l} \Pi_k^q A \Pi_l^q = \sum_{q,k,l} c_{kl}^q S_{kl}^q$$

where we have used the fact that $\Pi_k^q A \Pi_l^{q'} = 0$ for $q \neq q'$ and introduced the complex coefficients c_{kl}^q . Therefore $\mathcal{A} = \text{span} \{S_{kl}^q\}$. \square

Note that for $k = l$ the minimal isometries S_{kk}^q are actually the minimal projections Π_k^q , so the maximal set of minimal projections $\{\Pi_k^q\}$ is a subset of the maximal set of minimal isometries $\{S_{kl}^q\}$.

Although it was not very easy to get to the general result of Theorem 2.20, maximal sets of minimal isometries are quite easy to find in some canonical examples. For example, in the case of the full operator algebra $\mathcal{L}(\mathcal{H}_{qudit})$ of a qudit $\mathcal{H}_{qudit} = \text{span}\{|k\rangle\}_{k=1,\dots,d}$, the minimal isometries are simply the matrix units

$$S_{kl} = |k\rangle\langle l|.$$

Here the index q is suppressed because all $\{S_{kl}\}$ belong to the same block as we cannot partition them into subsets that are completely orthogonal to each other.

For a slightly more interesting example we may consider the qudit \mathcal{H}_{qudit} in a tensor product with a qubit $\mathcal{H}_{qubit} = \text{span}\{|0\rangle, |1\rangle\}$. Then, consider the algebra

$$\mathcal{A} = \{|q\rangle\langle q| \otimes A \mid q = 0, 1; A \in \mathcal{L}(\mathcal{H}_{qudit})\} \quad (2.5)$$

with the maximal set of minimal isometries

$$S_{kl}^q = |q\rangle\langle q| \otimes |k\rangle\langle l|.$$

Here the index $q = 0, 1$ distinguishes the two blocks of completely orthogonal isometries.

In both of the above examples, the initial and the final spaces of the isometries are one-dimensional $\text{tr}[S_{kl}^q S_{lk}^q] = 1$. In general, this is not the case and one should think of $\{S_{kl}^q\}$ as generalized matrix units that map between orthogonal subspaces of dimension one or higher. In the next section we will show how maximal sets of minimal isometries fully capture the structure of irreducible representations of operator algebras.

2.3 Bipartition tables and the irreps structure

In order to understand what a maximal set of minimal isometries tells us about the algebra we will introduce a neat visual aid that captures the implied structure. This visual aid is called a *bipartition table* and we will see that it specifies the structure of irreducible representations. The correspondence between maximal sets of minimal isometries and bipartition tables leads to the main result of the representation theory of (finite-dimensional) operator algebras known as the Wedderburn Decomposition.

Let us start with the definition.

Definition 2.21. A *bipartition table (BPT)* is an arrangement of some basis of the Hilbert space into a block-diagonal table. This arrangement is specified by a choice of orthonormal basis elements $\{|e_{ik}^q\rangle\}$ labeled with the indices of blocks q , rows i and columns k . For each

block q we construct the rectangular table

$$\begin{array}{|c|c|c|} \hline e_{1,1}^q & e_{1,2}^q & \cdots \\ \hline e_{2,1}^q & e_{2,2}^q & \cdots \\ \hline \vdots & \vdots & \ddots \\ \hline \end{array},$$

and the full bipartition table is given by the diagonal arrangement of all the blocks

$$\begin{array}{|c|c|} \hline e_{1,1}^1 & \cdots \\ \hline \vdots & \ddots \\ \hline \end{array} \quad \begin{array}{|c|c|} \hline e_{1,1}^2 & \cdots \\ \hline \vdots & \ddots \\ \hline \end{array} \quad \cdots \quad \begin{array}{|c|c|} \hline e_{1,1}^q & \cdots \\ \hline \vdots & \ddots \\ \hline \end{array} \quad \cdots$$

What makes BPTs useful is that they tell us how to construct maximal sets of minimal isometries. The construction is simple: Each pair of columns k, l in the block q , specifies the isometry

$$S_{kl}^q := \sum_i |e_{ik}^q\rangle \langle e_{il}^q|, \quad (2.6)$$

where i runs over all the rows in the block. The blocks of the BPT partition the minimal isometries into orthogonal subsets, that is $S_{kl}^q S_{k'l'}^{q'} = 0$ for $q \neq q'$. The subsets of the basis $\{|e_{il}^q\rangle\}_{i=1,\dots}$ and $\{|e_{ik}^q\rangle\}_{i=1,\dots}$ given by the columns l and k specify the initial and final spaces of the isometry S_{kl}^q . The alignment of basis elements across the rows specifies how the isometries map the vectors between the subspaces, that is, the basis element $|e_{il}^q\rangle$ is mapped to $|e_{ik}^q\rangle$ (these are the right and left singular vectors of S_{kl}^q).

It is easy to show that the set of isometries constructed in this way spans an algebra.

Proposition 2.22. *Let $\{S_{kl}^q\}$ be the set of partial isometries constructed from a bipartition table according to Eq. (2.6). Then, $\mathcal{A} = \text{span}\{S_{kl}^q\}$ is an operator algebra and $\{S_{kl}^q\}$ is a maximal set of minimal isometries in \mathcal{A} .*

Proof. Clearly, for all q, k, l we have $S_{kl}^q = S_{lk}^{q\dagger}$ and $S_{kl}^q S_{l'k'}^{q'} = \delta_{qq'} \delta_{ll'} S_{kk'}^q$. Therefore, for any $A_1, A_2 \in \text{span}\{S_{kl}^q\}$ and $c_1, c_2 \in \mathbb{C}$ we have: $c_1 A_1 + c_2 A_2 \in \text{span}\{S_{kl}^q\}$, and $A_1 A_2 \in \text{span}\{S_{kl}^q\}$, and $A_1^\dagger, A_2^\dagger \in \text{span}\{S_{kl}^q\}$. Thus by definition $\mathcal{A} = \text{span}\{S_{kl}^q\}$ is an operator algebra and $\{S_{kl}^q\}$ is a maximal set of minimal isometries in it. \square

Let us consider some examples of BPTs that specify the minimal isometries of some familiar algebras.

The minimal isometries $S_{kl} = |k\rangle \langle l|$ of the full operator algebra $\mathcal{L}(\mathcal{H}_{qudit})$ of the qudit $\mathcal{H}_{qudit} = \text{span}\{|k\rangle\}_{k=1,\dots,d}$, are constructed from the BPT

$$\begin{array}{|c|c|c|c|} \hline 1 & 2 & \cdots & d \\ \hline \end{array}.$$

There is only one block here and this block has only one row. Following the construction in Eq. (2.6) we can reproduce all the minimal isometries of $\mathcal{L}(\mathcal{H}_{qudit})$.

Adding a qubit $\mathcal{H}_{qubit} \otimes \mathcal{H}_{qudit}$ to the qudit we consider again the algebra in Eq. (2.5). Using the combined basis labels $|q, k\rangle \equiv |q\rangle_{qubit} \otimes |k\rangle_{qudit}$, we can see that all the minimal isometries are of the form

$$S_{kl}^q = |q\rangle \langle q| \otimes |k\rangle \langle l| \equiv |q, k\rangle \langle q, l|.$$

These isometries can be constructed from the BPT

$$\begin{array}{|c|c|c|c|} \hline 0, 1 & 0, 2 & \cdots & 0, d \\ \hline \end{array} \quad \begin{array}{|c|c|c|c|} \hline 1, 1 & 1, 2 & \cdots & 1, d \\ \hline \end{array}.$$

Here we have two blocks with one row each.

Lastly, still with the Hilbert space $\mathcal{H}_{qubit} \otimes \mathcal{H}_{qudit}$, consider the algebra of all the operators that act only on the qudit

$$\mathcal{A} = \{I_{qubit} \otimes A_{qudit} \mid A_{qudit} \in \mathcal{L}(\mathcal{H}_{qudit})\}.$$

The maximal set of minimal isometries in this case consists of

$$S_{kl} = I_{qubit} \otimes |k\rangle \langle l| = |0, k\rangle \langle 0, l| + |1, k\rangle \langle 1, l|$$

and the BPT that produces them is

$$\begin{array}{|c|c|c|c|} \hline 0, 1 & 0, 2 & \cdots & 0, d \\ \hline 1, 1 & 1, 2 & \cdots & 1, d \\ \hline \end{array}.$$

Here we have a single block with two rows.

In general, given a maximal set of minimal isometries of the algebra, we can always find a BPT that produces it.

Lemma 2.23. *Let $\{S_{kl}^q\}$ be a maximal set of minimal isometries. Then, there is a BPT that produces all $\{S_{kl}^q\}$ according to Eq. (2.6).*

Proof. Given $\{S_{kl}^q\}$ let us explicitly construct this BPT as follows:

1. Each q corresponds to a separate block of the BPT constructed independently.
2. Arbitrarily choose orthonormal basis $\{|e_{i1}^q\rangle\}_{i=1,\dots}$ for the eigenspace of S_{11}^q and assign them to the first column

$$\begin{array}{|c|} \hline e_{11}^q \\ \hline e_{21}^q \\ \hline \vdots \\ \hline \end{array}.$$

3. For every $k > 1$ map the first column to a new column in the block using the isometries $|e_{ik}^q\rangle = S_{k1}^q |e_{i1}^q\rangle$

$$\begin{array}{|c|c|c|c|} \hline e_{11}^q & \cdots & e_{1k}^q & \cdots \\ \hline e_{21}^q & \cdots & e_{2k}^q & \cdots \\ \hline \vdots & \vdots & \vdots & \ddots \\ \hline \end{array}.$$

Then, according to Eq. (2.6), the isometries constructed from this table are

$$\tilde{S}_{kl}^q = \sum_i |e_{ik}^q\rangle \langle e_{il}^q| = S_{k1}^q \left[\sum_i |e_{i1}^q\rangle \langle e_{i1}^q| \right] S_{1l}^q = S_{k1}^q S_{11}^q S_{1l}^q = S_{kl}^q.$$

□

Note that when $\{S_{kl}^q\}$ is not supported on the whole Hilbert space \mathcal{H} , the set of orthonormal basis $\{|e_{ik}^q\rangle\}$ constructed in the above lemma is not complete, and it only spans a proper subspace of \mathcal{H} where the algebra is supported. It can be shown that the algebra \mathcal{A} is supported on the whole Hilbert space \mathcal{H} , if and only if $I \in \mathcal{A}$.

The above Lemma closes the logical arc started with the Theorem 2.20 and Proposition 2.22: Every operator algebra is spanned by a maximal set of minimal isometries that can be constructed from a BPT, and every BPT constructs a set of minimal isometries that span an operator algebra. Thus, we can directly relate BPTs to operator algebras and operator algebras to BPTs.

We already know that by construction 2.6, the columns of the BPT specify a maximal set of minimal projections in the algebra. The rows of the BPT are also meaningful and they specify the following subspaces.

Definition 2.24. Let $\mathcal{A} \subseteq \mathcal{L}(\mathcal{H})$ be an operator algebra. The subspace $\mathcal{V} \subseteq \mathcal{H}$ is called an *invariant subspace* under \mathcal{A} if for all $|\psi\rangle \in \mathcal{V}$ and $A \in \mathcal{A}$ we have $A|\psi\rangle \in \mathcal{V}$. If, in addition, every proper subspace $\mathcal{V}' \subset \mathcal{V}$ is not invariant, then \mathcal{V} is called a *minimal invariant subspace*.

Proposition 2.25. Let $\{|e_{ik}^q\rangle\}$ be the orthonormal basis forming a BPT of the operator algebra \mathcal{A} . Then, every subspace $\mathcal{V} := \text{span} \{|e_{il}^q\rangle\}_{l=1,\dots}$ spanned by the basis elements in a

single row is a minimal invariant subspace.

Proof. With the minimal isometries constructed as in Eq. (2.6), we can express any $A \in \mathcal{A} = \text{span} \{S_{kl}^q\}$ as

$$A = \sum_{q', k', l'} c_{k'l'}^{q'} S_{k'l'}^{q'}.$$

Then,

$$A |e_{il}^q\rangle = \sum_{q', k', l'} c_{k'l'}^{q'} S_{k'l'}^{q'} |e_{il}^q\rangle = \sum_{k'} c_{k'l}^q |e_{ik'}^q\rangle \in \mathcal{V}, \quad (2.7)$$

so \mathcal{V} is an invariant subspace under \mathcal{A} . If \mathcal{V} is not minimal then there is subspace $\mathcal{V}' \subset \mathcal{V} = \mathcal{V}' \oplus \mathcal{V}''$, such that for every non-zero $|\psi'\rangle \in \mathcal{V}'$ and $|\psi''\rangle \in \mathcal{V}''$ we have $\langle \psi'' | A | \psi' \rangle = 0$ for all $A \in \mathcal{A}$. However, for every non-zero $|\psi'\rangle, |\psi''\rangle \in \mathcal{V} = \text{span} \{|e_{il}^q\rangle\}_{l=1, \dots}$, there is always at least one $S_{kl}^q \in \mathcal{A}$ such that $\langle \psi'' | S_{kl}^q | \psi' \rangle \neq 0$, therefore \mathcal{V} is minimal. \square

The rows of the BPT identify the subspaces on which \mathcal{A} acts irreducibly. Furthermore, it should be clear that the action of $A \in \mathcal{A}$ is identical on every row in the same block since the expression in Eq. (2.7) does not depend on the row index i . Therefore, all the rows in the same block carry equivalent irreducible representations of \mathcal{A} , and the number of rows in the block is the multiplicity of that irreducible representation.

The above statements are essentially the main result of the representation theory of finite-dimensional operator algebras, albeit, in the non-standard formulation that relies on the picture of BPTs. We will now present this result in the standard form known as the Wedderburn Decomposition.

Theorem 2.26. *Let $\mathcal{A} \subseteq \mathcal{L}(\mathcal{H})$ be an operator algebra supported on the whole Hilbert space \mathcal{H} . Then, there is a decomposition (Wedderburn Decomposition)*

$$\mathcal{H} \cong \bigoplus_q \mathcal{H}_{\nu_q} \otimes \mathcal{H}_{\mu_q}, \quad (2.8)$$

such that

$$\mathcal{A} \cong \bigoplus_q I_{\nu_q} \otimes \mathcal{L}(\mathcal{H}_{\mu_q}) := \left\{ \bigoplus_q I_{\nu_q} \otimes A_q \mid A_q \in \mathcal{L}(\mathcal{H}_{\mu_q}) \right\}.$$

Proof. Let $\{S_{kl}^q\}$ be a maximal set of minimal isometries in \mathcal{A} as provided by Theorem 2.20, and let $\{|e_{ik}^q\rangle\}$ be the orthonormal basis forming the BPT as provided by Lemma 2.23. Since \mathcal{A} is supported on the whole \mathcal{H} , we can define the map

$$V : |e_{ik}^q\rangle \mapsto |n_i^q\rangle \otimes |m_k^q\rangle$$

which isometrically maps the whole \mathcal{H} to the tensor products of $\mathcal{H}_{\nu_q} := \text{span} \{|n_i^q\rangle\}_{i=1, \dots}$ (associated with the row index) and $\mathcal{H}_{\mu_q} := \text{span} \{|m_k^q\rangle\}_{k=1, \dots}$ (associated with the column

index). Thus, we identify the isometric relation that specifies a decomposition of \mathcal{H} :

$$\mathcal{H} \cong V\mathcal{H} = \bigoplus_q \mathcal{H}_{\nu_q} \otimes \mathcal{H}_{\mu_q}.$$

The image of the algebra \mathcal{A} under V is then

$$\mathcal{A} \cong V\mathcal{A}V^\dagger = \text{span} \left\{ VS_{kl}^q V^\dagger \right\}.$$

We can now see that

$$VS_{kl}^q V^\dagger = \sum_i V |e_{ik}^q\rangle \langle e_{il}^q| V^\dagger = \sum_i |n_i^q\rangle \langle n_i^q| \otimes |m_k^q\rangle \langle m_l^q| = I_{\nu_q} \otimes |m_k^q\rangle \langle m_l^q|$$

and therefore

$$\mathcal{A} \cong \text{span} \left\{ I_{\nu_q} \otimes |m_k^q\rangle \langle m_l^q| \right\} = \bigoplus_q I_{\nu_q} \otimes \mathcal{L}(\mathcal{H}_{\mu_q}).$$

□

The decomposition in Eq. (2.8) is the general structure of irreducible representations of operator algebras. In the broader mathematical context, this leads to the realization that every operator algebra $\mathcal{A} \subseteq \mathcal{L}(\mathcal{H})$ is just (up to an isomorphism) a direct sum of full operator algebras $\mathcal{L}(\mathcal{H}_{\mu_q})$. When the algebra \mathcal{A} is not supported on the whole \mathcal{H} , this theorem applies to a proper subspace $\mathcal{H}' \subset \mathcal{H}$ where the operators of \mathcal{A} are supported.²

In the qubit-qudit example with the algebra of operators that act only on the qudit

$$\mathcal{A} = I_{\text{qubit}} \otimes \mathcal{L}(\mathcal{H}_{\text{qudit}}),$$

the Wedderburn Decomposition is simply $\mathcal{H} = \mathcal{H}_{\text{qubit}} \otimes \mathcal{H}_{\text{qudit}}$ by the definition of \mathcal{A} . The matrix form of all $A \in \mathcal{A}$ is then

$$A = I_{\text{qubit}} \otimes A_{\text{qudit}} = |0\rangle \langle 0| \otimes A_{\text{qudit}} + |1\rangle \langle 1| \otimes A_{\text{qudit}} = \begin{pmatrix} A_{\text{qudit}} & \\ & A_{\text{qudit}} \end{pmatrix}.$$

In general, Theorem 2.26 tells us that there is always a decomposition (2.8) where the operator algebra \mathcal{A} acts as the identity on \mathcal{H}_{ν_q} 's and as the full operator algebra on \mathcal{H}_{μ_q} 's, and it does not map between the sectors q . That is, with respect to the Wedderburn

²This should not be an issue for us since including the full identity I in the algebra will always be possible.

Decomposition, all $A \in \mathcal{A}$ are of the form

$$A \cong \bigoplus_q I_{\nu_q} \otimes A_q = \bigoplus_q \left[\sum_{i=1}^{\dim \mathcal{H}_{\nu_q}} |n_i^q\rangle \langle n_i^q| \otimes A_q \right] = \begin{pmatrix} A_1 & & & \\ & \ddots & & \\ & & A_1 & \\ \underbrace{\hspace{10em}}_{\dim \mathcal{H}_{\nu_1}} & & & \\ & A_2 & & \\ & & \ddots & \\ & & & A_2 \\ & & \underbrace{\hspace{10em}}_{\dim \mathcal{H}_{\nu_2}} & \\ & & & \ddots \end{pmatrix}.$$

From the explicit block-diagonal matrix form we can see that for each sector q , we have $\dim \mathcal{H}_{\nu_q}$ identical matrix blocks where A acts irreducibly with the matrices A_q . These matrix blocks correspond to the minimal invariant subspaces spanned by a single row in the BPT

$$\text{span} \{ |e_{ik}^q\rangle \}_{k=1,\dots} \cong \text{span} \{ |n_i^q\rangle \otimes |m_k^q\rangle \}_{k=1,\dots}.$$

We can see now that the BPT block index q distinguish between the classes of minimal invariant subspaces on which the action of $A \in \mathcal{A}$ is represented independently with distinct A_q 's. Then, inside the blocks, the BPT row index i distinguishes between the minimal invariant subspaces on which the action of $A \in \mathcal{A}$ is represented with the same A_q . In other words, the *rows* of the BPT correspond to the *irreducible matrix blocks* of A , while the *blocks* of the BPT correspond to the *super-blocks of identical irreducible matrix blocks* of A .

It should now be clear how BPTs specify the irreps structure by arranging the basis into a table.³ Our earlier assertion that BPTs correspond to operator algebras can now be restated in a stronger form: BPTs correspond to the irreps structures behind operator algebras.

We will now consider group algebras as a special case and derive the structure of group representations from the above results.

Definition 2.27. Given a finite or a Lie group \mathcal{G} with the unitary representation $U(\mathcal{G}) := \{U(g)\}_{g \in \mathcal{G}} \subset \mathcal{L}(\mathcal{H})$, the *group algebra* is denoted and defined as

$$\mathcal{A}_{U(\mathcal{G})} := \text{span} \{U(g)\}_{g \in \mathcal{G}}.$$

Clearly $U(\mathcal{G}) \subset \mathcal{A}_{U(\mathcal{G})}$ so with respect to the Wedderburn Decomposition (2.8), for all

³Note that BPTs only tell us how to arrange the basis *labels* into a table, they do not explicitly specify the basis themselves. Defining the basis behind the labels in the BPT is an essential information about the irreps structure.

$U(g) \in U(\mathcal{G})$ there are $U_{\mu_q}(g) \in \mathcal{L}(\mathcal{H}_{\mu_q})$ such that

$$U(g) \cong \bigoplus_q I_{\nu_q} \otimes U_{\mu_q}(g). \quad (2.9)$$

Theorem 2.28. *Let $U(\mathcal{G})$ be a unitary representation of the group \mathcal{G} on \mathcal{H} , and let Eq. (2.9) be the decomposition of the group action as given by the Theorem 2.26 for the group algebra $\mathcal{A}_{U(\mathcal{G})}$. Then, for all q , $U_{\mu_q}(\mathcal{G})$ are inequivalent irreducible unitary representations of \mathcal{G} on \mathcal{H}_{μ_q} .*

Proof. The fact that $U_{\mu_q}(\mathcal{G})$ are unitary representations of \mathcal{G} follows directly from the fact that $U(\mathcal{G})$ is a unitary representation of \mathcal{G} . According to Theorem 2.26, the group algebra $\mathcal{A}_{U(\mathcal{G})}$ acts on \mathcal{H}_{μ_q} as the full operator algebra $\mathcal{L}(\mathcal{H}_{\mu_q})$. Then, by the definition of group algebras, we must have

$$\text{span} \{U_{\mu_q}(g)\}_{g \in \mathcal{G}} = \mathcal{L}(\mathcal{H}_{\mu_q}).$$

There can be no proper invariant subspaces of \mathcal{H}_{μ_q} under the action of $U_{\mu_q}(\mathcal{G})$, because there are no proper invariant subspaces under the action of $\mathcal{L}(\mathcal{H}_{\mu_q}) = \text{span} \{U_{\mu_q}(g)\}_{g \in \mathcal{G}}$. Therefore, $U_{\mu_q}(\mathcal{G})$ acts irreducibly on \mathcal{H}_{μ_q} .

Furthermore, the general result of Theorem 2.26 implies that the algebra $\mathcal{A}_{U(\mathcal{G})}$ includes the projection $I_{\nu_q} \otimes I_{\mu_q}$ on the sector q . Then, there are coefficients $c(g) \in \mathbb{C}$ such that

$$\sum_{g \in \mathcal{G}} c(g) U(g) \cong \bigoplus_{q'} I_{\nu_{q'}} \otimes \left[\sum_{g \in \mathcal{G}} c(g) U_{\mu_{q'}}(g) \right] = I_{\nu_q} \otimes I_{\mu_q},$$

and so

$$\sum_{g \in \mathcal{G}} c(g) U_{\mu_{q'}}(g) = \delta_{qq'} I_{\mu_q}.$$

Therefore, for every $q' \neq q$ there must be some $g \in \mathcal{G}$ such that $U_{\mu_{q'}}(g) \neq U_{\mu_q}(g)$ and so the representations $U_{\mu_{q'}}(\mathcal{G})$ and $U_{\mu_q}(\mathcal{G})$ are not equivalent. \square

Theorem 2.28 tells us that the irreps structure of a group representation is, in fact, inherited from the irreps structure of the group algebra. We can therefore use all the insights about the irreps structure of operator algebras, in particular BPTs, to characterize the representations of groups.

As a simple example, consider the Hilbert space of two spins $\mathcal{H} = \frac{1}{2} \otimes \frac{1}{2}$ and the group of collective rotations. From group representation theory of $SU(2)$ we know that this Hilbert space decomposes as

$$\mathcal{H} = \frac{1}{2} \otimes \frac{1}{2} = \underline{1} \oplus \underline{0}$$

where the triplet (spin-1) and singlet (spin-0) subspaces are spanned by the basis

$$\begin{aligned}
|1; 1\rangle &= \left|\frac{1}{2}, \frac{1}{2}\right\rangle & |0; 0\rangle &\propto \left|\frac{1}{2}, -\frac{1}{2}\right\rangle - \left|-\frac{1}{2}, \frac{1}{2}\right\rangle \\
|1; 0\rangle &\propto \left|\frac{1}{2}, -\frac{1}{2}\right\rangle + \left|-\frac{1}{2}, \frac{1}{2}\right\rangle \\
|1; -1\rangle &= \left|-\frac{1}{2}, -\frac{1}{2}\right\rangle.
\end{aligned}$$

These basis identify the irreps structure of collective rotations on two spins which can be summarized with a BPT as

$$\begin{array}{|c|c|c|} \hline 1; 1 & 1; 0 & 1; -1 \\ \hline & & 0; 0 \\ \hline \end{array}.$$

The two blocks here identify the two inequivalent irreps of $SU(2)$, and each irrep is represented on a single invariant subspace, as per the number of rows in each block.

If we add a third qubit, the Hilbert space will decompose under collective rotations as

$$\mathcal{H} = \underline{\frac{1}{2}} \otimes \underline{\frac{1}{2}} \otimes \underline{\frac{1}{2}} = \underline{\frac{3}{2}} \oplus \underline{\frac{1}{2}} \oplus \underline{\frac{1}{2}}$$

with a single spin- $\frac{3}{2}$ subspace and two spin- $\frac{1}{2}$ subspaces. Given the basis of total spin $|j; m\rangle$, the BPT that specifies the irreps structure is

$$\begin{array}{|c|c|c|c|} \hline \frac{3}{2}, \frac{3}{2} & \frac{3}{2}, \frac{1}{2} & \frac{3}{2}, -\frac{1}{2} & \frac{3}{2}, -\frac{3}{2} \\ \hline & & & \\ \hline \end{array}
\begin{array}{|c|c|} \hline \frac{1}{2}, \frac{1}{2}, 1 & \frac{1}{2}, -\frac{1}{2}, 1 \\ \hline \frac{1}{2}, \frac{1}{2}, 2 & \frac{1}{2}, -\frac{1}{2}, 2 \\ \hline \end{array}.$$

These two blocks identify the irreps of spin- $\frac{3}{2}$ and spin- $\frac{1}{2}$. The second block has two rows since spin- $\frac{1}{2}$ is equivalently represented on two separate invariant subspaces labeled with $i = 1, 2$. The Wedderburn Decomposition implied by this BPT is

$$\mathcal{H} = \underline{\frac{1}{2}} \otimes \underline{\frac{1}{2}} \otimes \underline{\frac{1}{2}} \cong \mathcal{H}_{\mu_{3/2}} \oplus \mathcal{H}_{\nu_{1/2}} \otimes \mathcal{H}_{\mu_{1/2}},$$

where $\mathcal{H}_{\mu_{3/2}}$ and $\mathcal{H}_{\mu_{1/2}}$ are the inequivalent irreps, and $\dim \mathcal{H}_{\nu_{1/2}} = 2$ provides the two-dimensional multiplicity to the spin- $\frac{1}{2}$ irrep.

Group representations are commonly used to identify the symmetries of physically meaningful operators that commute with the group action. The commutant algebra of a symmetry group representation is therefore an interesting operator algebra that characterizes all the operators that have that symmetry. The following theorem allows us to immediately identify the commutant algebra from the BPT.

Theorem 2.29. *Let $\{|e_{ik}^q\rangle\}$ be the orthonormal basis forming the BPT of the operator algebra \mathcal{A} supported on the whole Hilbert space \mathcal{H} . Then, the transposition (interchanging rows with columns) of $\{|e_{ik}^q\rangle\}$ produces the BPT of the commutant algebra*

$$\mathcal{A}' = \{A' \in \mathcal{L}(\mathcal{H}) \mid [A', A] = 0 \quad \forall A \in \mathcal{A}\}.$$

Proof. By construction 2.6, the minimal isometries produced by the original and the transposed BPTs are

$$S_{kl}^q = \sum_i |e_{ik}^q\rangle \langle e_{il}^q|, \quad \tilde{S}_{ij}^q = \sum_k |e_{ik}^q\rangle \langle e_{jk}^q|.$$

Since \mathcal{A} is supported on the whole \mathcal{H} we have $I = \sum_{q,k} S_{kk}^q = \sum_{q,k} S_{kl}^q S_{lk}^q$ for any l . By the definition of \mathcal{A}' , for every $A' \in \mathcal{A}'$ and $S_{kl}^q \in \mathcal{A}$ we have $S_{kl}^q A' = A' S_{kl}^q$, and so

$$\begin{aligned} A' &= A' \sum_{q,k} S_{kl}^q S_{lk}^q = \sum_{q,k} S_{kl}^q A' S_{lk}^q = \sum_{q,k} \sum_i |e_{ik}^q\rangle \langle e_{il}^q| A' \sum_j |e_{jl}^q\rangle \langle e_{jk}^q| \\ &= \sum_{q,i,j} \langle e_{il}^q| A' |e_{jl}^q\rangle \sum_k |e_{ik}^q\rangle \langle e_{jk}^q| = \sum_{q,i,j} \langle e_{il}^q| A' |e_{jl}^q\rangle \tilde{S}_{ij}^q. \end{aligned}$$

Therefore, $\mathcal{A}' \subseteq \text{span} \{ \tilde{S}_{ij}^q \}$. By explicit multiplication we can see that $S_{kl}^{q'} \tilde{S}_{ij}^q = \tilde{S}_{ij}^q S_{kl}^{q'} = \delta_{qq'} |e_{ik}^q\rangle \langle e_{jl}^q|$, so $[\tilde{S}_{ij}^q, S_{kl}^{q'}] = 0$ and so $\text{span} \{ \tilde{S}_{ij}^q \} \subseteq \mathcal{A}'$. Therefore, $\mathcal{A}' = \text{span} \{ \tilde{S}_{ij}^q \}$. \square

In terms of the Wedderburn Decomposition, Theorem 2.29 tells us that

$$\mathcal{A} \cong \bigoplus_q I_{\nu_q} \otimes \mathcal{L}(\mathcal{H}_{\mu_q}) \quad \Leftrightarrow \quad \mathcal{A}' \cong \bigoplus_q \mathcal{L}(\mathcal{H}_{\nu_q}) \otimes I_{\mu_q}.$$

That is, operator algebras and their commutants have the same Wedderburn Decomposition with the roles of μ_q and ν_q exchanged. This theorem also trivially implies the following well known result.

Corollary 2.30. (*Bicommutant Theorem*) *Let \mathcal{A} be an operator algebra supported on the whole Hilbert space \mathcal{H} and let \mathcal{A}'' be its bicommutant (commutant of a commutant) algebra. Then, $\mathcal{A} = \mathcal{A}''$.*

Proof. According to Theorem 2.29, the BPT of \mathcal{A}'' is produced by transposing the BPT of \mathcal{A} twice, which leaves it unchanged. \square

In the example of three qubits, the commutant algebra of collective rotations is then given by the BPT

$$\begin{array}{|c|} \hline \frac{3}{2}, \frac{3}{2} \\ \hline \frac{3}{2}, \frac{1}{2} \\ \hline \frac{3}{2}, -\frac{1}{2} \\ \hline \frac{3}{2}, -\frac{3}{2} \\ \hline \end{array} \cdot \begin{array}{|c|c|} \hline \frac{1}{2}, \frac{1}{2}, 1 & \frac{1}{2}, \frac{1}{2}, 2 \\ \hline \frac{1}{2}, -\frac{1}{2}, 1 & \frac{1}{2}, -\frac{1}{2}, 2 \\ \hline \end{array}$$

Thus, all three-qubit operators that are symmetric under collective rotations are spanned by the five partial isometries:

$$S^{\frac{3}{2}} = \left| \frac{3}{2}, \frac{3}{2} \right\rangle \left\langle \frac{3}{2}, \frac{3}{2} \right| + \left| \frac{3}{2}, \frac{1}{2} \right\rangle \left\langle \frac{3}{2}, \frac{1}{2} \right| + \left| \frac{3}{2}, -\frac{1}{2} \right\rangle \left\langle \frac{3}{2}, -\frac{1}{2} \right| + \left| \frac{3}{2}, -\frac{3}{2} \right\rangle \left\langle \frac{3}{2}, -\frac{3}{2} \right|$$

$$\begin{aligned} S^{\frac{1}{2}}_{11} &= \left| \frac{1}{2}, \frac{1}{2}, 1 \right\rangle \left\langle \frac{1}{2}, \frac{1}{2}, 1 \right| + \left| \frac{1}{2}, -\frac{1}{2}, 1 \right\rangle \left\langle \frac{1}{2}, -\frac{1}{2}, 1 \right| & S^{\frac{1}{2}}_{22} &= \left| \frac{1}{2}, \frac{1}{2}, 2 \right\rangle \left\langle \frac{1}{2}, \frac{1}{2}, 2 \right| + \left| \frac{1}{2}, -\frac{1}{2}, 2 \right\rangle \left\langle \frac{1}{2}, -\frac{1}{2}, 2 \right| \\ S^{\frac{1}{2}}_{12} &= \left| \frac{1}{2}, \frac{1}{2}, 1 \right\rangle \left\langle \frac{1}{2}, \frac{1}{2}, 2 \right| + \left| \frac{1}{2}, -\frac{1}{2}, 1 \right\rangle \left\langle \frac{1}{2}, -\frac{1}{2}, 2 \right| & S^{\frac{1}{2}}_{21} &= \left| \frac{1}{2}, \frac{1}{2}, 2 \right\rangle \left\langle \frac{1}{2}, \frac{1}{2}, 1 \right| + \left| \frac{1}{2}, -\frac{1}{2}, 2 \right\rangle \left\langle \frac{1}{2}, -\frac{1}{2}, 1 \right|. \end{aligned}$$

The above construction of commutants provides some indication that there are benefit in using the BPT picture beyond the derivations and proofs of this chapter. In the following chapters we will use the BPT picture extensively. In Chapter 3 we will use it to describe the last step of the Scattering Algorithm that finds the irreps structures of arbitrarily generated operator algebras. In Chapters 5 and 4 we will define the reductions of states and Hamiltonians in terms of BPTs. In Chapter 6 we will take advantage of the visual representation in terms of BPTs to generalize state reductions beyond operator algebras. Thus, we will see that BPTs can be a useful tool for specifying, manipulating and producing tensor product structures, such as the structure of irreducible representations.

Chapter 3

Finding the irreps structure with the Scattering Algorithm

In Theorem 2.26 we have identified the general irreps structure of operator algebras; unfortunately, it was not a constructive result. We have learned that operator algebras can be specified via a set of generators (see Definition 2.8) but we do not know yet how to find the irreps structure of operator algebras specified this way. In this chapter we will take a constructive approach and address this problem.

Formally this problem can be stated as:

Given a finite set of self-adjoint operators $\mathcal{M} := \{M_1, M_2, \dots, M_n\}$ that generate the algebra $\langle \mathcal{M} \rangle$, find the basis that identify the irreps structure of $\langle \mathcal{M} \rangle$ as promised by Theorem 2.26.

It can be equivalently formulated (but not solved) in a simpler mathematical language:

Given a finite set of self-adjoint matrices $\mathcal{M} := \{M_1, M_2, \dots, M_n\}$, find the basis in which all $M_i \in \mathcal{M}$ are simultaneously block-diagonal with the smallest possible blocks.

When $\mathcal{M} = \{M\}$ is just one matrix, this means find the basis that diagonalize M . When \mathcal{M} is a set of matrices that commute, this means find the basis that simultaneously diagonalize all $M_i \in \mathcal{M}$. In general, for non-commuting matrices, the basis that identify the irreps structure of $\langle \mathcal{M} \rangle$ are the basis that simultaneously block-diagonalize all $M_i \in \mathcal{M}$ with the smallest possible blocks. Therefore, we can think of this problem as a problem of diagonalizing a set of matrices \mathcal{M} , where not all matrices necessarily commute.

Solving this problem is essential for the practical applications that require some form of reduction. More concretely, we would like to be able to answer questions such as:

- If $\mathcal{M} \subset \mathcal{L}(\mathcal{H})$ are terms in a Hamiltonian, how can we restrict the dynamics to lower dimensional subspaces where the Hamiltonian has a simpler form.
- If $\mathcal{M} \subset \mathcal{L}(\mathcal{H})$ is a subset of observables, how can we reduce the dimension of the Hilbert space while preserving all information about these observables?
- If $\mathcal{M} \subset \mathcal{L}(\mathcal{H})$ is a set of error operators of a noisy quantum channel, how can we encode information so it will not be affected by noise.

Just as we have a symbolic, not inherently numeric, algorithm for diagonalizing matrices using pen and paper, our goal is to introduce a symbolic algorithm for finding the irreps structure. The solution we propose is called the Scattering Algorithm. The idea of this algorithm was originally published in [54].

We are aware of two other approaches to this problem in the literature. First, a numerical algorithm was proposed by Murota *et al.* [72] in the context of semidefinite programming. A key step in their algorithm involves sampling for a random matrix in the algebra, which requires the ability to span the operator space of the algebra. Second, in a more physical context, Holbrook *et al.* [47] proposed an algorithm for computing the noise commutant of an error algebra associated with a noisy channel. Similarly to what we intend to achieve here, they propose a symbolic algorithm, however, this algorithm also requires the ability to span the operator space of the algebra. Unlike these approaches, the Scattering Algorithm does not require spanning the operator space of the algebra, which is not a trivial task given only the generators \mathcal{M} .

In the following, Section 3.1 is dedicated to describing and demonstrating how the Scattering Algorithm works without rigorous proofs. In Section 3.2 we will go over the details with more rigor and prove the correctness of the results.

3.1 How the Scattering Algorithm works

3.1.1 Overview

The main idea behind the Scattering Algorithm is to take the spectral projection of the generators and to break them down into minimal projections from which the irreps structure is built. The whole process proceeds in four steps:

1. Compile the initial set of projections from the spectral projections of the generators.
2. Apply the rank-reducing operation called scattering on all pairs of projections until no further reduction is possible.
3. Verify that all projections are minimal and the set is complete; fix it if necessary.
4. Construct minimal isometries and then the BPT basis that identify the irreps structure.

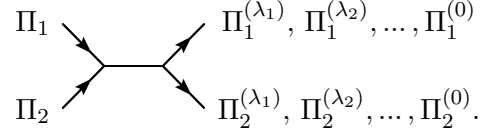
Phase 1

The first phase of the algorithm is just the spectral decomposition of all generators and the extraction of spectral projections on eigenspaces with distinct eigenvalues. After this, the original generators are left behind and their spectral projections move forward.

Phase 2

This phase is the heart of the algorithm where most of the calculations take place. In this phase we will apply the scattering operation defined as follows.

Definition 3.1. *Scattering* is an operation that takes a pair of projections and breaks each one into lower rank projections:



The lower rank projections are produced from the spectral decompositions of

$$\Pi_1 \Pi_2 \Pi_1 = \sum_{\lambda \neq 0} \lambda \Pi_1^{(\lambda)} \quad \text{and} \quad \Pi_2 \Pi_1 \Pi_2 = \sum_{\lambda \neq 0} \lambda \Pi_2^{(\lambda)},$$

with the addition of $\Pi_{i=1,2}^{(0)} := \Pi_i - \sum_{\lambda \neq 0} \Pi_i^{(\lambda)}$ called the *null projections*.

Note that we do not yet assume that the spectrum $\{\lambda\}$ is the same for both decompositions, however, we will later prove that it is. Also note that the null projections are not the projections on the kernel of $\Pi_i \Pi_j \Pi_i$ (the kernel projections are given by $I - \sum_{\lambda \neq 0} \Pi_i^{(\lambda)}$) and it is possible that $\Pi_i^{(0)} = 0$. We will treat the null projections just as $\lambda = 0$ elements of the set of spectral projections $\{\Pi_{i=1,2}^{(\lambda)}\}$. The projections produced by scattering are therefore the set $\{\Pi_{i=1,2}^{(\lambda)}\}$ of pairwise orthogonal projections that sum to their predecessor:

$$\Pi_i = \Pi_i^{(\lambda_1)} + \Pi_i^{(\lambda_2)} + \dots + \Pi_i^{(0)}.$$

Thus, in analogy with the scattering of particles, scattering of projections breaks them into smaller (lower rank) constituents of the original pair.

In Phase 2 of the algorithm we keep picking pairs of projections and applying the scattering operation (after each scattering only the resulting projections move forward) until all pairs have the following property.

Definition 3.2. A pair of projections Π_1, Π_2 is called *reflecting* if both projections remain unbroken under scattering, that is

$$\Pi_1 \Pi_2 \Pi_1 = \lambda \Pi_1 \tag{3.1}$$

$$\Pi_2 \Pi_1 \Pi_2 = \lambda \Pi_2. \tag{3.2}$$

The coefficient λ is then called a *reflection coefficient* and we will say that Π_1, Π_2 are *properly reflecting* if the reflection coefficient is not 0 (i.e. they are not orthogonal $\Pi_1 \Pi_2 \neq 0$).

We will later show that after one scattering, the resulting pairs $\{\Pi_1^{(\lambda)}, \Pi_2^{(\lambda')}\}$ are properly reflecting for all $\lambda = \lambda'$, and orthogonal for $\lambda \neq \lambda'$. By repetitively applying the scattering operation on non-reflecting pairs we are guaranteed to reach the state where all pairs are reflecting. That is because scattering reduces the ranks of projections (unless they are reflecting) and eventually we will either reach all reflecting pairs with ranks higher than 1 or we will reach projections of rank 1, which are always reflecting.

The final output of Phase 2 of the algorithm is a graph of reflection relations defined as follows.

Definition 3.3. A (proper) *reflection network* is a graph $G = \{V, E\}$ where the vertices set $V := \{\Pi_v\}$ consists of pairwise reflecting projections and every properly reflecting pair is connected with an edge (orthogonal pairs are unconnected)

$$E := \left\{ \{\Pi_v, \Pi_u\} \subset V \mid \begin{array}{l} \Pi_v \Pi_u \Pi_v = \lambda \Pi_v \\ \Pi_u \Pi_v \Pi_u = \lambda \Pi_u \end{array}, \lambda \neq 0 \right\}.$$

An *improper* reflection network is the generalization where not all projections are known to be reflecting so there are two kinds of edges: black edges for properly reflecting pairs and red edges for unknown relations.

Note that according to this definition only known orthogonal projections are not connected by any edge. In general, reflection networks may have multiple connected components formed by subsets of projections that are orthogonal to every projection outside the subset. It does not mean, however, that projections in the same connected component cannot be orthogonal; as long as there is a sequence of proper reflection (or unknown) relations connecting the projections, they will be in the same connected component.

With the above definition we can say that Phase 2 begins with an improper reflection network of projections produced in Phase 1. Then, as we keep applying the scattering operation, the reflection network evolves until it becomes a proper reflection network. The proper reflection network is what proceeds to the next phase.

Phase 3

In order to construct the irreps structure we have to establish that the reflection network has the following two properties:

1. (*minimality*) All projections in the reflection network are minimal projections.
2. (*completeness*) The reflection network has a maximal set of minimal projections

Phase 3 is where we establish that the reflection network produced in Phase 2 is indeed minimal and complete.

Although minimality is not guaranteed to hold for a proper reflection network, in practice, purely on empirical grounds, reflection networks produced in Phase 2 tend to always be minimal. Nevertheless, in the next section we will show how to check if this property holds and how to fix it if it does not.

Completeness is a rather trivial property that is guaranteed if any of the initial generators is supported on the whole Hilbert space. This can be arranged by adding the identity to the set of generators. When adding the identity is not feasible we will show in the next section how to complete the reflection network to have a maximal set.

Phase 4

In the last phase we take the proper reflection network that is minimal and complete and construct the BPT basis that specify the irreps structure. Each connected component in the reflection network will correspond to a block in the BPT. We construct the BPT basis by following the steps:

1. Select a maximal set of minimal projections $\{\Pi_k^q\}_{k=1,\dots}$ in the connected component q .
2. For each Π_k^q in the connected component q , take any path from Π_1^q to Π_k^q and construct the minimal isometry $S_{k1}^q \propto \Pi_k^q \cdots \Pi_1^q$ by taking the product of projections along the path (the proportionality coefficient is fixed after construction).
3. Use the minimal isometries S_{k1}^q to construct the BPT basis as described in the proof of Lemma 2.23.

3.1.2 Illustrative example

In order to see how the Scattering Algorithm works we consider the Hilbert space of three qubits $\mathcal{H} = \mathcal{H}_{qubit}^{\otimes 3}$ and study a peculiar Hamiltonian whose choice is mainly motivated by the fact that it presents a non-trivial problem in a relatively simple setting.

The Hamiltonian we consider consists of two terms $H(\epsilon) = H_{int} + \epsilon H_{z_1}$. Using the notation $|\pm\rangle = (|0\rangle \pm |1\rangle) / \sqrt{2}$, the term H_{int} is some interaction such that both $|++0\rangle$ and $|+11\rangle$ are the first (and only) excited states, and $|-00\rangle, |-01\rangle, |-10\rangle, |-11\rangle, |+01\rangle, |+ - 0\rangle$ are the ground states. The second term is $H_{z_1} = \sigma_z \otimes I_{23}$, where σ_z is a Pauli matrix acting on the first qubit so $|000\rangle, |001\rangle, |010\rangle, |011\rangle$ are the excited states. The excitation energy gap of H_{int} is normalized to 1, while ϵ is a free parameter that controls the gap of H_{z_1} . We would like to find out the spectrum and the eigenstates of $H(\epsilon)$ as a function of ϵ .

Since H_{int} and H_{z_1} do not commute, we cannot simultaneously diagonalize them. If ϵ is small we could use perturbation theory, but we do not want to assume that. What we can do instead is observe that for all ϵ , $H(\epsilon)$ is an element of the operator algebra generated by H_{int} and H_{z_1} . Thus, with respect to the Wedderburn Decomposition of this algebra, $H(\epsilon)$ may have a much simpler form. Another way to say it is this: although H_{int} and H_{z_1} cannot

be simultaneously diagonalized, they can be simultaneously block-diagonalized. Then, if the blocks are small and/or repetitive, the spectrum of $H(\epsilon)$ can be easier to analyze.

We will therefore find the irreps structure of the algebra $\langle H_{int}, H_{z_1} \rangle$ which amounts to finding its BPT basis.

Phase 1

Recall that the energy gap of H_{int} is 1 and we can shift the whole spectrum so that its ground energy is 0. Then, this Hamiltonian term is just a projection $H_{int} = \Pi_{int}$ on its excited states

$$\Pi_{int} := |++0\rangle\langle ++0| + |++1\rangle\langle ++1|.$$

The second Hamiltonian term consists of two spectral projections $H_{z_1} = \Pi_{z_1;0} - \Pi_{z_1;1}$ where

$$\Pi_{z_1;0} := |0\rangle\langle 0| \otimes I_{23} \quad \Pi_{z_1;1} := |1\rangle\langle 1| \otimes I_{23}.$$

Overall, we compile the three spectral projections $\{\Pi_{int}, \Pi_{z_1;0}, \Pi_{z_1;1}\}$.⁴

Phase 2

The initial (improper) reflection network is shown Fig. 3.1 where the red edges indicate unknown relations and the absent edge between $\Pi_{z_1;0}$ and $\Pi_{z_1;1}$ indicates our prior knowledge that they are orthogonal.

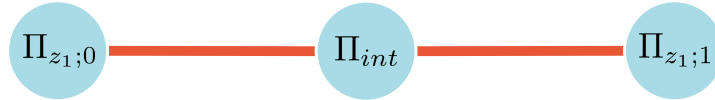


Figure 3.1: An example of the initial (improper) reflection network.

For the first scattering we pick any pair connected by a red edge, say $\{\Pi_{z_1;0}, \Pi_{int}\}$. For the scattering calculation it is convenient to first calculate the product

$$\Pi_{z_1;0}\Pi_{int} = \frac{1}{\sqrt{2}}|0+0\rangle\langle ++0| + \frac{1}{\sqrt{2}}|011\rangle\langle ++1|,$$

⁴We could shift the spectrum again and drop the second projection $\Pi_{z_1;1}$ but then none of the generators will be supported on the whole Hilbert space. This will result in an incomplete reflection network, which is easy to fix, but there is no reason to deliberately create this complication.

and then it is easy to get the scattering result for both projections

$$\begin{aligned}\Pi_{int}\Pi_{z_1;0}\Pi_{int} &= \frac{1}{2} |++0\rangle \langle ++0| + \frac{1}{2} |++11\rangle \langle ++11| = \frac{1}{2}\Pi_{int} \\ \Pi_{z_1;0}\Pi_{int}\Pi_{z_1;0} &= \frac{1}{2} |0+0\rangle \langle 0+0| + \frac{1}{2} |011\rangle \langle 011| =: \frac{1}{2}\Pi_{z_1;0}^{(1/2)}.\end{aligned}$$

After scattering, Π_{int} remains unbroken and $\Pi_{z_1;0}$ breaks into $\Pi_{z_1;0}^{(1/2)}$ and the null projection

$$\Pi_{z_1;0}^{(0)} := \Pi_{z_1;0} - \Pi_{z_1;0}^{(1/2)} = |0-0\rangle \langle 0-0| + |001\rangle \langle 001|.$$

At this point, one can explicitly verify that Π_{int} is reflecting with $\Pi_{z_1;0}^{(1/2)}$ and orthogonal to $\Pi_{z_1;0}^{(0)}$ (in fact, this verification is unnecessary since this is a general property of projections produced by scattering that we will prove in Theorem 3.4). We also know that $\Pi_{z_1;1}$ is orthogonal to both $\Pi_{z_1;0}^{(1/2)}$ and $\Pi_{z_1;0}^{(0)}$ since it was orthogonal to their predecessor. The updated reflection network is shown in Fig. 3.2.

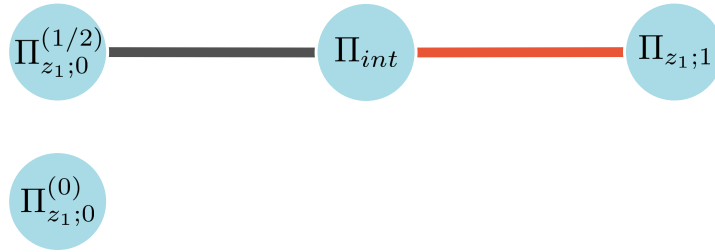


Figure 3.2: An example of the intermediate reflection network after one scattering.

The only remaining red edge is between the pair $\{\Pi_{z_1;1}, \Pi_{int}\}$ which after scattering similarly yields

$$\begin{aligned}\Pi_{int}\Pi_{z_1;1}\Pi_{int} &= \frac{1}{2} |++0\rangle \langle ++0| + \frac{1}{2} |++11\rangle \langle ++11| = \frac{1}{2}\Pi_{int} \\ \Pi_{z_1;1}\Pi_{int}\Pi_{z_1;1} &= \frac{1}{2} |1+0\rangle \langle 1+0| + \frac{1}{2} |111\rangle \langle 111| =: \frac{1}{2}\Pi_{z_1;1}^{(1/2)}.\end{aligned}$$

Again, Π_{int} remains unbroken and $\Pi_{z_1;1}$ breaks into $\Pi_{z_1;1}^{(1/2)}$ and the null projection

$$\Pi_{z_1;1}^{(0)} := \Pi_{z_1;1} - \Pi_{z_1;1}^{(1/2)} = |1-0\rangle \langle 1-0| + |101\rangle \langle 101|.$$

The final and proper reflection network is shown in Fig. 3.3.

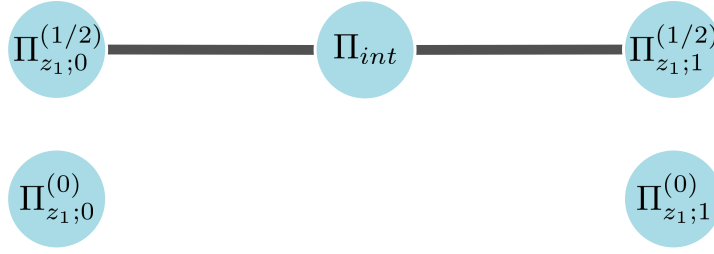


Figure 3.3: An example of the final (proper) reflection network after two scatterings.

Phase 3

Since we had not discussed yet how to check minimality and completeness of the reflection network, we will just assert that these properties hold.

Phase 4

In the final reflection network in Fig. 3.3 we identify three connected components that will correspond to three blocks in the BPT. The two connected components with a single projection have a single column given by the eigenspace of the projection. Since we are free to choose the basis for the first column in each block, we will stick with $|0 - 0\rangle$, $|001\rangle$ for $\Pi_{z_1;0}^{(0)}$, and with $|1 - 0\rangle$, $|101\rangle$ for $\Pi_{z_1;1}^{(0)}$.

For the last block we need to choose a maximal subset of minimal projections whose eigenspaces will correspond to the columns. In this case it can only be $\{\Pi_{z_1;0}^{(1/2)}, \Pi_{z_1;1}^{(1/2)}\}$ and we pick $\Pi_{z_1;0}^{(1/2)}$ to be the first column. Again, we naturally choose the first column basis to be the eigenstates $|0 + 0\rangle$, $|011\rangle$ of $\Pi_{z_1;0}^{(1/2)}$. For the second column in this block we cannot freely choose the basis. Instead, we get the second column basis by mapping the first column with the minimal isometry

$$S_{01}^{(1/2)} \propto \Pi_{z_1;1}^{(1/2)} \Pi_{int} \Pi_{z_1;0}^{(1/2)} = \frac{1}{2} |1 + 0\rangle \langle 0 + 0| + \frac{1}{2} |111\rangle \langle 011|$$

constructed by taking the product of projections along the connecting path in the reflection network (the factors $\frac{1}{2}$ are removed by normalization). Thus, the second column also consists of the familiar basis $|1 + 0\rangle$, $|111\rangle$ but we could not know that a priori.

The final result of the Scattering Algorithm is summarized by the BPT

0 - 0				
001				
	1 - 0			
	101			
		0 + 0	1 + 0	
		011	111	

Returning to our original question, the Wedderburn Decomposition given by the above BPT is

$$\mathcal{H}_{qubit}^{\otimes 3} \cong \mathcal{H}_{\nu_a} \oplus \mathcal{H}_{\nu_b} \oplus \mathcal{H}_{\nu_c} \otimes \mathcal{H}_{\mu_c}$$

where we have labeled the three blocks as a, b, c . Since $H(\epsilon) \in \langle H_{int}, H_{z_1} \rangle$, for all ϵ this Hamiltonian must have the block-diagonal form

$$H(\epsilon) = I_{\nu_a} \alpha(\epsilon) \oplus I_{\nu_b} \beta(\epsilon) \oplus I_{\nu_c} \otimes H_{\mu_c}(\epsilon) = \begin{pmatrix} \alpha(\epsilon) & & & & & & \\ & \alpha(\epsilon) & & & & & \\ & & \beta(\epsilon) & & & & \\ & & & \beta(\epsilon) & & & \\ & & & & H_{\mu_c}(\epsilon) & & \\ & & & & & H_{\mu_c}(\epsilon) & \\ & & & & & & H_{\mu_c}(\epsilon) \end{pmatrix}$$

where $\alpha(\epsilon), \beta(\epsilon)$ are ϵ -dependent scalars and $H_{\mu_c}(\epsilon)$ is an ϵ -dependent 2×2 matrix.

We can calculate these scalars and matrix elements using the original definition

$$H(\epsilon) = H_{int} + \epsilon H_{z_1} = |++0\rangle\langle ++0| + |++1\rangle\langle ++1| + \epsilon \sigma_z \otimes I_{23}.$$

Since all rows in the same block of the BPT are identical representations of $H(\epsilon)$, we only need to calculate the matrix elements for a single row in each BPT block:

$$\begin{aligned} \alpha(\epsilon) &= \langle 001 | H(\epsilon) | 001 \rangle = \epsilon & \beta(\epsilon) &= \langle 101 | H(\epsilon) | 101 \rangle = -\epsilon \\ H_{\mu_c}(\epsilon) &= \begin{pmatrix} \langle 011 | H(\epsilon) | 011 \rangle & \langle 011 | H(\epsilon) | 111 \rangle \\ \langle 111 | H(\epsilon) | 011 \rangle & \langle 111 | H(\epsilon) | 111 \rangle \end{pmatrix} = \begin{pmatrix} \frac{1}{2} + \epsilon & \frac{1}{2} \\ \frac{1}{2} & \frac{1}{2} - \epsilon \end{pmatrix}. \end{aligned}$$

Therefore, using the basis arranged in the BPT (reading the BPT top to bottom, left to right)

$$\{|0-0\rangle, |001\rangle, |1-0\rangle, |101\rangle, |0+0\rangle, |1+0\rangle, |011\rangle, |111\rangle\},$$

results in the block-diagonal matrix representation of this Hamiltonian

$$H(\epsilon) = \begin{pmatrix} \epsilon & & & & & & & \\ & \epsilon & & & & & & \\ & & -\epsilon & & & & & \\ & & & -\epsilon & & & & \\ & & & & \frac{1}{2} + \epsilon & \frac{1}{2} & & \\ & & & & \frac{1}{2} & \frac{1}{2} - \epsilon & & \\ & & & & & & \frac{1}{2} + \epsilon & \frac{1}{2} \\ & & & & & & \frac{1}{2} & \frac{1}{2} - \epsilon \end{pmatrix}.$$

The states $\{|0-0\rangle, |001\rangle\}$ and $\{|1-0\rangle, |101\rangle\}$ are clearly the eigenvectors with the eigenvalues $\epsilon, -\epsilon$ respectively. The 2×2 matrix block $H_{\mu_c}(\epsilon)$ can be decomposed into Pauli matrices

$$H_{\mu_c}(\epsilon) = \frac{1}{2}\sigma_x + \epsilon\sigma_z + \frac{1}{2}I$$

and we can disregard the identity as it only generates a phase factor. Then we can see that $H_{\mu_c}(\epsilon)$ is just the Hamiltonian of a single spin in transverse fields. The “up” and “down” states of this spin are $\{|0+0\rangle, |1+0\rangle\}$ for one matrix block and $\{|011\rangle, |111\rangle\}$ for the other. Thus, the whole task reduces to analyzing a single spin in transverse fields, which is a significant simplification of the original problem.

3.2 The Scattering Algorithm in detail

With the above overview and example we are in a good position to formally go over the details of the Scattering Algorithm and prove the correctness of the solution that it finds.

The input of this algorithm is a finite set of self-adjoint matrices $\mathcal{M} \subseteq \mathcal{L}(\mathcal{H})$ that generate the algebra $\mathcal{A} := \langle \mathcal{M} \rangle$. The output is a set of BPT basis $\{|e_{ik}^q\rangle\}$ where the indices q specify the distinct irreps, i specify the multiple instances of identical irreps, and k specify the distinct basis elements inside each irrep. The BPT basis specify the irreps structure (Wedderburn Decomposition) of \mathcal{A} as described in the proof of Theorem 2.26.

The main procedure of the algorithm is as follows:

Algorithm 3.1 The Scattering Algorithm

- 1: **procedure** FINDIRREPSTRUCTURE(\mathcal{M})
 - 2: $SpecProjections \leftarrow$ GETALLSPECTRALPROJECTIONS(\mathcal{M})
 - 3: $ReflectNet \leftarrow$ SCATTERPROJECTIONS($SpecProjections$)
 - 4: $ReflectNet \leftarrow$ ESTABLISHMINIMALITY($ReflectNet$)
 - 5: $ReflectNet \leftarrow$ ESTABLISHCOMPLETENESS($ReflectNet$)
 - 6: $BptBasis \leftarrow$ CONSTRUCTBPTBASIS($ReflectNet$)
 - 7: **return** $BptBasis$
 - 8: **end procedure**
-

We will now go over the details of each procedure (except the trivial first step of getting all the spectral projections from the generators) and prove the accompanying facts. In Section 3.2.5 we will prove the correctness of the whole algorithm.

3.2.1 Scattering of projections

Following the Definitions 3.1 and 3.2 of scattering and reflecting projections, we will now prove a few useful facts.

The most important fact about the scattering operation is that regardless of what the initial projections Π_1, Π_2 are, the resulting projections are always a series of reflecting pairs $\Pi_1^{(\lambda)}, \Pi_2^{(\lambda)}$ with reflection coefficients λ , and every pair is orthogonal to any other pair.

Theorem 3.4. *Let Π_1, Π_2 be a pair of projections before scattering and let $\{\Pi_1^{(\lambda)}\}, \{\Pi_2^{(\lambda)}\}$ be the resulting projections after scattering. Then:*

- (1) *The non-zero eigenvalues $\{\lambda\}$ are the same for both $\Pi_1\Pi_2\Pi_1$ and $\Pi_2\Pi_1\Pi_2$.*
- (2) *For all $\lambda \neq \lambda'$ the pairs of projections $\Pi_1^{(\lambda)}, \Pi_2^{(\lambda')}$ are orthogonal.*
- (3) *For all $\lambda = \lambda'$ the pairs of projections $\Pi_1^{(\lambda)}, \Pi_2^{(\lambda)}$ are reflecting with reflection coefficient λ .*

Proof. We will assume that $\{\lambda\}$ are the eigenvalues of $\Pi_1\Pi_2\Pi_1$ while the eigenvalues of $\Pi_2\Pi_1\Pi_2$ are unknown. Since all $\{\Pi_1^{(\lambda)}\}$ are pairwise orthogonal and sum to Π_1 , we have $\Pi_1^{(\lambda)}\Pi_1 = \Pi_1\Pi_1^{(\lambda)} = \Pi_1^{(\lambda)}$ for all λ . Then, if we multiply the definition of scattering $\Pi_1\Pi_2\Pi_1 = \sum_{\lambda'' \neq 0} \lambda'' \Pi_1^{(\lambda'')}$ from left and right with $\Pi_1^{(\lambda)}$ and $\Pi_1^{(\lambda')}$, we get the identity

$$\Pi_1^{(\lambda)}\Pi_2\Pi_1^{(\lambda')} = \delta_{\lambda\lambda'}\lambda\Pi_1^{(\lambda)}. \quad (3.3)$$

This equation holds for all λ including $\lambda = 0$ regardless of whether $\Pi_1^{(0)} = 0$ or not. In particular

$$\left(\Pi_1^{(0)}\Pi_2\right)\left(\Pi_1^{(0)}\Pi_2\right)^\dagger = \Pi_1^{(0)}\Pi_2\Pi_1^{(0)} = 0$$

so $\Pi_1^{(0)}\Pi_2 = \Pi_2\Pi_1^{(0)} = 0$. Therefore,

$$\begin{aligned} \Pi_2\Pi_1\Pi_2 &= \Pi_2\left(\Pi_1 - \Pi_1^{(0)}\right)\Pi_2 = \Pi_2\left(\sum_{\lambda \neq 0} \Pi_1^{(\lambda)}\right)\Pi_2 = \sum_{\lambda \neq 0} \lambda \left(\frac{1}{\lambda}\Pi_2\Pi_1^{(\lambda)}\Pi_2\right) \\ &= \sum_{\lambda \neq 0} \lambda \tilde{\Pi}_2^{(\lambda)}, \end{aligned} \quad (3.4)$$

where the last step suggests the definition $\tilde{\Pi}_2^{(\lambda)} := \frac{1}{\lambda}\Pi_2\Pi_1^{(\lambda)}\Pi_2$. The operators $\tilde{\Pi}_2^{(\lambda)}$ are clearly self-adjoint and, using Eq. (3.3), we have

$$\tilde{\Pi}_2^{(\lambda)}\tilde{\Pi}_2^{(\lambda')} = \frac{1}{\lambda\lambda'}\Pi_2\Pi_1^{(\lambda)}\Pi_2\Pi_1^{(\lambda')}\Pi_2 = \delta_{\lambda\lambda'}\frac{1}{\lambda}\Pi_2\Pi_1^{(\lambda)}\Pi_2 = \delta_{\lambda\lambda'}\tilde{\Pi}_2^{(\lambda)}.$$

Therefore, the operators $\{\tilde{\Pi}_2^{(\lambda)}\}$ form a set of pairwise orthogonal projections. In that case,

Eq. (3.4) is the spectral decomposition of $\Pi_2\Pi_1\Pi_2$. Since the spectral decomposition is unique we must have $\tilde{\Pi}_2^{(\lambda)} = \Pi_2^{(\lambda)}$ for all $\lambda \neq 0$ and so the non-zero eigenvalues are the same for both $\Pi_1\Pi_2\Pi_1$ and $\Pi_2\Pi_1\Pi_2$. This proves claim 1 and produces the identity

$$\Pi_2^{(\lambda)} = \frac{1}{\lambda} \Pi_2 \Pi_1^{(\lambda)} \Pi_2. \quad (3.5)$$

Using the identities (3.5) and (3.3), we get another identity

$$\Pi_1^{(\lambda)} \Pi_2^{(\lambda')} = \frac{1}{\lambda'} \Pi_1^{(\lambda)} \Pi_2 \Pi_1^{(\lambda')} \Pi_2 = \delta_{\lambda\lambda'} \Pi_1^{(\lambda)} \Pi_2,$$

which proves claim 2. In particular, for $\lambda = \lambda'$, we can multiply the last identity with its own adjoint from both sides

$$\begin{aligned} \Pi_1^{(\lambda)} \Pi_2^{(\lambda)} \Pi_1^{(\lambda)} &= \Pi_1^{(\lambda)} \Pi_2 \Pi_1^{(\lambda)} \\ \Pi_2^{(\lambda)} \Pi_1^{(\lambda)} \Pi_2^{(\lambda)} &= \Pi_2 \Pi_1^{(\lambda)} \Pi_2. \end{aligned}$$

Then, using the identity (3.3) in the first line, and the identity (3.5) in the second, we get

$$\begin{aligned} \Pi_1^{(\lambda)} \Pi_2^{(\lambda)} \Pi_1^{(\lambda)} &= \lambda \Pi_1^{(\lambda)} \\ \Pi_2^{(\lambda)} \Pi_1^{(\lambda)} \Pi_2^{(\lambda)} &= \lambda \Pi_2^{(\lambda)}, \end{aligned}$$

which proves claim 3. □

Note that Eq. (3.5) tells us how to calculate the projections $\{\Pi_2^{(\lambda \neq 0)}\}$ if we know $\{\Pi_1^{(\lambda \neq 0)}\}$. That is, we only need to calculate one spectral decomposition of $\Pi_1\Pi_2\Pi_1$, and then get the spectral decomposition of $\Pi_2\Pi_1\Pi_2$ for free. In practice, it is often easier to get the spectral projections of both $\Pi_1\Pi_2\Pi_1$ and $\Pi_2\Pi_1\Pi_2$ from the left and right singular vectors of $\Pi_1\Pi_2$.

Another useful fact that we will need is:

Proposition 3.5. *Let Π_1, Π_2 be a pair of properly reflecting projections with the reflection coefficient $\lambda \neq 0$, then, Π_1 and Π_2 have the same rank. If in addition $\lambda = 1$ then $\Pi_1 = \Pi_2$.*

Proof. If we take the trace on both sides of Eqs. (3.1), (3.2) we get

$$\text{tr}(\Pi_1\Pi_2) = \lambda \text{tr}(\Pi_1), \quad \text{tr}(\Pi_1\Pi_2) = \lambda \text{tr}(\Pi_2).$$

Since λ 's are the same (see Theorem 3.4) then $\text{tr}(\Pi_1) = \frac{\text{tr}(\Pi_1\Pi_2)}{\lambda} = \text{tr}(\Pi_2)$ and so they have the same rank. If $\lambda = 1$ then

$$\begin{aligned} (\Pi_1 - \Pi_1\Pi_2)(\Pi_1 - \Pi_1\Pi_2)^\dagger &= \Pi_1 - \Pi_1\Pi_2\Pi_1 = \Pi_1 - \lambda\Pi_1 = 0 \\ (\Pi_2 - \Pi_2\Pi_1)(\Pi_2 - \Pi_2\Pi_1)^\dagger &= \Pi_2 - \Pi_2\Pi_1\Pi_2 = \Pi_2 - \lambda\Pi_2 = 0. \end{aligned}$$

Therefore, $\Pi_1 - \Pi_1 \Pi_2 = 0$ and $(\Pi_2 - \Pi_2 \Pi_1)^\dagger = 0$ so $\Pi_1 = \Pi_1 \Pi_2 = \Pi_2$. \square

The first statement of the above proposition implies that all the projections that belong to the same connected component of a proper reflection network (see Definition 3.3) have the same rank. The second statement of the above proposition implies that whenever we scatter the pair Π_1, Π_2 and there is a $\lambda = 1$ in the spectrum, then $\Pi_1^{(\lambda=1)} = \Pi_2^{(\lambda=1)}$ (recall claim 3 in Theorem 3.4). This situation occurs when the eigenspaces of Π_1 and Π_2 have a common subspace so $\Pi_{i=1,2}^{(\lambda=1)}$ is the common projection on it. During the scattering procedure we can eliminate either $\Pi_1^{(\lambda=1)}$ or $\Pi_2^{(\lambda=1)}$ in order to avoid redundant operations in the future (it is not strictly necessary though).

We can now consider how a single scattering operation changes the reflection network (recall Definition 3.3 of the reflection network). According to Theorem 3.4, a pair of projections Π_1, Π_2 whose relation is initially unknown (red edge) scatters into a series of reflecting pairs (black edges except for $\lambda = 0$), and each pair is orthogonal (no edges) to all other pairs. Since both projections Π_1, Π_2 are part of a larger network, we have to specify how the resulting projections $\{\Pi_{i=1,2}^{(\lambda)}\}$ inherit the relations with the rest of the network; see Fig. 3.4.

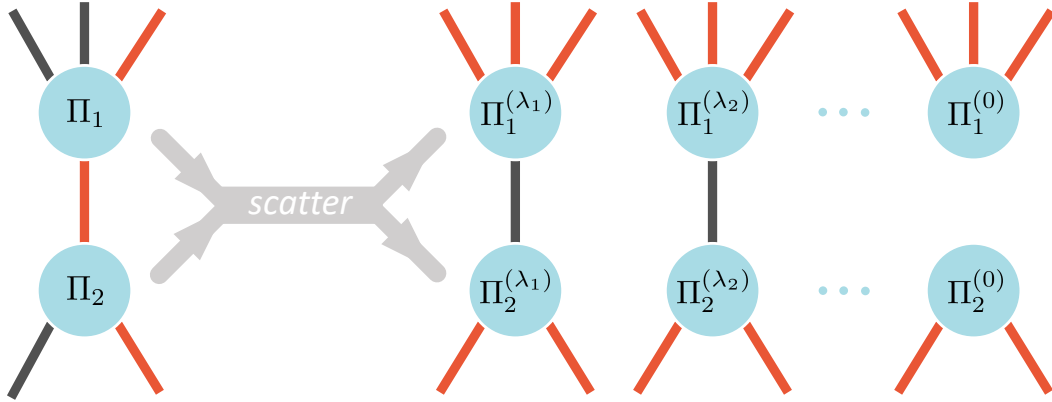


Figure 3.4: Generic update rules for the reflection relations after scattering. The red edges represent unknown reflection relations, black edges represent properly reflecting pairs, absent edges represent orthogonal pairs. Open ended edges stand for the reflection relations with the other projections in the network. In the generic case each $\Pi_{i=1,2}$ breaks into $\{\Pi_{i=1,2}^{(\lambda)}\}$ and the result is a series of properly reflecting pairs (for $\lambda = 0$ the pair is orthogonal) as described in Theorem 3.4. The open ended (external) edges are inherited from $\Pi_{i=1,2}$ by each of $\{\Pi_{i=1,2}^{(\lambda)}\}$ with the black edges being reset to red (assuming $\Pi_{i=1,2}$ did break under scattering).

First, note that orthogonality with other (external) projections is preserved under scattering so we do not need to add new edges that we did not already have. Second, the external red edges also do not need to be updated since every unknown relation that $\Pi_{i=1,2}$ had, remains unknown for $\{\Pi_{i=1,2}^{(\lambda)}\}$. The external black edges, however, do not survive

when a projection is broken into smaller rank projections. That is because properly reflecting pairs must have the same rank (see Proposition 3.5) so when one of the projections in the pair is broken, the resulting projections are necessarily of lower rank than the projection that was on the other side of that black edge. Therefore, the black edges that $\Pi_{i=1,2}$ had before scattering have to be reset to red when inherited by $\{\Pi_{i=1,2}^{(\lambda)}\}$, unless $\Pi_{i=1,2}$ did not break under scattering.

The special case where only one of the projections in the pair breaks under scattering is presented in Fig. 3.5. When both projections in the pair do not break (this is not shown in the figures), we only need to update the connecting red edge to black.

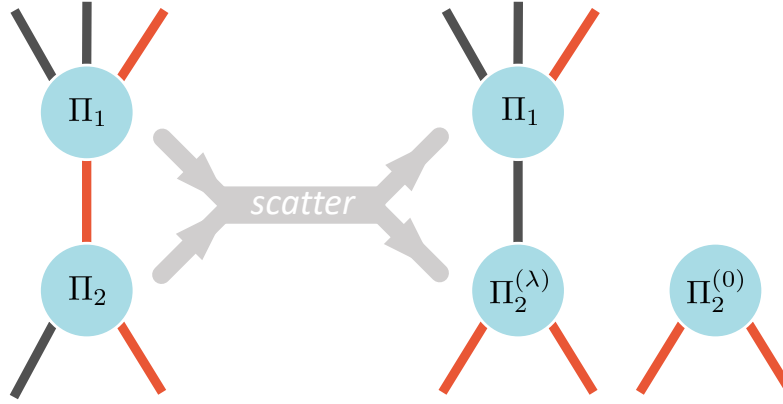


Figure 3.5: Update rules for the reflection relations in the case where only one of the projections breaks. In this case, Π_2 may break to at most two projections (if Π_2 also does not break then the red edge of $\{\Pi_1, \Pi_2\}$ is just set to black). The difference from the generic case is that the external black edges of the unbroken projection Π_1 are not reset to red.

The procedure SCATTERPROJECTIONS in the Scattering Algorithm 3.1 proceeds as follows:

1. Construct the improper reflection network from the initial spectral projections and initializing all edges to red except for the ones that are known to be reflecting (rank 1 and orthogonal projections).
2. Repeat until all edges are black: pick a pair of projections connected by a red edge, scatter it and update the relations in the network according to the rules given by Figs. 3.4 and 3.5.

As was discussed after Theorem 3.4, we don't have to keep the duplicates if the scattered projections share a common subspace. Also, we can argue heuristically that lower rank projection are less likely to break under scattering which triggers the resets of the previously established black edges. Thus, we may reduce the overall number of scatterings needed if we prioritize scattering the projections of lower ranks first.

The above procedure finishes when the reflection network is proper, that is, when all edges are black. The fact that it always successfully finishes in a finite number of steps is proven in the following lemma.

Lemma 3.6. *Given a finite number of input projections $\{\Pi_i\}$, the procedure SCATTERPROJECTIONS described above finishes in a finite number of steps and produces a proper reflection network.*

Proof. Let $\{\Pi_{i;t}\}$ be the set of projections in the reflection network at step $t = 0, 1, \dots$ of the procedure. At each t consider the total number of projections N_t , the total number of red edges R_t , and the total rank of all the projection $\gamma_t = \sum_i \text{rank} \Pi_{i;t}$. By the Definition 3.1, the scattering operation does not change the total rank of projections between input and output so for all t we have $\gamma_t = \gamma_0$. At each step, only two things can happen: Either both projections do not break so $N_{t+1} = N_t$ and the connecting red edge becomes black so $R_{t+1} = R_t - 1$; or at least one projection breaks so for some $n_t, r_t > 0$ we have $N_{t+1} = N_t + n_t$ and the value $R_{t+1} = R_t \pm r_t$ can increase or decrease (it will decrease only if the broken projections were not connected to any other projection in the network). Now, consider the progression of the coordinate (N_t, R_t) on a two-dimensional grid. At each step it can either move one position down or it can move diagonally but always to the right:

$$(N_t, R_t) \mapsto (N_{t+1}, R_{t+1}) = \begin{cases} (N_t, R_t - 1) \\ (N_t + n_t, R_t \pm r_t). \end{cases}$$

Furthermore, we have the upper bound $N_t \leq \gamma_t = \gamma_0$ because projections cannot have ranks lower than 1. We also know that N_0 and R_0 are finite because $\{\Pi_i\}$ is finite. Therefore, after a finite number of steps we will either reach $R_t = 0$ which means the reflection network is now proper, or we will reach $N_t = \gamma_0$, after which every step will decrease R_t by 1 until it reaches 0. \square

3.2.2 Establishing minimality of the reflection network

Establishing minimality of a reflection network means making sure that all the projections in the network are minimal projections in the algebra that they generate. Minimality can be established by considering the paths in the network.

A path in a reflection network is given by an ordered set of vertices $\pi = (v_1, v_2, \dots, v_n)$ that identifies a sequence of connected projections in the reflection network. By taking the product of all projections along the path and normalizing we define an isometry

$$S_\pi := \frac{1}{\lambda_\pi} \Pi_{v_1} \Pi_{v_2} \cdots \Pi_{v_n}, \quad (3.6)$$

where the normalization λ_π is the unique non-zero singular value of the product of projections. We will refer to these operators as *path-isometries* that map from the initial space

given by Π_{v_n} to the final space given by Π_{v_1} , along the path π . It should be clear that S_π^\dagger is a path-isometry along the same path as S_π but in reverse direction.

The minimality of reflection network can then be established using the following lemma.

Lemma 3.7. *Let $\{\Pi_v\}$ be a set of projections forming a proper reflection network such that all path-isometries in the network are proportional $S_\pi \propto S_{\pi'}$ wherever the paths π and π' have the same initial and final vertices. Then, all the projections $\{\Pi_v\}$ are minimal in the algebra that they generate $\mathcal{A} := \langle \{\Pi_v\} \rangle$.*

Proof. Every element $A \in \mathcal{A}$ is a linear combination of products of $\{\Pi_v\}$, therefore $\mathcal{A} = \text{span}\{S_\pi\}$ where $\{S_\pi\}$ are all the path isometries in the network. Then, all the projections $\{\Pi_v\}$ are minimal if $\Pi_{v_0} S_\pi \Pi_{v_0} \propto \Pi_{v_0}$ for all v_0 and π . When the path π does not start or end next to v_0 , we have $\Pi_{v_0} S_\pi = 0$ or $S_\pi \Pi_{v_0} = 0$ so the relation $\Pi_{v_0} S_\pi \Pi_{v_0} = 0 \propto \Pi_{v_0}$ trivially holds. Let us now consider $\pi := (v_1, v_2, \dots, v_n)$ such that $\Pi_{v_0} S_\pi \Pi_{v_0} \neq 0$. We can therefore append v_0 to the beginning and the end of π to get the circular path $\tilde{\pi} := (v_0, v_1, v_2, \dots, v_n, v_0)$. Another circular path from v_0 to itself is the trivial path (v_0, v_0) , and so

$$\Pi_{v_0} S_\pi \Pi_{v_0} \propto S_{\tilde{\pi}} \propto S_{(v_0, v_0)} \propto \Pi_{v_0} \Pi_{v_0} = \Pi_{v_0}.$$

Therefore, all $\{\Pi_{v_0}\}$ are minimal in $\mathcal{A} = \text{span}\{S_\pi\}$. \square

By checking whether the path-isometries in a reflection network depend only on the initial and final vertices independently from the paths, we can verify that all projections are minimal. Note that projections of rank 1 are minimal so connected components with rank 1 projections are always minimal.

In case minimality could not be established, Lemma 3.7 also implies a correction that can be implemented.

Lemma 3.8. *In the setting of Lemma 3.7, let π, π' be two paths that share the same initial v_{in} and final v_{fin} vertices, but $S_\pi \not\propto S_{\pi'}$. Then, the spectral projections of $U_{\pi\pi'} := S_\pi S_{\pi'}^\dagger$ are not reflecting with $\Pi_{v_{fin}}$.*

Proof. The operator $U_{\pi\pi'}$ is an isometry from the eigenspace of $\Pi_{v_{fin}}$ to itself, so it is a unitary on the eigenspace of $\Pi_{v_{fin}}$. We therefore have the spectral projections $\Pi^{(\omega)}$ with the non-zero eigenvalues ω such that $U_{\pi\pi'} = \sum_\omega \omega \Pi^{(\omega)}$ and $\sum_\omega \Pi^{(\omega)} = \Pi_{v_{fin}}$. If there was only one non-zero eigenvalue ω then $U_{\pi\pi'} = \omega \Pi^{(\omega)} = \omega \Pi_{v_{fin}}$ so $U_{\pi\pi'} = S_\pi S_{\pi'}^\dagger \propto \Pi_{v_{fin}} = S_{\pi'} S_\pi^\dagger$, but that implies $S_\pi \propto S_{\pi'}$. Therefore, there is more than one spectral projection $\{\Pi^{(\omega)}\}$ and so $\Pi_{v_{fin}} \Pi^{(\omega)} \Pi_{v_{fin}} = \Pi^{(\omega)} \not\propto \Pi_{v_{fin}}$. \square

The procedure ESTABLISHMINIMALITY in the Scattering Algorithm 3.1 proceeds as follows:

1. Check whether path-isometries in the reflection network depend only on the initial and final vertices and if they are, finish.

2. If not, given the paths π, π' that violate the premise of Lemma 3.7, take $U_{\pi\pi'} = S_\pi S_{\pi'}^\dagger$ and add its spectral projections $\{\Pi^{(\omega)}\}$ to the connected component where π and π' reside.
3. Initiate another round of scatterings on the connected component with the new projections until the reflection network is proper again, then repeat step 1.

In step 1 only connected components with projections of rank higher than 1 need to be checked. This procedure is guaranteed to stop because it either finishes on step 1 or it reduces the rank of projections in the connected component, and minimality trivially holds if it reaches projections of rank 1.

3.2.3 Establishing completeness of the reflection network

Completeness of a reflection network means that there is a subset of vertices in the network that forms a maximal set of minimal projections. If any of the initial generators of the algebra are supported on the whole Hilbert space, which means their spectral projections sum to the identity, then completeness is guaranteed and we don't have to do anything here. That is because after scattering, the descendants of these spectral projections in the proper reflection network will still sum to the identity, so they will form a maximal set of minimal projections.

If we can always add the identity to the initial set of generators, completeness becomes a trivial property. Nevertheless, it is also possible (and sometimes easier) to scatter the initial projections regardless of them being supported on the whole Hilbert space, and then fix the completeness of the final reflection network after the fact.

Given the projections $\{\Pi_v\}$ forming a reflection network we will assume that at this point minimality has been established. Consider the largest subset of pairwise orthogonal projections $\{\Pi_{v_k}\} \subseteq \{\Pi_v\}$ where $\Pi_{v_k} \Pi_{v_l} = \delta_{kl} \Pi_{v_k}$. From the perspective of graphs this is the maximal independent set of vertices in the network and it does not have to be unique. The subset $\{\Pi_{v_k}\}$ is a maximal set of minimal projections if the operator

$$I_{\mathcal{A}} := \sum_k \Pi_{v_k} \quad (3.7)$$

acts as the identity on every operator in the algebra $\mathcal{A} := \langle \{\Pi_v\} \rangle$, meaning $I_{\mathcal{A}} \Pi_v = \Pi_v$ for all v . If it is not, we can use the result of the following lemma to complete $I_{\mathcal{A}}$ to act as the identity.

Lemma 3.9. *Let Π_v be a minimal projection in a reflection network such that $I_{\mathcal{A}} \Pi_v \neq \Pi_v$ with $I_{\mathcal{A}}$ defined in Eq. (3.7). Then, with the appropriate normalization factor c , the operator*

$$\tilde{\Pi}_v := \frac{1}{c} (I - I_{\mathcal{A}}) \Pi_v (I - I_{\mathcal{A}}), \quad (3.8)$$

where I is the full identity matrix, has the following properties:

- (1) $\tilde{\Pi}_v$ is a minimal projection in $\mathcal{A} := \langle \{\Pi_v\} \rangle$.
- (2) $\tilde{\Pi}_v$ is orthogonal to all Π_{v_k} in Eq. (3.7).
- (3) The operator $\tilde{I}_{\mathcal{A}} := I_{\mathcal{A}} + \tilde{\Pi}_v$ is such that $\tilde{I}_{\mathcal{A}}\Pi_v = \Pi_v$.

Proof. If we distribute the terms in Eq. (3.8) we will get $c\tilde{\Pi}_v = \Pi_v - I_{\mathcal{A}}\Pi_v - \Pi_v I_{\mathcal{A}} + I_{\mathcal{A}}\Pi_v I_{\mathcal{A}}$ so clearly $\tilde{\Pi}_v$ is a self-adjoint operator in \mathcal{A} . Since Π_v is minimal we have

$$\Pi_v (I - I_{\mathcal{A}}) \Pi_v = \Pi_v - \Pi_v I_{\mathcal{A}} \Pi_v = (1 - \lambda) \Pi_v. \quad (3.9)$$

Here λ is the proportionality factor in the minimality relation $\Pi_v I_{\mathcal{A}} \Pi_v \propto \Pi_v$ and λ is not 1 because that would contradict $I_{\mathcal{A}}\Pi_v \neq \Pi_v$. Then, choosing $c = 1 - \lambda$ and taking the square of $\tilde{\Pi}_v$ we get

$$\begin{aligned} \tilde{\Pi}_v \tilde{\Pi}_v &= \frac{1}{c^2} (I - I_{\mathcal{A}}) \Pi_v (I - I_{\mathcal{A}}) \Pi_v (I - I_{\mathcal{A}}) \\ &= \frac{1}{(1 - \lambda)^2} (I - I_{\mathcal{A}}) (1 - \lambda) \Pi_v (I - I_{\mathcal{A}}) = \tilde{\Pi}_v. \end{aligned}$$

Therefore, $\tilde{\Pi}_v$ is a projection. It is minimal because for any $A \in \mathcal{A}$ we have

$$\tilde{\Pi}_v A \tilde{\Pi}_v = \frac{1}{c^2} (I - I_{\mathcal{A}}) \Pi_v \tilde{A} \Pi_v (I - I_{\mathcal{A}})$$

where $\tilde{A} := (I - I_{\mathcal{A}}) A (I - I_{\mathcal{A}})$. Since $\tilde{A} \in \mathcal{A}$ and Π_v is minimal we get $\Pi_v \tilde{A} \Pi_v \propto \Pi_v$ and so $\tilde{\Pi}_v A \tilde{\Pi}_v \propto \tilde{\Pi}_v$. This proves statement 1. Statement 2 follows from $(I - I_{\mathcal{A}}) \Pi_{v_k} = \Pi_{v_k} - \Pi_{v_k} = 0$ so $\tilde{\Pi}_v \Pi_{v_k} = 0$. Finally, recalling that $c = 1 - \lambda$ and using the identity (3.9) again, we get

$$\tilde{\Pi}_v \Pi_v = \frac{1}{c} (I - I_{\mathcal{A}}) \Pi_v (I - I_{\mathcal{A}}) \Pi_v = (I - I_{\mathcal{A}}) \Pi_v.$$

Thus, $\tilde{I}_{\mathcal{A}}\Pi_v = I_{\mathcal{A}}\Pi_v + (I - I_{\mathcal{A}}) \Pi_v = \Pi_v$, which proves statement 3. \square

The procedure ESTABLISHCOMPLETENESS in the Scattering Algorithm 3.1 proceeds as follows:

1. Choose the largest subset of pairwise orthogonal projections in the network $\{\Pi_{v_k}\}$ and if $I_{\mathcal{A}} = \sum_k \Pi_{v_k}$ acts as the identity on all other projections, finish.
2. If it does not, then for each projection such that $I_{\mathcal{A}}\Pi_v \neq \Pi_v$ construct the complementary projection $\tilde{\Pi}_v$ as defined in Eq. (3.8) and add it to the network.

Since by construction $\tilde{\Pi}_v$'s are minimal projections in the same algebra, they do not render the reflection network improper. Lemma 3.9 then ensures that after the completion of the network all the new $\tilde{\Pi}_v$'s will join the largest subset of pairwise orthogonal projections in the network and sum to $\tilde{I}_{\mathcal{A}}$ that acts as the identity on every element. It should be noted

again that this procedure is only needed if none of the original generators were supported on the whole Hilbert space.

3.2.4 Constructing the bipartition table

We already know from Lemma 2.23 how to construct BPTs from maximal sets of minimal isometries. What we need then is to construct a maximal set of minimal isometries from the reflection network. This is achieved with the help of the following lemma.

Lemma 3.10. *Let $\{\Pi_v\}$ be the projections of a reflection network for which minimality and completeness holds. Then, there is a set $\{S_{kl}^q\}$ of path-isometries in the network that is a maximal set of minimal isometries in the algebra $\mathcal{A} := \langle \{\Pi_v\} \rangle$.*

Proof. Let $\{\Pi_{v_k^q}\} \subseteq \{\Pi_v\}$ be a maximal set of minimal projections partitioned into connected components q . Let $\Pi_{v_1^q}$ be an arbitrarily chosen first element in this set for each connected component q . Then, for every $k \geq 1$ there is a path π between $\Pi_{v_1^q}$ and $\Pi_{v_k^q}$ identifying the path-isometries $S_{k1}^q \equiv S_\pi$ and $S_{1k}^q \equiv S_\pi^\dagger$ as in Eq. 3.6. For all $k, l \geq 1$ we can identify $S_{kl}^q := S_{k1}^q S_{1l}^q$ which are path-isometries from $\Pi_{v_l^q}$ to $\Pi_{v_k^q}$ via $\Pi_{v_1^q}$. Isometries defined this way have the properties $S_{kl}^q = S_{lk}^{q\dagger}$ and $S_{kl}^q S_{l'k'}^{q'} = \delta_{qq'} \delta_{ll'} S_{kk'}^q$ as required by the Definition 2.19 of maximal sets of minimal isometries. The final property that we need to show is that $\{S_{kl}^q\}$ spans \mathcal{A} . Since \mathcal{A} is spanned by products of $\{\Pi_v\}$ that are proportional to path-isometries $\{S_\pi\}$, it is sufficient to show that for any path π the path-isometry S_π is spanned by $\{S_{kl}^q\}$. Since completeness holds, the sum $\sum_{q,k} \Pi_{v_k^q} = I_{\mathcal{A}}$ acts as the identity of the algebra. Therefore,

$$S_\pi = I_{\mathcal{A}} S_\pi I_{\mathcal{A}} = \sum_{kl} \Pi_{v_k^q} S_\pi \Pi_{v_l^q}, \quad (3.10)$$

where q is the connected component that contains the path π . By definition of path-isometries, every non-vanishing term $\Pi_{v_k^q} S_\pi \Pi_{v_l^q}$ is proportional to the path-isometry $S_{(v_k^q, \pi, v_l^q)}$. Since minimality holds, according to Lemma 2.16 the path-isometries $S_{(v_k^q, \pi, v_l^q)} \propto S_{kl}^q$ are proportional because they have the same initial and final spaces. Therefore, for all k, l in Eq. (3.10), $\Pi_{v_k^q} S_\pi \Pi_{v_l^q} \propto S_{kl}^q$ so S_π is in the span of $\{S_{kl}^q\}$. \square

The procedure CONSTRUCTBPTBASIS in the Scattering Algorithm 3.1 proceeds as follows:

1. Identify a maximal set of orthogonal projections $\{\Pi_{v_k^q}\}$ in each connected component q and arbitrarily designate the first element $\Pi_{v_1^q}$.
2. In each connected component q construct the path-isometries $\{S_{k1}^q\}$ from $\Pi_{v_1^q}$ to every other element $\Pi_{v_k^q}$.
3. Use the path-isometries $\{S_{k1}^q\}$ to construct the BPT basis as described in the proof of Lemma 2.23.

Note that the reason that we can use Lemma 2.23 in step 3 is because S_{k1}^q are minimal isometries as established by Lemma 3.10.

3.2.5 Why the Scattering Algorithm works: putting it all together

Following the above results we are almost ready to prove that the output of the Scattering Algorithm is correct. What remains before we can put it all together is to show that the algebra generated by the final reflection network is the same algebra generated by the input \mathcal{M} .

Lemma 3.11. *Let $\{\Pi_v\}$ be the projections in the final reflection network (after minimality and completeness have been established) produced by the Scattering Algorithm 3.1. Then, the algebra generated by the projections $\langle\{\Pi_v\}\rangle$ and the algebra generated by the input $\langle\mathcal{M}\rangle$ is the same algebra.*

Proof. Let $\mathcal{A} := \langle\mathcal{M}\rangle$. All the spectral projections of the operators in \mathcal{M} span the operators in \mathcal{M} and are themselves in the algebra \mathcal{A} (with Eq. 2.4 we can show that this is true for every spectral projection of any $A \in \mathcal{A}$). Therefore, the algebra \mathcal{A} is generated by the output of GETALLSPECTRALPROJECTIONS. During the procedure SCATTERPROJECTIONS, we repeat the scattering operation where we replace a pair of projections Π_1, Π_2 with the spectral projections $\{\Pi_1^{(\lambda)}\}, \{\Pi_2^{(\lambda)}\}$ as specified in the Definition 3.1. Since $\{\Pi_{i=1,2}^{(\lambda)}\}$ are the spectral projections of $\Pi_i \Pi_j \Pi_i$, and $\Pi_i \Pi_j \Pi_i \in \mathcal{A}$, each $\Pi_{i=1,2}^{(\lambda)}$ (including the null projections) is an element of \mathcal{A} . Conversely, the sum of $\{\Pi_{i=1,2}^{(\lambda)}\}$ gives back $\Pi_{i=1,2}$, so replacing the pair Π_1, Π_2 with $\{\Pi_1^{(\lambda)}\}, \{\Pi_2^{(\lambda)}\}$ does not change the generating power of projections in the reflection network. Therefore, the set of projection in the output of SCATTERPROJECTIONS still generates the same algebra \mathcal{A} . During the procedure ESTABLISHMINIMALITY, we may add the spectral projections of $U_{\pi\pi'}$, but once again, since $U_{\pi\pi'} \in \mathcal{A}$ its spectral projections are elements of \mathcal{A} so the output of ESTABLISHMINIMALITY still generates the same algebra \mathcal{A} . During the procedure ESTABLISHCOMPLETENESS we may add more projections as provided by Lemma 3.9 but it guarantees that they are all in \mathcal{A} , so the output of ESTABLISHCOMPLETENESS still generates \mathcal{A} . \square

Theorem 3.12. *The BPT basis $\{|e_{ik}^q\rangle\}$ produced by the Scattering Algorithm 3.1 on the input \mathcal{M} , identify the irreps structure of the algebra $\langle\mathcal{M}\rangle$ as established by Theorem 2.26.*

Proof. The procedure GETALLSPECTRALPROJECTIONS outputs the projections that will form the initial improper reflection network. Lemma 3.6 ensures that the procedure SCATTERPROJECTIONS will take the initial improper reflection network and output a proper reflection network in a finite number of steps. Lemma 3.7 ensures that the procedure ESTABLISHMINIMALITY correctly identifies whether the reflection network consists of minimal projections. Lemma 3.8 ensures that ESTABLISHMINIMALITY correctly modifies the

reflection network to consist of minimal projections if it did not initially. Lemma 3.9 ensures that the procedure ESTABLISHCOMPLETENESS correctly modifies the reflection network to include a maximal set of minimal projections. At this point we have a minimal and complete reflection network that consists of projections $\{\Pi_v\}$. Since minimality and completeness hold, Lemma 3.10 ensures that the procedure CONSTRUCTBPTBASIS finds minimal isometries and, following Lemma 2.23, constructs the BPT basis $\{|e_{ik}^q\rangle\}$ for the algebra $\langle\{\Pi_v\}\rangle$. Lemma 3.11 then ensures that $\{|e_{ik}^q\rangle\}$ are also the BPT basis for the algebra $\langle\mathcal{M}\rangle$. Finally, the proof of Theorem 2.26 demonstrates how the BPT basis $\{|e_{ik}^q\rangle\}$ identify the irreps structure of the algebra $\langle\mathcal{M}\rangle$. \square

Chapter 4

Reduction of states

In this chapter we will consider reductions of states and their implications in the form of superselection and decoherence. By reduction of states we loosely mean the reduction of information contained in the quantum state as a result of some operational constraint. The best known reduction of states is the partial trace map. By shifting the focus from subsystems to operator algebras we will consider more general reductions of states.

The reduced states produced by the partial trace map were motivated by the need to describe the states of individual subsystems, even when they are entangled. Identifying such reduced states turned out to be more than a mathematical exercise because without it we could not define decoherence and understand its role in the emergence of classicality (see [105, 87] for a review of the decoherence program). The idea that other physically motivated (but more general) state reductions can lead to decoherence and emergence of classicality has been explored in [25, 26, 40, 81, 60, 4, 31, 24].

A shift in perspective on the notion of a subsystem and the accompanying state reduction is due to Zanardi *et al.* [102, 104, 59, 94], that have defined the concept of a *virtual* subsystem via operator algebras. This idea found many applications in the quantum error correction community with the development of decoherence free subsystems and operator quantum error correction (a.k.a. subsystem codes) [59, 57, 65, 64, 63, 62, 8, 14, 15]. These ideas have also percolated into the study of bulk reconstruction in AdS/CFT correspondence where the holographic-error-correcting-code approach was introduced [5, 78]. Beyond quantum error correction, the definition of subsystems via operator algebras (in particular group algebras) plays a central role in ideas such as generalized entanglement [9, 10], quantum reference frames [11, 51] and quantum state compression [13].

In the following, Section 4.1 is dedicated to re-examining the partial trace map and re-framing it as an instance of a state reduction map that arises from an operational constraint. We will derive an alternative representation of the partial trace map and show how it is visually captured by a bipartition table. This alternative representation will then be used to describe the process of decoherence without referring to the interacting subsystems (without the system-environment split).

In Section 4.2 we will consider state reductions due to more general operational constraints that go beyond inaccessible subsystems. We will see that in general, operational constraints lead to a combination of superselection and decoherence.

In order to clarify these ideas we will study a few examples. In the first example we will

consider the operational constraint of not having a shared reference frame and see how that leads to superselection. In the second example we will demonstrate how an operational constraint can lead to decoherence in a simple system such as the Hydrogen atom even when no interactions or couplings to an external environment are present. In the last example we will identify the possible encodings of quantum information into a decoherence free subsystem by considering the noise as an operational constraint. In this example we will demonstrate how the Scattering Algorithm allows us to expand the scope of treatable operational constraints beyond group representations.

4.1 State reductions and decoherence due to inaccessible subsystems

The partial trace map is the prototypical example of quantum state reduction. It is usually introduced by the following reasoning: We are given the bipartite Hilbert space $\mathcal{H}_{AB} := \mathcal{H}_A \otimes \mathcal{H}_B$ and the operational constraint that allows measurements only on subsystem B . Then, we consider the map tr_A that reduces the full states of AB to the states of B and preserves all information about B . In other words, the partial trace map tr_A is defined by the condition that for all $\rho \in \mathcal{L}(\mathcal{H}_{AB})$ and all $O_B \in \mathcal{L}(\mathcal{H}_B)$ it produces reduced states $\rho_B := \text{tr}_A[\rho]$ such that

$$\text{tr}[O_B \rho_B] = \text{tr}[I_A \otimes O_B \rho]. \quad (4.1)$$

If $\{|a_i\rangle\}$ are some basis in \mathcal{H}_A , the map tr_A can be expressed in the operator sum representation as

$$\text{tr}_A[\rho] := \sum_i K_i \rho K_i^\dagger, \quad (4.2)$$

where $K_i := \langle a_i| \otimes I_B$. Since $\sum_i K_i^\dagger K_i = I_{AB}$, it is completely positive and trace preserving (CPTP) so it maps quantum states to quantum states. Using the cyclical property of the trace (not partial) and linearity we can show that the condition in Eq. (4.1) holds for the map in Eq. (4.2):

$$\begin{aligned} \text{tr}[O_B \rho_B] &= \text{tr} \left[O_B \left(\sum_i \langle a_i| \otimes I_B \rho |a_i\rangle \otimes I_B \right) \right] \\ &= \text{tr} \left[\sum_i |a_i\rangle \langle a_i| \otimes O_B \rho \right] \\ &= \text{tr}[I_A \otimes O_B \rho]. \end{aligned}$$

We will now derive an alternative representation of the partial trace map in the framework of operator algebras. First, we note that the operational constraint dictates that only observables of the form $I_A \otimes O_B$ are physically relevant. Therefore, the operational

constraint identifies the operator algebra

$$\mathcal{A} := \{I_A \otimes O_B \mid O_B \in \mathcal{L}(\mathcal{H}_B)\} \quad (4.3)$$

that contains all the relevant observables. Since $\mathcal{A} = I_A \otimes \mathcal{L}(\mathcal{H}_B)$, it can be reduced to \mathcal{H}_B by mapping $I_A \otimes O_B \mapsto O_B$. The accompanying state reduction map $\rho_B := \text{tr}_A[\rho]$ must comply with the condition (4.1). By linearity, it is sufficient to satisfy this condition for the minimal isometries $S_{kl} := I_A \otimes |b_k\rangle\langle b_l|$ that span \mathcal{A} , so we require the condition

$$\text{tr}[|b_k\rangle\langle b_l| \rho_B] = \text{tr}[S_{kl} \rho].$$

With the above condition and the resolution of identity $I_B = \sum_l |b_l\rangle\langle b_l|$, we can express

$$\rho_B = \left(\sum_l |b_l\rangle\langle b_l| \right) \rho_B \left(\sum_k |b_k\rangle\langle b_k| \right) = \sum_{kl} \text{tr}[|b_k\rangle\langle b_l| \rho_B] |b_l\rangle\langle b_k| = \sum_{kl} \text{tr}[S_{kl} \rho] |b_l\rangle\langle b_k|.$$

Since $\rho_B = \text{tr}_A[\rho]$, we have derived above a new representation for the partial trace map

$$\text{tr}_A[\rho] := \sum_{kl} \text{tr}[S_{kl} \rho] |b_l\rangle\langle b_k|. \quad (4.4)$$

Such representations of maps between operators are known as “Input/Output” or “Tomographic” [71]. The easiest way to see that 4.4 is the same partial trace map as (4.2), is to verify that both representations yield

$$\text{tr}_A[|a_i\rangle\langle a_j| \otimes |b_l\rangle\langle b_k|] = \delta_{ij} |b_l\rangle\langle b_k|.$$

Then, by linearity both maps have to be identical since $\{|a_i\rangle\langle a_j| \otimes |b_l\rangle\langle b_k|\}$ span all the operators in $\mathcal{L}(\mathcal{H}_{AB})$.

As an illustration, consider the Hilbert space $\mathcal{H} := \mathbb{C} \otimes \frac{1}{2}$ of spin- l and spin- $\frac{1}{2}$. The algebra of observables on spin- $\frac{1}{2}$ is spanned by the minimal isometries $S_{mm'} := I_l \otimes |\frac{1}{2}, m\rangle\langle \frac{1}{2}, m'|$ for $m, m' = \pm \frac{1}{2}$. Then, for any pure state $|\psi\rangle \in \mathcal{H}$ we can express the partial trace over spin- l using (4.4) as

$$|\psi\rangle \mapsto \text{tr}_l[|\psi\rangle\langle \psi|] = \sum_{m, m' = \pm \frac{1}{2}} \langle \psi | S_{mm'} | \psi \rangle \left| \frac{1}{2}, m' \right\rangle \left\langle \frac{1}{2}, m \right| = \begin{pmatrix} \langle \psi | S_{\frac{1}{2}, \frac{1}{2}} | \psi \rangle & \langle \psi | S_{-\frac{1}{2}, \frac{1}{2}} | \psi \rangle \\ \langle \psi | S_{\frac{1}{2}, -\frac{1}{2}} | \psi \rangle & \langle \psi | S_{-\frac{1}{2}, -\frac{1}{2}} | \psi \rangle \end{pmatrix}. \quad (4.5)$$

Let us now consider how the partial trace map looks in the BPT picture. The algebra of relevant observables for the partial trace over A is $I_A \otimes \mathcal{L}(\mathcal{H}_B)$, so for some product basis $|e_{ik}\rangle := |a_i\rangle |b_k\rangle$, where $i = 1, \dots, d_A$ and $k = 1, \dots, d_B$, the irreps of this algebra are given by the BPT

$e_{1,1}$	$e_{1,2}$	\cdots	e_{1,d_B}
$e_{2,1}$	$e_{2,2}$	\cdots	e_{2,d_B}
\vdots	\vdots	\ddots	\vdots
$e_{d_A,1}$	$e_{d_A,2}$	\cdots	e_{d_A,d_B}
\downarrow	\downarrow		\downarrow
b_1	b_2	\cdots	b_{d_B}

We have added an additional single row on the bottom which represents the Hilbert space of reduced states.

This picture implies that states that are supported on a single column $|\varphi_k\rangle = \sum_i c_i |e_{ik}\rangle$ —we will call them *column kets*—reduce as

$$|\varphi_k\rangle \mapsto |b_k\rangle.$$

That is because column kets are the product states $|\varphi_k\rangle = |\varphi_{A;k}\rangle |b_k\rangle$ for some $|\varphi_{A;k}\rangle \in \mathcal{H}_A$.

A general pure state $|\psi\rangle \in \mathcal{H}$ that is supported on multiple columns can then be expressed as a sum of unnormalized column kets $|\psi\rangle = \sum_k |\varphi_k\rangle$. Then, using the representation (4.4) of the partial trace map, all pure states reduce as

$$|\psi\rangle \mapsto \rho_B = \sum_{kl} \langle \varphi_k | S_{kl} | \varphi_l \rangle |b_l\rangle \langle b_k|. \quad (4.6)$$

Observe that in the reduced state ρ_B , the probability weights of the diagonal terms $|b_k\rangle \langle b_k|$ are given by the overlaps $\langle \varphi_k | S_{kk} | \varphi_k \rangle = \langle \varphi_k | \varphi_k \rangle$ of the column kets with themselves (these are their square norms). In general, the weights and phases of the reduced coherence terms $|b_l\rangle \langle b_k|$ are given by the overlaps $\langle \varphi_k | S_{kl} | \varphi_l \rangle$ of the corresponding column kets. The overlap is calculated by mapping the kets to the same column with the isometries S_{kl} .

In the following section we will use this perspective in order to make sense of the process of decoherence in reduced states that arise from more general operational constraints. Before we do that, however, let us describe the process of decoherence using this perspective in a familiar setting where the reduced states are given by the partial trace over a subsystem.

Going back to the composite system of spin- l and spin- $\frac{1}{2}$, we adopt the shorter notation for the product basis $|m, \pm \frac{1}{2}\rangle := |l, m\rangle |\frac{1}{2}, \pm \frac{1}{2}\rangle$. The BPT picture of the partial trace over spin- l is then

$$\begin{array}{|c|c|} \hline +l, +\frac{1}{2} & +l, -\frac{1}{2} \\ \hline \vdots & \vdots \\ \hline 0, +\frac{1}{2} & 0, -\frac{1}{2} \\ \hline \vdots & \vdots \\ \hline -l, +\frac{1}{2} & -l, -\frac{1}{2} \\ \hline \end{array} \downarrow \downarrow \begin{array}{|c|c|} \hline +\frac{1}{2} & -\frac{1}{2} \\ \hline \end{array} .$$

This BPT specifies the minimal isometries and the partial trace map over spin- l as given in Eq. 4.5.

Now, consider the dynamics in the form of the interaction Hamiltonian

$$H_{int} = -\epsilon L_z \otimes \sigma_z,$$

with the operator $\sigma_z = \Pi^{(+)} - \Pi^{(-)}$, where $\Pi^{(\pm)} = |\pm\frac{1}{2}\rangle \langle \pm\frac{1}{2}|$. Let us separate H_{int} into two terms supported on the two columns of the above BPT

$$H_{int} = -\epsilon \left(L_z \otimes \Pi^{(+)} - L_z \otimes \Pi^{(-)} \right) = H_{int}^{(+)} \otimes \Pi^{(+)} + H_{int}^{(-)} \otimes \Pi^{(-)},$$

where $H_{int}^{(\pm)} := \mp \epsilon L_z$. Using the fact that $\Pi^{(+)}$ and $\Pi^{(-)}$ are orthogonal, the overall time evolution is given by

$$\begin{aligned} e^{-itH_{int}} &= \sum_{n=0}^{\infty} \frac{1}{n!} \left(-itH_{int}^{(+)} \otimes \Pi^{(+)} - itH_{int}^{(-)} \otimes \Pi^{(-)} \right)^n \\ &= \sum_{n=0}^{\infty} \frac{1}{n!} \left(-itH_{int}^{(+)} \right)^n \otimes \Pi^{(+)} + \sum_{n=0}^{\infty} \frac{1}{n!} \left(-itH_{int}^{(-)} \right)^n \otimes \Pi^{(-)} \\ &= e^{-itH_{int}^{(+)}} \otimes \Pi^{(+)} + e^{-itH_{int}^{(-)}} \otimes \Pi^{(-)}. \end{aligned}$$

We can now see that $H_{int}^{(+)}$ generates the time evolution inside the subspace of the left column of the BPT, and $H_{int}^{(-)}$ generates the evolution inside the right column. Since $H_{int}^{(+)}$ and $H_{int}^{(-)}$ differ in the overall sign (this traces back to the eigenvalues of σ_z), the column kets evolve in opposite directions inside the columns. From that we conclude that the Hamiltonian H_{int} will drive the column kets apart, which will reduce their overlap, and that kills off the coherence terms in the reduced states.

For concreteness, consider the initial product state

$$|\psi\rangle_{AB} := |\varphi\rangle \left(\alpha \left| +\frac{1}{2} \right\rangle + \beta \left| -\frac{1}{2} \right\rangle \right).$$

After some time t we will have

$$|\psi(t)\rangle_{AB} = |\varphi_+(t)\rangle \left| +\frac{1}{2} \right\rangle + |\varphi_-(t)\rangle \left| -\frac{1}{2} \right\rangle,$$

where

$$|\varphi_+(t)\rangle := \alpha e^{-itH_{int}^{(+)}} |\varphi\rangle, \quad |\varphi_-(t)\rangle := \beta e^{-itH_{int}^{(-)}} |\varphi\rangle.$$

The coefficient of the reduced coherence term $\left| +\frac{1}{2} \right\rangle \left\langle -\frac{1}{2} \right|$ of $\text{spin-}\frac{1}{2}$ is given by the overlap of the corresponding column kets

$$\langle \varphi_-(t) | \left\langle -\frac{1}{2} \right| S_{-\frac{1}{2}, \frac{1}{2}} |\varphi_+(t)\rangle \left| +\frac{1}{2} \right\rangle = \langle \varphi_-(t) | \varphi_+(t)\rangle = \beta^* \alpha \langle \varphi | e^{itH_{int}^{(-)}} e^{-itH_{int}^{(+)}} |\varphi\rangle.$$

Unless $|\varphi\rangle$ is an eigenstate of $H_{int}^{(\pm)}$, the overlap $\langle \varphi | e^{itH_{int}^{(-)}} e^{-itH_{int}^{(+)}} |\varphi\rangle$ will vanish with time (the rate depends on the coupling strength ϵ and the magnitude of $\text{spin-}l$).

In Fig. 4.1 we have plotted the purity $\text{tr}(\rho_B^2)$ of the reduced state of $\text{spin-}\frac{1}{2}$ coupled to $\text{spin-}100$ with the initial state

$$|\psi\rangle_{AB} := |m_x = 100\rangle \left(\frac{1}{\sqrt{2}} \left| +\frac{1}{2} \right\rangle + \frac{1}{\sqrt{2}} \left| -\frac{1}{2} \right\rangle \right).$$

Here $|m_x = 100\rangle$ is the maximally \hat{x} -polarized eigenstate of L_x .

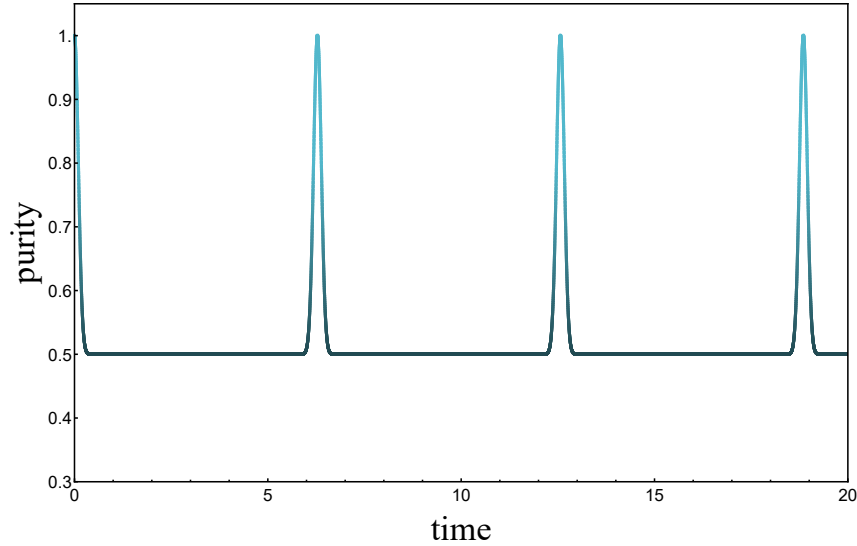


Figure 4.1: Time dependent purity of $\text{spin-}\frac{1}{2}$ coupled to $\text{spin-}100$.

As we can see, starting with the maximal purity of 1 the purity rapidly drops to its minimal value of 0.5 and stays there until it reaches periodic brief revivals back to 1. This can be understood from the behavior of the overlaps between two column kets as they evolve. Initially, both column kets correspond to the same state of $\text{spin-}100$ that is polarized

in the \hat{x} direction. As they evolve with the opposite Hamiltonians $H_{int}^{(\pm)} = \mp \frac{\epsilon}{2} L_z$, they rotate in opposite directions in the $\hat{x} - \hat{y}$ plane; see Fig. 4.2. Thus, the overlap between the two column kets rapidly vanishes, and after a while it briefly revives as they periodically meet in the $\hat{x} - \hat{y}$ plane.

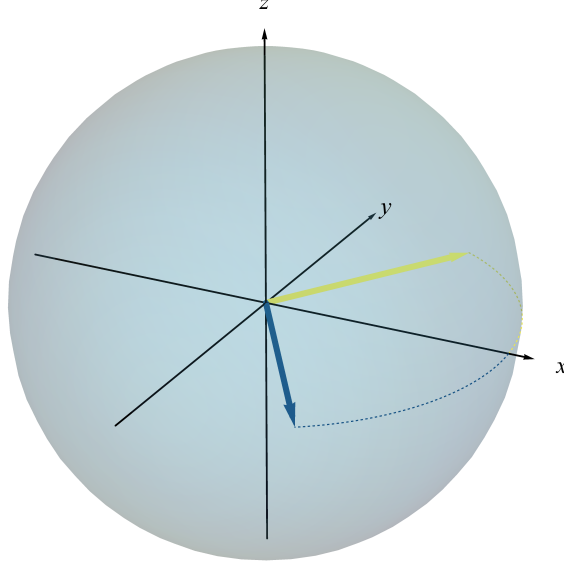


Figure 4.2: Column kets of maximally polarized spin states rotate in opposite directions in the $\hat{x} - \hat{y}$ plane. The periodic brief alignments of the kets is responsible for the periodic brief revivals of coherence.

As simplistic as the above example is, it demonstrates how the decoherence of reduced states can be described without referring to subsystems and instead focus on the BPT that specifies the state reduction. We can solidify this observation by considering how the interaction terms and the non-interaction terms of the Hamiltonian act on the BPT in the generic bipartite system $\mathcal{H}_A \otimes \mathcal{H}_B$.

The self-Hamiltonian of system A acts identically on all the columns of the BPT as

$$H_{self:A} := H_A \otimes I_B = \sum_k H_A \otimes |b_k\rangle \langle b_k|.$$

This means that $H_{self:A}$ drives all the column kets in sync, and that does not diminish their overlaps and does not cause decoherence. The self-Hamiltonian of system B does not generate dynamics inside the columns at all, instead it generates dynamics inside the row subspaces

$$H_{self:B} := I_A \otimes H_B = \sum_i |a_i\rangle \langle a_i| \otimes H_B.$$

This, of course, changes the reduced states but it does so unitarily.

What causes decoherence are the Hamiltonian terms that generate unsynchronized

evolutions inside the column subspaces which eliminates the overlaps between the column kets; see Fig. 4.3 for an illustration. This property is what characterizes the generic interaction term

$$H_{int} := \sum_k H_{A_k} \otimes |k\rangle \langle k|,$$

where the column Hamiltonians H_{A_k} vary with k .

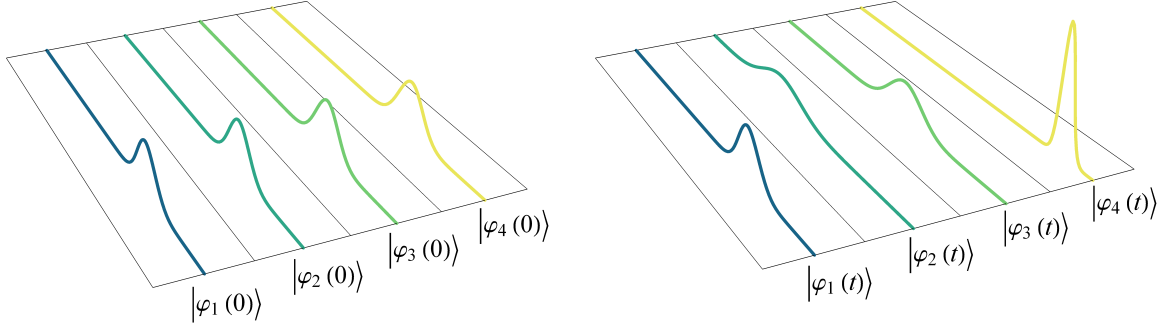


Figure 4.3: Generic picture of column kets on a bipartition table before (left) and after (right) unsynchronized evolution inside the columns caused by the interaction term. The diminishing overlaps between the different column kets translates into diminishing coherence terms in the reduced state.

4.2 State reductions and decoherence due to operational constraints

In the previous section we have derived the partial trace map by imposing the operational constraint such that only the observables from the algebra $I_A \otimes \mathcal{L}(\mathcal{H}_B)$ are accessible. This does not imply that all the observables $I_A \otimes O_B$ have to be accessible, but it does exclude what definitely cannot be accessed (information about A in this case). The resulting state reduction map accounts for the operational constraint of not having access to one of the subsystems.

It is then natural to consider the operational constraints that go beyond the restriction to physical subsystems. These constraints can be the result of having only access to collective observables of a composite system, or having a noisy quantum channel that renders some observables irrelevant by randomizing their outcomes. In such scenarios, what specifies the operational constraint is not the physical subsystem decomposition, such as the system-environment split, but an algebra $\mathcal{A} \subset \mathcal{L}(\mathcal{H})$ of relevant observables. This algebra, of course, may be an overstatement of the practical reality and not all $O \in \mathcal{A}$ are necessarily accessible, but it is still a useful notion that excludes what is definitely out of reach.

For example, consider again the Hilbert space $\mathcal{H} := \underline{l} \otimes \underline{\frac{1}{2}}$ of spin- l and spin- $\frac{1}{2}$ and let us assume that in principle we can measure whatever we want. However, there is some uncontrollable effect that applies an unknown random rotation $U_l(R) \otimes I$ on the spin- l subsystem, while leaving spin- $\frac{1}{2}$ unaffected. Since we do not know what rotation has been applied, this effect renders the orientation of spin- l completely random. Under such circumstances the only observables that remain relevant are the ones that are unaffected by the unknown rotations. Therefore, this uncontrollable effect imposes an operational constraint that restricts the algebra of relevant observables to the ones that commute with all the rotations of spin- l :

$$\mathcal{A} = \{O \in \mathcal{L}(\mathcal{H}) \mid [O, U_l(R) \otimes I] = 0 \quad \forall R\}. \quad (4.7)$$

Once the algebra of relevant observables is identified, we would like to define the state reduction map that accounts for the limitations imposed by the operational constraints. Such reduced state will then be the effective state of the system that we have access to in light of the operational constraints.

Following the operator-algebraic derivation of the partial trace map in the previous section, we can adopt the same approach to produce state reduction maps for any operator algebra (provided we can find its irreps structure). The derivation of the general state reduction map is outlined as follows:

1. Identify the operator algebra $\mathcal{A} \subseteq \mathcal{L}(\mathcal{H})$ of relevant observables.
2. Find its irreps structure $\mathcal{H} \cong \bigoplus_q \mathcal{H}_{\nu_q} \otimes \mathcal{H}_{\mu_q}$ and identify the minimal isometries $\{S_{kl}^q\}$.
3. The Hilbert space of reduced states is given by

$$\mathcal{H}_{\{\mu_q\}} := \bigoplus_q \mathcal{H}_{\mu_q}, \quad (4.8)$$

and the state reduction map is

$$\text{tr}_{\{\nu_q\}}[\rho] := \bigoplus_q \sum_{kl} \text{tr}[S_{kl}^q \rho] |m_l^q\rangle \langle m_k^q|. \quad (4.9)$$

The physical meaning of state reduction maps depends on the physical context. For the usual partial trace map, the reduced state is the effective state of a physical subsystem. In the more general case we can think of reduced states as the states of some virtual subsystems which embody the degrees of freedom associated with the algebra of relevant observables. Ultimately, it is the algebra of the relevant observables that gives meaning to the reduced state.

Returning to our example of spin- l and spin- $\frac{1}{2}$, the irreps of rotations $U_l(R) \otimes I$ are specified by the BPT

$+l, +\frac{1}{2}$	\cdots	$0, +\frac{1}{2}$	\cdots	$-l, +\frac{1}{2}$
$+l, -\frac{1}{2}$	\cdots	$0, -\frac{1}{2}$	\cdots	$-l, -\frac{1}{2}$

Since the algebra of relevant observables (4.7) is the commutant of these rotations, the irreps we are interested in are given by the transposition of this BPT

$+l, +\frac{1}{2}$	$+l, -\frac{1}{2}$
\vdots	\vdots
$0, +\frac{1}{2}$	$0, -\frac{1}{2}$
\vdots	\vdots
$-l, +\frac{1}{2}$	$-l, -\frac{1}{2}$
\downarrow	\downarrow
$+\frac{1}{2}$	$-\frac{1}{2}$

As we have seen in the previous section, this BPT defines the partial trace over spin- l . Not surprisingly, the appropriate state reduction map that accounts for having the spin- l subsystem randomly rotated, is the erasure of all information about the state of spin- l .

In the more general cases of state reductions, the reduced Hilbert space (4.8) is a direct sum of orthogonal sectors $\{\mathcal{H}_{\mu_q}\}$ identified by the distinct inequivalent irreps of the algebra. These sectors are commonly referred to as *superselection sectors*. In the case of the partial trace map we have only one distinct irrep so the reduced Hilbert space has only one superselection sector. When multiple superselection sectors are present (that is when the BPT has multiple blocks), the state reduction map eliminates all coherence terms between the basis elements belonging to distinct superselection sectors, regardless of the state.

We will see how the superselection sectors arise from operational constraints in the more elaborate examples below. There is one extremal case, however, that we can briefly point out here.

Consider the operational constraint that allows only one observable $O \in \mathcal{L}(\mathcal{H})$ to be measured. In this case, the algebra of relevant observables is just $\langle O \rangle$. The minimal isometries of this algebra are the spectral projections $\{\Pi^{(\lambda)}\}$ of O , where the eigenvalues $\lambda \neq 0$ identify the distinct one-dimensional irreps. Because the irreps are one-dimensional, the reduced Hilbert space (4.8) in this case is just $\bigoplus_{\lambda} |\lambda\rangle$. The state reduction map (4.9) is then

$$\rho \longmapsto \bigoplus_{\lambda} \text{tr} [\Pi^{(\lambda)} \rho] |\lambda\rangle \langle \lambda|.$$

The resulting reduced state is completely diagonal and it represents the probability distribution over the observable's outcomes $\{\lambda\}$.

Not surprisingly, when we constrain the measurements to a single observable, the state reduction map becomes the mapping of the quantum state ρ to the classical probability distribution $p(\lambda) := \text{tr} [\Pi^{(\lambda)} \rho]$ over the outcomes of that observable. As we can see, the

extremal constraint of having only one observable leads to the complete elimination of coherence terms. Therefore, when more observables are available, we expect an intermediate outcome where the coherence terms between some subspaces are eliminated while the coherence terms inside these subspaces are preserved.

Such elimination of coherence terms by the state reduction map is what we call superselection, and it is distinct from the dynamical elimination of coherence terms in the process of decoherence.⁵

In order to clarify these ideas we will now study three more elaborate examples.

Example 1

In this example we will study a simple case where the superselection sectors appear due to the lack of a shared reference frame. See [11] for a review of this topic.

When the agent that prepares the states (Alice) and the agent that measures them (Bob) do not share a common reference frame, it imposes an operational constraint on the latter. Let us consider such situation with the same system $\mathcal{H} := \underline{l} \otimes \underline{\frac{1}{2}}$ of spin- l and spin- $\frac{1}{2}$.

We will assume that Alice and Bob share a common reference frame for the \hat{z} axis but they are misaligned in the $\hat{x} - \hat{y}$ plane by an unknown angle θ . If Alice can send multiple states to Bob then he could implement some protocol for aligning his reference frame with Alice by inferring the angle θ from the collection of states. If, however, Bob receives only one state then from his perspective it is rotated by an unknown angle around \hat{z} . The only relevant observables that remain for Bob are the ones that commute with $U_{\hat{z}}(\theta)$ for all θ . Our goal is to find the state reduction map that accounts for the lack of common reference frame in the $\hat{x} - \hat{y}$ plane.

The abelian group $\{U_{\hat{z}}(\theta)\}$ is generated by the single J_z component of the total angular momentum operator. The irreps of this group are all one-dimensional and are given by the eigenvectors $|j, m\rangle$ of J_z , with distinct eigenvalues m identifying distinct irreps. For brevity, let us specialize to $l = 1$ so $j = 1 \pm \frac{1}{2}$.

The one-dimensional irreps of $\{U_{\hat{z}}(\theta)\}$ are summarized by the BPT

$$\begin{array}{c} \boxed{\frac{3}{2}, \frac{3}{2}} \\ \boxed{\frac{3}{2}, \frac{1}{2}} \\ \boxed{\frac{1}{2}, \frac{1}{2}} \\ \boxed{\frac{3}{2}, -\frac{1}{2}} \\ \boxed{\frac{1}{2}, -\frac{1}{2}} \\ \boxed{\frac{3}{2}, -\frac{3}{2}} \end{array} .$$

Note that the abelian group $\{U_{\hat{z}}(\theta)\}$ acts on the states in each BPT block with a different phase factor; this is why the eigenvalues of J_z distinguish the irreps.

⁵The dynamical elimination of coherence terms is sometimes referred to as *einselection*, which stands for environment-induced-superselection [105].

The commutant algebra, and the implied state reduction map, are given by the transposition of the BPT (note that we re-use the same labels for the reduced basis on the bottom)

$$\begin{array}{cccccc}
 \boxed{\frac{3}{2}, \frac{3}{2}} & & & & & \\
 & \boxed{\frac{3}{2}, \frac{1}{2}} & \boxed{\frac{1}{2}, \frac{1}{2}} & & & \\
 & & & \boxed{\frac{3}{2}, -\frac{1}{2}} & \boxed{\frac{1}{2}, -\frac{1}{2}} & \\
 & & & & & \boxed{\frac{3}{2}, -\frac{3}{2}} \\
 \downarrow & \downarrow & \downarrow & \downarrow & \downarrow & \downarrow \\
 \boxed{\frac{3}{2}, \frac{3}{2}} & \boxed{\frac{3}{2}, \frac{1}{2}} & \boxed{\frac{1}{2}, \frac{1}{2}} & \boxed{\frac{3}{2}, -\frac{1}{2}} & \boxed{\frac{1}{2}, -\frac{1}{2}} & \boxed{\frac{3}{2}, -\frac{3}{2}}
 \end{array}$$

Instead of explicitly specifying all the minimal isometries needed for the definition of the state reduction map as given in Eq. (4.9), we can read the implied state reduction map directly from the BPT. It tells us that all the basis elements reduce to themselves but only the coherence terms between elements in the same row remain in tact; all other coherence terms are eliminated.

One can verify explicitly using the definition in Eq. (4.9) that the implied state reduction map reduces the pure states $|\psi\rangle = \sum_{j,m} c_{j,m} |j, m\rangle$ to

$$|\psi\rangle \mapsto \rho_{Bob} = \begin{pmatrix} \left|c_{\frac{3}{2}, \frac{3}{2}}\right|^2 & & & & & \\ & \left|c_{\frac{3}{2}, \frac{1}{2}}\right|^2 & c_{\frac{3}{2}, \frac{1}{2}} c_{\frac{1}{2}, \frac{1}{2}}^* & & & \\ & c_{\frac{1}{2}, \frac{1}{2}} c_{\frac{3}{2}, \frac{1}{2}}^* & \left|c_{\frac{1}{2}, \frac{1}{2}}\right|^2 & & & \\ & & & \left|c_{\frac{3}{2}, -\frac{1}{2}}\right|^2 & c_{\frac{3}{2}, -\frac{1}{2}} c_{\frac{1}{2}, -\frac{1}{2}}^* & \\ & & & c_{\frac{1}{2}, -\frac{1}{2}} c_{\frac{3}{2}, -\frac{1}{2}}^* & \left|c_{\frac{1}{2}, -\frac{1}{2}}\right|^2 & \\ & & & & & \left|c_{\frac{3}{2}, -\frac{3}{2}}\right|^2 \end{pmatrix}.$$

The coherence terms that got eliminated are exactly where the unknown phase factors due to the unknown rotation $U_{\hat{z}}(\theta)$ were present. Since Bob has no access to this phase factor, whether Alice sends him $|\psi_1\rangle$ or $|\psi_2\rangle = U_{\hat{z}}(\theta') |\psi_1\rangle$ (for any θ'), there is nothing he can do that will differentiate the two cases. The resulting state reduction map accounts for that by eliminating the coherence terms whose values remain unknown within Bob's operational constraint.

In this example we saw a state reduction map that enforces superselection between states with different eigenvalues of J_z due to the lack of common reference frame. In the next example we will see a state reduction map that combines superselection with a partial-trace-like map.

Example 2

In this example we will consider the dynamics of a reduced state. The main takeaway here is that decoherence does not have to be only the consequence of interactions with inaccessible subsystems, it can also arise from other combinations of dynamics and operational constraints.

Let us consider the composite system $\mathcal{H} := \underline{l} \otimes \underline{\frac{1}{2}} \otimes \underline{\frac{1}{2}}$ of two spin- $\frac{1}{2}$'s and an integer angular momentum l , such as the Hydrogen atom. Assume that we have a large ensemble of N Hydrogen atoms and we have come up with a procedure that allows us to prepare all of them in the same arbitrary state $|\psi\rangle \in \mathcal{H}$. Unfortunately, we cannot control the individual orientations of the atoms so instead of having the collective state $|\psi\rangle^{\otimes N}$, each atom ends up in the state $U(R)|\psi\rangle$, where $U(R)$ is a random rotation that is independently chosen for each atom. If we sample a single atom from this ensemble, what is the effective state of this atom?

The operational constraint that the limitation of state preparations imposes, is the restriction to rotationally invariant measurements. The algebra of relevant observables is therefore the commutant of the $SU(2)$ group. We can find the irreps structure of this algebra from the representation theory of $SU(2)$.

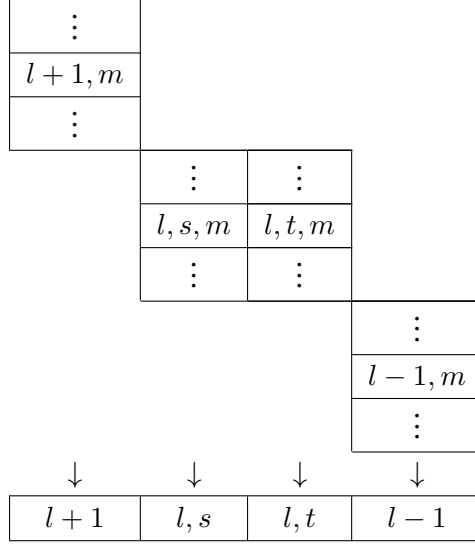
We know that our Hilbert space decomposes into

$$\underline{l} \otimes \underline{\frac{1}{2}} \otimes \underline{\frac{1}{2}} = \underline{l} \otimes (\underline{1} \oplus \underline{0}) = \underline{l+1} \oplus \underline{l} \oplus \underline{l-1} \oplus \underline{l}.$$

That is, under $SU(2)$ rotations we have one irrep that transforms as $j = l + 1$, one that transforms as $j = l - 1$, and two irreps that transform as $j = l$. Note that the two $j = l$ irreps can be distinguished by whether the spins are in the singlet or triplet states. We thus have the $j = l \pm 1$ total angular momentum basis $|l \pm 1, m\rangle$, and the singlet / triplet variants $\alpha = s, t$ of the $j = l$ total angular momentum basis $|l, \alpha, m\rangle$. The irreps of $SU(2)$ can then be specified by the BPT (in each row $m = j, \dots, -j$).

...	$l + 1, m$...							
			...	l, s, m	...				
			...	l, t, m	...				
						...	$l - 1, m$...	

The irreps structure of the commutant algebra is given by its transposition



The reduced Hilbert space consists of the basis $|l+1\rangle, |l, s\rangle, |l, t\rangle, |l-1\rangle$.

The pure state $|\psi\rangle$ can now be expanded in the column kets of the above BPT

$$|\psi\rangle = |\varphi_{l+1}\rangle + |\varphi_{l,s}\rangle + |\varphi_{l,t}\rangle + |\varphi_{l-1}\rangle.$$

Since different BPT blocks specify distinct irreps, no coherences between column kets supported on different blocks are preserved; this is superselection. In the central block, however, where we have two columns, the reduced coherence terms are given by the overlaps $\langle\varphi_{l,t}|S_{ts}|\varphi_{l,s}\rangle$ (where $S_{ts} := \sum_{m=-l}^l |l, t, m\rangle\langle l, s, m|$) between the column kets; this is the partial-trace-like reduction. Overall, the state reduction map is summarized as

$$|\psi\rangle \mapsto \rho = \begin{pmatrix} \langle\varphi_{l+1}|\varphi_{l+1}\rangle & & & \\ & \langle\varphi_{l,s}|\varphi_{l,s}\rangle & \langle\varphi_{l,t}|S_{ts}|\varphi_{l,s}\rangle & \\ & \langle\varphi_{l,s}|S_{st}|\varphi_{l,t}\rangle & \langle\varphi_{l,t}|\varphi_{l,t}\rangle & \\ & & & \langle\varphi_{l-1}|\varphi_{l-1}\rangle \end{pmatrix}.$$

Therefore, the only information we are left with is the one qubit encoded between the triplet and singlet variants of the $j = l$ irrep, and the overall probability distribution over the total angular momentum $j = l+1, l, l-1$. The consequence of such operational constraint is even more pronounced if we consider unitary dynamics acting on this system.

Even the simple Hamiltonian of uniform magnetic field along the \hat{y} axis (without spin-spin or spin-orbit interactions)

$$H = \epsilon L_y + S_{1;y} + S_{2;y}$$

can induce decoherence in such reduced states. Here $L_y, S_{1;y}, S_{2;y}$ are the \hat{y} components of the individual angular momentum operators, and ϵ is the coupling strength of the orbital angular momentum to the external field (for the two spins it is normalized to 1). We will

now see that the non-uniformity of the coupling strengths is responsible for the decoherence.

Let us separate the Hamiltonian into the uniform and the difference parts:

$$H = \epsilon (L_y + S_{1;y} + S_{2;y}) + (1 - \epsilon) (S_{1;y} + S_{2;y}).$$

Now, consider how these two terms act on the above column kets. The first term is the component $J_y = L_y + S_{1;y} + S_{2;y}$ of the total angular momentum operator so it generates global rotations around the \hat{y} axis according to the representations $j = l + 1, l, l - 1$. Therefore, the term J_y generates identical time evolutions inside the two columns of total angular momentum $j = l$, and it does not map between the columns.

The second Hamiltonian term is the \hat{y} component of the total spin operator $S_y = S_{1;y} + S_{2;y}$. This operator acts trivially on the singlet spin states $|\varphi_{l,s}\rangle$, but otherwise, it does not preserve the total angular momentum j and it is free to map between all $\alpha \neq s$ columns. So, for $\epsilon \neq 1$ the overlap between the column kets $|\varphi_{l,s}\rangle$ and $|\varphi_{l,t}\rangle$ will fluctuate as one column ket will remain stationary while the other will not.

Following the above distinction between the two terms of the Hamiltonian, we can label them as the effective “self” and “interaction” terms

$$H = \epsilon H_{self} + (1 - \epsilon) H_{int}$$

$$H_{self} := L_y + S_{1;y} + S_{2;y} \quad H_{int} := S_{1;y} + S_{2;y}.$$

The term H_{self} only changes the global orientation of the system (which we are completely ignorant of due to the operational constraint), so we can think of H_{self} as the self Hamiltonian of the inaccessible environment. We can then think of the other term H_{int} , as the effective interaction term because it couples the singlet-triplet qubit to the global orientation of the system.

For concreteness, let us assume that $l = 3$ and $\epsilon = 0$ so there is only the effective interaction term $H = H_{int}$. If the initial unreduced state is

$$|\psi\rangle = \frac{1}{\sqrt{2}} |l, s, 0\rangle + \frac{1}{\sqrt{2}} |l, t, 0\rangle,$$

then the initial reduced state is

$$\rho = \frac{1}{2} \begin{pmatrix} 0 & & & \\ & 1 & 1 & \\ & 1 & 1 & \\ & & & 0 \end{pmatrix}.$$

The purity of ρ as a function of time under the evolution with H is shown in Fig. 4.4. This illustrates how the singlet-triplet qubit periodically decoheres into the effective envi-

environment imposed by the operational constraint.

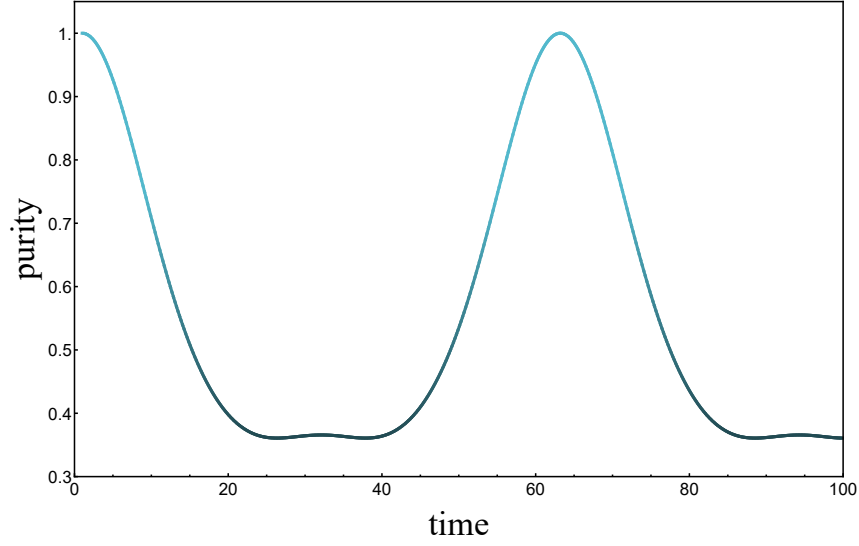


Figure 4.4: The purity of the reduced state under the evolution with $H = H_{int}$.

In Fig. 4.5 we can see the BPT perspective on this decoherence process. At $t = 0$ the initial state is the even superposition of the two basis elements in the two $j = l$ columns. As time progresses, the column ket of the singlet remains unchanged while the column ket of the triplet evolves both inside the $j = l$ column and it leaks into the $j = l \pm 1$ columns. Thus, the overlap between the initial singlet and triplet column kets diminishes. Periodically, as the spin rotations complete a full cycle, the triplet column ket returns to its initial configuration (around $t = 63$ for the first time), which results in the revivals of coherence.

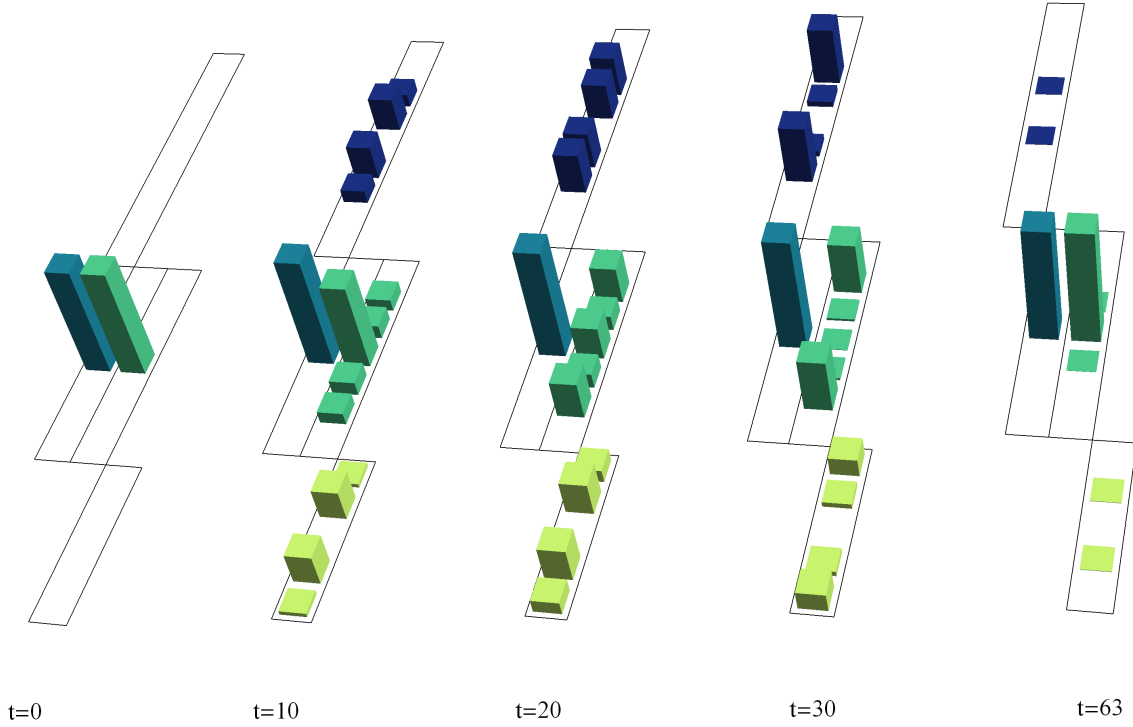


Figure 4.5: The column kets of the unreduced state as it evolves on the BPT. The height of each bar corresponds to the absolute value of the coefficient of the underlying BPT basis element. The distinct bar color is assigned to each column for contrast and has no numeric meaning.

In conclusion, there is no conceptual difference between decoherence in this example and decoherence from coupling to a physical environment. Ultimately, it is the combination of operational constraints and unitary dynamics that leads to non-unitary evolutions of reduced states.

Example 3

A basic question in quantum information is how to encode a logical qubit in a physical system in a way that will be least susceptible to noise. The idea of decoherence free subspaces and subsystems [59, 57, 65, 64] has emerged to address this question. The main obstacle to finding decoherence free subspaces and subsystems is finding the relevant irreps structure, so it is only the irreps of group representations that are commonly treated. In this example we will demonstrate how the Scattering Algorithm can expand the scope of treatable problems beyond group representations.

As before, we consider the composite system $\mathcal{H} := \underline{l} \otimes \frac{1}{2}$ of spin- l (either integer or half integer) and spin- $\frac{1}{2}$. Assume that Alice wants to send some quantum information to Bob by encoding it into the physical state of this system. Furthermore, Alice knows that on its

way it will be susceptible to noise dominated by the Ising interaction $L_z \otimes S_z$, and spin- $\frac{1}{2}$ rotations generated by $I \otimes S_x$. The question is how can Alice encode quantum information (and how many qubits) without it being affected by the dominant sources of noise.

We can answer this question by considering the noise as an imposed operational constraint such that only the observables that commute with both $L_z \otimes S_z$ and $I \otimes S_x$ remain relevant. The reduced states will then contain all the information that is unaffected by noise and the state reduction map will tell us how to encode and decode it.

In order to address this problem we need to find the irreps of the commutant of the algebra generated by both $L_z \otimes S_z$ and $I \otimes S_x$. We know the irreps of the individual terms—they are given by their eigenvectors—but we do not know the irreps structure of the combined algebra.

In the following we will use the product basis $|m, \uparrow\rangle, |m, \downarrow\rangle$, where $m = l, \dots, -l$ and \uparrow, \downarrow are the spin-up spin-down states along \hat{z} , or alternatively $|m, +\rangle, |m, -\rangle$ where $+, -$ are the spin-up spin-down states along \hat{x} . Before we address the problem for general l , let us solve it for $l = \frac{1}{2}$.

The combination of the irreps of $L_z \otimes S_z$ and of $I \otimes S_x$ can be expressed as the addition of BPTs

$$\begin{array}{|c|} \hline \frac{1}{2}, \uparrow \\ \hline -\frac{1}{2}, \downarrow \\ \hline \end{array} + \begin{array}{|c|} \hline \frac{1}{2}, + \\ \hline -\frac{1}{2}, + \\ \hline \end{array} \begin{array}{|c|} \hline \frac{1}{2}, \downarrow \\ \hline -\frac{1}{2}, \uparrow \\ \hline \end{array} \begin{array}{|c|} \hline \frac{1}{2}, - \\ \hline -\frac{1}{2}, - \\ \hline \end{array}$$

The left BPT consists of two single-column blocks that correspond to the distinct eigenvalues of $L_z \otimes S_z$ with the two degenerate eigenvectors in each columns. The right BPT comes from $I \otimes S_x$ with similar interpretation. The scattering calculations in the case of $l = \frac{1}{2}$ are very simple, however, in a anticipation of the general case let us simplify things even further.

First, we note that separate blocks of BPTs can be detached into separate terms in the sum, that is

$$\begin{array}{|c|} \hline \frac{1}{2}, \uparrow \\ \hline -\frac{1}{2}, \downarrow \\ \hline \end{array} + \begin{array}{|c|} \hline \frac{1}{2}, + \\ \hline -\frac{1}{2}, + \\ \hline \end{array} \begin{array}{|c|} \hline \frac{1}{2}, \downarrow \\ \hline -\frac{1}{2}, \uparrow \\ \hline \end{array} \begin{array}{|c|} \hline \frac{1}{2}, - \\ \hline -\frac{1}{2}, - \\ \hline \end{array} = \begin{array}{|c|} \hline \frac{1}{2}, \uparrow \\ \hline -\frac{1}{2}, \downarrow \\ \hline \end{array} + \begin{array}{|c|} \hline \frac{1}{2}, \downarrow \\ \hline -\frac{1}{2}, \uparrow \\ \hline \end{array} + \begin{array}{|c|} \hline \frac{1}{2}, + \\ \hline -\frac{1}{2}, + \\ \hline \end{array} + \begin{array}{|c|} \hline \frac{1}{2}, - \\ \hline -\frac{1}{2}, - \\ \hline \end{array}$$

We can do that because the set of operators that we can generate from either side of this equation is the same, so it is the same algebra.

The second simplification is that we can drop redundant terms in the combination. If we know that some terms can be generated by other terms then they do not add anything to the combined algebra, and therefore can be dropped. In this case we can drop any one of the columns because the sole projection that it defines can be spanned by the other three.

We end up with the following combination of BPTs

$$\begin{array}{|c|} \hline \frac{1}{2}, \uparrow \\ \hline -\frac{1}{2}, \downarrow \\ \hline \end{array} + \begin{array}{|c|} \hline \frac{1}{2}, \downarrow \\ \hline -\frac{1}{2}, \uparrow \\ \hline \end{array} + \begin{array}{|c|} \hline \frac{1}{2}, + \\ \hline -\frac{1}{2}, + \\ \hline \end{array}.$$

The three projections defined by these columns are

$$\begin{aligned} \Pi_{zz; \frac{1}{4}} &:= \left| \frac{1}{2}, \uparrow \right\rangle \left\langle \frac{1}{2}, \uparrow \right| + \left| -\frac{1}{2}, \downarrow \right\rangle \left\langle -\frac{1}{2}, \downarrow \right| & \Pi_{zz; -\frac{1}{4}} &:= \left| \frac{1}{2}, \downarrow \right\rangle \left\langle \frac{1}{2}, \downarrow \right| + \left| -\frac{1}{2}, \uparrow \right\rangle \left\langle -\frac{1}{2}, \uparrow \right| \\ \Pi_{x; \frac{1}{2}} &:= \left| \frac{1}{2}, + \right\rangle \left\langle \frac{1}{2}, + \right| + \left| -\frac{1}{2}, + \right\rangle \left\langle -\frac{1}{2}, + \right|. \end{aligned}$$

The subscripts $zz; \pm \frac{1}{4}$ refers to the $\pm \frac{1}{4}$ eigenvalues of $L_z \otimes S_z$, and $x; \frac{1}{2}$ refers to the $\frac{1}{2}$ eigenvalue of $I \otimes S_x$. By scattering



we learn that these projections are reflecting so the resulting reflection network is shown in Fig 4.6.

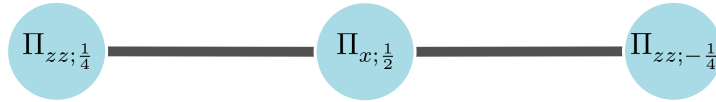


Figure 4.6: The final reflection network for $l = \frac{1}{2}$.

The condition of minimality holds because the reflection network has no cycles so all path-isometries between the same vertices have to follow the same paths and therefore be equal. The condition of completeness holds because $\Pi_{zz; \frac{1}{4}} + \Pi_{zz; -\frac{1}{4}} = I$.

The columns of the new BPT are determined by the maximal independent set in the network, which is $\left\{ \Pi_{zz; \frac{1}{4}}, \Pi_{zz; -\frac{1}{4}} \right\}$. The choice and alignment of basis elements in the columns of the new BPT is given by the path-isometry that connects the independent vertices, which is

$$S_{-\frac{1}{4}, \frac{1}{4}} \propto \Pi_{zz; -\frac{1}{4}} \Pi_{x; \frac{1}{2}} \Pi_{zz; \frac{1}{4}} \propto \left| \frac{1}{2}, \downarrow \right\rangle \left\langle \frac{1}{2}, \uparrow \right| + \left| -\frac{1}{2}, \uparrow \right\rangle \left\langle -\frac{1}{2}, \downarrow \right|.$$

The resulting BPT is therefore

$$\begin{array}{|c|} \hline \frac{1}{2}, \uparrow \\ \hline -\frac{1}{2}, \downarrow \\ \hline \end{array} + \begin{array}{|c|} \hline \frac{1}{2}, \downarrow \\ \hline -\frac{1}{2}, \uparrow \\ \hline \end{array} + \begin{array}{|c|} \hline \frac{1}{2}, + \\ \hline -\frac{1}{2}, + \\ \hline \end{array} = \begin{array}{|c|c|} \hline \frac{1}{2}, \uparrow & \frac{1}{2}, \downarrow \\ \hline -\frac{1}{2}, \downarrow & -\frac{1}{2}, \uparrow \\ \hline \end{array}.$$

In order to get the irreps of the commutant we transpose the resulting BPT and label

the reduced basis according to the common state of spin- l in each column:

$$\begin{array}{|c|c|} \hline \frac{1}{2}, \uparrow & -\frac{1}{2}, \downarrow \\ \hline \frac{1}{2}, \downarrow & -\frac{1}{2}, \uparrow \\ \hline \end{array} \quad \begin{array}{c} \downarrow \\ \downarrow \end{array} \quad \begin{array}{|c|c|} \hline \frac{1}{2} & -\frac{1}{2} \\ \hline \end{array}.$$

For the state reduction map we explicitly define the minimal isometries given by the alignment of columns

$$S_{\frac{1}{2}, \frac{1}{2}} := \left| \frac{1}{2}, \uparrow \right\rangle \left\langle \frac{1}{2}, \uparrow \right| + \left| \frac{1}{2}, \downarrow \right\rangle \left\langle \frac{1}{2}, \downarrow \right| \quad S_{-\frac{1}{2}, -\frac{1}{2}} := \left| -\frac{1}{2}, \downarrow \right\rangle \left\langle -\frac{1}{2}, \downarrow \right| + \left| -\frac{1}{2}, \uparrow \right\rangle \left\langle -\frac{1}{2}, \uparrow \right|$$

$$S_{-\frac{1}{2}, \frac{1}{2}} := \left| -\frac{1}{2}, \downarrow \right\rangle \left\langle \frac{1}{2}, \uparrow \right| + \left| -\frac{1}{2}, \uparrow \right\rangle \left\langle \frac{1}{2}, \downarrow \right|.$$

The state reduction map is then given by

$$|\psi\rangle \mapsto \rho_{Bob} = \begin{pmatrix} \langle \psi | S_{\frac{1}{2}, \frac{1}{2}} | \psi \rangle & \langle \psi | S_{-\frac{1}{2}, \frac{1}{2}} | \psi \rangle \\ \langle \psi | S_{-\frac{1}{2}, \frac{1}{2}}^\dagger | \psi \rangle & \langle \psi | S_{-\frac{1}{2}, -\frac{1}{2}} | \psi \rangle \end{pmatrix}.$$

The above BPT identifies a bipartition of the Hilbert space into two virtual subsystems, and the state reduction map is the partial-trace-like map over one of these subsystems. It may be tempting to think of this state reduction map as the partial trace over the second spin, but it is not quite the case. Although the product states such as $|\pm\frac{1}{2}, \uparrow\rangle$ or $|\pm\frac{1}{2}, \downarrow\rangle$ reduce with this map to $|\pm\frac{1}{2}\rangle$, other product states such as $|\psi\rangle = \frac{1}{\sqrt{2}} |\frac{1}{2}, \downarrow\rangle + \frac{1}{\sqrt{2}} |-\frac{1}{2}, \downarrow\rangle$ do not reduce to $\frac{1}{\sqrt{2}} |\frac{1}{2}\rangle + \frac{1}{\sqrt{2}} |-\frac{1}{2}\rangle$ but to the completely mixed state

$$|\psi\rangle \mapsto \rho_{Bob} = \begin{pmatrix} \frac{1}{2} & 0 \\ 0 & \frac{1}{2} \end{pmatrix}.$$

We can summarize this distinction by observing that the BPT that corresponds to the partial trace over the second spin is

$$\begin{array}{|c|c|} \hline \frac{1}{2}, \uparrow & -\frac{1}{2}, \uparrow \\ \hline \frac{1}{2}, \downarrow & -\frac{1}{2}, \downarrow \\ \hline \end{array}$$

which is not quite the same as the one we have derived above.

Thus, Alice can encode one qubit of information into the subspaces of $|\frac{1}{2}, \uparrow\rangle$ and $|\frac{1}{2}, \downarrow\rangle$ (or $|\frac{1}{2}, \downarrow\rangle$ and $|\frac{1}{2}, \uparrow\rangle$), and Bob can decode it by applying the above state reduction map. Since this qubit is encoded in a subsystem given by the commutant of $L_z \otimes S_z$ and $I \otimes S_x$, it is a decoherence free subsystem that is not affected by such noise.

Now we will address the case of general l . The combination of the irreps of $L_z \otimes S_z$ and of $I \otimes S_x$ is given by the sum BPTs

$$\begin{array}{c}
\begin{array}{|c|} \hline l, \uparrow \\ \hline -l, \downarrow \\ \hline \end{array} \\
\begin{array}{|c|} \hline l-1, \uparrow \\ \hline 1-l, \downarrow \\ \hline \end{array} \\
\vdots \\
\begin{array}{|c|} \hline 1-l, \uparrow \\ \hline l-1, \downarrow \\ \hline \end{array} \\
\begin{array}{|c|} \hline -l, \uparrow \\ \hline l, \downarrow \\ \hline \end{array}
\end{array}
+
\begin{array}{c}
\begin{array}{|c|} \hline l, + \\ \hline \vdots \\ \hline -l, + \\ \hline \end{array} \\
\begin{array}{|c|} \hline l, - \\ \hline \vdots \\ \hline -l, - \\ \hline \end{array}
\end{array}
.$$

The $2l + 1$ column-blocks of the left BPT correspond to the eigenvalues $\lambda = \frac{l}{2}, \dots, -\frac{l}{2}$ of $L_z \otimes S_z$, and the two column-blocks of the right BPT correspond to the two eigenvalues $\pm \frac{1}{2}$ of $I \otimes S_x$. Using the same reasoning as in the case of $l = \frac{1}{2}$, we rearrange this combination of BPTs as follows

$$\left(\begin{array}{|c|} \hline 0, \uparrow \\ \hline 0, \downarrow \\ \hline \end{array} \right) + \dots + \left(\begin{array}{|c|} \hline 1-l, \uparrow \\ \hline l-1, \downarrow \\ \hline \end{array} + \begin{array}{|c|} \hline l-1, \uparrow \\ \hline 1-l, \downarrow \\ \hline \end{array} \right) + \left(\begin{array}{|c|} \hline l, \uparrow \\ \hline -l, \downarrow \\ \hline \end{array} + \begin{array}{|c|} \hline -l, \uparrow \\ \hline l, \downarrow \\ \hline \end{array} \right) + \begin{array}{|c|} \hline l, + \\ \hline \vdots \\ \hline -l, + \\ \hline \end{array}.$$

Here we have dropped the redundant second column of the $-\frac{1}{2}$ eigenvalue of $I \otimes S_x$, and grouped together the columns of $L_z \otimes S_z$ according to the magnitude of the eigenvalues λ . Note that the $\lambda = 0$ column on the left is special since it is alone in its group and it only exists if l is integer. We will assume integer l since this is the more general case while the case of half integer l can be considered as a simplification. The above grouping and ordering of columns has been chosen in anticipation of how the scattering calculations will unfold.

In the following, we will denote the spectral projections of $L_z \otimes S_z$ as

$$\Pi_{zz;\lambda} := |\lambda, \uparrow\rangle \langle \lambda, \uparrow| + |-\lambda, \downarrow\rangle \langle -\lambda, \downarrow|.$$

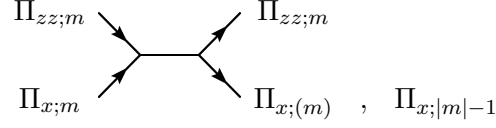
We also conveniently define the projections

$$\Pi_{x;m} := \sum_{m'=-m}^m |m', +\rangle \langle m', +|,$$

such that for $m = l$ and $m = -l$ we get the $+\frac{1}{2}$ spectral projection of $I \otimes S_x$. For any $m = l, \dots, -l$ we can calculate

$$\Pi_{zz;m} \Pi_{x;m} = \frac{1}{\sqrt{2}} |m, \uparrow\rangle \langle m, +| + \frac{1}{\sqrt{2}} | -m, \downarrow\rangle \langle -m, +|,$$

which implies that for any $m \neq 0$ we get the scatterings (the $m = 0$ case is shown later)



Here we had to introduce another projection

$$\Pi_{x;(m)} := |m, +\rangle \langle m, +| + |-m, +\rangle \langle -m, +|$$

(note that $\Pi_{x;(m)} = \Pi_{x;(-m)}$).

The above general scattering calculation can then be used to combine the BPT columns starting from the right side and proceeding toward the left. In the first step we consider the reflection network of $\Pi_{zz;l}, \Pi_{zz;-l}, \Pi_{x;l}$, which after scattering is shown in Fig. 4.7.

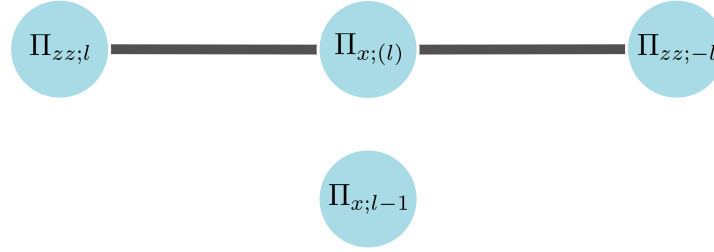


Figure 4.7: The first step reflection network for general l .

Then we include the next two columns $\Pi_{zz;l-1}, \Pi_{zz;1-l}$ which are orthogonal to $\Pi_{zz;l}, \Pi_{zz;-l}, \Pi_{x;(l)}$ but not to $\Pi_{x;l-1}$. After scattering with $\Pi_{x;l-1}$ we get the reflection network shown in Fig. 4.8.

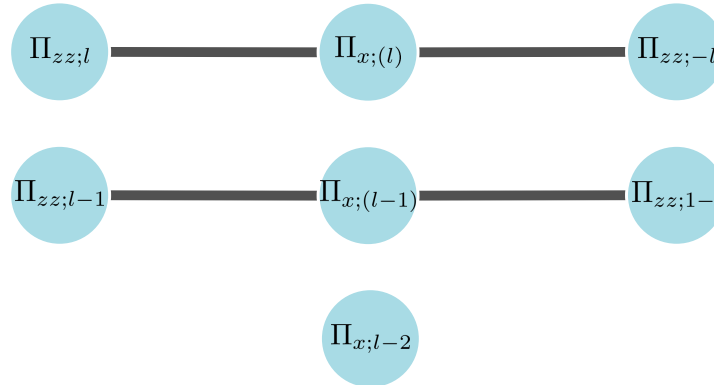
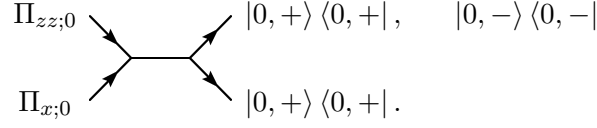


Figure 4.8: The second step reflection network for general l .

This pattern repeats as we fold in the columns until (assuming l is integer) we are

left with the last column $\Pi_{zz;0} = |0, \uparrow\rangle \langle 0, \uparrow| + |0, \downarrow\rangle \langle 0, \downarrow|$ and the leftover projection $\Pi_{x;0} = |0, +\rangle \langle 0, +|$ from the previous scatterings. They scatter differently than before:



The final reflection network is shown in Fig. 4.9.

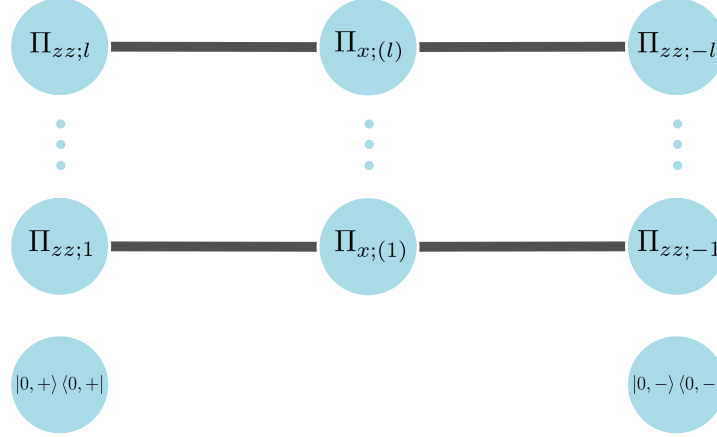


Figure 4.9: The final reflection network for integer l . When l is half integer the last two projections $|0, +\rangle \langle 0, +|$ and $|0, -\rangle \langle 0, -|$ do not exist.

Each connected component with three vertices corresponds to a 2×2 BPT block, as in the $l = \frac{1}{2}$ case, and the last two isolated vertices correspond to two single-celled blocks. As we did in the $l = \frac{1}{2}$ case we construct the 2×2 blocks, and then transpose them, which results in the BPT

$$\begin{array}{|c|c|} \hline l, \uparrow & -l, \downarrow \\ \hline l, \downarrow & -l, \uparrow \\ \hline \end{array} \quad \ddots \quad \begin{array}{|c|c|} \hline 1, \uparrow & -1, \downarrow \\ \hline 1, \downarrow & -1, \uparrow \\ \hline \end{array} \quad \begin{array}{|c|} \hline 0, + \\ \hline \end{array} \quad \begin{array}{|c|} \hline 0, - \\ \hline \end{array} .$$

The form of the resulting BPT implies that there are $m = 1, \dots, l$ alternative decoherence free subsystems that Alice can choose from; she can still encode only one qubit though. Since there are l alternative orthogonal subspaces to choose from (not counting $l = 0$), Alice can also encode $\log l$ classical bits in addition to the qubit.

It is important to note that the derivation of the irreps structure for general l was only possible because we could carry out all the calculations analytically, without specifying

the value of l . This demonstrates the key advantage of the Scattering Algorithm over the numeric approaches in that it can be applied symbolically.

Chapter 5

Reduction of dynamics

In this chapter we will consider two notions of reduction of dynamics. The common idea here is that the Hamiltonian is block-diagonalizable by the irrep basis of any non-trivial algebra that the Hamiltonian belongs to. Such block-diagonalization leads to the reduction of dynamics onto the irreps. With this basic idea in mind we will first consider the reduction of dynamics with symmetries, and then proceed to the symmetry-agnostic approach.

The idea of reduction of dynamics with symmetries traces back to the seminal work by Emmy Noether [76]. Today, symmetry related methods are a well established staple in physics with many dedicated textbooks such as [29, 90, 42]. With the advancement of finite-dimensional quantum mechanics driven by the development of quantum information and quantum computing, the central role of the irreps structures associated with symmetries was gradually recognized in applications [103, 101, 59, 11, 67, 69].

In Section 5.1 we will briefly outline the role of the irreps structure in the reduction of dynamics with symmetries. This will lead to the realization that the usual notion of symmetry is too restrictive and even groups that do not commute with the Hamiltonian may still be useful for the reduction of dynamics. This idea is summarized in Theorem 5.1 and we will illustrate it with an example of a quantum walk with a broken symmetry. As a secondary goal we will use this example to demonstrate how the the Scattering Algorithm constructs irreps of a non-trivial finite group.

In Section 5.2 we will demonstrate how the same kind of reduction of dynamics can be performed without the need to recognize symmetries. Such symmetry-agnostic approach is possible with the Scattering Algorithm as it allows us to directly focus on the irreps structure generated by the Hamiltonian terms. We will illustrate this idea with two examples from the literature on qubit implementations in quantum dots. Specifically, we will show how the symmetry-agnostic approach can be used to reduce the control Hamiltonian in order to find the possible qubit encodings.

5.1 Reduction of Hamiltonians with symmetries

We will begin by describing the central role of the irreps structure in the usual reduction of Hamiltonians with symmetries.

Let us consider the Hamiltonian $H \in \mathcal{L}(\mathcal{H})$ and the group \mathcal{G} represented by the unitaries $U(\mathcal{G}) := \{U(g)\}_{g \in \mathcal{G}}$. We say that \mathcal{G} is a symmetry of H (as represented by $U(\mathcal{G})$) if

$[H, U(g)] = 0$ for all $g \in \mathcal{G}$. This identifies H as an element of the commutant $U(\mathcal{G})'$ of $U(\mathcal{G})$.

In general, the group algebra $\mathcal{A}_{U(\mathcal{G})}$ (recall Definition 2.27) identifies the irreps structure

$$\mathcal{H} \cong \bigoplus_q \mathcal{H}_{\nu_q} \otimes \mathcal{H}_{\mu_q} \quad (5.1)$$

such that all the unitaries $U(g)$ reduce to

$$U(g) \cong \bigoplus_q I_{\nu_q} \otimes U_{\mu_q}(g),$$

where $U_{\mu_q}(g)$ are the irreducible unitary representations of \mathcal{G} (see Theorem 2.28). Since $H \in U(\mathcal{G})'$, it reduces in a complementary manner (see Theorem 2.29)

$$H \cong \bigoplus_q H_{\nu_q} \otimes I_{\mu_q}.$$

This block-diagonal form constitutes a reduction of dynamics where we have reduced the action of H from the whole \mathcal{H} to the smaller Hamiltonians H_{ν_q} acting on \mathcal{H}_{ν_q} . This form rules out any transitions between states supported on different irreps, so the the irrep value q is a conserved quantity. Thus, the irreps structure (5.1) of the symmetry group $U(\mathcal{G})$ identifies the constants of motion and the subsystems \mathcal{H}_{ν_q} on which the dynamics reduce.

As an example, consider the three spin Heisenberg interaction Hamiltonian

$$H = \epsilon_{12} \vec{S}_1 \cdot \vec{S}_2 + \epsilon_{23} \vec{S}_2 \cdot \vec{S}_3,$$

where ϵ_{ij} are arbitrary coupling strengths and $\vec{S}_i = (S_{i,x}, S_{i,y}, S_{i,z})$ are the spin operators. This Hamiltonian commutes with the $SU(2)$ group of rotations $[H, U(R)] = 0$ that have the familiar irreps structure of total spin

$$\mathcal{H} \cong \mathcal{H}_{\mu_{3/2}} \oplus \mathcal{H}_{\nu_{1/2}} \otimes \mathcal{H}_{\mu_{1/2}}. \quad (5.2)$$

These irreps are identified by the total spin basis $|j, \alpha, m\rangle$ where $j = \frac{3}{2}, \frac{1}{2}$, $m = -j, \dots, j$ and $\alpha = s, t$ distinguishes the two variants of the $j = \frac{1}{2}$ irrep. The conserved quantity here is the total spin $j = \frac{3}{2}, \frac{1}{2}$, as identified by the irreps.

The irreps structure (5.1) tells us that the Hamiltonian reduces to

$$H \cong h_{\nu_{3/2}} I_{\mu_{3/2}} \oplus H_{\nu_{1/2}} \otimes I_{\mu_{1/2}}$$

where $h_{\nu_{3/2}}$ is a scalar (since $\mathcal{H}_{\nu_{3/2}}$ is one-dimensional) and $H_{\nu_{1/2}}$ is a 2×2 matrix. Therefore,

in the total spin basis, H is given by the five matrix elements

$$h_{\nu_{3/2}} = \left\langle \frac{3}{2}, m \left| H \right| \frac{3}{2}, m \right\rangle = \frac{1}{4} (\epsilon_{12} + \epsilon_{23}),$$

$$H_{\nu_{1/2}} = \begin{pmatrix} \langle \frac{1}{2}, s, m | H | \frac{1}{2}, s, m \rangle & \langle \frac{1}{2}, s, m | H | \frac{1}{2}, t, m \rangle \\ \langle \frac{1}{2}, t, m | H | \frac{1}{2}, s, m \rangle & \langle \frac{1}{2}, t, m | H | \frac{1}{2}, t, m \rangle \end{pmatrix} = \frac{1}{4} \begin{pmatrix} -3\epsilon_{23} & \sqrt{3}\epsilon_{12} \\ \sqrt{3}\epsilon_{12} & \epsilon_{23} - 2\epsilon_{12} \end{pmatrix} \quad (5.3)$$

where the choice of m does not matter and all other matrix elements are zero.

In the standard applications of symmetries, as in the above example, only the groups such that $[H, U(g)] = 0$ are considered. The symmetry condition $[H, U(g)] = 0$, however, is too restrictive and the irreps structure (5.1) can still be useful with groups that fail to commute with the Hamiltonian.

For example, we can add the symmetry breaking term $S_{tot,z} = S_{1,z} + S_{2,z} + S_{3,z}$ to the Hamiltonian

$$H = \epsilon_{12} \vec{S}_1 \cdot \vec{S}_2 + \epsilon_{23} \vec{S}_2 \cdot \vec{S}_3 + S_{tot,z}.$$

Now $[H, U(R)] \neq 0$ so the $SU(2)$ group is not a symmetry and it would appear that the above reduction of dynamics is no longer relevant. This, however, is not the case and the irreps structure of the $SU(2)$ group is still useful for the reduction of this Hamiltonian. The reason for that is because the symmetry breaking term $S_{tot,z}$ is itself one of the generators of the $SU(2)$ group (it breaks the symmetry because the group is not Abelian). This means that $S_{tot,z}$ is an element of the $SU(2)$ group algebra and so with respect to its irreps (5.2) it is confined to the form⁶

$$S_{tot,z} \cong S_{\mu_{3/2},z} \oplus I_{\nu_{1/2}} \otimes S_{\mu_{1/2},z},$$

so

$$H \cong \left(h_{\nu_{3/2}} I_{\mu_{3/2}} + S_{\mu_{3/2},z} \right) \oplus \left(H_{\nu_{1/2}} \otimes I_{\mu_{1/2}} + I_{\nu_{1/2}} \otimes S_{\mu_{1/2},z} \right).$$

Thus, we can still say that the original exchange interaction generates dynamics via the $H_{\nu_{1/2}}$ term in the $\mathcal{H}_{\nu_{1/2}}$ subsystem, while the new $S_{\mu_{3/2},z}$ and $S_{\mu_{1/2},z}$ terms generates dynamics in the $\mathcal{H}_{\mu_{3/2}}$ and $\mathcal{H}_{\mu_{1/2}}$ subsystems. The critical detail here is that each subsystem evolves independently as there are no interaction terms between them so the dynamics can be reduced to the subsystems identified by the irreps structure (5.2). Also note that the total spin is still a constant of motion even though the group that identifies it is not a symmetry of the Hamiltonian.

The general result that extends the application of group representations beyond symmetries is give by the following theorem.

Theorem 5.1. *Let $H \in \mathcal{L}(\mathcal{H})$ and let \mathcal{G} be a finite or a compact Lie group represented by the*

⁶In this example it is even more obvious because the symmetry breaking term $S_{tot,z}$ is diagonal in the total spin basis $|j, \alpha, m\rangle$.

unitaries $U(\mathcal{G}) := \{U(g)\}_{g \in \mathcal{G}} \subset \mathcal{L}(\mathcal{H})$, such that

$$[H, U(g)] \in \mathcal{A}_{U(\mathcal{G})} \quad \forall g \in \mathcal{G}.$$

Then, with respect to the irreps structure of the group algebra $\mathcal{A}_{U(\mathcal{G})}$

$$\mathcal{H} \cong \bigoplus_q \mathcal{H}_{\nu_q} \otimes \mathcal{H}_{\mu_q},$$

the operator H reduces to

$$H = H_\nu + H_\mu \cong \bigoplus_q H_{\nu_q} \otimes I_{\mu_q} + \bigoplus_q I_{\nu_q} \otimes H_{\mu_q}$$

for some $H_{\nu_q} \in \mathcal{L}(\mathcal{H}_{\nu_q})$ and $H_{\mu_q} \in \mathcal{L}(\mathcal{H}_{\mu_q})$.

Proof. Let $A(g) := [H, U(g)]$ so

$$H = U(g) H U(g)^\dagger + A(g) U(g)^\dagger.$$

If \mathcal{G} is finite we can sum both sides over all $g \in \mathcal{G}$ and normalize it by the order of \mathcal{G} :

$$H = \frac{1}{|\mathcal{G}|} \sum_{g \in \mathcal{G}} U(g) H U(g)^\dagger + \frac{1}{|\mathcal{G}|} \sum_{g \in \mathcal{G}} A(g) U(g)^\dagger.$$

In the more general case, if \mathcal{G} is a compact Lie group there is a normalized invariant measure (Haar measure) $d\mu(g)$ over \mathcal{G} such that

$$H = \underbrace{\int_{\mathcal{G}} d\mu(g) U(g) H U(g)^\dagger}_{H_\nu} + \underbrace{\int_{\mathcal{G}} d\mu(g) A(g) U(g)^\dagger}_{H_\mu}.$$

For all $g \in \mathcal{G}$ both $U(g)^\dagger$ and $A(g)$ are in the group algebra $\mathcal{A}_{U(\mathcal{G})}$. Therefore, $H_\mu \in \mathcal{A}_{U(\mathcal{G})}$ so according to Theorem 2.26 it reduces to

$$H_\mu \cong \bigoplus_q I_{\nu_q} \otimes H_{\mu_q}.$$

The term H_ν , on the other hand, is in the commutant $\mathcal{A}'_{U(\mathcal{G})}$ because it commutes with all $U(g)$:

$$H_\nu U(g) = \int_{\mathcal{G}} d\mu(g') U(g') H U(g'^{-1}g)^\dagger = \int_{\mathcal{G}} d\mu(gg') U(gg') H U(g')^\dagger = U(g) H_\nu$$

(here we have used the invariance of the measure $d\mu(gg') = d\mu(g)$). Therefore, $H_\nu \in \mathcal{A}'_{U(\mathcal{G})}$ so according to Theorem 2.29 it reduces to

$$H_\nu \cong \bigoplus_q H_{\nu_q} \otimes I_{\mu_q}.$$

Thus,

$$H = H_\nu + H_\mu \cong \bigoplus_q H_{\nu_q} \otimes I_{\mu_q} + \bigoplus_q I_{\nu_q} \otimes H_{\mu_q}.$$

□

This theorem implies that symmetry groups are the special case when $[H, U(g)] = 0 \in \mathcal{A}_{U(\mathcal{G})}$. The generalization is that now we can also consider groups such that the Hamiltonian consists of both an invariant term—identified by H_ν —and a symmetry breaking term—identified by H_μ . The restriction is that the symmetry breaking term H_μ still has to be an element of the group algebra $\mathcal{A}_{U(\mathcal{G})}$. Once we have identified such group, the dynamics reduce to the subsystems of the group's irreps structure, that is

$$e^{-itH} = e^{-itH_\nu} e^{-itH_\mu} = \bigoplus_q e^{-itH_{\nu_q}} \otimes e^{-itH_{\mu_q}}.$$

In particular, the value q that distinguishes the irreps is a conserved quantity.

We will now consider a more elaborate example of such reduction of dynamics.

Example

In this example we will analyze the dynamics of a continuous-time quantum walk (CTQW) on binary trees. CTQW is the quantum analog of a continuous-time random walk on graphs. The idea that a CTQW model can provide an exponentially faster way of searching for distinguished vertices on certain problems, was first introduced by Farhi and Gutmann in [39]. Since some computational problems can be formulated as searches on graphs, the CTQW model turned out to be an alternative paradigm to quantum Fourier transform for designing quantum algorithms with an exponential speed-up.

What is interesting about the CTQW paradigm is that it is relatively easy to understand where the exponential speed-up is coming from. It was observed in [27, 28] that the exponential speed-up can be explained by the exponential reduction of dynamics. This observation was analyzed exactly for a search on binary trees and the reduction was traced back to the symmetries of the graph. In the following, we will reproduce this argument by finding the irreps of symmetries of the binary tree and show that the exponential reduction of dynamics holds even when the symmetry is broken.

The Hilbert space of a CTQW model is spanned by the vertices V of a graph G :

$$\mathcal{H} := \text{span } V.$$

The Hamiltonian of a CTQW model can be defined by the edges E of a graph G as follows

$$H := - \sum_{\langle i,j \rangle \in E} (|i\rangle \langle j| + |j\rangle \langle i| - |i\rangle \langle i| - |j\rangle \langle j|). \quad (5.4)$$

The graph G that we will consider here is shown in Fig. 5.1.

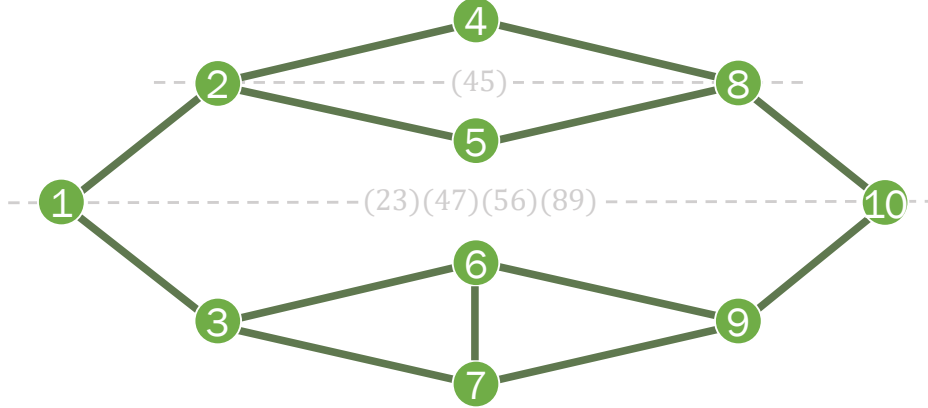


Figure 5.1: Two “glued” binary trees with a symmetry breaking edge $\langle 6, 7 \rangle$. The two generators of the permutation symmetry are shown in grey using the cyclic notation (ij) . The dashed lines are the axis of reflection associated with the permutations.

Note that we can permute the vertices 4 with 5 or 6 with 7 without changing the definition of the Hamiltonian 5.4. This is so because these permutations do not change how the vertices are connected. This is not true, for example, for the permutation of 2 with 4 because initially 4 is not connected to 1 or 5, but after this permutation it is. Therefore, the permutations $\pi_2 := (45)$ and $\pi_3 := (67)$ are symmetries of this Hamiltonian.⁷

Any permutation π of the vertices V is represented on the Hilbert space \mathcal{H} by the unitaries

$$U(\pi) := \sum_{i \in V} |\pi(i)\rangle \langle i|.$$

In particular, the 2-cycle permutations (ij) are represented by

$$U((ij)) := |i\rangle \langle j| + |j\rangle \langle i| + \sum_{k \neq i,j} |k\rangle \langle k| = |i\rangle \langle j| + |j\rangle \langle i| + I - |i\rangle \langle i| - |j\rangle \langle j|.$$

We can therefore express the Hamiltonian (5.4) as a sum of 2-cycle permutations

$$H = - \sum_{\langle i,j \rangle \in E} (U((ij)) - I) = - \sum_{\langle i,j \rangle \in E} U((ij)) + |E| I$$

and we can drop the constant identity $|E| I$. Observe that the permutation $U((67))$ is both a

⁷The subscripts 2 and 3 refer to the root vertices of the sub-trees where these permutations apply.

symmetry of H and an additive term in H . Theorem 5.1 then implies that we can consider symmetries that do not commute with $U((67))$, as long as they commute with the rest of H and $U((67))$ is itself an element of that symmetry. In the notation of Theorem 5.1 we split $H = H_\nu + H_\mu$ where $H_\mu := -U((67))$ and H_ν are all the other terms.

If we exclude the term H_μ (on the graph this means deleting the edge $\langle 6, 7 \rangle$) the remaining term H_ν has more symmetry. That is, in addition to π_2 and π_3 another permutation is also a symmetry:

$$\pi_1 := (23)(47)(56)(89).$$

For the full H it is not a symmetry because $U(\pi_3)$ and $U(\pi_1)$ do not commute. However, since the finite group \mathcal{G} generated by π_1 , π_2 and π_3 is a symmetry of H_ν and $H = H_\nu + (-U(\pi_3))$, the condition of Theorem 5.1 holds:

$$[H, U(\pi_i)] = [-U(\pi_3), U(\pi_i)] \in \mathcal{A}_{U(\mathcal{G})}.$$

In order to reduce the dynamics with the group $U(\mathcal{G})$ we need to find its irreps structure. Note that the group element π_3 is redundant as $\pi_3 = \pi_1\pi_2\pi_1$ so we only need to consider the generators π_1 and π_2 . First, we find the spectral projections of $U(\pi_1)$ and $U(\pi_2)$. Using the shorthand notation for the states

$$\left| \begin{smallmatrix} +i_1, i_2, \dots \\ -j_1, j_2, \dots \end{smallmatrix} \right\rangle := \frac{1}{\sqrt{N}} (|i_1\rangle + |i_2\rangle + \dots - |j_1\rangle - |j_2\rangle - \dots) \quad (5.5)$$

we can diagonalize the generator

$$U(\pi_2) = |4\rangle\langle 5| + |5\rangle\langle 4| + \sum_{k \neq 4,5} |k\rangle\langle k| = \left| \begin{smallmatrix} +4,5 \\ - \end{smallmatrix} \right\rangle \left\langle \begin{smallmatrix} +4,5 \\ - \end{smallmatrix} \right| - \left| \begin{smallmatrix} +4 \\ -5 \end{smallmatrix} \right\rangle \left\langle \begin{smallmatrix} +4 \\ -5 \end{smallmatrix} \right| + \sum_{k \neq 4,5} |k\rangle\langle k|$$

so its spectral projections are

$$\begin{aligned} \Pi_{2,+} &:= \left| \begin{smallmatrix} +4,5 \\ - \end{smallmatrix} \right\rangle \left\langle \begin{smallmatrix} +4,5 \\ - \end{smallmatrix} \right| + |1\rangle\langle 1| + |2\rangle\langle 2| + |3\rangle\langle 3| + |6\rangle\langle 6| + |7\rangle\langle 7| + |8\rangle\langle 8| + |9\rangle\langle 9| + |10\rangle\langle 10| \\ \Pi_{2,-} &:= \left| \begin{smallmatrix} +4 \\ -5 \end{smallmatrix} \right\rangle \left\langle \begin{smallmatrix} +4 \\ -5 \end{smallmatrix} \right|. \end{aligned}$$

Similarly, we have

$$U(\pi_1) = \Pi_{1,+} - \Pi_{1,-}$$

where

$$\begin{aligned} \Pi_{1,+} &:= |1\rangle\langle 1| + \left| \begin{smallmatrix} +2,3 \\ - \end{smallmatrix} \right\rangle \left\langle \begin{smallmatrix} +2,3 \\ - \end{smallmatrix} \right| + \left| \begin{smallmatrix} +4,7 \\ - \end{smallmatrix} \right\rangle \left\langle \begin{smallmatrix} +4,7 \\ - \end{smallmatrix} \right| + \left| \begin{smallmatrix} +5,6 \\ - \end{smallmatrix} \right\rangle \left\langle \begin{smallmatrix} +5,6 \\ - \end{smallmatrix} \right| + \left| \begin{smallmatrix} +8,9 \\ - \end{smallmatrix} \right\rangle \left\langle \begin{smallmatrix} +8,9 \\ - \end{smallmatrix} \right| + |10\rangle\langle 10| \\ \Pi_{1,-} &:= \left| \begin{smallmatrix} +2 \\ -3 \end{smallmatrix} \right\rangle \left\langle \begin{smallmatrix} +2 \\ -3 \end{smallmatrix} \right| + \left| \begin{smallmatrix} +4 \\ -7 \end{smallmatrix} \right\rangle \left\langle \begin{smallmatrix} +4 \\ -7 \end{smallmatrix} \right| + \left| \begin{smallmatrix} +5 \\ -6 \end{smallmatrix} \right\rangle \left\langle \begin{smallmatrix} +5 \\ -6 \end{smallmatrix} \right| + \left| \begin{smallmatrix} +8 \\ -9 \end{smallmatrix} \right\rangle \left\langle \begin{smallmatrix} +8 \\ -9 \end{smallmatrix} \right|. \end{aligned}$$

Since both sets of spectral projections sum to I , one of the projections is redundant so

we will drop $\Pi_{2;+}$. It is now straight forward to calculate the scatterings



where

$$\Pi_{1;+}^{(1/2)} := \begin{vmatrix} +4,7 \\ -5,6 \end{vmatrix} \begin{vmatrix} +4,7 \\ -5,6 \end{vmatrix} \quad \Pi_{1;-}^{(1/2)} := \begin{vmatrix} +4,6 \\ -5,7 \end{vmatrix} \begin{vmatrix} +4,6 \\ -5,7 \end{vmatrix}$$

and

$$\Pi_{1;+}^{(0)} := \Pi_{1;+} - \Pi_{1;+}^{(1/2)} = |1\rangle \langle 1| + \begin{vmatrix} +2,3 \\ - \end{vmatrix} \begin{vmatrix} +2,3 \\ - \end{vmatrix} + \begin{vmatrix} +4,5,6,7 \\ - \end{vmatrix} \begin{vmatrix} +4,5,6,7 \\ - \end{vmatrix} + \begin{vmatrix} +8,9 \\ - \end{vmatrix} \begin{vmatrix} +8,9 \\ - \end{vmatrix} + |10\rangle \langle 10|$$

$$\Pi_{1;-}^{(0)} := \Pi_{1;-} - \Pi_{1;-}^{(1/2)} = \begin{vmatrix} +2 \\ -3 \end{vmatrix} \begin{vmatrix} +2 \\ -3 \end{vmatrix} + \begin{vmatrix} +4,5 \\ -6,7 \end{vmatrix} \begin{vmatrix} +4,5 \\ -6,7 \end{vmatrix} + \begin{vmatrix} +8 \\ -9 \end{vmatrix} \begin{vmatrix} +8 \\ -9 \end{vmatrix}.$$

The resulting reflection network consists of the three connected components shown in Fig. 5.2.

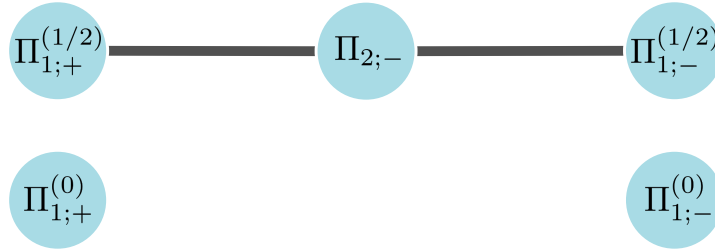


Figure 5.2: The reflection network from the generators of the group $U(\mathcal{G})$.

This, in turn, implies the following BPT

1			
$\begin{vmatrix} +2,3 \\ - \end{vmatrix}$			
$\begin{vmatrix} +4,5,6,7 \\ - \end{vmatrix}$			
$\begin{vmatrix} +8,9 \\ - \end{vmatrix}$			
10			
	$\begin{vmatrix} +2 \\ -3 \end{vmatrix}$		
	$\begin{vmatrix} +4,5 \\ -6,7 \end{vmatrix}$		
	$\begin{vmatrix} +8 \\ -9 \end{vmatrix}$		
		$\begin{vmatrix} +4,7 \\ -5,6 \end{vmatrix}$	$\begin{vmatrix} +4,6 \\ -5,7 \end{vmatrix}$

From the last block (bottom row) of the BPT we see that $U(\mathcal{G})$ acts as a two-dimensional

irrep on the subspace

$$\mathcal{H}_{\mu_3} := \text{span} \left\{ \begin{bmatrix} +4,7 \\ -5,6 \end{bmatrix}, \begin{bmatrix} +4,6 \\ -5,7 \end{bmatrix} \right\}.$$

Since the multiplicity of this irrep is one, the multiplicity subsystem \mathcal{H}_{ν_3} is absorbed into \mathcal{H}_{μ_3} . The two other blocks in the BPT identify two distinct one-dimensional irreps. Since these irreps are one-dimensional the irrep subsystems \mathcal{H}_{μ_1} and \mathcal{H}_{μ_2} are absorbed into the multiplicity subsystems

$$\begin{aligned} \mathcal{H}_{\nu_1} &:= \text{span} \left\{ |1\rangle, \begin{bmatrix} +2,3 \\ - \end{bmatrix}, \begin{bmatrix} +4,5,6,7 \\ - \end{bmatrix}, \begin{bmatrix} +8,9 \\ - \end{bmatrix}, |10\rangle \right\} \\ \mathcal{H}_{\nu_2} &:= \text{span} \left\{ \begin{bmatrix} +2 \\ -3 \end{bmatrix}, \begin{bmatrix} +4,5 \\ -6,7 \end{bmatrix}, \begin{bmatrix} +8 \\ -9 \end{bmatrix} \right\}. \end{aligned}$$

Overall, the $U(\mathcal{G})$ irrep decomposition of the Hilbert space is

$$\mathcal{H} \cong \mathcal{H}_{\nu_1} \oplus \mathcal{H}_{\nu_2} \oplus \mathcal{H}_{\mu_3}.$$

The two Hamiltonian terms $H = H_\nu + H_\mu$ are such that $H_\mu \in U(\mathcal{G})$ and $H_\nu \in U(\mathcal{G})'$. Therefore, with respect to the above irreps structure they reduce to

$$\begin{aligned} H_\mu &\cong I_{\nu_1} h_{\mu_1} \oplus I_{\nu_2} h_{\mu_2} \oplus H_{\mu_3} \\ H_\nu &\cong H_{\nu_1} \oplus H_{\nu_2} \oplus h_{\nu_3} I_{\mu_3}. \end{aligned}$$

Here $h_{\mu_1}, h_{\mu_2}, h_{\nu_3}$ are scalars and $H_{\nu_1}, H_{\nu_2}, H_{\mu_3}$ are 5×5 , 3×3 and 2×2 matrices respectively.

The important outcome from these analysis is that the dynamics are restricted to the irrep sectors $\mathcal{H}_{\nu_1}, \mathcal{H}_{\nu_2}, \mathcal{H}_{\mu_3}$. In particular, the sector \mathcal{H}_{ν_1} is spanned by the states $|1\rangle, \begin{bmatrix} +2,3 \\ - \end{bmatrix}, \begin{bmatrix} +4,5,6,7 \\ - \end{bmatrix}, \begin{bmatrix} +8,9 \\ - \end{bmatrix}, |10\rangle$ that dissect the graph into the layers of the binary trees. Explicit construction of the Hamiltonian term H_{ν_1} will show that it generates a CTQW on a one-dimensional line constructed from these layer states. In fact, we can present all the Hamiltonian terms as CTQW over the irrep states that we have found.

In Fig. 5.3 we can see the term H_{ν_1} represented by the bottom line, the term H_{ν_2} represented by the middle line, and the top vertical pair represents the term H_{μ_3} . The terms H_{ν_1} and H_{ν_2} traverse the graph across layers while H_{μ_3} generates dynamics inside the central layer. Since each term generates dynamics in a different orthogonal subspace, each connected component in this graph evolves independently from the others. In particular, this picture explains the direct propagation from root 1 to root 10 over a subspace that is exponentially smaller than the full tree. Therefore, what we have shown here is that this speed-up holds even in the non-symmetric version of the graph.



Figure 5.3: The irrep basis representation of the continuous-time quantum walk Hamiltonian over the binary trees in Fig. 5.1. In the irrep basis, the Hamiltonian decomposes into three terms that correspond to the three connected components. The connected component in the bottom row indicates the direct propagation from root 1 to root 10 that happens in a subspace exponentially smaller than the full tree. The symmetry breaking term of the Hamiltonian contributes to the dynamics in the top component, but it does not affect the dynamics in the bottom row.

5.2 Symmetry-agnostic reduction of Hamiltonians

In the previous section we have studied how the irreps structures of symmetries lead to the reduction of Hamiltonians. In this section we will demonstrate that it is not always necessary to identify the symmetries in order to reduce Hamiltonians. Instead, we will focus on directly finding the irreps structure that leads to the reduction.

The key takeaway from the discussion of symmetries is that the statement “ $U(\mathcal{G})$ is a symmetry of H ” can be rephrased as “ H is an element of the commutant algebra $U(\mathcal{G})'$ ”. It is the observation that H is an element of some non-trivial algebra that leads to the reduction; the fact that this algebra happens to be the commutant of a symmetry group is not important. Therefore, if we can recognize that “ H is an element of the algebra \mathcal{A} ”, for some non-trivial algebra \mathcal{A} , then we can reduce H using the irreps structure of \mathcal{A} .

We can specialize the above idea as follows: The most obvious algebra that we can use to restrict H is the algebra generated by its additive terms. That is, whenever we have $H = \sum_k \epsilon_k H_k$ we can say that H is an element of the algebra generated by the terms H_k and therefore it reduces to the irreps of $\langle \{H_k\} \rangle$. The illustrative example of the Scattering Algorithm that was given in Section 3.1 is exactly such a symmetry-agnostic reduction of Hamiltonians.

As another simple example, consider again the spin-orbit coupled system $\mathcal{H} = \underline{l} \otimes \underline{\frac{1}{2}}$ for some integer l and the Hamiltonian

$$H(\epsilon) = L_z \otimes S_z + \epsilon I \otimes S_x$$

for arbitrary real constant ϵ . Instead of identifying the symmetries (which will still require finding the irreps structure) we recognize that for all ϵ , $H(\epsilon)$ is an element of the algebra \mathcal{A} generated by $L_z \otimes S_z$ and $I \otimes S_x$. In the last example of Section 4.2 we have derived the irreps structure of \mathcal{A} to be given by the BPT

$$\begin{array}{|c|c|} \hline l, \uparrow & l, \downarrow \\ \hline -l, \downarrow & -l, \uparrow \\ \hline \end{array} \quad \ddots \quad \begin{array}{|c|c|} \hline 1, \uparrow & 1, \downarrow \\ \hline -1, \downarrow & -1, \uparrow \\ \hline \end{array} \quad \begin{array}{|c|} \hline 0, + \\ \hline \end{array} \quad \begin{array}{|c|} \hline 0, - \\ \hline \end{array}$$

(note that in Section 4.2 this BPT was transposed since we were interested in the commutant of \mathcal{A}). This BPT identifies the irrep decomposition

$$\mathcal{H} \cong |0, -\rangle \oplus |0, +\rangle \oplus \left[\bigoplus_{q=1}^l \mathcal{H}_{\nu_q} \otimes \mathcal{H}_{\mu_q} \right],$$

where both \mathcal{H}_{ν_q} and \mathcal{H}_{μ_q} are two-dimensional virtual subsystems for all $q = 1, \dots, l$.

Since $H(\epsilon) \in \mathcal{A}$, this irreps structure implies that the Hamiltonian reduces to

$$H(\epsilon) = h_-(\epsilon) |0, -\rangle \langle 0, -| + h_+(\epsilon) |0, +\rangle \langle 0, +| + \bigoplus_{q=1}^l I_{\nu_q} \otimes H_{\mu_q}(\epsilon)$$

where $h_{\pm}(\epsilon)$ are scalars, $H_{\mu_q}(\epsilon)$ are 2×2 matrices and I_{ν_q} are 2×2 identities. The explicit matrix elements are then given by

$$h_{\pm}(\epsilon) = \langle 0, \pm | H(\epsilon) | 0, \pm \rangle = \pm \frac{\epsilon}{2}$$

$$H_{\mu_q}(\epsilon) = \begin{pmatrix} \langle q, \uparrow | H(\epsilon) | q, \uparrow \rangle & \langle q, \uparrow | H(\epsilon) | q, \downarrow \rangle \\ \langle q, \downarrow | H(\epsilon) | q, \uparrow \rangle & \langle q, \downarrow | H(\epsilon) | q, \downarrow \rangle \end{pmatrix} = \frac{1}{2} \begin{pmatrix} q & \epsilon \\ \epsilon & -q \end{pmatrix}.$$

Thus, for each $q = 1, \dots, l$, the Hamiltonian terms $L_z \otimes S_z$ and $\epsilon I \otimes S_x$ act as $q\sigma_z$ and $\epsilon\sigma_x$ (where σ_x, σ_z are Pauli matrices) on the virtual subsystems \mathcal{H}_{μ_q} . If ϵ is a tunable parameter then we can use $H_{\mu_q}(\epsilon)$ as the control Hamiltonian for the logical qubit encoded in \mathcal{H}_{μ_q} . If, on the other hand, ϵ is the uncontrollable random noise then \mathcal{H}_{ν_q} can be used as

a decoherence free subsystem.

In order to further demonstrate the potential applications of the symmetry-agnostic approach, we will analyze two examples dealing with the qubit encodings in quantum dot arrays.

The idea of qubit implementations in quantum dots was first proposed in [66]. In this setting, individual electrons are trapped in manufactured potential wells (referred to as “dots”) where they can be controlled by the electric potentials that set the barriers between adjacent dots, and by applying external magnetic fields. The overall dynamics of such systems are described by the Hubbard model [18], where the degrees of freedom are the occupation numbers of electrons in the individual dots (also referred to as “orbital” or “charge” degree of freedom), and the spin degrees of freedom.

Because of the multiple degrees of freedom, there is a variety of possible qubit encodings in quantum dots; see [85] for an overview. Different qubit encodings have different advantages and disadvantages⁸ and it is not our goal to explore these issues here. What we will focus on is how to identify the possible qubit encodings in the first place, which at the very least should accommodate arbitrary Bloch sphere rotations.

In the following two examples we will consider the effective control Hamiltonian of a quantum dot system and find the possible qubit encodings where arbitrary Bloch sphere rotations can be performed. This will be achieved by adopting the symmetry-agnostic approach and finding out how the independent terms of the Hamiltonian can be reduced. The reduced subspaces (or subsystems) of the independent terms will then identify the possible encodings.

Example 1

In this example we will consider the charge quadrupole qubit that was proposed in [41]. The charge quadrupole qubit is designed to be a more robust version of the charge dipole qubit against the electric potential noise. By taking the symmetry-agnostic approach we will show that there is a continuum of possible qubit encodings between the charge quadrupole and the charge dipole cases that has not been considered. Due to the systematic nature of this approach we will also rule out the possibility of any other charge-qubit encodings in this setting.

Our system consists of a single electron trapped in a triple quantum dot where it can occupy the dots $|1\rangle$, $|2\rangle$, $|3\rangle$. We will disregard the spin degree of freedom so our Hilbert space is just $\mathcal{H} = \text{span}\{|1\rangle, |2\rangle, |3\rangle\}$. As discussed in [41], the effective control Hamiltonian has five tunable parameters

⁸The key characteristics are the levels and sources of noise from gate operations and the complexity of two-qubit gates.

$$H = \begin{pmatrix} u_1 & t_{12} & 0 \\ t_{12} & u_2 & t_{23} \\ 0 & t_{23} & u_3 \end{pmatrix} = \begin{pmatrix} \epsilon_d & t_{12} & 0 \\ t_{12} & \epsilon_q & t_{23} \\ 0 & t_{23} & -\epsilon_d \end{pmatrix} + \epsilon_0 I$$

where t_{12}, t_{23} are the tunneling amplitudes, and u_1, u_2 , and u_3 are the dot potentials that can be re-stated as the detuning parameters

$$\epsilon_d = \frac{u_1 - u_3}{2} \quad \epsilon_q = u_2 - \frac{u_1 + u_3}{2} \quad \epsilon_0 = \frac{u_1 + u_3}{2}.$$

The independent Hamiltonian terms here are

$$T_{12} := \begin{pmatrix} 0 & 1 & 0 \\ 1 & 0 & 0 \\ 0 & 0 & 0 \end{pmatrix} \quad T_{23} := \begin{pmatrix} 0 & 0 & 0 \\ 0 & 0 & 1 \\ 0 & 1 & 0 \end{pmatrix} \quad D := \begin{pmatrix} 1 & 0 & 0 \\ 0 & 0 & 0 \\ 0 & 0 & -1 \end{pmatrix} \quad Q := \begin{pmatrix} 0 & 0 & 0 \\ 0 & 1 & 0 \\ 0 & 0 & 0 \end{pmatrix},$$

so

$$H = t_{12}T_{12} + t_{23}T_{23} + \epsilon_d D + \epsilon_q Q$$

and we have dropped the inconsequential identity term.

In principle, we can assert that $H \in \langle T_{12}, T_{23}, D, Q \rangle$ but it is not a very helpful assertion because, as we will see shortly, the algebra $\langle T_{12}, T_{23}, D, Q \rangle$ is the trivial irreducible algebra $\mathcal{L}(\mathcal{H})$. However, since there are excessive degrees of freedom here (we only need two independent parameters for arbitrary Bloch sphere rotations) we can constrain some of the parameters such that the constrained terms will become reducible.

First, we show that t_{12} and t_{23} cannot be both independent because the algebra $\langle T_{12}, T_{23} \rangle$ is irreducible. The spectral projections of $T_{ij} = \Pi_{ij,+} - \Pi_{ij,-}$ are given by

$$\Pi_{ij,+} := \begin{vmatrix} +i, j \\ - \end{vmatrix} \begin{vmatrix} +i, j \\ - \end{vmatrix} \quad \Pi_{ij,-} := \begin{vmatrix} +i \\ -j \end{vmatrix} \begin{vmatrix} +i \\ -j \end{vmatrix}$$

where we have used the shorthand state notation of Eq. (5.5). Since these spectral projections are rank-1 they are all reflecting, resulting in the reflection network shown in Fig. 5.4.

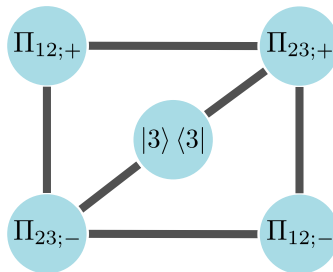


Figure 5.4: The reflection network from the generators T_{12}, T_{23} .

Note that both T_{12} and T_{23} are not supported on the whole Hilbert space ($\Pi_{ij;+} + \Pi_{ij;-} \neq I$) so the resulting reflection network was incomplete. The projection $|3\rangle\langle 3|$ was added by the completion procedure described in Section 3.2.3. The resulting BPT is

$$\begin{array}{|c|c|c|} \hline +1,2 & +1 & \\ - & -2 & 3 \\ \hline \end{array}$$

which defines the full operator algebra $\mathcal{L}(\mathcal{H})$.⁹ Therefore, the action of both T_{12} and T_{23} is irreducible on \mathcal{H} .

Assuming that t_{12} and t_{23} have the same sign, we constrain these two independent parameters to be $t_{12} = \alpha t$ and $t_{23} = (1 - \alpha)t$ for a constant $0 \leq \alpha \leq 1$ and the new common parameter t . The new constrained term is

$$T_\alpha := \alpha T_{12} + (1 - \alpha) T_{23} = \begin{pmatrix} 0 & \alpha & 0 \\ \alpha & 0 & 1 - \alpha \\ 0 & 1 - \alpha & 0 \end{pmatrix}$$

so the Hamiltonian is $H = tT_\alpha + \epsilon_d D + \epsilon_q Q$.

For $\alpha = 0, 1$ the problem reduces to a double quantum dot where (assuming $\alpha = 1$) the positions $|1\rangle, |2\rangle$ identify the logical qubit basis $|0_L\rangle, |1_L\rangle$ and

$$H = \begin{pmatrix} \epsilon_d & t & 0 \\ t & \epsilon_q & 0 \\ 0 & 0 & -\epsilon_d \end{pmatrix}.$$

Thus, $T_{\alpha=1} = T_{12}$ serves as the Pauli σ_x operator and D or Q can serve as $\frac{1}{2}(I \pm \sigma_z)$ operators. This encoding is known as charge dipole.

For $0 < \alpha < 1$ we observe that the parameters ϵ_d and ϵ_q also cannot be both independent since the three terms T_α, D, Q cannot be reduced onto a two-dimensional subspace. We can see this by considering the three spectral projections $\Pi_{i=1,2,3} := |i\rangle\langle i|$ provided by D and Q . All three $\Pi_{i=1,2,3}$ are rank-1 and orthogonal but we also have to include the spectral projections of T_α . Since $\Pi_1 T_\alpha \Pi_2 \neq 0$ and $\Pi_2 T_\alpha \Pi_3 \neq 0$ the resulting reflection network will have a single connected component that contains all three projections $\Pi_{i=1,2,3}$. The resulting BPT will therefore be that of the trivial operator algebra $\mathcal{L}(\mathcal{H})$ which implies the irreducibility of $\langle T_\alpha, D, Q \rangle$.

Assuming that ϵ_d and ϵ_q can have opposite signs, we constrain them as $\epsilon_d = \beta\epsilon$ and $\epsilon_q = (1 - |\beta|)\epsilon$ for a constant $-1 \leq \beta \leq 1$ and the new common parameter ϵ . The new

⁹This is always the case when the reflection network consists of a single connected component of rank-1 projections and is supported on the whole \mathcal{H} .

constrained term is

$$E_\beta := \beta D + (1 - |\beta|) Q = \begin{pmatrix} \beta & 0 & 0 \\ 0 & 1 - |\beta| & 0 \\ 0 & 0 & -\beta \end{pmatrix}$$

so the Hamiltonian is $H = tT_\alpha + \epsilon E_\beta$.

For $\beta \neq 0, \pm 1, \pm \frac{1}{2}$ it is easy to see the spectral projections of E_β are still the three rank-1 projections $\Pi_{i=1,2,3}$ so the algebra $\langle T_\alpha, E_\beta \rangle$ is still irreducible. It is less obvious that $\langle T_\alpha, E_\beta \rangle$ is irreducible even for $\beta = \pm 1, \pm \frac{1}{2}$, however, that is also the case. When $\beta = \pm 1$ the projection Π_2 is initially not a spectral projection of E_β but the resulting reflection network will be incomplete. The completion procedure will add Π_2 and we will have $\Pi_{i=1,2,3}$ once again in the same connected component. When $\beta = \pm \frac{1}{2}$ one of the spectral projections of E_β is rank-2 but it will scatter with the spectral projection of T_α and form a single connected component of rank-1 projections. Either way, for all $\beta \neq 0$ we will have a single connected component of rank-1 projections which implies the irreducibility of $\langle T_\alpha, E_\beta \rangle$.

We are therefore left with $\beta = 0$, that is, $E_{\beta=0} = Q$ and the only spectral projection of Q is Π_2 . The eigenvalues of T_α are $\pm \lambda_\alpha = \pm \sqrt{\alpha^2 + (1 - \alpha)^2}$ and the eigenvectors are

$$|\alpha; \pm\rangle := \frac{\alpha |1\rangle \pm \lambda_\alpha |2\rangle + (1 - \alpha) |3\rangle}{\lambda_\alpha \sqrt{2}}.$$

The two spectral projections of T_α are therefore $\Pi_{\alpha;\pm} := |\alpha; \pm\rangle \langle \alpha; \pm|$ and the reflection network of the algebra $\langle T_\alpha, Q \rangle$ is shown in Fig. 5.5.

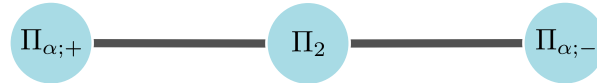


Figure 5.5: The reflection network of $\langle T_\alpha, Q \rangle$.

The resulting BPT is

$$\boxed{\alpha; + \quad \alpha; -}$$

so T_α and Q reduce to the subspace spanned by $|\alpha; +\rangle$ and $|\alpha; -\rangle$. There is a freedom of choice for the logical qubit basis, but if we want to be consistent with the choice we made for the case $\alpha = 0, 1$ we will choose

$$|0_L\rangle = \frac{|\alpha; +\rangle + |\alpha; -\rangle}{\sqrt{2}} = \frac{\alpha |1\rangle + (1 - \alpha) |3\rangle}{\lambda_\alpha}$$

$$|1_L\rangle = \frac{|\alpha; +\rangle - |\alpha; -\rangle}{\sqrt{2}} = |2\rangle.$$

The operator T_α then acts on $|0_L\rangle, |1_L\rangle$ as $\lambda_\alpha \sigma_x$, and the operator Q acts as $\frac{1}{2}(I - \sigma_z)$. By turning the terms T_α and Q on and off we can perform arbitrary Bloch sphere rotations.

In [41] the authors have identified the charge quadrupole qubit that corresponds to the case of $\alpha = \frac{1}{2}$. Here, using the symmetry-agnostic approach, we have identified qubit encodings for the continuum $0 \leq \alpha \leq 1$ where the edge cases $\alpha = 0, 1$ correspond to the charge dipole encodings.

Example 2

In quantum dot arrays where each dot is occupied by one electron, a controlled variation of electric potentials allows the realization of Heisenberg interactions between adjacent electrons [66]. If the qubits are encoded in the spin degree of freedom of the trapped electrons (as envisioned in [66]), then in addition to the electric potentials the qubit gate operations require the use of variable magnetic fields. The necessity of variable magnetic fields complicates the design and reduces the performance of this qubits due to the additional sources of noise and the relatively weak coupling of the magnetic field to the electron spins.

The surprising resolution to this issue was brought forward by DiVincenzo *et al.* [33] (see also [7]), where the encoding of a single qubit in a subspace of three (or four) electron spins was proposed. The key advantage of this encoding is that all qubit gates can be performed with the Heisenberg interaction only, which in quantum dots is realized by electric potentials without the need in variable magnetic fields.

In the following, we will first discuss how this qubit encoding is identified by the irreps of the $SU(2)$ symmetry of the Heisenberg interaction. Then, by adopting the symmetry-agnostic approach we will show that additional encodings in four spins can be found. These additional encodings are not identified by the $SU(2)$ symmetry alone and they were not recognized in the original proposal [7].

The basic idea in [33, 7] is to encode the qubit in a non-periodic spin-chain of three (as in [33]) or four (as in [7]) spins with tunable nearest neighbor interactions

$$H = \epsilon_{12} \vec{S}_1 \cdot \vec{S}_2 + \epsilon_{23} \vec{S}_2 \cdot \vec{S}_3 + \epsilon_{34} \vec{S}_3 \cdot \vec{S}_4$$

(the term $\epsilon_{34} \vec{S}_3 \cdot \vec{S}_4$ is only relevant for the four-spin case). Since H is an element of the commutant of the $SU(2)$ group, it reduces to the irreps of this commutant (these structures are sometimes referred to as decoherence free subspaces and subsystems). The possible qubit encodings can therefore be identified from the irreps of the commutant of $SU(2)$.

The commutant's irreps are given by the transposition of the BPT of the $SU(2)$ irreps. In the total spin basis $|j, \alpha, m\rangle$, the transposed BPT for the three-spin case is

$$\begin{array}{c}
\begin{array}{|c|} \hline \frac{3}{2}, +\frac{3}{2} \\ \hline \vdots \\ \hline \frac{3}{2}, -\frac{3}{2} \\ \hline \end{array} \\
\begin{array}{|c|c|} \hline \frac{1}{2}, s, +\frac{1}{2} & \frac{1}{2}, t, +\frac{1}{2} \\ \hline \frac{1}{2}, s, -\frac{1}{2} & \frac{1}{2}, t, -\frac{1}{2} \\ \hline \end{array} \\
\begin{array}{ccc} \downarrow & & \downarrow \\ \hline \begin{array}{|c|c|} \hline 0_L & 1_L \\ \hline \end{array} & & \hline \end{array}
\end{array} \cdot$$

From this BPT we can see that in the three-spin case, the candidates for the qubit encodings are the two-dimensional invariant subspaces of $j = \frac{1}{2}$ and $m = \frac{1}{2}$ or $j = \frac{1}{2}$ and $m = -\frac{1}{2}$ (top and bottom rows of the right block). As we have seen in Eq. (5.3), the Heisenberg interaction Hamiltonian acts on these subspaces as

$$H_{\nu_{1/2}} = \frac{1}{4} \begin{pmatrix} -3\epsilon_{23} & \sqrt{3}\epsilon_{12} \\ \sqrt{3}\epsilon_{12} & \epsilon_{23} - 2\epsilon_{12} \end{pmatrix} = \frac{\epsilon_{12}}{4} (\sqrt{3}\sigma_x + \sigma_z - I) + \frac{\epsilon_{23}}{8} (\sigma_z + 5I).$$

One can change the basis inside these subspaces to get a more convenient form of $H_{\nu_{1/2}}$ in terms of Pauli matrices. Regardless of the choice of basis, we can implement arbitrary qubit rotations in this subspace by controlling the couplings ϵ_{12} , ϵ_{23} .

Thus, the irreps of the commutant of $SU(2)$ identify the two-dimensional subspaces on which the independent interaction terms of the Hamiltonian can be reduced. Note that in the case of three spins there are exactly two independent parameters ϵ_{12} , ϵ_{23} which is the minimal number of parameters needed to control a qubit. We will now see that with four spins, where there are three independent parameters, we can utilize the extra degree of freedom to find qubit subspaces that are not captured by the $SU(2)$ symmetry alone.¹⁰

Let us first identify the four-spin qubit encoding using $SU(2)$ symmetry. In this case, the representation of $SU(2)$ decomposes as

$$\begin{aligned}
\frac{1}{2}^{\otimes 4} &= \left[\frac{1}{2} \otimes \frac{1}{2} \right] \otimes \left[\frac{1}{2} \otimes \frac{1}{2} \right] = [\underline{1} \oplus \underline{0}] \otimes [\underline{1} \oplus \underline{0}] \\
&= (\underline{1} \otimes \underline{1}) \oplus (\underline{1} \otimes \underline{0}) \oplus (\underline{0} \otimes \underline{1}) \oplus (\underline{0} \otimes \underline{0}) \\
&= (\underline{2} \oplus \underline{1} \oplus \underline{0}) \oplus (\underline{1}) \oplus (\underline{1}) \oplus (\underline{0}).
\end{aligned}$$

In order to distinguish the different variant of equivalent irreps we will use the labels $\alpha = tt, ts, st, ss$ that specify whether the left and right pairs of spins are in the singlet or triplet states. For $j = 2$ there are no variants to distinguish and $\alpha = tt$; for $j = 1$ we have

¹⁰In the case of three spins in a periodic configuration we could also have three independent parameters but the Hilbert space is too small to take advantage of that.

interaction terms of the left and right pairs of spins are diagonal in the $|\alpha\rangle$ basis

$$\begin{aligned} [\vec{S}_1 \cdot \vec{S}_2] &= \frac{1}{4} |tt\rangle \langle tt| + \frac{1}{4} |ts\rangle \langle ts| - \frac{3}{4} |st\rangle \langle st| \\ [\vec{S}_3 \cdot \vec{S}_4] &= \frac{1}{4} |tt\rangle \langle tt| + \frac{1}{4} |st\rangle \langle st| - \frac{3}{4} |ts\rangle \langle ts|. \end{aligned}$$

The interaction term of the central pair of spins $\vec{S}_2 \cdot \vec{S}_3$ is similarly diagonal but in a different basis

$$[\vec{S}_2 \cdot \vec{S}_3] = \frac{1}{4} |t\rangle \langle t| + \frac{1}{4} |s\rangle \langle s| - \frac{3}{4} |t\rangle \langle s|.$$

In this notation the top letter t or s refers to the triplet or singlet state of the central pair of spins (2, 3), and the bottom letter refers to the state of the pair of boundary spins (1, 4). Explicitly these are

$$\begin{aligned} |t_s\rangle &= \frac{|\uparrow\uparrow\downarrow\rangle - |\downarrow\uparrow\uparrow\rangle}{\sqrt{2}} = \frac{|ts\rangle + |st\rangle - \sqrt{2}|tt\rangle}{2} \\ |s_t\rangle &= \frac{|\uparrow\downarrow\uparrow\rangle - |\uparrow\uparrow\downarrow\rangle}{\sqrt{2}} = \frac{|ts\rangle + |st\rangle + \sqrt{2}|tt\rangle}{2} \\ |t\rangle &= \frac{|\uparrow\uparrow\downarrow\rangle + |\uparrow\downarrow\uparrow\rangle - |\uparrow\uparrow\uparrow\rangle - |\downarrow\uparrow\uparrow\rangle}{2} = \frac{|st\rangle - |ts\rangle}{\sqrt{2}}. \end{aligned}$$

Let us now constrain the two independent terms $\vec{S}_1 \cdot \vec{S}_2$ and $\vec{S}_3 \cdot \vec{S}_4$ into one independent term. That is, for some $0 \leq \beta \leq 1$ we have the new term

$$[S_\beta] := \beta [\vec{S}_1 \cdot \vec{S}_2] + (1 - \beta) [\vec{S}_3 \cdot \vec{S}_4] = \frac{1}{4} |tt\rangle \langle tt| + \left(\beta - \frac{3}{4}\right) |ts\rangle \langle ts| + \left(\frac{1}{4} - \beta\right) |st\rangle \langle st|.$$

Note that the degeneracy of the eigenspaces of $[S_\beta]$ changes when $\beta = 0, \frac{1}{2}, 1$. For $\beta \neq 0, \frac{1}{2}, 1$, its spectral projections are $|tt\rangle \langle tt|$, $|ts\rangle \langle ts|$, $|st\rangle \langle st|$ which end up in a fully connected reflection network if we scatter them with the spectral projections of $[\vec{S}_2 \cdot \vec{S}_3]$. This means that $[S_\beta]$ and $[\vec{S}_2 \cdot \vec{S}_3]$ are irreducible for $\beta \neq 0, \frac{1}{2}, 1$.

For $\beta = 1$ or $\beta = 0$ we disregard one of the interactions $[\vec{S}_3 \cdot \vec{S}_4]$ or $[\vec{S}_1 \cdot \vec{S}_2]$ and focus on the interactions between three spins. This will lead to a reduction of the remaining two terms onto a two dimensional subspace inside the $j = 1, m = 1$ subspace. We will not elaborate on this reduction since it is not much different than the three-spin encoding.

The genuinely different encoding that is possible here is for $\beta = \frac{1}{2}$. The spectral projections of $[S_{\beta=\frac{1}{2}}]$ are

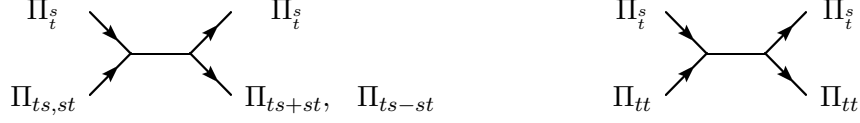
$$\Pi_{ts,st} = |ts\rangle \langle ts| + |st\rangle \langle st| \quad \Pi_{tt} = |tt\rangle \langle tt|$$

and the spectral projections of $[\vec{S}_2 \cdot \vec{S}_3]$ are

$$\Pi_{t_t} = |t\rangle \langle t| + |s\rangle \langle s| \quad \Pi_t = |t\rangle \langle t|.$$

Since both pairs of spectral projections sum to the identity on this subspace, one of these projections is redundant so we drop $\Pi_{t,ts}$.

The scattering calculation is then



where the new projections are $\Pi_{ts \pm st} := |ts \pm st\rangle \langle ts \pm st|$ and

$$|ts \pm st\rangle := \frac{|ts\rangle \pm |st\rangle}{\sqrt{2}}.$$

The resulting reflection network is shown in Fig. 5.6.

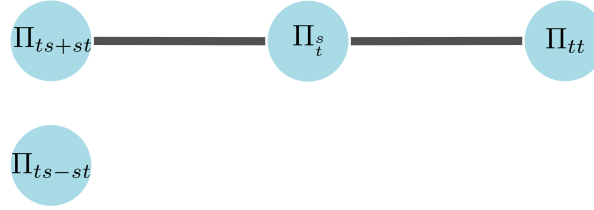


Figure 5.6: The reflection network from the spectral projections of $[\vec{S}_2 \cdot \vec{S}_3]$ and $[S_{\beta=\frac{1}{2}}]$.

Therefore, in the three-dimensional subspace of $j = 1, m = 1$ there is a two-dimensional subspace on which both $[S_{\beta=\frac{1}{2}}]$ and $[\vec{S}_2 \cdot \vec{S}_3]$ reduce. This subspace is identified by the BPT constructed from the reflection network in Fig. 5.6:

$$\begin{array}{c} \boxed{ts - st} \\ \downarrow \\ \begin{array}{|c|c|} \hline ts + st & tt \\ \hline \end{array} \\ \downarrow \quad \downarrow \\ \begin{array}{|c|c|} \hline 0_L & 1_L \\ \hline \end{array} \end{array}.$$

The possible qubit basis for $j = 1, m = 1$ are then

$$\begin{aligned} |0_L\rangle &= |ts + st\rangle = \frac{|\uparrow\downarrow\uparrow\uparrow\rangle - |\downarrow\uparrow\uparrow\uparrow\rangle + |\uparrow\uparrow\uparrow\downarrow\rangle - |\uparrow\uparrow\downarrow\uparrow\rangle}{2} \\ |1_L\rangle &= |tt\rangle = \frac{|\uparrow\downarrow\uparrow\uparrow\rangle + |\downarrow\uparrow\uparrow\uparrow\rangle - |\uparrow\uparrow\uparrow\downarrow\rangle - |\uparrow\uparrow\downarrow\uparrow\rangle}{2}. \end{aligned}$$

It is easy to verify that the Hamiltonian terms restricted to this subspace act as

$$\begin{aligned} \left[S_{\beta=\frac{1}{2}} \right] &= -\frac{1}{4} |0_L\rangle \langle 0_L| + \frac{1}{4} |1_L\rangle \langle 1_L| = -\frac{1}{4} \sigma_z \\ \left[\vec{S}_2 \cdot \vec{S}_3 \right] &= \frac{1}{4} |+_L\rangle \langle +_L| - \frac{3}{4} |-_L\rangle \langle -_L| = \frac{1}{2} \sigma_x - \frac{1}{4} I \end{aligned}$$

where $|\pm_L\rangle \propto |0_L\rangle \pm |1_L\rangle$. Thus, we have identified a controllable qubit encoded in the subspace of $j = 1, m = 1$. Similar encodings can be found in the subspaces of $j = 1, m = 0$ and $j = 1, m = -1$.

In retrospect, we recognize that the new qubit encodings can be found by imposing the permutation symmetry that swaps both $1 \leftrightarrow 4$ and $2 \leftrightarrow 3$ spins.¹² In order to comply with this symmetry we would have to constrain the independent parameters $\epsilon_{12} = \epsilon_{34}$, which is the same as fixing $\beta = \frac{1}{2}$. Then, the irreps of the commutant of the combined symmetry of $SU(2)$ and these permutations would point to this qubit encoding.

In the symmetry-agnostic approach we do not have to come up with the additional symmetries to impose and construct the combined irreps. Instead, we follow the systematic procedure where we introduce the constraint β , note the special values $\beta = 0, \frac{1}{2}, 1$ where the degeneracies change, and then identify the qubit by reducing the constrained terms with the Scattering Algorithm.

¹²The original H does not have this symmetry but it has redundant degrees of freedom that can be fixed by imposing additional symmetries.

Chapter 6

Beyond operator algebras

In the previous chapters we have formulated the idea of reduction based on the solid mathematical framework of operator algebras. In this chapter we will push the formalism of bipartition tables to its limits and advance the idea of reduction beyond operator algebras.

The fact that certain subspaces of observables, not algebras, can identify new notions of bipartition and entanglement, has been brought forward by Barnum, Viola, *et al.* in [10, 95, 93] (see also [4]). The need for generalized bipartition beyond tensor products and operator algebras has also been expressed in [43], motivated by the definition of local entanglement in the theories of quantum gravity.

In the following, we will derive such generalized notion of bipartition by relaxing the rigid structure of bipartition tables and operator algebras. Despite the relaxation, the essence of bipartition tables will remain the same and the resulting structure naturally generalizes tensor products to become *partial* bipartitions, and virtual subsystems to become *partial* subsystems. The associated state reductions produced by tracing out a partial subsystem are analogous to coarse-graining of classical probability distributions. Such reductions will therefore be called *quantum coarse-graining*. The ideas of quantum coarse-graining were originally published in [52].

Similar adaptations of the classical notion of coarse-graining in quantum theory have been explored in [37, 34, 30] (for other approaches to the quantum notion of coarse-graining see [89, 32, 35]). Our main contribution is in deriving the general operational meaning of such notion of coarse-graining in quantum theory, and rigorously demonstrating its relation to the analogous classical notion.

Before formally introducing the new ideas, we will begin in Section 6.1 with a motivating example that demonstrates why the operator-algebraic structure is too rigid and how it can be relaxed. In Section 6.2 we will proceed with an illustrative example of the classical notion of coarse-graining. We will then generalize the formalism of bipartition tables to partial bipartitions and make the connection with classical coarse-graining. Finally, we will derive the operational meaning of quantum coarse-graining in Theorem 6.3 which generalizes the operational meaning of the partial trace map beyond tensor products.

6.1 Motivating example

In this section we will investigate a simple example where the operator-algebraic approach falls short of providing a satisfying solution. We will see how the irreps structure of operator algebras can be too rigid and that a relaxation of this structure has benefits. This motivates a more serious investigation of such relaxed structures that we will end up calling partial bipartitions in the next section.

Consider a communication scenario where Alice has a spin-1 system in the state

$$|\psi\rangle = \alpha_1 |1\rangle + \alpha_0 |0\rangle + \alpha_{-1} |-1\rangle$$

(the basis are the eigenvectors of the z -component of the spin operator) and she wants to send it to Bob. Unfortunately, Alice cannot send the spin-1 system directly but she can prepare and send a single qubit in any (pure or mixed) state ρ_{qubit} . It is, of course, not possible to genuinely encode a three-dimensional system into a two-dimensional one without losing some information. So, Alice has to prioritize the observables of the spin-1 system that she wants to preserve.

Assume that Alice's top priority is the observable

$$Z = |0\rangle\langle 0| - |1\rangle\langle 1| - |-1\rangle\langle -1|$$

that distinguishes the state $|0\rangle$ from the rest. Alice can then encode

$$|\psi\rangle \mapsto \rho_{qubit} = \begin{pmatrix} |\alpha_0|^2 & 0 \\ 0 & |\alpha_1|^2 + |\alpha_{-1}|^2 \end{pmatrix}$$

and Bob can recover all the statistical information about Z from the Pauli observable σ_z . This encoding treats the qubit as a classical bit so the interesting question here is how can Alice take advantage of the full qubit to communicate additional information about the spin-1 system.

Let us first try the operator-algebraic approach to address this question.

We may consider the encoding into a qubit as a quantum state reduction. If only the observable Z is considered, the state reduction is given by the irreps structure of the algebra $\langle Z \rangle$:

$$\begin{array}{c} \boxed{0} \\ \downarrow \\ \boxed{0_L} \end{array} \quad \begin{array}{c} \boxed{1} \\ \boxed{-1} \\ \downarrow \\ \boxed{1_L} \end{array} .$$

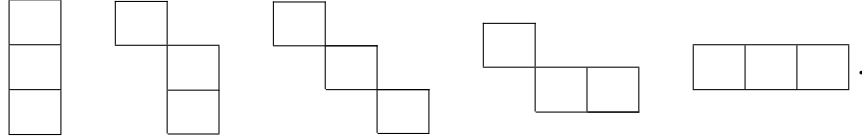
The minimal isometries here are just the spectral projections of Z

$$\Pi_0 := |0\rangle\langle 0| \quad \Pi_{\pm 1} := |1\rangle\langle 1| + |-1\rangle\langle -1|.$$

Using the general construction of state reduction maps in Eq. 4.9, we will get the encoding we know

$$|\psi\rangle \mapsto \rho_{qubit} = \begin{pmatrix} \langle\psi|\Pi_0|\psi\rangle & \\ & \langle\psi|\Pi_{\pm 1}|\psi\rangle \end{pmatrix} = \begin{pmatrix} |\alpha_0|^2 & 0 \\ 0 & |\alpha_1|^2 + |\alpha_{-1}|^2 \end{pmatrix}.$$

If in addition to Z Alice wants encode information about any other observable X , she has to consider the irreps of $\langle Z, X \rangle$. There is, however, only five “shapes” that the BPT can have in a three-dimensional Hilbert space. The possibilities are



The first shape (from the left) corresponds to a reduction onto a one-dimensional system that preserves no information. The second shape is what we got for $\langle Z \rangle$. Therefore, unless X has the same spectral projections as Z (which makes it the same observable up to eigenvalues), the irreps structure of $\langle Z, X \rangle$ will have one of the last three shapes. The last three shapes, however, correspond to reductions onto a three-dimensional system so it will not work as a qubit encoding.

Therefore, the operator-algebraic perspective suggests that it is not possible to encode in a qubit another (distinct) observable together with Z .

We should now point out that in the operator-algebraic approach the state reduction map is not just concerned with the generators of the algebra but with the whole algebra. For $\langle Z \rangle$ the associated state reduction map preserves the expectation values not just of Z , but also of Z^n for all n . In particular, the spectral projections Π_0 and $\Pi_{\pm 1}$ are also in $\langle Z \rangle$ so their expectation values, which are the probabilities of the two outcomes, are also preserved. This suggests that if we want to include another observable X we may be able to compromise on preserving only its expectation values without preserving the probabilities of the individual outcomes.

This brings us to the main point: The irreps structure of operator algebras is too rigid for some tasks and a more flexible structure is desired. Since BPTs are the visual representations of irreps structures, we can relax the rigidity of irreps structures by relaxing the rigidity of bipartition tables.

By their original Definition 2.21, BPTs can only have a block diagonal form where each block is rectangular, that is, each row (or column) in the block has the same number of cells. In Lemma 2.23 we have showed that all operator algebras correspond to BPTs defined this way. We will now relax the requirement for BPT blocks to be rectangular and such BPTs

will not correspond to any operator algebra.

Consider, for example, the arrangement (and the implied state reduction) given by the BPT

$$\begin{array}{|c|c|} \hline 0 & 1 \\ \hline & -1 \\ \hline \end{array} \begin{array}{c} \downarrow \\ \downarrow \end{array} \begin{array}{|c|c|} \hline 0_L & 1_L \\ \hline \end{array}.$$

There is only one block here and the number of cells in the first and second rows is not the same. Such BPT cannot arise from any operator algebra, however, we can still use this arrangement to construct partial isometries (we will not call them “minimal” anymore because we no longer have an algebra). Following the original construction of isometries from BPTs given in Eq. (2.6), we get the projections Π_0 and $\Pi_{\pm 1}$ as before, but now we also get the proper isometries

$$S_{0,1} := |0\rangle \langle 1| \quad S_{1,0} := |1\rangle \langle 0|.$$

The state reduction map is defined as before only now we have the additional proper isometries that preserve some of the coherences

$$|\psi\rangle \mapsto \rho_{qubit} = \begin{pmatrix} \langle \psi | \Pi_0 | \psi \rangle & \langle \psi | S_{1,0} | \psi \rangle \\ \langle \psi | S_{0,1} | \psi \rangle & \langle \psi | \Pi_{\pm 1} | \psi \rangle \end{pmatrix} = \begin{pmatrix} |\alpha_0|^2 & \alpha_1^* \alpha_0 \\ \alpha_0^* \alpha_1 & |\alpha_1|^2 + |\alpha_{-1}|^2 \end{pmatrix}.$$

It is easy to verify that ρ_{qubit} is a positive operator of trace 1, so it is a proper quantum state.

As before, Bob can recover all the statistical information about Z (including the probabilities of the individual outcomes) from the Pauli observable σ_z . Since the coherence terms between $|0\rangle$ and $|1\rangle$ are also preserved, Bob can now recover the expectation values of observables such as

$$\begin{aligned} X &:= S_{1,0} + S_{0,1} = |1\rangle \langle 0| + |0\rangle \langle 1| \\ Y &:= iS_{1,0} - iS_{0,1} = i|1\rangle \langle 0| - i|0\rangle \langle 1| \end{aligned}$$

from the expectation values of the Pauli operators σ_x and σ_y . It is easy to verify that

$$\begin{aligned} \text{tr}[X |\psi\rangle \langle \psi|] &= \alpha_1^* \alpha_0 + \alpha_0^* \alpha_1 = \text{tr}[\sigma_x \rho_{qubit}] \\ \text{tr}[Y |\psi\rangle \langle \psi|] &= i\alpha_1^* \alpha_0 - i\alpha_0^* \alpha_1 = \text{tr}[\sigma_y \rho_{qubit}]. \end{aligned}$$

The surprising feature of this encoding is that even though the expectation values of X and Y are preserved, the probabilities of the individual outcomes are not. For example,

since the $+1$ eigenvectors of X and σ_x are

$$\begin{bmatrix} +0,1 \\ - \end{bmatrix} := \frac{|0\rangle + |1\rangle}{\sqrt{2}} \quad |+_L\rangle := \frac{|0_L\rangle + |1_L\rangle}{\sqrt{2}}$$

we calculate the corresponding probabilities to be

$$\begin{aligned} \text{tr} \left[\begin{bmatrix} +0,1 \\ - \end{bmatrix} \left\langle \begin{bmatrix} +0,1 \\ - \end{bmatrix} \middle| \psi \right\rangle \langle \psi | \right] &= \frac{\alpha_0^* \alpha_1 + \alpha_1^* \alpha_0 + |\alpha_0|^2 + |\alpha_1|^2}{2} \\ \text{tr} [|+_L\rangle \langle +_L| \rho_{qubit}] &= \frac{\alpha_0^* \alpha_1 + \alpha_1^* \alpha_0 + |\alpha_0|^2 + |\alpha_1|^2 + |\alpha_{-1}|^2}{2}. \end{aligned}$$

We see that in the qubit the probability of $+1$ has increased by $|\alpha_{-1}|^2/2$.¹³

So far, the additional preserved observables X, Y were the result of arbitrary rearrangement of the basis elements in the BPT. If we want a specific observable to be preserved in addition to Z , we will have to be more deliberate about how we choose the basis elements in the BPT.

We can change the basis in the subspace $\{|1\rangle, |-1\rangle\}$ of the second column

$$\begin{array}{c} \begin{array}{|c|c|} \hline 0 & e_1 \\ \hline & e_2 \\ \hline \end{array} \\ \downarrow \quad \downarrow \\ \begin{array}{|c|c|} \hline 0_L & 1_L \\ \hline \end{array} \end{array}.$$

This does not change the fact that the spectral projections

$$\begin{aligned} \Pi_0 &:= |0\rangle \langle 0| \\ \Pi_{\pm 1} &:= |e_1\rangle \langle e_1| + |e_2\rangle \langle e_2| = |1\rangle \langle 1| + |-1\rangle \langle -1| \end{aligned}$$

of Z are still the isometries constructed from this BPT. The proper isometries, however, are now different

$$S_{0,1} := |0\rangle \langle e_1| \quad S_{1,0} := |e_1\rangle \langle 0|.$$

Thus, by changing the basis $|e_1\rangle, |e_2\rangle$ we can choose the preserved observables.

Alice may choose, for example, to preserve the expectation value of the x component of spin. Using the subscripts x, y, z to distinguish the eigenvectors of different components of the spin operator (so $|1\rangle, |0\rangle, |-1\rangle$ are now $|1_z\rangle, |0_z\rangle, |-1_z\rangle$) we note that

$$|\pm 1_x\rangle = \frac{|0_y\rangle \pm |0_z\rangle}{\sqrt{2}}.$$

¹³It should not be too surprising since in the original system the probabilities for the outcomes of $+1$ and -1 did not have to sum to 1 as there was another outcome, 0. In the qubit the probabilities for the two outcomes must sum to 1 so we cannot expect the original probabilities to stay unchanged.

The x component of spin can then be expressed as

$$S_x = |1_x\rangle \langle 1_x| - |-1_x\rangle \langle -1_x| = |0_y\rangle \langle 0_z| + |0_z\rangle \langle 0_y|.$$

Before, when $|e_1\rangle = |1_z\rangle$ we preserved the expectations of

$$X = |1_z\rangle \langle 0_z| + |0_z\rangle \langle 1_z|.$$

This suggests that in order to preserve the expectations of S_x we need to choose

$$|e_1\rangle = |0_y\rangle = \frac{|1_z\rangle + |-1_z\rangle}{\sqrt{2}}.$$

The resulting qubit encoding is

$$|\psi\rangle \mapsto \rho_{qubit} = \begin{pmatrix} \langle \psi | \Pi_0 | \psi \rangle & \langle \psi | 0_y \rangle \langle 0_z | \psi \rangle \\ \langle \psi | 0_z \rangle \langle 0_y | \psi \rangle & \langle \psi | \Pi_{\pm 1} | \psi \rangle \end{pmatrix} = \begin{pmatrix} |\alpha_0|^2 & \frac{\alpha_1^* + \alpha_{-1}^*}{\sqrt{2}} \alpha_0 \\ \alpha_0^* \frac{\alpha_1 + \alpha_{-1}}{\sqrt{2}} & |\alpha_1|^2 + |\alpha_{-1}|^2 \end{pmatrix}$$

and the expectation value of S_x is recovered from the expectation value of σ_x

$$\text{tr}[S_x |\psi\rangle \langle \psi|] = \frac{\alpha_1^* + \alpha_{-1}^*}{\sqrt{2}} \alpha_0 + \alpha_0^* \frac{\alpha_1 + \alpha_{-1}}{\sqrt{2}} = \text{tr}[\sigma_x \rho_{qubit}].$$

In the following we will see that only the expectation values of observables spanned by the isometries constructed from the BPT are preserved. Then, the explanation to why some probabilities of outcomes may not be preserved is as follows: Since the isometries constructed from the relaxed BPTs do not span an algebra, it is possible for an observable to be in the span but not for its spectral projections.

6.2 Partial bipartitions and quantum coarse-graining

The example in the previous section implies that it may be beneficial to consider the structure of non-rectangular bipartition tables more seriously. In this section we will identify this structure as a *partial* bipartition and establish its operational meaning. We will see that such structure naturally generalizes virtual subsystems and lays the foundation to more general state reduction maps called quantum coarse-graining.

6.2.1 Classical analogy

An illuminating perspective on partial bipartitions and coarse-graining can be gained by considering its analogues in probability theory. In the classical formalism it is quite natural to reduce one probabilistic state into another state that provides a coarser probabilistic account of the same system. Thus, it is instructive to first establish the notions of partial

bipartitions and coarse-graining in the classical formalism where its reasoning is more natural.

As an illustrative example, consider the weather in Vancouver that can be sunny or rainy, and warm or cold (say above or below 15 C°). Precipitation and temperature are correlated and historical data may tell us that on October 1st it is 50% likely to be rainy and cold (rc), 30% sunny and cold (sc), 15% rainy and warm (rw), and 5% sunny and warm (sw).¹⁴ We can then produce a coarser account of the weather in Vancouver by only distinguishing between sunny and rainy, or warm and cold. These coarser accounts are associated with a (non-partial) bipartition of the four-outcome state space into two state spaces of two outcomes each. The reduced probabilities of it being sunny or rainy, and warm or cold are given by summing over the columns and rows of the following bipartition table

5% sw	15% rw	→	20% warm
30% sc	50% rc	→	80% cold
↓	↓		
35% sunny	65% rainy		

The above reduction of probabilities is called *marginalization* and it is the classical analogue of the partial trace map. Just like the partial trace map, marginalization takes the joint probability distribution of two random variables and produces the probability distribution of one random variable. Since marginalized probability distributions distinguish between fewer outcomes, we can say that marginalization is a kind of coarse-graining of probability distributions.

In the context of classical probability theory it is also reasonable to consider coarse-grainings that go beyond the usual notion of marginalization. For example, whenever it is sunny and warm I wear a shirt, when it is sunny and cold or rainy and warm I wear a jacket, and when it is rainy and cold I wear a coat. Also, I wear some kind of hat when it is cold or sunny. The probability of me wearing a shirt, a jacket, or a coat, with or without a hat, on October 1st in Vancouver is given by summations over the rows and column of the following partial BPT

	15% rw		→	15% no hat
5% sw	30% sc	50% rc	→	85% hat
↓	↓	↓		
5% shirt	45% jacket	50% coat		

Since my clothing and hat combinations are perfectly correlated with the weather, instead of “sunny and cold” we can label the same outcome as “jacket and hat”, and similarly for other outcomes. Even though not all combinations of clothing and hat are possible (“shirt and no hat” or “coat and no hat” never happen), it is still perfectly reasonable to

¹⁴These probabilities come from a subjective approximation based on the experiences of the author and not an actual meteorological data.

coarse-grain the probability distribution this way in order to get the reduced probabilities for my clothing or hat choices.

Our goal is to import the same kind of reasoning into quantum theory where instead of probability distributions we will coarse-grain quantum states. In order to do that we will have to further develop our formalism to incorporate partial BPTs.

6.2.2 The formalism of partial bipartitions

Let us forget for now about irreps and operator algebras and consider what, in essence, rectangular bipartition tables tell us. By arranging the basis elements into a two-dimensional grid we identify two distinct degrees of freedom; one degree of freedom varies horizontally and the other vertically. These two degrees of freedom can then be associated with two subsystems (virtual or otherwise) that constitute a bipartition of the Hilbert space.

In order to make this statement more precise, consider the generic rectangular BPT with a single block¹⁵ and the implied reductions of rows and columns

$$\begin{array}{ccccccc}
 \begin{array}{|c|c|c|c|} \hline e_{1,1} & e_{1,2} & \cdots & e_{1,d_B} \\ \hline e_{2,1} & e_{2,2} & \cdots & e_{2,d_B} \\ \hline \vdots & \vdots & \ddots & \vdots \\ \hline e_{d_A,1} & e_{d_A,2} & \cdots & e_{d_A,d_B} \\ \hline \end{array} & \rightarrow & \begin{array}{|c|} \hline a_1 \\ \hline a_2 \\ \hline \vdots \\ \hline a_{d_A} \\ \hline \end{array} \\
 \downarrow & & & & & & \\
 \begin{array}{|c|c|c|c|} \hline b_1 & b_2 & \cdots & b_{d_B} \\ \hline \end{array} & & & & & &
 \end{array}$$

(d_A and d_B are the number of rows and columns in the BPT). The choice and arrangement of basis in the BPT tells us how to map the original Hilbert space \mathcal{H} spanned by $\{|e_{ik}\rangle\}$, onto a bipartite Hilbert space $\mathcal{H}_A \otimes \mathcal{H}_B$ spanned by $\{|a_i\rangle \otimes |b_k\rangle\}$. In other words, the BPT defines a Hilbert space isometry

$$\begin{aligned}
 V : \quad \mathcal{H} &\longrightarrow \mathcal{H}_A \otimes \mathcal{H}_B \\
 |e_{ik}\rangle &\longmapsto |a_i\rangle \otimes |b_k\rangle
 \end{aligned} \tag{6.1}$$

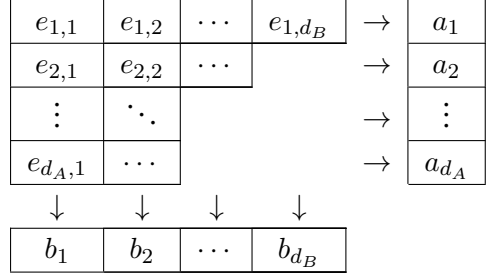
from the original Hilbert space to the bipartite Hilbert space. Thus, as the name suggests, the essence of a bipartition table is to identify a tensor product bipartition of the Hilbert space

$$\mathcal{H} \cong \mathcal{H}_A \otimes \mathcal{H}_B.$$

With this perspective we realize that the same construction can also be applied to non-rectangular BPTs such as¹⁶

¹⁵In this section we will only consider BPTs with a single block to avoid unnecessary clutter but it naturally generalizes to multi-block BPTs where each block is considered separately.

¹⁶Earlier we assumed that $\dim \mathcal{H} = d_A d_B$, now we assume that $\dim \mathcal{H} < d_A d_B$.



Even though the dimensions of rows and columns can now vary, it still defines a Hilbert space isometry as in Eq. (6.1), only now the indices i, k are constrained by the non-rectangular shape of the BPT. As a result, \mathcal{H} is not mapped *onto* but *into* $\mathcal{H}_A \otimes \mathcal{H}_B$, that is, \mathcal{H} is mapped onto a subspace of $\mathcal{H}_A \otimes \mathcal{H}_B$.

We may still think of such mapping as a bipartition of \mathcal{H} but it is no longer a tensor product bipartition. We will call such generalized bipartitions *partial* since not all product basis $|a_i\rangle \otimes |b_k\rangle$ can be found in the original Hilbert space. We introduce the notation

$$\mathcal{H} \cong \mathcal{H}_A \circ \mathcal{H}_B$$

for partial bipartitions that emphasizes the fact that it is a generalization of the tensor product. We will also say that \mathcal{H}_A and \mathcal{H}_B are (the Hilbert spaces of) *partial subsystems*, generalizing the notion of a virtual subsystem.

Now that we have defined partial bipartitions we can define state reduction maps given by tracing out one of the partial subsystems. By elevating the isometry (6.1) to act on operators

$$\mathcal{V}(\rho) := V\rho V^\dagger,$$

we define the state reduction map as the composition

$$\text{tr}_{(A)} := \text{tr}_A \circ \mathcal{V}.$$

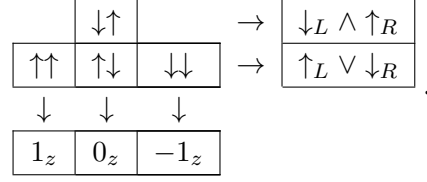
The map $\text{tr}_{(A)}$ is CPTP (so it reduces proper quantum states to proper quantum states) because it can be expressed in the operator sum representation [75]

$$\text{tr}_{(A)}(\rho) = \sum_i (K_i V) \rho (K_i V)^\dagger$$

where K_i are the Kraus operators of tr_A .

With this formalism we can reproduce the classical reasoning of Section 6.2.1 in a quantum setting. Let us map the classical states of $\{\text{sw, sc, rw, rc}\}$ (sunny and warm, ... , rainy and cold) to the product basis of two spins $\{|\uparrow\uparrow\rangle, |\uparrow\downarrow\rangle, |\downarrow\uparrow\rangle, |\downarrow\downarrow\rangle\}$ spanning \mathcal{H} . The coarse-graining that we have considered before is now given by the partial BPT ¹⁷

¹⁷Note that in the quantum case we do not specify any probabilities in the BPT because they are complex



Observe that the three columns distinguish between the states of total spin $1, 0, -1$ along \hat{z} . Similarly, the two rows distinguish between states that can be described as “left ↓ *and* right ↑” and “left ↑ *or* right ↓”. We then label the basis for the partial subsystems according to what they distinguish

$$\mathcal{H}_B := \text{span} \{ |1_z\rangle, |0_z\rangle, |-1_z\rangle \} \quad (6.2)$$

$$\mathcal{H}_A := \text{span} \{ |\downarrow_L \wedge \uparrow_R\rangle, |\uparrow_L \vee \downarrow_R\rangle \}. \quad (6.3)$$

The partial bipartition $\mathcal{H} \cong \mathcal{H}_A \otimes \mathcal{H}_B$ is defined by an isometry $V : \mathcal{H} \longrightarrow \mathcal{H}_A \otimes \mathcal{H}_B$ where

$$\begin{aligned} V |\uparrow\uparrow\rangle &= |\uparrow_L \vee \downarrow_R\rangle \otimes |1_z\rangle \\ V |\uparrow\downarrow\rangle &= |\uparrow_L \vee \downarrow_R\rangle \otimes |0_z\rangle \\ V |\downarrow\uparrow\rangle &= |\downarrow_L \wedge \uparrow_R\rangle \otimes |0_z\rangle \\ V |\downarrow\downarrow\rangle &= |\uparrow_L \vee \downarrow_R\rangle \otimes |-1_z\rangle. \end{aligned}$$

The remaining two states $|\downarrow_L \wedge \uparrow_R\rangle \otimes |\pm 1_z\rangle$ are impossible spin states and they are not in the image of V (so they are annihilated by V^\dagger). The reduced states are given by tracing out one of the partial subsystems A or B . That is, for any $\rho \in \mathcal{L}(\mathcal{H})$ the reduced states are

$$\begin{aligned} \rho_B &= \text{tr}_{(A)} [\rho] = \text{tr}_A [V \rho V^\dagger] \in \mathcal{L}(\mathcal{H}_B) \\ \rho_A &= \text{tr}_{(B)} [\rho] = \text{tr}_B [V \rho V^\dagger] \in \mathcal{L}(\mathcal{H}_A). \end{aligned}$$

If ρ is a classical probabilistic state such as

$$\rho := p_{\uparrow\uparrow} |\uparrow\uparrow\rangle \langle\uparrow\uparrow| + p_{\uparrow\downarrow} |\uparrow\downarrow\rangle \langle\uparrow\downarrow| + p_{\downarrow\uparrow} |\downarrow\uparrow\rangle \langle\downarrow\uparrow| + p_{\downarrow\downarrow} |\downarrow\downarrow\rangle \langle\downarrow\downarrow|$$

then its reduced states are

$$\begin{aligned} \rho_B &= p_{\uparrow\uparrow} |1_z\rangle \langle 1_z| + (p_{\uparrow\downarrow} + p_{\downarrow\uparrow}) |0_z\rangle \langle 0_z| + p_{\downarrow\downarrow} |-1_z\rangle \langle -1_z| \\ \rho_A &= p_{\downarrow\uparrow} |\downarrow_L \wedge \uparrow_R\rangle \langle \downarrow_L \wedge \uparrow_R| + (p_{\uparrow\uparrow} + p_{\uparrow\downarrow} + p_{\downarrow\downarrow}) |\uparrow_L \vee \downarrow_R\rangle \langle \uparrow_L \vee \downarrow_R|. \end{aligned}$$

Apparently, when applied to classical states the reduction map is just the classical coarse-graining of probabilities that sums them up over the rows and columns of the BPT.

amplitudes and their reduction is more than a summation over the rows and columns.

If ρ is a pure quantum state such as

$$|\psi\rangle := \alpha_{\uparrow\uparrow} |\uparrow\uparrow\rangle + \alpha_{\uparrow\downarrow} |\uparrow\downarrow\rangle + \alpha_{\downarrow\uparrow} |\downarrow\uparrow\rangle + \alpha_{\downarrow\downarrow} |\downarrow\downarrow\rangle,$$

we calculate the reduced states to be (the ordering of the reduced basis is as in Eqs. (6.2) and 6.3)

$$\rho_B = \begin{pmatrix} |\alpha_{\uparrow\uparrow}|^2 & \alpha_{\uparrow\uparrow}\alpha_{\uparrow\downarrow}^* & \alpha_{\uparrow\uparrow}\alpha_{\downarrow\downarrow}^* \\ \alpha_{\uparrow\downarrow}\alpha_{\uparrow\uparrow}^* & |\alpha_{\uparrow\downarrow}|^2 + |\alpha_{\downarrow\uparrow}|^2 & \alpha_{\uparrow\downarrow}\alpha_{\downarrow\downarrow}^* \\ \alpha_{\downarrow\uparrow}\alpha_{\uparrow\uparrow}^* & \alpha_{\downarrow\uparrow}\alpha_{\uparrow\downarrow}^* & |\alpha_{\downarrow\downarrow}|^2 \end{pmatrix}$$

$$\rho_A = \begin{pmatrix} |\alpha_{\downarrow\uparrow}|^2 & \alpha_{\downarrow\uparrow}\alpha_{\uparrow\downarrow}^* \\ \alpha_{\uparrow\downarrow}\alpha_{\downarrow\uparrow}^* & |\alpha_{\uparrow\uparrow}|^2 + |\alpha_{\uparrow\downarrow}|^2 + |\alpha_{\downarrow\downarrow}|^2 \end{pmatrix}.$$

From the diagonal matrix elements we see that even in the pure quantum case the classical coarse-graining of probabilities persists, however, now it also preserves some of the coherence terms.

We conclude that the probability distribution over the outcomes of observables that distinguish between the basis are coarse-grained by the state reduction map as in the classical case. Thus, by promoting distinguishable states to orthogonal basis and probability distributions to quantum states we reproduce the classical notion of coarse-graining by tracing out a partial subsystem. However, in the quantum setting there are more observables than just a distinction of certain basis, and there is more to tracing out a partial subsystem than just a summation of probabilities. In order to understand how all observables are affected by tracing out a partial subsystem we need to derive the operational meaning of such state reductions.

6.2.3 The operational meaning of quantum coarse-graining

From here on, we will use the notions of state reduction, tracing out a partial subsystem, and quantum coarse-graining interchangeably. In order to derive the operational meaning of quantum coarse-graining we will have to establish a few more facts.

Using the tomographic representation (4.4) of the partial trace map we derive

$$\text{tr}_{(A)}(\rho) = \text{tr}_A[V\rho V^\dagger] = \sum_{k,l=1}^{d_B} \text{tr}[\tilde{S}_{kl}V\rho V^\dagger] |b_l\rangle\langle b_k| = \sum_{k,l=1}^{d_B} \text{tr}[(V^\dagger\tilde{S}_{kl}V)\rho] |b_l\rangle\langle b_k|$$

where $\tilde{S}_{kl} := I_A \otimes |b_k\rangle\langle b_l|$ are partial isometries in $\mathcal{H}_A \otimes \mathcal{H}_B$. We define partial isometries in \mathcal{H} as $S_{kl} := V^\dagger\tilde{S}_{kl}V$ and then the map that traces out a partial subsystem can also be given

in the tomographic representation

$$\text{tr}_{(A)}(\rho) = \sum_{k,l=1}^{d_B} \text{tr}[S_{kl}\rho] |b_l\rangle \langle b_k|. \quad (6.4)$$

This representation simplifies things since the partial isometries $\{S_{kl}\}$ can be constructed directly from the non-rectangular BPT. In order to see that, let us explicitly define

$$V = \sum_{ik} |a_i\rangle \otimes |b_k\rangle \langle e_{ik}|,$$

where the row and column indices i, k are constrained by the shape of the BPT, that is

$$V^\dagger |a_i\rangle \otimes |b_k\rangle = \begin{cases} |e_{ik}\rangle & \text{The cell } i, k \text{ is present in the BPT} \\ 0 & \text{The cell } i, k \text{ is absent in the BPT.} \end{cases}$$

The aforementioned partial isometries then reduce to

$$\begin{aligned} S_{kl} &= V^\dagger \tilde{S}_{kl} V = V^\dagger \left(\sum_{i=1}^{d_A} |a_i\rangle \langle a_i| \right) \otimes |b_k\rangle \langle b_l| V \\ &= \sum_{i \in \text{CR}(k,l)} |e_{ik}\rangle \langle e_{il}| \end{aligned} \quad (6.5)$$

where the set $\text{CR}(k, l)$ contains the common row indices of cells that are present in both columns k and l .

The result in Eq. (6.5) tells us how S_{kl} is constructed directly from the BPT according to the alignment of elements in the columns k and l . When the BPT is rectangular the set $\text{CR}(k, l)$ always contains all the rows. When the BPT is non-rectangular some rows are shorter than others so not every row is present in every column. Compare the original construction of partial isometries from BPTs in Eq. (2.6) (assuming a single block) to the new construction in Eq. 6.5, and verify that the later generalizes the former.

So far, it seems like we do not really have to make a distinction between rectangular and non-rectangular BPTs. The isometries are constructed according to the same general prescription in Eq. 6.5, and the state reduction map is given by the same Eq. 6.4 in terms of the isometries. The obvious question then is how does the non-rectangular shape generalize operator algebras associated with the rectangular shape. The answer to that begins with the following definition.

Definition 6.1. An operator system is a subset of operators $\mathcal{O} \subseteq \mathcal{L}(\mathcal{H})$ such that:

- (1) For all $O_1, O_2 \in \mathcal{O}$ and $c_1, c_2 \in \mathbb{C}$ we have $c_1 O_1 + c_2 O_2 \in \mathcal{O}$.
- (2) For all $O \in \mathcal{O}$ we have $O^\dagger \in \mathcal{O}$.

(3) There is a projection $I_{\mathcal{O}} \in \mathcal{O}$ such that $I_{\mathcal{O}}O = O$ for all $O \in \mathcal{O}$.

Operator systems generalize operator algebras in that the products of operators do not have to remain in the set. In other words, operator systems are just subspaces of operators that are closed under conjugation and contain a projection that serves as the identity.¹⁸

It turns out that for rectangular BPTs the constructed isometries span operator algebras, but when non-rectangular BPTs are considered they span operator systems. Furthermore, the constructed isometries $\{S_{kl}\}$ form a basis for the operator system that they span. These facts are shown in the following proposition.

Proposition 6.2. *Let $\mathcal{H} \cong \mathcal{H}_A \otimes \mathcal{H}_B$ be a partial bipartition and let $\{S_{kl}\}$ be the isometries constructed according to Eq. (6.5). Then, $\text{span}\{S_{kl}\}$ is an operator system and the set $\{S_{kl}\}$ forms an operator basis that are orthogonal with respect to the Hilbert-Schmidt (HS) inner product*

$$\langle S_{k'l'}, S_{kl} \rangle_{HS} = \delta_{kk'} \delta_{ll'} |\text{CR}(k, l)|.$$

Proof. Condition (1) of Definition 6.1 trivially holds as $\text{span}\{S_{kl}\}$ is a vector space. Condition (2) holds because $S_{kl}^\dagger = S_{lk}$. For condition (3) we construct $I_{\mathcal{O}} := \sum_{k'} S_{k'k'}$ so

$$\begin{aligned} I_{\mathcal{O}} S_{kl} &= \sum_{k'} \left(\sum_{i' \in \text{CR}(k', k')} |e_{i'k'}\rangle \langle e_{i'k'}| \right) \left(\sum_{i \in \text{CR}(k, l)} |e_{ik}\rangle \langle e_{il}| \right) \\ &= \sum_{i \in \text{CR}(k, l)} \sum_{k'} \sum_{i' \in \text{CR}(k', k')} \delta_{ii'} \delta_{kk'} |e_{i'k'}\rangle \langle e_{il}| = \sum_{i \in \text{CR}(k, l)} |e_{ik}\rangle \langle e_{il}| = S_{kl}. \end{aligned}$$

Finally, using the definition of the HS inner product $\langle X, Y \rangle_{HS} := \text{tr}[X^\dagger Y]$ we derive

$$\begin{aligned} \langle S_{k'l'}, S_{kl} \rangle_{HS} &= \text{tr} \left[\left(\sum_{i' \in \text{CR}(k', l')} |e_{i'l'}\rangle \langle e_{i'l'}| \right) \left(\sum_{i \in \text{CR}(k, l)} |e_{ik}\rangle \langle e_{il}| \right) \right] \\ &= \sum_{i' \in \text{CR}(k', l')} \sum_{i \in \text{CR}(k, l)} \delta_{kk'} \delta_{ll'} \delta_{ii'} = \delta_{kk'} \delta_{ll'} |\text{CR}(k, l)|. \end{aligned}$$

□

Note that the basis $\{S_{kl}\}$ are not normalized since

$$\|S_{kl}\|_{HS}^2 = \langle S_{kl}, S_{kl} \rangle_{HS} = |\text{CR}(k, l)|.$$

The normalized basis will be denoted as

$$\hat{S}_{kl} := \frac{S_{kl}}{\sqrt{|\text{CR}(k, l)|}}.$$

¹⁸In finite-dimensional operator algebras the existence of the identity was not part of the definition because it could be derived.

Finally, we are ready to discuss the operational meaning of state reductions associated with partial bipartitions. When the bipartition $\mathcal{H} \cong \mathcal{H}_A \otimes \mathcal{H}_B$ is a proper tensor product, the operational meaning of the reduced state $\rho_B = \text{tr}_A(\rho)$ is that it preserves the expectation values of all the observables of the form $O = I_A \otimes O_B$. That is, for every observable $O \in I_A \otimes \mathcal{L}(\mathcal{H}_B)$ there is an observable $O_B \in \mathcal{L}(\mathcal{H}_B)$ such that $\text{tr}[O\rho] = \text{tr}[O_B\rho_B]$, and vice versa. The correspondence between these observables is trivially given by

$$O_B \longleftrightarrow O = I_A \otimes O_B.$$

The following theorem generalizes this statement to partial bipartitions.

Theorem 6.3. *Let $\mathcal{H} \cong \mathcal{H}_A \otimes \mathcal{H}_B$ be a partial bipartition with the isometries $\{S_{kl}\}$ as constructed in Eq. (6.5), and let $\rho \in \mathcal{L}(\mathcal{H})$ and $\rho_B = \text{tr}_{(A)}(\rho)$. Then, for every observable $O \in \text{span}\{S_{kl}\}$ there is an observable $O_B \in \mathcal{L}(\mathcal{H}_B)$ such that $\text{tr}[O\rho] = \text{tr}[O_B\rho_B]$, and vice versa. This correspondence of observables is explicitly given by*

$$O_B \longmapsto O := \sum_{k,l=1}^{d_B} \text{tr}[O_B |b_l\rangle \langle b_k|] S_{kl} \quad (6.6)$$

$$O \longmapsto O_B := \sum_{k,l=1}^{d_B} \frac{\text{tr}(S_{lk}O)}{|\text{CR}(k,l)|} |b_k\rangle \langle b_l|. \quad (6.7)$$

Proof. To see that the correspondence (6.6) holds we recall the definition (6.4) of $\text{tr}_{(A)}(\rho)$ and use the linearity of trace to derive

$$\text{tr}[O_B\rho_B] = \text{tr}\left[O_B \left(\sum_{k,l=1}^{d_B} |b_l\rangle \langle b_k| \text{tr}[S_{kl}\rho]\right)\right] = \text{tr}\left[\left(\sum_{k,l=1}^{d_B} \text{tr}[O_B |b_l\rangle \langle b_k|] S_{kl}\right) \rho\right] = \text{tr}[O\rho].$$

For the converse, using the fact that $O \in \text{span}\{S_{kl}\}$ we can expand it in the $\{\hat{S}_{kl}\}$ basis as

$$O = \sum_{k,l=1}^{d_B} \langle \hat{S}_{kl}, O \rangle_{HS} \hat{S}_{kl} = \sum_{k,l=1}^{d_B} \frac{\text{tr}(S_{lk}O)}{|\text{CR}(k,l)|} S_{kl}.$$

so

$$\text{tr}[O\rho] = \sum_{k,l=1}^{d_B} \frac{\text{tr}(S_{lk}O)}{|\text{CR}(k,l)|} \text{tr}[S_{kl}\rho].$$

Then, using the correspondence (6.7) we can check that $\text{tr}[O\rho] = \text{tr}[O_B\rho_B]$ holds

$$\begin{aligned}\text{tr}[O_B\rho_B] &= \text{tr} \left[\left(\sum_{k,l=1}^{d_B} \frac{\text{tr}(S_{lk}O)}{|\text{CR}(k,l)|} |b_k\rangle \langle b_l| \right) \left(\sum_{k',l'=1}^{d_B} \text{tr}[S_{k'l'}\rho] |b_{l'}\rangle \langle b_{k'}| \right) \right] \\ &= \sum_{k,l=1}^{d_B} \frac{\text{tr}(S_{lk}O)}{|\text{CR}(k,l)|} \text{tr}[S_{kl}\rho] = \text{tr}[O\rho].\end{aligned}$$

□

Thus, the above theorem tells us that the operational meaning of the reduced state ρ_B is that it preserves the expectation values of all the observables $O \in \text{span}\{S_{kl}\}$. It is also worth noting that the correspondences (6.6) and (6.7) can be concisely expressed element-wise as

$$|b_l\rangle \langle b_k| \longleftrightarrow S_{kl}. \quad (6.8)$$

The surprising feature of tracing out a partial subsystem is that even when the expectation values of some observable are preserved, it does not mean that the probabilities of its individual outcomes are preserved. The reason for that is because the statement $O \in \text{span}\{S_{kl}\}$ does not imply that the spectral projections $\{\Pi_i\}$ of O are also in $\text{span}\{S_{kl}\}$ (unless $\text{span}\{S_{kl}\}$ is an algebra so the bipartition is not partial). Since the probabilities of individual outcomes are given by the expectation values of the spectral projections, they are not guaranteed to be preserved.

As an example, let us go back to the two spin Hilbert space $\mathcal{H} = \frac{1}{2} \otimes \frac{1}{2}$ and change to the total spin basis $|j, m_z\rangle$. The partial bipartition that we now want to consider is given by the following BPT

$$\begin{array}{ccc} & \boxed{0, 0_z} & \\ \boxed{1, +1_z} & \boxed{1, 0_z} & \boxed{1, -1_z} \end{array} \rightarrow \begin{array}{c} \boxed{s} \\ \boxed{t} \end{array}.$$

$$\begin{array}{ccc} \downarrow & \downarrow & \downarrow \\ \boxed{1_z} & \boxed{0_z} & \boxed{-1_z} \end{array}$$

As before, the columns distinguish between the states with different m_z . The rows now distinguish between the singlet (s) and triplet (t) states. The partial subsystems are therefore

$$\begin{aligned}\mathcal{H}_B &:= \text{span}\{|1_z\rangle, |0_z\rangle, |-1_z\rangle\} \\ \mathcal{H}_A &:= \text{span}\{|s\rangle, |t\rangle\}.\end{aligned}$$

The question then is what observable information is preserved if we trace out the singlet-triplet subsystem?

The short answer is that the preserved information is given by the expectation values of all the observables $O \in \text{span} \{S_{kl}\}$, where S_{kl} are constructed from the BPT according to Eq. (6.5) as

$$S_{kl} = \sum_{j \in \text{CR}(k,l)} |j, k_z\rangle \langle j, l_z| = \begin{cases} |0, 0_z\rangle \langle 0, 0_z| + |1, 0_z\rangle \langle 1, 0_z| & k = l = 0 \\ |1, k_z\rangle \langle 1, l_z| & \text{otherwise} \end{cases}.$$

In particular, for $k = l$ the projections $\{S_{kk}\}$ are the spectral projections of the total spin component

$$J_z = \sum_{j,k} k |j, k\rangle \langle j, k| = \sum_k k S_{kk}.$$

Thus, all the statistical information about the observable J_z is preserved and, according to the correspondence (6.8), the reduced observable is

$$J_z \mapsto J_{z;B} = \sum_k k |k_z\rangle \langle k_z|.$$

As expected, J_z corresponds to the \hat{z} component of the reduced spin-1 system and $|k_z\rangle$ are its eigenstates.

The total spin ladder operators J_{\pm} are also in $\text{span} \{S_{kl}\}$ since they can be expanded as

$$\begin{aligned} J_+ &= \sqrt{2} |1, 1_z\rangle \langle 1, 0_z| + \sqrt{2} |1, 0_z\rangle \langle 1, -1_z| = \sqrt{2} S_{1,0} + \sqrt{2} S_{0,-1} \\ J_- &= \sqrt{2} |1, -1_z\rangle \langle 1, 0_z| + \sqrt{2} |1, 0_z\rangle \langle 1, 1_z| = \sqrt{2} S_{-1,0} + \sqrt{2} S_{0,1}. \end{aligned}$$

This means that the other two total spin components J_x and J_y are in $\text{span} \{S_{kl}\}$ as well. From the correspondence (6.8) we have

$$\begin{aligned} J_+ &\mapsto J_{+;B} = \sqrt{2} |1_z\rangle \langle 0_z| + \sqrt{2} |0_z\rangle \langle -1_z| \\ J_- &\mapsto J_{-;B} = \sqrt{2} |-1_z\rangle \langle 0_z| + \sqrt{2} |0_z\rangle \langle 1_z| \end{aligned}$$

and so

$$\begin{aligned} J_x &\mapsto J_{x;B} = \frac{J_{+;B} + J_{-;B}}{2} = \frac{|1_z\rangle \langle 0_z| + |0_z\rangle \langle -1_z| + |-1_z\rangle \langle 0_z| + |0_z\rangle \langle 1_z|}{\sqrt{2}} \\ J_y &\mapsto J_{y;B} = \frac{J_{+;B} - J_{-;B}}{2i} = \frac{|1_z\rangle \langle 0_z| + |0_z\rangle \langle -1_z| - |-1_z\rangle \langle 0_z| - |0_z\rangle \langle 1_z|}{\sqrt{2}i}. \end{aligned}$$

That is, J_x and J_y correspond to the \hat{x} and \hat{y} components of the reduced spin-1 system.

Unlike J_z , however, the spectral projections of J_x and J_y are not present in $\text{span} \{S_{kl}\}$.

If they were, then J_x^2 (similarly J_y^2) would also be in $\text{span}\{S_{kl}\}$ but that is not the case as

$$\begin{aligned} J_x^2 &= \left(\frac{J_+ + J_-}{2} \right)^2 = \frac{1}{2} (S_{1,0} + S_{0,-1} + S_{-1,0} + S_{0,1})^2 \\ &= \frac{1}{2} (S_{1,-1} + S_{1,1} + S_{-1,-1} + S_{-1,1}) + |1, 0_z\rangle \langle 1, 0_z|. \end{aligned}$$

Since $|1, 0_z\rangle \langle 1, 0_z|$ is not in $\text{span}\{S_{kl}\}$ (because $S_{00} = |0, 0_z\rangle \langle 0, 0_z| + |1, 0_z\rangle \langle 1, 0_z|$) then neither is J_x^2 .

Therefore, by tracing out the singlet-triplet partial subsystem we can preserve all the statistical information about the component J_z of total spin, but for J_x and J_y only the expectation values are preserved and not their higher moments. These, of course, are not all the observables in $\text{span}\{S_{kl}\}$ and there is more observable information that is preserved in the reduced states.

Chapter 7

The uncertainty principle on a lattice

In this chapter we will carry out a case study of the uncertainty principle on a lattice. Unlike previous chapters where the emphasis was on the methods, here we will focus on specific physical questions. Because a much simpler notion of coarse-graining is needed here, the analysis in this chapter will not rely on the contents of previous chapters. These results were originally published in [53].

Heisenberg's uncertainty principle is colloquially understood as the fact that arbitrarily precise values of position and momentum cannot simultaneously be determined (see [20, 22] for a review). A rigorous formulation of the uncertainty principle is often conflated with the uncertainty relations for states $\sigma_x \sigma_p \geq \hbar/2$, where σ_x and σ_p refer to the standard deviations of independently measured position and momentum of a particle in the same state. This inequality rules out the possibility of quantum states with arbitrarily sharp values of both position and momentum. It does not, however, rule out the possibility of measurements that simultaneously determine both of these values with arbitrary precision. The essential effect behind the uncertainty principle that rules out the latter possibility is the mutual disturbance between measurements of incompatible observables.

According to the original formulation by Heisenberg [46], due to the unavoidable disturbance by measurements, it is not possible to localize a particle in a phase space cell of the size of the Planck constant or smaller. However, when phase space cells much coarser than the Planck constant are considered, Heisenberg argued that the values of both observables can be estimated at the expense of lower resolution. The picture that emerges from Heisenberg's original arguments is that the Planck constant sets a resolution scale in phase space that separates the quantum regime from the classical (see Fig. 7.1(a)). There is, of course, a continuum of scales so it is natural to ask for a characteristic function that outlines how the uncertainty principle transitions to the classical regime as the resolution of measurements decreases.

A rigorous formulation of the measurement uncertainty principle has been extensively debated in recent years [77, 23, 16, 61, 19, 84], producing multiple perspectives on the fundamental limits of simultaneous measurability of incompatible observables. These formulations are similar to the uncertainty relations for states as they capture the trade-off between the resolution and disturbance of measurements (which may also depend on the

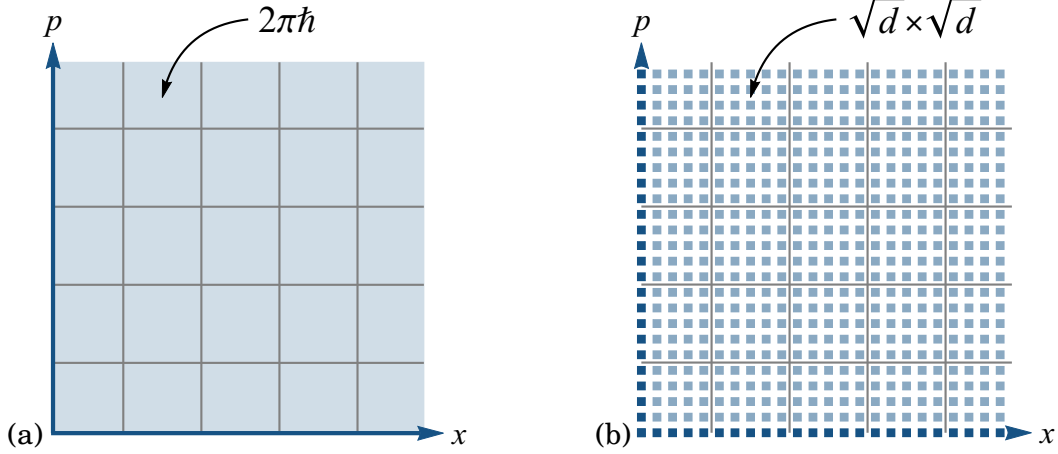


Figure 7.1: (a) The continuous phase space where the cells with the area $2\pi\hbar$ represent the resolution scale associated with the uncertainty principle. (b) The discretized phase space of a lattice of integer length d . The cells with the area $\sqrt{d} \times \sqrt{d}$ arise from the scale \sqrt{d} associated with the uncertainty principle on a lattice. The Planck constant $2\pi\hbar$ can be recovered from \sqrt{d} by converting the phase space area $\sqrt{d} \times \sqrt{d}$ to proper units.

states). However, the picture of how the uncertainty principle transitions to the regime where joint measurability is possible is not so clear from these perspectives.

Furthermore, the picture of continuous phase space as a fundamental concept has been challenged by the various approaches to quantum gravity [2]. The existence of minimal length in space is indicated by many thought experiments that point to the impossibility of probing length scales close to the Planck length $\delta x \sim 10^{-35}$ m (see [48] for a review). It then follows that due to the existence of minimal length in space, the canonical commutation relations and the associated mutual disturbance effects have to be modified; this is known as the *generalized uncertainty principle* [2]. There is great interest in identifying any observable effects associated with the modifications of the uncertainty principle due to minimal length, and in recent years there have been at least two experimental proposals [3, 82] based on this idea.

In this chapter we will study the effects of the uncertainty principle as a function of measurement resolution. In Section 7.1 we will introduce and analyze an operationally defined measure of mutual disturbance that is responsible for the uncertainty principle. This measure is based on the probability that an instantaneous succession of coarse-grained measurements of position-momentum-position will agree on both outcomes of position. The analysis will be carried out on a finite-dimensional periodic lattice of integer length d , where the continuous space can be recovered by introducing the minimal length δx and taking the limits $d \rightarrow \infty$, $\delta x \rightarrow 0$. As a result, we will derive a rigorous characteristic function that quantifies the transition of the uncertainty principle from quantum to classical regimes, in both continuous and discrete settings.

In Section 7.2 we will study the implications of the uncertainty principle on a lattice.

One implication is that the transition of the uncertainty principle to the classical regimes is perturbed by the discontinuity of the lattice. We will see how this perturbation can be quantified by our operationally defined characteristic function.

Another implication is related to the question of how classicality emerges in isolated finite-dimensional systems. Such questions have been considered in [83] and [79], and in particular Kofler and Brukner [60] have demonstrated that for a spin- j system, incompatible spin components can simultaneously be determined if the resolution of measurements is coarse compared to \sqrt{j} .

Our analysis show that the same conclusion applies to position and momentum on a lattice, where both variables can simultaneously be determined if the resolution of measurements is coarse compared to \sqrt{d} . We will then discuss how the unitless scale \sqrt{d} factorizes the Planck constant (see Fig. 7.1 (b)) and defines a new length scale given by the geometric mean $\sqrt{\delta x L}$ of the *minimal* length δx and the *maximal* length L .

7.1 From quantum to classical regimes on a lattice

Let us consider the simple, operationally meaningful quantity p_{agree} , which is the probability that an instantaneous succession of position-momentum-position measurements will agree on both outcomes of position, regardless of the outcomes. When all measurements have arbitrarily fine resolution, the second measurement in this succession prepares a sharp momentum state that is nearly uniformly distributed in position space. Then, the probability that the first and the last measurements of position will agree is vanishingly small $p_{\text{agree}} \approx 0$. As we decrease the resolution of measurements, we expect the probability p_{agree} to grow from 0 to 1 because coarser momentum measurement will cause less spread in the position space, and coarser position measurements will be more likely to agree on the estimate of position.

Now, consider the average $\langle p_{\text{agree}} \rangle$ over all states. In general, the average value $\langle p_{\text{agree}} \rangle$ does not inform us about how strongly the measurements disturb each other for any particular state ρ . However, when the average $\langle p_{\text{agree}} \rangle$ is close to 0 or 1, the value of $p_{\text{agree}}(\rho)$ has to converge to the average for almost all states ρ . That is because $p_{\text{agree}} \in [0, 1]$ so its variance has to vanish as the average gets close to the edges. Therefore, the value of $\langle p_{\text{agree}} \rangle$ indicates how close we are to the regime $\langle p_{\text{agree}} \rangle \approx 0$ where the measurements strongly disturb each other for almost all states, or the regime $\langle p_{\text{agree}} \rangle \approx 1$ where the mutual disturbance is inconsequential for almost all states. We can therefore utilize $\langle p_{\text{agree}} \rangle$ as a characteristic function that quantifies the relevance of the uncertainty principle and outlines the transition between quantum and classical regimes.

For the rest of this section we will focus on deriving and studying the explicit expression for $\langle p_{\text{agree}} \rangle$ as a function of measurement resolution. The most technical calculations concerned with the upper and lower bounds on $\langle p_{\text{agree}} \rangle$ are deferred to the Appendix. The

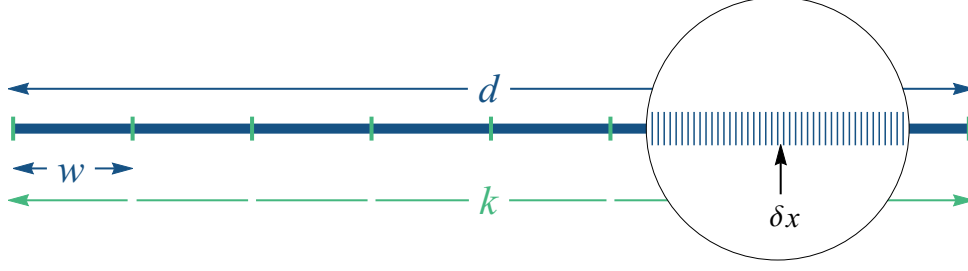


Figure 7.2: Periodic one dimensional lattice with d lattice sites in total, w lattice sites in each coarse-graining interval, and $k = d/w$ intervals. The lattice unit of length is δx .

final result is the explicit expression for $\langle p_{\text{agree}} \rangle$ in Eq. (7.9) along with the bounds (7.11), (7.12), and the plot presented in Fig. 7.3.

In order to calculate the value of $\langle p_{\text{agree}} \rangle$ as a function of measurement resolution, we turn to the canonical setting of finite-dimensional quantum mechanics. In this setting we consider a particle on a periodic one-dimensional lattice with d lattice sites. Initially, both lattice units of position and momentum will be set to unity $\delta x \equiv 1$, $\delta p \equiv 1$. Later, we will introduce proper units and consider the continuum limit.

Following the construction in [96, 49], the Hilbert space of our system is given by the span of position basis $|X; n\rangle$ for $n = 0, \dots, d-1$. The momentum basis are related to the position basis via the discrete Fourier transform F

$$|X; n\rangle = F^\dagger |P; n\rangle = \frac{1}{\sqrt{d}} \sum_{m=0}^{d-1} e^{-i2\pi mn/d} |P; m\rangle$$

$$|P; m\rangle = F |X; m\rangle = \frac{1}{\sqrt{d}} \sum_{n=0}^{d-1} e^{i2\pi mn/d} |X; n\rangle.$$

In principle, realistic finite resolution measurements should be modeled as unsharp POVMs [21, 79]. For our purposes, however, it will be sufficient to consider the idealized version in the form of coarse-grained projective measurements.

We introduce the integer parameters w_x, w_p to specify the widths of the coarse-graining intervals for the corresponding observables (larger w means lower resolution). The variable $k = d/w$ specifies the number of coarse-graining intervals which we will also assume to be an integer. See Fig. 7.2 for a diagrammatic summary of the relevant lengths.

The coarse-grained position and momentum observables are constructed from the spec-

tral projections

$$\Pi_{X;\nu} = \sum_{n=\nu w_x}^{\nu w_x + w_x - 1} |X; n\rangle \langle X; n| \quad (7.1)$$

$$\Pi_{P;\mu} = \sum_{m=\mu w_p}^{\mu w_p + w_p - 1} |P; m\rangle \langle P; m| \quad (7.2)$$

associated with the eigenvalues of coarse-grained position $\nu = 0, \dots, k_x - 1$ and momentum $\mu = 0, \dots, k_p - 1$. In the following we will only need these spectral projections, so we do not have to explicitly define the operators of coarse-grained position and momentum.

Let us now calculate the probability of getting the outcomes ν, μ, ν in an instantaneous sequence of position-momentum-position measurements on the initial state ρ . Using the intermediate post-measurement states in this sequence

$$\rho^{(\nu)} = \frac{\Pi_{X;\nu} \rho \Pi_{X;\nu}}{\text{tr} [\Pi_{X;\nu} \rho]} \quad \rho^{(\nu\mu)} = \frac{\Pi_{X;\mu} \rho^{(\nu)} \Pi_{X;\mu}}{\text{tr} [\Pi_{X;\mu} \rho^{(\nu)}]}$$

we can express this probability as

$$\begin{aligned} p_{xpx}(\nu, \mu, \nu | \rho) &= \text{tr} [\Pi_{X;\nu} \rho] \text{tr} [\Pi_{P;\mu} \rho^{(\nu)}] \text{tr} [\Pi_{X;\nu} \rho^{(\nu\mu)}] \\ &= \text{tr} [(\Pi_{X;\nu} \Pi_{P;\mu} \Pi_{X;\nu})^2 \rho]. \end{aligned} \quad (7.3)$$

Then, the probability that both position outcomes agree, regardless of the outcomes, is

$$\begin{aligned} p_{\text{agree}}(\rho) &= \sum_{\nu=0}^{k_x-1} \sum_{\mu=0}^{k_p-1} p_{xpx}(\nu, \mu, \nu | \rho) \\ &= \text{tr} \left[\sum_{\nu=0}^{k_x-1} \sum_{\mu=0}^{k_p-1} (\Pi_{X;\nu} \Pi_{P;\mu} \Pi_{X;\nu})^2 \rho \right]. \end{aligned} \quad (7.4)$$

From Eq. (7.4) we identify the observable

$$\Lambda_{\text{agree}} = \sum_{\nu=0}^{k_x-1} \sum_{\mu=0}^{k_p-1} (\Pi_{X;\nu} \Pi_{P;\mu} \Pi_{X;\nu})^2$$

whose expectation values are the probabilities $p_{\text{agree}}(\rho) = \text{tr}(\Lambda_{\text{agree}} \rho)$. Since $p_{\text{agree}}(\rho)$ is linear in ρ , the average $\langle p_{\text{agree}} \rangle$ is given by $p_{\text{agree}}(\langle \rho \rangle)$, where $\langle \rho \rangle = \frac{1}{d} I$ is the average state, thus

$$\langle p_{\text{agree}} \rangle = p_{\text{agree}}\left(\frac{1}{d} I\right) = \frac{1}{d} \text{tr} [\Lambda_{\text{agree}}].$$

In order to calculate $\langle p_{\text{agree}} \rangle$ as an explicit function of w_x and w_p , we will have to establish a few identities.

Let us introduce the lattice translation operators T_X , T_P in position and momentum defined by their action on the basis (addition on the lattice is mod d)

$$\begin{aligned} T_X |X; n\rangle &= |X; n+1\rangle & T_X^\dagger |X; n\rangle &= |X; n-1\rangle \\ T_P |P; m\rangle &= |P; m+1\rangle & T_P^\dagger |P; m\rangle &= |P; m-1\rangle. \end{aligned}$$

By expanding the position basis in momentum basis and vice versa, it is straight forward to verify that

$$\begin{aligned} T_P |X; n\rangle &= e^{i2\pi n/d} |X; n\rangle & T_P^\dagger |X; n\rangle &= e^{-i2\pi n/d} |X; n\rangle \\ T_X |P; m\rangle &= e^{-i2\pi m/d} |P; m\rangle & T_X^\dagger |P; m\rangle &= e^{i2\pi m/d} |P; m\rangle. \end{aligned}$$

Therefore, T_P commutes with $|X; n\rangle \langle X; n|$ and T_X commutes with $|P; m\rangle \langle P; m|$. By extension, T_P commutes with $\Pi_{X;\nu}$ and T_X commutes with $\Pi_{P;\mu}$.

Using the translation operators we can express the coarse-grained position and momentum projections (7.1), (7.2) as

$$\begin{aligned} \Pi_{X;\nu} &= \sum_{n=0}^{w_x-1} T_X^{\nu w_x} |X; n\rangle \langle X; n| T_X^{\nu w_x \dagger} = T_X^{\nu w_x} \Pi_{X;0} T_X^{\nu w_x \dagger} \\ \Pi_{P;\mu} &= \sum_{m=0}^{w_p-1} T_P^{\mu w_p} |P; m\rangle \langle P; m| T_P^{\mu w_p \dagger} = T_P^{\mu w_p} \Pi_{P;0} T_P^{\mu w_p \dagger}. \end{aligned}$$

Then, using the commutativity of projections with translations we get the identity

$$\Pi_{X;\nu} \Pi_{P;\mu} \Pi_{X;\nu} = T_P^{\mu w_p} (\Pi_{X;\nu} \Pi_{P;0} \Pi_{X;\nu}) T_P^{\mu w_p \dagger} = T_P^{\mu w_p} T_X^{\nu w_x} (\Pi_{X;0} \Pi_{P;0} \Pi_{X;0}) T_X^{\nu w_x \dagger} T_P^{\mu w_p \dagger}.$$

With this identity we can simplify

$$\begin{aligned} \langle p_{\text{agree}} \rangle &= \frac{1}{d} \text{tr} [\Lambda_{\text{agree}}] = \frac{1}{d} \sum_{\nu=0}^{k_x-1} \sum_{\mu=0}^{k_p-1} \text{tr} [(\Pi_{X;\nu} \Pi_{P;\mu} \Pi_{X;\nu})^2] \\ &= \frac{k_x k_p}{d} \text{tr} [(\Pi_{X;0} \Pi_{P;0} \Pi_{X;0})^2]. \end{aligned} \tag{7.5}$$

Let us then express

$$\Pi_{X;0} \Pi_{P;0} \Pi_{X;0} = \sum_{m=0}^{w_p-1} \Pi_{X;0} |P; m\rangle \langle P; m| \Pi_{X;0} = \frac{1}{k_x} \sum_{m=0}^{w_p-1} |P_0; m\rangle \langle P_0; m|. \tag{7.6}$$

Here we have defined the *truncated* momentum states

$$|P_\nu; m\rangle := \sqrt{k_x} \Pi_{X;\nu} |P; m\rangle = \frac{1}{\sqrt{w_x}} \sum_{n=\nu w_x}^{\nu w_x + w_x - 1} e^{i2\pi mn/d} |X; n\rangle$$

given by normalizing the support of the m 'th momentum state on the ν 'th position interval. In general, these states are not orthogonal to each other and their overlap is given by

$$\langle P_{\nu'}; m' | P_\nu; m\rangle = \delta_{\nu', \nu} k_x \langle P; m' | \Pi_{X;\nu} |P; m\rangle = \delta_{\nu', \nu} \frac{k_x}{d} \sum_{n=\nu w_x}^{\nu w_x + w_x - 1} e^{i2\pi(m-m')n/d}.$$

It will be convenient to express such sums by defining the function

$$\Delta_q(x) := \frac{1}{q} \sum_{n=0}^{q-1} e^{i2\pi xn/q} = \frac{e^{i\pi(x-x/q)} \sin(\pi x)}{q \sin(\pi x/q)} \quad (7.7)$$

over real x and integer $q \geq 1$ (note that $\Delta_q(0) = 1$). Then, for $\nu' = \nu = 0$ the overlaps of truncated momentum states are give by

$$\langle P_0; m' | P_0; m\rangle = \Delta_{w_x} \left(\frac{m - m'}{k_x} \right). \quad (7.8)$$

Then, with (7.6) and (7.7) we can express

$$\begin{aligned} \langle \mathbf{p}_{\text{agree}} \rangle &= \frac{k_x k_p}{d} \text{tr} \left[(\Pi_{X;0} \Pi_{P;0} \Pi_{X;0})^2 \right] = \frac{1}{d} \frac{k_p}{k_x} \sum_{m, m'=0}^{w_p-1} |\langle P_0; m' | P_0; m\rangle|^2 \\ &= \frac{1}{d} \frac{k_p}{k_x} \sum_{m, m'=0}^{w_p-1} \left| \Delta_{w_x} \left(\frac{m - m'}{k_x} \right) \right|^2. \end{aligned}$$

Noting that the summand depends only on the difference $n = m - m'$, we simplify

$$\langle \mathbf{p}_{\text{agree}} \rangle = \frac{1}{d} \frac{k_p}{k_x} \sum_{n=1-w_p}^{w_p-1} (w_p - |n|) \left| \Delta_{w_x} \left(\frac{n}{k_x} \right) \right|^2.$$

Since the summed function is symmetric $|\Delta_{w_x}(x)|^2 = |\Delta_{w_x}(-x)|^2$, we further simplify

$$\langle \mathbf{p}_{\text{agree}} \rangle = \frac{1}{d} \frac{k_p}{k_x} \left[w_p |\Delta_{w_x}(0)|^2 + 2 \sum_{n=1}^{w_p-1} (w_p - n) \left| \Delta_{w_x} \left(\frac{n}{k_x} \right) \right|^2 \right].$$

Finally, by substituting the explicit form (7.7) of Δ_{w_x} and recalling that $k_x = d/w_x$, $k_p =$

d/w_p and $\Delta_{w_x}(0) = 1$, we find out how $\langle p_{\text{agree}} \rangle$ varies as a function of w_x and w_p :

$$\begin{aligned}\langle p_{\text{agree}} \rangle &= \frac{1}{d} \frac{w_x}{w_p} \left[w_p + 2 \sum_{n=1}^{w_p-1} (w_p - n) \frac{1}{w_x^2} \frac{\sin^2\left(\frac{\pi n w_x}{d}\right)}{\sin^2\left(\frac{\pi n}{d}\right)} \right] \\ &= \frac{w_x}{d} + \frac{2}{w_x w_p d} \sum_{n=1}^{w_p-1} (w_p - n) \frac{\sin^2\left(\frac{\pi n w_x}{d}\right)}{\sin^2\left(\frac{\pi n}{d}\right)}.\end{aligned}\quad (7.9)$$

The apparent asymmetry under the exchange of w_x with w_p traces back to the apparent asymmetry under the exchange between $\Pi_{X;0}$ and $\Pi_{P;0}$ in Eq. (7.5). These asymmetries are only apparent because

$$\text{tr} \left[(\Pi_{X;0} \Pi_{P;0} \Pi_{X;0})^2 \right] = \text{tr} [\Pi_{X;0} \Pi_{P;0} \Pi_{X;0} \Pi_{P;0}] = \text{tr} \left[(\Pi_{P;0} \Pi_{X;0} \Pi_{P;0})^2 \right].$$

If we were to exchange $\Pi_{X;0}$ with $\Pi_{P;0}$ we would have to exchange w_x with w_p , and end up with

$$\langle p_{\text{agree}} \rangle = \frac{w_p}{d} + \frac{2}{w_x w_p d} \sum_{n=1}^{w_x-1} (w_x - n) \frac{\sin^2\left(\frac{\pi n w_p}{d}\right)}{\sin^2\left(\frac{\pi n}{d}\right)}.\quad (7.10)$$

The symmetry under the exchange of w_x with w_p can also be seen in Fig. 7.3(a) where we have used Eq. 7.9 to plot $\langle p_{\text{agree}} \rangle$ as a function of w_x and w_p . In Fig. 7.3(b) we plot $\langle p_{\text{agree}} \rangle$ for the diagonal $w = w_x = w_p$, together with the upper and lower bounds

$$\langle p_{\text{agree}} \rangle \leq w^2/d \quad w < \sqrt{d} \quad (7.11)$$

$$\langle p_{\text{agree}} \rangle \geq 1 - \frac{2}{\pi^2} \frac{\ln(w^2/d) + 3\pi^2/2}{w^2/d} \quad w > \sqrt{d} \quad (7.12)$$

See the Appendix for the derivation of these bounds.

The upper bound (7.11) tells us that when $w < \sqrt{d}$, the value of $\langle p_{\text{agree}} \rangle$ falls to 0 at least as fast as $\sim w^2$. The lower bound (7.12) tells us that when $w > \sqrt{d}$, the value of $\langle p_{\text{agree}} \rangle$ climbs to 1 at least as fast as $\sim 1 - \frac{\ln w^2}{w^2}$. This implies that along the diagonal $w = w_x = w_p$, there is an inflection in $\langle p_{\text{agree}} \rangle$ around $w = \sqrt{d}$. Therefore, \sqrt{d} is a natural boundary that separates the scales of the quantum and classical regimes.

The above observation can be extended to the entire plane of w_x, w_p , where the curve $w_x w_p = d$ generalizes the boundary $w = \sqrt{d}$. According to the plot in Fig. 7.3(a), as we get farther from the curve $w_x w_p = d$, we get deeper into one of the regimes, and an inflection in $\langle p_{\text{agree}} \rangle$ occurs somewhere near the curve. The fact that the curve $w_x w_p = d$ separates the scales of the quantum and classical regimes follows from the observation that $\langle p_{\text{agree}} \rangle \approx 0.656$ holds almost everywhere on this curve (except for the far ends).

In order to see that, we assume that d is large (otherwise the lattice does not approxi-

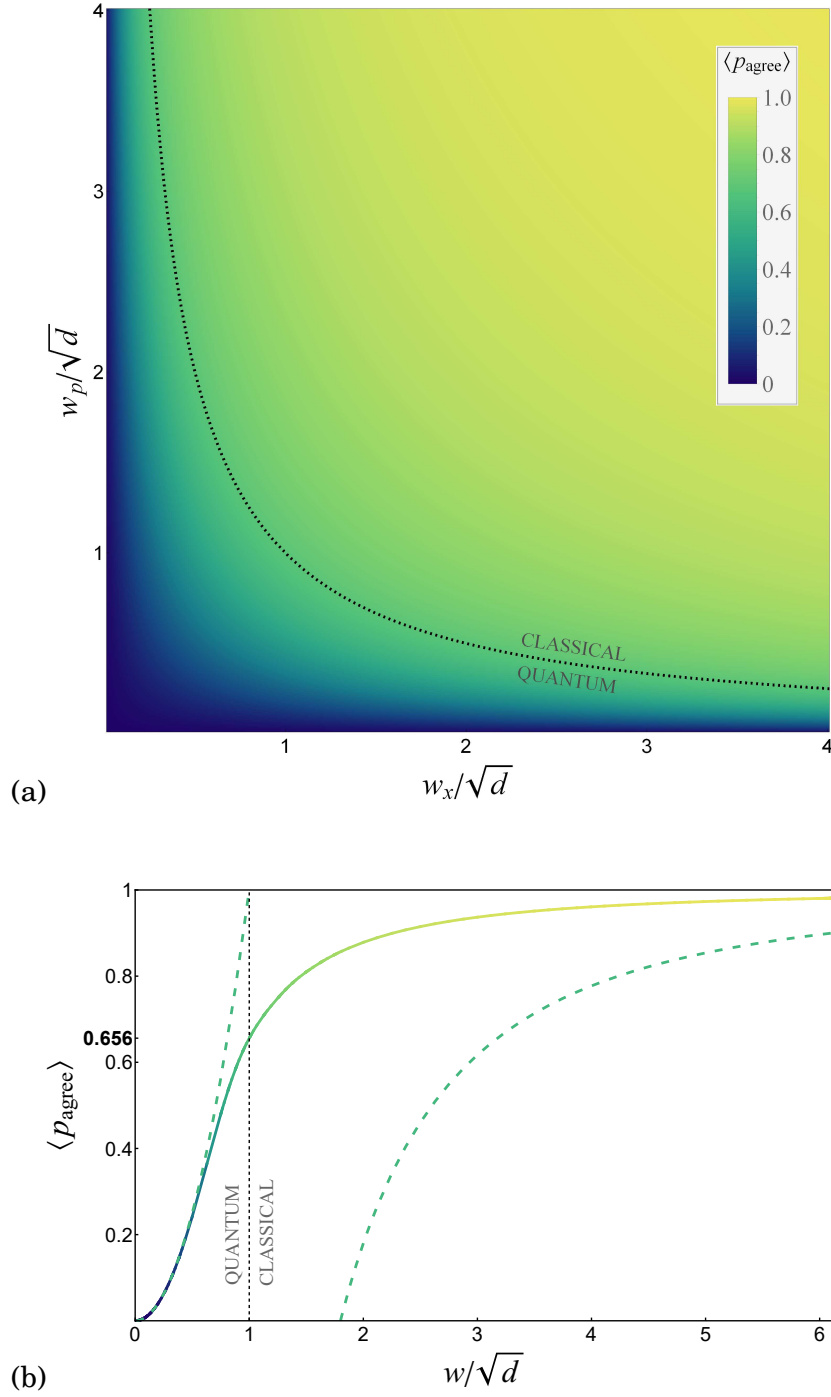


Figure 7.3: (a) The plot of the average probability $\langle p_{\text{agree}} \rangle$ that an instantaneous succession of position-momentum-position measurements will agree on both outcomes of position as a function of the resolution parameters w_x, w_p on a lattice of length d . The dotted curve $w_x w_p = d$ is the boundary that outlines the transitional scale with respect to which we distinguish the quantum and classical regimes. (b) The plot of $\langle p_{\text{agree}} \rangle$ (solid) along the diagonal $w = w_x = w_p$ with the upper and lower bounds (dashed) from Eqs. (7.11) and (7.12).

mate a continuum) but finite. On the curve $w_x w_p = d$ so Eq. (7.9) simplifies to

$$\langle p_{\text{agree}} \rangle = \frac{1}{w_p} + \frac{2}{d^2} \sum_{n=1}^{w_p-1} (w_p - n) \frac{\sin^2\left(\frac{\pi n}{w_p}\right)}{\sin^2\left(\frac{\pi n}{d}\right)}. \quad (7.13)$$

In the intermediate range of values $1 \ll w_p \ll d$ we have $\frac{n}{d} \ll 1$ since $n < w_p$. We can then approximate $\sin^{-2}\left(\frac{\pi n}{d}\right) \approx \left(\frac{\pi n}{d}\right)^{-2}$, so

$$\langle p_{\text{agree}} \rangle \approx \frac{1}{w_p} + \frac{2}{\pi^2} \sum_{n=1}^{w_p-1} (w_p - n) \frac{\sin^2\left(\frac{\pi n}{w_p}\right)}{n^2}. \quad (7.14)$$

Since the intermediate range also implies that $1 \ll w_p$, we can approximate the sum with an integral by introducing the variable $\alpha = \frac{n}{w_p} \in [0, 1]$ and $d\alpha = \frac{1}{w_p}$. Then,

$$\begin{aligned} \langle p_{\text{agree}} \rangle &\approx \frac{1}{w_p} + \frac{2}{\pi^2} \sum_{n=1}^{w_p-1} \frac{1}{w_p} \left(1 - \frac{n}{w_p}\right) \frac{\sin^2\left(\pi \frac{n}{w_p}\right)}{n^2/w_p^2} \\ &\approx d\alpha + \frac{2}{\pi^2} \int_0^1 d\alpha (1 - \alpha) \frac{\sin^2(\pi\alpha)}{\alpha^2} \approx 0.656. \end{aligned}$$

Thus, for the intermediate range $1 \ll w_p \ll d$ on the curve of $w_x w_p = d$, we have $\langle p_{\text{agree}} \rangle \approx 0.656$.

Then we ask, for what values of w_p does the approximation $\langle p_{\text{agree}} \rangle \approx 0.656$ breaks? For $w_p \sim 1$ Eq. (7.14) still holds (since $w_p \ll d$) and its numeric values are

w_p	1	2	3	4	...	15	16	...
$\langle p_{\text{agree}} \rangle$	1.00	0.703	0.675	0.667	...	0.657	0.656	0.656

Thus, on one end of the curve $w_x w_p = d$, the approximation $\langle p_{\text{agree}} \rangle \approx 0.656$ breaks for $w_p < 16$ (considering 3 significant figures). Since w_x and w_p are interchangeable, on the other end of this curve (where $w_x \sim 1$) the approximation breaks for $w_x < 16$. Therefore, if d is large then the approximation $\langle p_{\text{agree}} \rangle \approx 0.656$ holds almost everywhere on the curve $w_x w_p = d$, with the exception of the far ends $w_p < 16$ or $w_x < 16$.

The curve $w_x w_p = d$ is significant not because there is something special about the value 0.656, but because it allows us to say that

$$\begin{cases} \langle p_{\text{agree}} \rangle \approx 1 & w_x w_p \gg d \\ \langle p_{\text{agree}} \rangle \approx 0 & w_x w_p \ll d. \end{cases}$$

In other words, the significance of the curve $w_x w_p = d$ is that it outlines the transitional scale in phase space with respect to which we distinguish the quantum scale from the classical scale.

7.2 The implications of the uncertainty principle on a lattice

7.2.1 Inferring the size of the lattice

Let us briefly point out one simple implication: it is possible to infer the size of the lattice from the scale at which the transition to the classical regime takes place. The general idea is that if we take a generic state ρ and probe the probability $p_{\text{agree}}(\rho)$ at various scales of coarse-graining, the scale where $p_{\text{agree}}(\rho) \sim 0.656$ is the scale where $w_x w_p \sim d$ so the product $w_x w_p$ is an estimation of the value of d . Given concrete assumptions about the limitations of state preparation and measurements, a more specific protocol for determining d can be designed around this general idea.

7.2.2 The continuum limit and lattice perturbations

We will now introduce proper units to the lattice.

The total length of the lattice in proper units is $L = \delta x d$, where δx is the smallest unit of length associated with one lattice spacing. The smallest unit of inverse length, or a wavenumber, is then $1/L$. With the de Broglie relation $p = 2\pi\hbar/\lambda$, we can convert wavenumbers $1/\lambda$ to momenta, so the smallest unit of momentum is $\delta p = 2\pi\hbar/L$.¹⁹ The coarse-graining intervals w_x and w_p become $\Delta x = \delta x w_x$ and $\Delta p = \delta p w_p$ when expressed in proper units.

The continuum limit is achieved by taking $\delta x \rightarrow 0$ and $d \rightarrow \infty$ while keeping L constant. The coarse-graining interval of position $\Delta x = \delta x w_x$ is kept constant by fixing the total number of intervals $k_x = d/w_x$ while $w_x \rightarrow \infty$. Unlike δx , $\delta p = 2\pi\hbar/L$ does not vanish in the continuum limit (the momentum of a particle in a box remains quantized) so the coarse-graining intervals of momentum $\Delta p = \delta p w_p$ are unaffected and w_p remains a finite integer.

We may now ask what happens to $\langle p_{\text{agree}} \rangle$ as we take the continuum limit. Since $w_x/d = \Delta x/L$, the expression (7.9) can be re-stated using the proper units of length as

$$\langle p_{\text{agree}} \rangle = \frac{\Delta x}{L} + \frac{L}{\Delta x} \frac{2}{w_p} \sum_{n=1}^{w_p-1} (w_p - n) \frac{\sin^2\left(\frac{\pi n \Delta x}{L}\right)}{\left[d \sin\left(\frac{\pi n}{d}\right)\right]^2}. \quad (7.15)$$

We do not have to change to the proper units of momentum because

$$w_p = \frac{\Delta p}{\delta p} = \frac{\Delta p}{2\pi\hbar} L,$$

which is a legitimate quantity even in the continuum limit (provided that L is finite).

¹⁹Note that the de Broglie relation is the source of the Planck constant in all of the following equations

The only evidence for the lattice structure that remains in Eq. (7.15) is the d -dependence of the factors

$$\left[d \sin \left(\frac{\pi n}{d} \right) \right]^{-2} = \frac{1}{\pi^2 n^2} + \frac{1}{3d^2} + O \left(\frac{1}{d^3} \right). \quad (7.16)$$

In the continuum limit these factors reduce to $1/\pi^2 n^2$, but when the minimal length $\delta x = L/d$ is above 0, these factors are perturbed with the leading order contribution of $1/3d^2 = \delta x^2/3L^2$.

7.2.3 Factorizing the Planck constant

Observe that the smallest unit of phase space area on a lattice is $\delta x \delta p = 2\pi\hbar/d$.²⁰ Therefore, the curve $w_x w_p = d$ that outlines the transitional scale in phase space becomes

$$\Delta x \Delta p = \delta x \delta p w_x w_p = \delta x \delta p d = 2\pi\hbar. \quad (7.17)$$

Thus, we have recovered Heisenberg's original argument where the Planck constant identifies the transitional scale in phase space. We now see that in the unitless lattice setting (where $\delta x \equiv 1$ and $\delta p \equiv 1$) the constant d is the unitless "Planck constant".²¹

In the continuous phase space the uncertainty principle is only associated with the constant $2\pi\hbar$, which does not admit a preferred factorization into position and momentum. On the lattice, however, the same constant is given by $\delta x \delta p d$, which can be factorized as $\delta x \sqrt{d}$ and $\delta p \sqrt{d}$. We will now argue that the constants $\delta x \sqrt{d}$ and $\delta p \sqrt{d}$ are more than arbitrary factors of the Planck constant. In fact, these are the primary scales associated with the uncertainty principle on a lattice and the Planck constant is a secondary quantity derived from their product.

Returning to the unitless picture of Fig. 7.3(a), observe that if the localization in position w_x approaches \sqrt{d} from above, in order to stay in the classical regime the localization in momentum w_p has to diverge faster than the convergence in w_x . In contrast, as long as both $w_x, w_p \gg \sqrt{d}$, the classical regime is insensitive to the variations in these variables and there is no need to compensate the increase in localization for one variable with the decrease in localization for the other.

We can then define the transitional scale for a single variable as the scale around which increases in localization for one variable (say position) result in *higher* decreases in localization for the other variable (say momentum). This definition is only meaningful on a lattice because it requires the fundamental units δx and δp in terms of which we can compare the changes in localization for both variables.²² From the plot in Fig. 7.3(a) we see

²⁰This is a well known constraint that comes up in the construction of Generalized Clifford Algebras in finite-dimensional quantum mechanics. See [88] for an overview and the references therein.

²¹Note that unlike $2\pi\hbar$, the constant d depends on the size of the system. This inconstancy traces back to the fact that in the unitless case we define $\delta p \equiv 1$, while in proper units we have $\delta p = 2\pi\hbar/L$, which depends on the total length L .

²²In the continuum we cannot tell how the localization for one variable compares to the other because the

that \sqrt{d} is the transitional scale for a single unitless variable. It then follows that the uncertainty principle on a lattice is primarily associated with the unitless constant \sqrt{d} , that in turn defines the transitional scales $\delta x\sqrt{d}$ and $\delta p\sqrt{d}$ for position and momentum, and then the transitional scale in phase space is given by

$$\left(\delta x\sqrt{d}\right)\left(\delta p\sqrt{d}\right) = \delta x\delta p d = 2\pi\hbar.$$

With proper units we conclude that on a lattice, in addition to the minimal length δx and the total length L , quantum mechanics imposes another fundamental length

$$l_u = \delta x\sqrt{d}.$$

The length l_u is directly related to the minimal length δx via the total length $L = \delta x d$ as $l_u = \sqrt{\delta x L}$ or $\delta x = l_u^2/L$. The length l_u is therefore the geometric mean of the minimal length δx and the maximal length L . It can also be framed as the length for which there are as many intervals l_u in L as there are δx in l_u . In the continuum limit, where the minimal length δx vanishes, the length $l_u = \sqrt{\delta x L}$ must also be 0. Therefore, if we can establish that $l_u > 0$ then it follows that $\delta x > 0$.

The advantage of l_u as an indicator of the discontinuity of space is that it is greater than δx by orders of magnitude. For instance, for $L \sim 1$ m of the order of a macroscopic box and $\delta x \sim 10^{-35}$ m of the order of Planck length, we have $l_u \sim 10^{-17.5}$ m which is much closer to the scale of experiments than 10^{-35} m.

It is not clear at this point what are the observable effects associated with the fundamental length l_u . However, if such effects can be identified then the discontinuity of space can be probed at scales that are many orders of magnitude greater than the Planck length.

answer depends on the arbitrary choice of units.

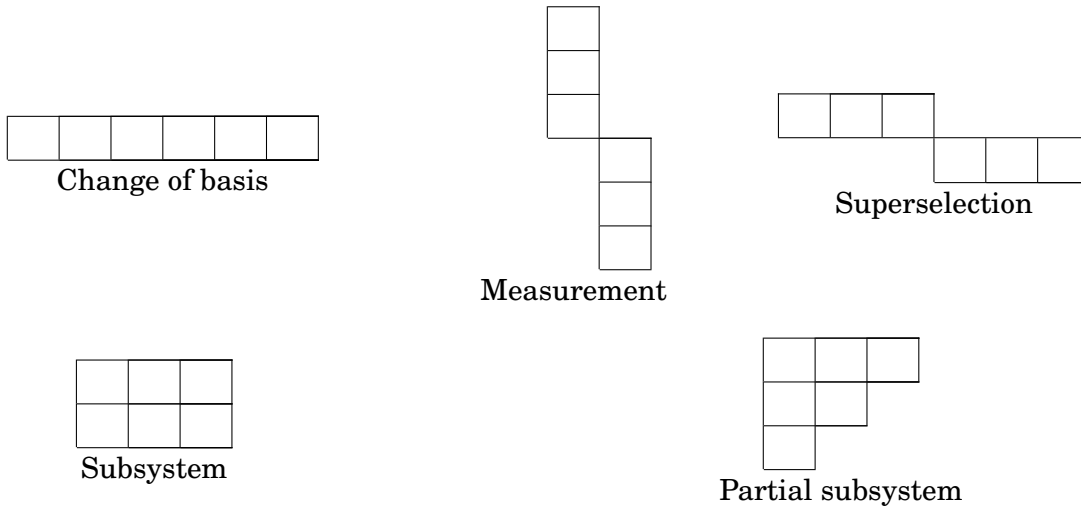
Chapter 8

Conclusion

Inspired by the methods of symmetries, we have studied an operator algebraic approach to reductions in finite-dimensional quantum mechanics, and its extension to operator systems. For this purpose we have identified a convenient representation of the irreps structure in the form of bipartition tables, and introduced the Scattering Algorithm to find the irreps structures of operator algebras. The applications of this approach have been subdivided into reductions of states and reductions of dynamics, and studied separately. The extension of operator algebras to operator systems has led to the formulation of the quantum notion of coarse-graining that is analogous to its classical counterpart.

We started with an observation that in finite-dimensional settings the structure of irreducible representations of groups is in fact associated with operator algebras. Thus, the simplifications that are usually associated with symmetries can be attributed to operator algebras. We studied the representation theory of finite-dimensional operator algebras in Chapter 2 and concluded that all the important aspects of irreps of operator algebras, such as minimal projections and invariant subspaces, are captured by bipartition tables.

Throughout this thesis we saw many examples of bipartition tables. We summarize below the possible shapes of bipartition tables and the corresponding reductions.²³



Thus, bipartition tables unite a broad class of important concepts in finite-dimensional quantum mechanics in a single picture.

²³To this list we have added the change of basis transformation that can be specified by linearly arranging the new basis in place of the old basis.

The principal problem that arises in applications of operator algebras is the derivation of the irreps structure from the generators of the algebra. In Chapter 3 we have addressed this problem by introducing the Scattering Algorithm. The idea of the algorithm is to apply the scattering operation to break the initial spectral projections of the generators into minimal projections, and use them to construct the bipartition tables specifying the irreps structure.

As we have emphasized, the Scatting Algorithm is designed to allow analytical derivations of the irreps structure without having to specify the operators numerically. The execution of the algorithm mostly involves multiplications and diagonalizations of operators, and we saw multiple non-trivial examples that are simple enough to derive the irreps structure with pen and paper.

Applications associated with the reduction of states were studied in Chapter 4. We first observed that the prototypical state reduction in the form of the partial trace map can be understood as a map that accounts for operational constraints. By adopting this perspective we defined state reductions as maps that account for operational constraints given by a restriction of observables to a subalgebra. Such state reduction maps were illustrated with examples that involve lacking a common reference frame and encoding of quantum information in a noiseless subsystem.

An important consequence of constraining the observables to a subsystem is the decoherence of the reduced state. There is nothing special, however, about constraining the observables to a subsystem, and in principle decoherence can be the consequence of any operational constraint. We saw how simple rotations (without interactions) can cause decoherence under the operational constraint of not having a common reference frame of direction in space. Not only such reduced states decohere, but we can also single out the effective interaction term of the Hamiltonian by considering the irreps structure of the operational constraint. Thus, from this broader perspective all the implications of the decoherence program follow primarily from operational constraints, of which the restriction to subsystems is a special case.

Applications associated with the reduction of dynamics were studied in Chapter 5. The reduction of Hamiltonians with symmetries was reexamined and the condition for a group to be a symmetry was relaxed. Specifically, we showed that the Hamiltonian may have a symmetry breaking term and still be reducible, as long as this term is itself an element of the group algebra. We then introduced the symmetry-agnostic approach to the reduction of Hamiltonians where we shifted the focus from symmetries to operator algebras. This approach was demonstrated in two problems concerned with finding the possible qubit encodings for a control Hamiltonian in quantum dot arrays.

The aim of the symmetry-agnostic approach is not to replace the concept of symmetries but rather provide an alternative for problems where identifying the symmetries is not easy. In particular, when dealing with Hamiltonians that have multiple different terms it

may not be obvious what their common symmetry group is. In addition, when the symmetry group is identified, it is still necessary to find the irreps structure of the group in order to reduce the dynamics. In the symmetry-agnostic approach we also have to find the irreps structure of the algebra generated by the Hamiltonian terms. However, it is no longer necessary to identify any symmetries and we can start with the problem of finding the irreps directly.

When considering a simple reduction problem of compressing a qutrit into a qubit we observed that it does not seem to have a satisfying solution in the framework of operator algebras. This has lead in Chapter 6 to the extension of the mathematical framework of state reductions from operator algebras to operator systems. The resulting state reduction maps turned out to be the quantum analogue of the classical notion of coarse-graining that so far did not have an equivalent in quantum theory.

In applications such as quantum state compression or tomography, we have a set of physically available observables and we want to find a reduction map that represents the state compression or the tomographic reconstruction of the state. If we assume that these observables form an operator algebra, we can use the Scattering Algorithm to produce the bipartition tables from which the reduction map is constructed. Physically available observables, however, do not usually form an operator algebra so it is more realistic to assume an operator system instead.

Finally, in Chapter 7 we studied the effects of the uncertainty principle as a function of measurement resolution on a lattice. By introducing a measure of mutual disturbance between incompatible observables we characterized the transition of the uncertainty principle to the classical regime with decreasing resolution of measurements. From this characteristic function we were able to conclude that the resolution scale that separates the quantum and classical regimes is given by the square root of the unitless length of the lattice.

The analysis of the uncertainty principle on a lattice implies certain effects that can be associated with the discontinuity of space. Specifically, we saw that the probability that a successive measurement of position-momentum-position will agree on both outcomes of position is perturbed by the existence of minimal length on the lattice. We also noted that if the minimal length exists, then the geometric mean of the minimal length and the maximal length is a special length scale that is singled out by the uncertainty principle. In principle, this special length scale is directly related to the discontinuity of space, but it is much longer than the minimal length itself. However, it is not yet clear what measurable effects can be associated with it.

Regarding the directions of future research, there are a few questions that are worth exploring further.

We saw that bipartition tables can represent various maps such as the partial trace, unitary transformation, and a measurement; in the most general case partial bipartition

tables represent quantum coarse-graining. It would be interesting to find out what class of CPTP maps can be represented with bipartition tables, and whether we can use bipartition tables to represent CPTP maps in general.

Even though we have designed the Scattering Algorithm for purely analytical uses, it would be good to have a rigorous complexity analysis of its runtime and compare it to numeric implementations. For calculations it is also desirable to have a computer implementation of the Scattering Algorithm in a symbolic calculation software such as the Wolfram Mathematica.

More importantly, just as we have the Scattering Algorithm for constructing bipartition tables from a generating set of an operator algebra, we want to be able to construct partial bipartition tables from a spanning set of an operator system. Without something like the Scattering Algorithm for operator systems, the idea of reduction by quantum coarse-graining is difficult to implement in applications.

We have pointed out that all the implications of the decoherence program follow primarily from operational constraints. That is, decoherence is not just the result of how the observed system interact with other systems, it is also the result of how the observer interacts with the observed system. It would be interesting to find out whether implications such as the emergence of classicality can be attributed to operational limitations that go beyond the paradigm of the system-environment split.

Bibliography

- [1] Milton Abramowitz and Irene A Stegun. *Handbook of mathematical functions with formulas, graphs, and mathematical tables*, volume 55. US Government printing office, 1972.
- [2] Ahmed Farag Ali, Saurya Das, and Elias C Vagenas. Discreteness of space from the generalized uncertainty principle. *Physics Letters B*, 678(5):497–499, 2009. doi: 10.1016/j.physletb.2009.06.061.
- [3] Ahmed Farag Ali, Saurya Das, and Elias C Vagenas. Proposal for testing quantum gravity in the lab. *Physical Review D*, 84(4):044013, 2011.
- [4] R. Alicki, M. Fannes, and M. Pogorzelska. Quantum generalized subsystems. *Phys. Rev. A*, 79:052111, May 2009. doi: 10.1103/PhysRevA.79.052111. URL <https://link.aps.org/doi/10.1103/PhysRevA.79.052111>.
- [5] Ahmed Almheiri, Xi Dong, and Daniel Harlow. Bulk locality and quantum error correction in ads/cft. *Journal of High Energy Physics*, 2015(4):163, 2015.
- [6] Horst Alzer. On some inequalities for the gamma and psi functions. *Mathematics of computation*, 66(217):373–389, 1997. doi: /10.1090/S0025-5718-97-00807-7.
- [7] D. Bacon, J. Kempe, D. A. Lidar, and K. B. Whaley. Universal fault-tolerant quantum computation on decoherence-free subspaces. *Phys. Rev. Lett.*, 85:1758–1761, Aug 2000. doi: 10.1103/PhysRevLett.85.1758. URL <https://link.aps.org/doi/10.1103/PhysRevLett.85.1758>.
- [8] Dave Bacon. Operator quantum error-correcting subsystems for self-correcting quantum memories. *Phys. Rev. A*, 73:012340, Jan 2006. doi: 10.1103/PhysRevA.73.012340. URL <https://link.aps.org/doi/10.1103/PhysRevA.73.012340>.
- [9] Howard Barnum, Emanuel Knill, Gerardo Ortiz, and Lorenza Viola. Generalizations of entanglement based on coherent states and convex sets. *Phys. Rev. A*, 68:032308, Sep 2003. doi: 10.1103/PhysRevA.68.032308. URL <https://link.aps.org/doi/10.1103/PhysRevA.68.032308>.
- [10] Howard Barnum, Emanuel Knill, Gerardo Ortiz, Rolando Somma, and Lorenza Viola. A subsystem-independent generalization of entanglement. *Phys. Rev. Lett.*, 92:

- 107902, Mar 2004. doi: 10.1103/PhysRevLett.92.107902. URL <https://link.aps.org/doi/10.1103/PhysRevLett.92.107902>.
- [11] Stephen D. Bartlett, Terry Rudolph, and Robert W. Spekkens. Reference frames, superselection rules, and quantum information. *Rev. Mod. Phys.*, 79:555–609, Apr 2007. doi: 10.1103/RevModPhys.79.555. URL <https://link.aps.org/doi/10.1103/RevModPhys.79.555>.
 - [12] Cédric Bény and Florian Richter. Algebraic approach to quantum theory: a finite-dimensional guide. *arXiv preprint arXiv:1505.03106*, 2015.
 - [13] Andreas Bluhm, Lukas Rauber, and Michael M. Wolf. Quantum Compression Relative to a Set of Measurements. *Annales Henri Poincaré*, 19(6):1891–1937, Jun 2018. doi: 10.1007/s00023-018-0660-z.
 - [14] Robin Blume-Kohout, Hui Khoon Ng, David Poulin, and Lorenza Viola. Characterizing the structure of preserved information in quantum processes. *Phys. Rev. Lett.*, 100:030501, Jan 2008. doi: 10.1103/PhysRevLett.100.030501. URL <https://link.aps.org/doi/10.1103/PhysRevLett.100.030501>.
 - [15] Robin Blume-Kohout, Hui Khoon Ng, David Poulin, and Lorenza Viola. Information-preserving structures: A general framework for quantum zero-error information. *Phys. Rev. A*, 82:062306, Dec 2010. doi: 10.1103/PhysRevA.82.062306. URL <https://link.aps.org/doi/10.1103/PhysRevA.82.062306>.
 - [16] Cyril Branciard. Error-tradeoff and error-disturbance relations for incompatible quantum measurements. *Proceedings of the National Academy of Sciences*, 110(17):6742–6747, 2013.
 - [17] Heinz-Peter Breuer, Francesco Petruccione, et al. *The theory of open quantum systems*. Oxford University Press on Demand, 2002.
 - [18] Guido Burkard, Daniel Loss, and David P. DiVincenzo. Coupled quantum dots as quantum gates. *Phys. Rev. B*, 59:2070–2078, Jan 1999. doi: 10.1103/PhysRevB.59.2070. URL <https://link.aps.org/doi/10.1103/PhysRevB.59.2070>.
 - [19] Francesco Buscemi, Michael JW Hall, Masanao Ozawa, and Mark M Wilde. Noise and disturbance in quantum measurements: an information-theoretic approach. *Physical review letters*, 112(5):050401, 2014.
 - [20] Paul Busch and Christopher Shilladay. Complementarity and uncertainty in mach-zehnder interferometry and beyond. *Physics Reports*, 435(1):1–31, 2006. doi: 10.1016/j.physrep.2006.09.001.

- [21] Paul Busch, Pekka J Lahti, and Peter Mittelstaedt. *The quantum theory of measurement*. Springer, 1996. doi: 10.1007/978-3-540-37205-9_3.
- [22] Paul Busch, Teiko Heinonen, and Pekka Lahti. Heisenberg’s uncertainty principle. *Physics reports*, 452(6):155–176, 2007. doi: 10.1016/j.physrep.2007.05.006.
- [23] Paul Busch, Pekka Lahti, and Reinhard F. Werner. Proof of heisenberg’s error-disturbance relation. *Phys. Rev. Lett.*, 111:160405, Oct 2013. doi: 10.1103/PhysRevLett.111.160405. URL <https://link.aps.org/doi/10.1103/PhysRevLett.111.160405>.
- [24] Sean M. Carroll and Ashmeet Singh. Quantum mereology: Factorizing hilbert space into subsystems with quasi-classical dynamics, 2020.
- [25] Mario Castagnino and Olimpia Lombardi. Self-induced decoherence: a new approach. *Studies in the History and Philosophy of Modern Physics*, 35(1):73–107, Jan 2004. doi: 10.1016/j.shpsb.2003.03.001.
- [26] Mario Castagnino, Sebastian Fortin, Olimpia Lombardi, and Roberto Laura. A general theoretical framework for decoherence in open and closed systems. *Class. Quant. Grav.*, 25:154002, 2008. doi: 10.1088/0264-9381/25/15/154002.
- [27] Andrew M Childs, Edward Farhi, and Sam Gutmann. An example of the difference between quantum and classical random walks. *Quantum Information Processing*, 1(1-2):35–43, 2002.
- [28] Andrew M Childs, Richard Cleve, Enrico Deotto, Edward Farhi, Sam Gutmann, and Daniel A Spielman. Exponential algorithmic speedup by a quantum walk. In *Proceedings of the thirty-fifth annual ACM symposium on Theory of computing*, pages 59–68, 2003.
- [29] John F Cornwell. *Group theory in physics: An introduction*. Academic press, 1997.
- [30] Pedro Silva Correia, Paola Concha Obando, Raúl O Vallejos, and Fernando de Melo. Macro-to-micro quantum mapping and the emergence of nonlinearity. *arXiv preprint arXiv:2007.14370*, 2020.
- [31] Jordan S Cotler, Geoffrey R Penington, and Daniel H Ranard. Locality from the spectrum. *Communications in Mathematical Physics*, 368(3):1267–1296, 2019.
- [32] Olivia Di Matteo, Luis L. Sánchez-Soto, Gerd Leuchs, and Markus Grassl. Coarse graining the phase space of N qubits. *Physical Review A*, 95(2):022340, Feb 2017. doi: 10.1103/PhysRevA.95.022340.

- [33] David P DiVincenzo, Dave Bacon, Julia Kempe, Guido Burkard, and K Birgitta Whaley. Universal quantum computation with the exchange interaction. *Nature*, 408 (6810):339, 2000.
- [34] Cristhiano Duarte, Gabriel Dias Carvalho, Nadja K Bernardes, and Fernando de Melo. Emerging dynamics arising from coarse-grained quantum systems. *Physical Review A*, 96(3):032113, 2017.
- [35] Cristhiano André Duarte. Compatibility between agents as a tool for coarse-grained descriptions of quantum systems. *Journal of Physics A: Mathematical and Theoretical*, 2020.
- [36] Paul Ehrenfest and Tatiana Ehrenfest. *The conceptual foundations of the statistical approach in mechanics*. Dover, New York, 1990. Originally published in: Enzyklopadie der Mathematischen Wissenschaften, Leipzig 1912.
- [37] Philippe Faist. *Quantum Coarse-Graining: An Information-theoretic Approach to thermodynamics*. PhD thesis, ETH Zurich, 2016.
- [38] Douglas R Farenick. *Algebras of linear transformations*. Springer Science & Business Media, 2012.
- [39] Edward Farhi and Sam Gutmann. Quantum computation and decision trees. *Phys. Rev. A*, 58:915–928, Aug 1998. doi: 10.1103/PhysRevA.58.915. URL <https://link.aps.org/doi/10.1103/PhysRevA.58.915>.
- [40] Sebastian Fortin, Olimpia Lombardi, and Mario Castagnino. Decoherence: A Closed-System Approach. *Brazilian Journal of Physics*, 44(1):138–153, Feb 2014. doi: 10.1007/s13538-013-0151-0.
- [41] Mark Friesen, Joydip Ghosh, MA Eriksson, and SN Coppersmith. A decoherence-free subspace in a charge quadrupole qubit. *Nature communications*, 8(1):1–7, 2017.
- [42] Howard Georgi. *Lie algebras in particle physics: from Isospin To Unified Theories*. CRC Pressy, 2018.
- [43] Sudip Ghosh and Suvrat Raju. Quantum information measures for restricted sets of observables. *Phys. Rev. D*, 98:046005, Aug 2018. doi: 10.1103/PhysRevD.98.046005. URL <https://link.aps.org/doi/10.1103/PhysRevD.98.046005>.
- [44] Alexander N Gorban, Nikolaos K Kazantzis, Ioannis G Kevrekidis, Hans Christian Öttinger, and Constantinos Theodoropoulos. *Model reduction and coarse-graining approaches for multiscale phenomena*. Springer, 2006.
- [45] Daniel Harlow. The ryu–takayanagi formula from quantum error correction. *Communications in Mathematical Physics*, 354(3):865–912, 2017.

- [46] Werner Heisenberg. Über den anschaulichen inhalt der quantentheoretischen kinematik und mechanik. *Z. Physik*, 43:172–198, 1927.
- [47] John A Holbrook, David W Kribs, and Raymond Laflamme. Noiseless subsystems and the structure of the commutant in quantum error correction. *Quantum Information Processing*, 2(5):381–419, 2003.
- [48] Sabine Hossenfelder. Minimal length scale scenarios for quantum gravity. *Living Reviews in Relativity*, 16(1):2, 2013. doi: 10.12942/lrr-2013-2.
- [49] R Jagannathan, TS Santhanam, and R Vasudevan. Finite-dimensional quantum mechanics of a particle. *International Journal of Theoretical Physics*, 20(10):755–773, 1981. doi: 10.1007/BF00674253.
- [50] Vaughan F. R. Jones. Von Neumann Algebras. 2015. URL <http://inspirehep.net/record/1662882/files/VonNeumann2015.pdf>.
- [51] Oleg Kabernik. Quantum reference frames and the poincaré symmetry. Master’s thesis, University of Waterloo, 2014.
- [52] Oleg Kabernik. Quantum coarse graining, symmetries, and reducibility of dynamics. *Phys. Rev. A*, 97:052130, May 2018. doi: 10.1103/PhysRevA.97.052130. URL <https://link.aps.org/doi/10.1103/PhysRevA.97.052130>.
- [53] Oleg Kabernik. Quantifying the uncertainty principle and the effects of minimal length from a finite-dimensional perspective. *arXiv preprint quant-ph/2002.01564*, 2020.
- [54] Oleg Kabernik, Jason Pollack, and Ashmeet Singh. Quantum state reduction: Generalized bipartitions from algebras of observables. *Phys. Rev. A*, 101:032303, Mar 2020. doi: 10.1103/PhysRevA.101.032303. URL <https://link.aps.org/doi/10.1103/PhysRevA.101.032303>.
- [55] Leo P Kadanoff. *Statistical physics: statics, dynamics and renormalization*. World Scientific Publishing Company, 2000.
- [56] Leo P Kadanoff. More is the same; phase transitions and mean field theories. *Journal of Statistical Physics*, 137(5-6):777, 2009.
- [57] J. Kempe, D. Bacon, D. A. Lidar, and K. B. Whaley. Theory of decoherence-free fault-tolerant universal quantum computation. *Phys. Rev. A*, 63:042307, Mar 2001. doi: 10.1103/PhysRevA.63.042307. URL <https://link.aps.org/doi/10.1103/PhysRevA.63.042307>.

- [58] Alexei Kitaev, Dominic Mayers, and John Preskill. Superselection rules and quantum protocols. *Phys. Rev. A*, 69:052326, May 2004. doi: 10.1103/PhysRevA.69.052326. URL <https://link.aps.org/doi/10.1103/PhysRevA.69.052326>.
- [59] Emanuel Knill, Raymond Laflamme, and Lorenza Viola. Theory of quantum error correction for general noise. *Phys. Rev. Lett.*, 84:2525–2528, Mar 2000. doi: 10.1103/PhysRevLett.84.2525. URL <https://link.aps.org/doi/10.1103/PhysRevLett.84.2525>.
- [60] Johannes Kofler and Āaslav Brukner. Classical World Arising out of Quantum Physics under the Restriction of Coarse-Grained Measurements. *Physical Review Letters*, 99(18):180403, Nov 2007. doi: 10.1103/PhysRevLett.99.180403.
- [61] Kamil Korzekwa, David Jennings, and Terry Rudolph. Operational constraints on state-dependent formulations of quantum error-disturbance trade-off relations. *Physical Review A*, 89(5):052108, 2014.
- [62] David Kribs, Raymond Laflamme, and David Poulin. Unified and generalized approach to quantum error correction. *Physical review letters*, 94(18):180501, 2005.
- [63] David W Kribs, Raymond Laflamme, David Poulin, and Maia Lesosky. Operator quantum error correction. *Quantum Information & Computation*, 6(4):382–399, 2006.
- [64] Daniel A Lidar. Review of decoherence free subspaces, noiseless subsystems, and dynamical decoupling. *Adv. Chem. Phys.*, 154:295–354, 2014.
- [65] Daniel A Lidar and K Birgitta Whaley. Decoherence-free subspaces and subsystems. In *Irreversible quantum dynamics*, pages 83–120. Springer, 2003.
- [66] Daniel Loss and David P. DiVincenzo. Quantum computation with quantum dots. *Phys. Rev. A*, 57:120–126, Jan 1998. doi: 10.1103/PhysRevA.57.120. URL <https://link.aps.org/doi/10.1103/PhysRevA.57.120>.
- [67] Iman Marvian and Robert W Spekkens. The theory of manipulations of pure state asymmetry: I. basic tools, equivalence classes and single copy transformations. *New Journal of Physics*, 15(3):033001, 2013.
- [68] Iman Marvian and Robert W. Spekkens. Modes of asymmetry: The application of harmonic analysis to symmetric quantum dynamics and quantum reference frames. *Phys. Rev. A*, 90:062110, Dec 2014. doi: 10.1103/PhysRevA.90.062110. URL <https://link.aps.org/doi/10.1103/PhysRevA.90.062110>.
- [69] Iman Marvian and Robert W Spekkens. Extending noether’s theorem by quantifying the asymmetry of quantum states. *Nature communications*, 5(1):1–8, 2014.

- [70] William D McComb, WD McComb, et al. *Renormalization methods: a guide for beginners*. Oxford University Press, 2004.
- [71] Simon Milz, Felix A Pollock, and Kavan Modi. An introduction to operational quantum dynamics. *Open Systems & Information Dynamics*, 24(04):1740016, 2017.
- [72] Kazuo Murota, Yoshihiro Kanno, Masakazu Kojima, and Sadayoshi Kojima. A numerical algorithm for block-diagonal decomposition of matrix *-algebras with application to semidefinite programming. *Japan Journal of Industrial and Applied Mathematics*, 27(1):125–160, Jun 2010. ISSN 1868-937X. doi: 10.1007/s13160-010-0006-9. URL <https://doi.org/10.1007/s13160-010-0006-9>.
- [73] Francis J Murray and J v Neumann. On rings of operators. *Annals of Mathematics*, pages 116–229, 1936.
- [74] J v Neumann. Zur algebra der funktionaloperationen und theorie der normalen operatoren. *Mathematische Annalen*, 102(1):370–427, 1930.
- [75] Michael A Nielsen and Isaac L Chuang. *Quantum Computation and Quantum Information*. Cambridge University Press, 2010.
- [76] Emmy Noether. Invariante variationsprobleme. *Nachrichten von der Gesellschaft der Wissenschaften zu Gottingen, Math-phys. Klasse*, 2:235–257, 1918.
- [77] Masanao Ozawa. Universally valid reformulation of the heisenberg uncertainty principle on noise and disturbance in measurement. *Phys. Rev. A*, 67:042105, Apr 2003. doi: 10.1103/PhysRevA.67.042105. URL <https://link.aps.org/doi/10.1103/PhysRevA.67.042105>.
- [78] Fernando Pastawski, Beni Yoshida, Daniel Harlow, and John Preskill. Holographic quantum error-correcting codes: Toy models for the bulk/boundary correspondence. *Journal of High Energy Physics*, 2015(6):149, 2015.
- [79] Asher Peres. *Quantum theory: concepts and methods (Chapter 12)*, volume 57. Springer Science & Business Media, 2006. doi: 10.1007/0-306-47120-5.
- [80] D Perez-Garcia, F Verstraete, MM Wolf, and JI Cirac. Matrix product state representations. *Quantum Information & Computation*, 7(5):401–430, 2007.
- [81] Federico Piazza. Glimmers of a pre-geometric perspective. *Foundations of Physics*, 40(3):239–266, 2010.
- [82] Igor Pikovski, Michael R Vanner, Markus Aspelmeyer, MS Kim, and Ćaslav Brukner. Probing planck-scale physics with quantum optics. *Nature Physics*, 8(5):393, 2012. doi: 10.1038/nphys2262.

- [83] David Poulin. Macroscopic observables. *Physical Review A*, 71(2):022102, 2005. doi: 10.1103/PhysRevA.71.022102.
- [84] Lee A Rozema, Dylan H Mahler, Alex Hayat, and Aephraim M Steinberg. A note on different definitions of momentum disturbance. *Quantum Studies: Mathematics and Foundations*, 2(1):17–22, 2015. doi: 10.1007/s40509-014-0027-1.
- [85] Maximilian Russ and Guido Burkard. Three-electron spin qubits. *Journal of Physics: Condensed Matter*, 29(39):393001, 2017.
- [86] Wilhelmus HA Schilders, Henk A Van der Vorst, and Joost Rommes. *Model order reduction: theory, research aspects and applications*, volume 13. Springer, 2008.
- [87] Maximilian Schlosshauer. Decoherence the measurement problem, and interpretations of quantum mechanics. *Rev. Mod. Phys.*, 76:1267–1305, Feb 2005. doi: 10.1103/RevModPhys.76.1267. URL <https://link.aps.org/doi/10.1103/RevModPhys.76.1267>.
- [88] Ashmeet Singh and Sean M. Carroll. Modeling position and momentum in finite-dimensional hilbert spaces via generalized clifford algebra. *arXiv preprint quant-ph/1806.10134*, 2018.
- [89] Ashmeet Singh and Sean M. Carroll. Quantum decimation in hilbert space: Coarse graining without structure. *Phys. Rev. A*, 97:032111, Mar 2018. doi: 10.1103/PhysRevA.97.032111. URL <https://link.aps.org/doi/10.1103/PhysRevA.97.032111>.
- [90] Wu-Ki Tung. *Group theory in physics: an introduction to symmetry principles, group representations, and special functions in classical and quantum physics*. World Scientific Publishing Company, 1985.
- [91] F. Verstraete and J. I. Cirac. Matrix product states represent ground states faithfully. *Phys. Rev. B*, 73:094423, Mar 2006. doi: 10.1103/PhysRevB.73.094423. URL <https://link.aps.org/doi/10.1103/PhysRevB.73.094423>.
- [92] G. Vidal. Entanglement renormalization. *Phys. Rev. Lett.*, 99:220405, Nov 2007. doi: 10.1103/PhysRevLett.99.220405. URL <https://link.aps.org/doi/10.1103/PhysRevLett.99.220405>.
- [93] Lorenza Viola and Howard Barnum. Entanglement and subsystems, entanglement beyond subsystems, and all that. *Philosophy of quantum information and entanglement*, pages 16–43, 2010.
- [94] Lorenza Viola, Emanuel Knill, and Raymond Laflamme. Constructing qubits in physical systems. *Journal of Physics A: Mathematical and General*, 34(35):7067, 2001.

- [95] Lorenza Viola, Howard Barnum, Emanuel Knill, Gerardo Ortiz, and Rolando Somma. Entanglement beyond subsystems. *arXiv preprint quant-ph/0403044*, 2004.
- [96] Apostolos Vourdas. Quantum systems with finite hilbert space. *Reports on Progress in Physics*, 67(3):267, 2004. doi: 10.1088/0034-4885/67/3/r03.
- [97] Xiaoting Wang, Mark Byrd, and Kurt Jacobs. Numerical method for finding decoherence-free subspaces and its applications. *Physical Review A*, 87(1):012338, 2013.
- [98] Steven Weinberg. *The quantum theory of fields*, volume 1. Cambridge university press, 1995.
- [99] Eugene Paul Wigner. Group theory and its application to the quantum mechanics of atomic spectra. 1959.
- [100] Kenneth G. Wilson. The renormalization group: Critical phenomena and the kondo problem. *Rev. Mod. Phys.*, 47:773–840, Oct 1975. doi: 10.1103/RevModPhys.47.773. URL <https://link.aps.org/doi/10.1103/RevModPhys.47.773>.
- [101] P. Zanardi and M. Rasetti. Noiseless quantum codes. *Phys. Rev. Lett.*, 79:3306–3309, Oct 1997. doi: 10.1103/PhysRevLett.79.3306. URL <https://link.aps.org/doi/10.1103/PhysRevLett.79.3306>.
- [102] Paolo Zanardi. Virtual quantum subsystems. *Physical Review Letters.*, 87:077901, 2001. doi: 10.1103/PhysRevLett.87.077901.
- [103] Paolo Zanardi and Mario Rasetti. Error avoiding quantum codes. *Modern Physics Letters B*, 11(25):1085–1093, 1997.
- [104] Paolo Zanardi, Daniel A. Lidar, and Seth Lloyd. Quantum tensor product structures are observable induced. *Physical Review Letters*, 92:060402, 2004. doi: 10.1103/PhysRevLett.92.060402.
- [105] Wojciech Hubert Zurek. Decoherence, einselection, and the quantum origins of the classical. *Reviews of modern physics*, 75(3):715, 2003.

Appendix

A calculation of the bounds (7.11) and (7.12)

Here we will assume $w = w_x = w_p$ and $k = k_x = k_p$.

In order to calculate the bounds on $\langle p_{\text{agree}} \rangle$ we will have to find a different way to express $\Pi_{X;0}\Pi_{P;0}\Pi_{X;0}$. Recalling Eq. (7.8) and the function (7.7) we now have

$$|\langle P_0; m' | P_0; m \rangle| = \left| \Delta_w \left(\frac{m - m'}{k} \right) \right| = \frac{\sin \left(\pi \frac{m - m'}{k} \right)}{w \sin \left(\pi \frac{m - m'}{d} \right)}.$$

Observe that the truncated momentum states are orthogonal when the difference $m - m'$ is an integer number of k 's. That is, for any integers c, c' and n the states $|P_0; ck + n\rangle$ and $|P_0; c'k + n\rangle$ are orthogonal.

In Eq. 7.6 we have derived the form

$$\Pi_{X;0}\Pi_{P;0}\Pi_{X;0} = \frac{1}{k} \sum_{m=0}^{w-1} |P_0; m\rangle \langle P_0; m| \quad (8.1)$$

where $|P_0; m\rangle \langle P_0; m|$ are rank 1 projections. Since some of these projections are pairwise orthogonal, we can group them together and express $\Pi_{X;0}\Pi_{P;0}\Pi_{X;0}$ as a smaller sum of higher rank projections.

In order to do that, let us first assume that $\gamma = w/k$ is a non-zero integer (we will not need this assumption in general). Then the set of integers $\{m = 0, \dots, w - 1\}$ can be partitioned into k subsets $\Omega_n = \{ck + n \mid c = 0, \dots, \gamma - 1\}$ with $n = 0, \dots, k - 1$. Thus, we can group up the orthogonal elements in the sum (8.1) as

$$\Pi_{X;0}\Pi_{P;0}\Pi_{X;0} = \frac{1}{k} \sum_{n=0}^{k-1} \sum_{m \in \Omega_n} |P_0; m\rangle \langle P_0; m| = \frac{1}{k} \sum_{n=0}^{k-1} \Pi^{(n)}$$

where we have introduced the rank γ projections

$$\Pi^{(n)} = \sum_{m \in \Omega_n} |P_0; m\rangle \langle P_0; m| = \sum_{c=0}^{\gamma-1} |P_0; ck + n\rangle \langle P_0; ck + n|.$$

When $\gamma = w/k$ is not an integer, the accounting of indices is more involved. We have to

introduce the integer part $g = \lfloor \gamma \rfloor$ and the remainder part $r = w - k \lfloor \gamma \rfloor$ of γ . As before, we partition the set $\{m = 0, \dots, w - 1\}$ into subsets

$$\Omega_n := \begin{cases} \{ck + n \mid c = 0, \dots, g\} & n < r \\ \{ck + n \mid c = 0, \dots, g - 1\} & n \geq r \end{cases}$$

but now they are not of equal size and the range of n depends on whether $\gamma \geq 1$. When $\gamma \geq 1$ then $|\Omega_n|$ is $g + 1$ for $n < r$ and g for $n \geq r$. When $\gamma < 1$ so $g = 0$ and $r = w$, then $|\Omega_n| = 1$ for $n < w$ but $|\Omega_n| = 0$ for $n \geq w$ so we do not need to count Ω_n for $n \geq w$. Noting that the condition $\gamma \geq 1$ is equivalent to $\min(k, w) = k$ and the condition $\gamma < 1$ is equivalent to $\min(k, w) = w$, we conclude that we only have to count Ω_n for $n < \min(k, w)$. Therefore, for the general γ we have

$$\Pi_{X;0}\Pi_{P;0}\Pi_{X;0} = \frac{1}{k} \sum_{n=0}^{\min(k,w)-1} \sum_{m \in \Omega_n} |P_0; m\rangle \langle P_0; m| = \frac{1}{k} \sum_{n=0}^{\min(k,w)-1} \Pi^{(n)} \quad (8.2)$$

and the projections

$$\Pi^{(n)} = \sum_{m \in \Omega_n} |P_0; m\rangle \langle P_0; m| = \sum_{c=0}^{g_n-1} |P_0; ck + n\rangle \langle P_0; ck + n|$$

are now of the rank

$$g_n = \begin{cases} g + 1 & n < r \\ g & n \geq r. \end{cases}$$

Using the new form (8.2), we can re-express Eq. 7.5 as

$$\langle p_{\text{agree}} \rangle = \frac{k^2}{d} \text{tr} \left[(\Pi_{X;0}\Pi_{P;0}\Pi_{X;0})^2 \right] = \frac{1}{d} \sum_{n,n'=0}^{\min(k,w)-1} \text{tr} \left[\Pi^{(n)} \Pi^{(n')} \right]. \quad (8.3)$$

The upper bound

The quantity $\text{tr} \left[\Pi^{(n)} \Pi^{(n')} \right]$ is the Hilbert-Schmidt inner product $\langle \Pi^{(n)}, \Pi^{(n')} \rangle$ (also known as Frobenius inner product) of the operators $\Pi^{(n)}$ and $\Pi^{(n')}$. Therefore, it obeys the Cauchy-Schwarz inequality

$$\left| \text{tr} \left[\Pi^{(n)} \Pi^{(n')} \right] \right|^2 = \left| \langle \Pi^{(n)}, \Pi^{(n')} \rangle \right|^2 \leq \langle \Pi^{(n)}, \Pi^{(n)} \rangle \langle \Pi^{(n')}, \Pi^{(n')} \rangle = \text{tr} \left[\Pi^{(n)} \right] \text{tr} \left[\Pi^{(n')} \right].$$

Since the value

$$\text{tr} \left[\Pi^{(n)} \Pi^{(n')} \right] = \sum_{m \in \Omega_n} \sum_{m' \in \Omega_{n'}} |\langle P_0; m \mid P_0; m' \rangle|^2$$

is clearly real and positive, we get

$$\text{tr} \left[\Pi^{(n)} \Pi^{(n')} \right] \leq \sqrt{\text{tr} \left[\Pi^{(n)} \right] \text{tr} \left[\Pi^{(n')} \right]}.$$

The value of $\text{tr} \left[\Pi^{(n)} \right]$ is the rank of the projection which is either g or $g + 1$ so

$$\text{tr} \left[\Pi^{(n)} \Pi^{(n')} \right] \leq g + 1.$$

Therefore, the form of $\langle p_{\text{agree}} \rangle$ in Eq. (8.3) implies that

$$\langle p_{\text{agree}} \rangle \leq \frac{1}{d} \sum_{n, n'=0}^{\min(k, w)-1} (g + 1) = (g + 1) \frac{\min(k, w)^2}{d}.$$

When $\gamma \geq 1$, this upper bound is greater or equal to 1 because

$$(g + 1) \frac{\min(k, w)^2}{d} = (g + 1) \frac{k^2}{d} \geq \gamma \frac{k^2}{d} = w \frac{k}{d} = 1$$

which is not helpful since we already know that $\langle p_{\text{agree}} \rangle \leq 1$ for it is a probability. When $\gamma < 1$, on the other hand, we have $g = 0$ and so

$$(g + 1) \frac{\min(k, w)^2}{d} = \frac{w^2}{d}.$$

Thus, when $\gamma < 1$, which translates to $w < k = d/w$ so $w < \sqrt{d}$, we have the upper bound

$$\langle p_{\text{agree}} \rangle \leq \frac{w^2}{d}.$$

The lower bound

We will now focus on the lower bound of the inner product $\text{tr} \left[\Pi^{(n)} \Pi^{(n')} \right]$ for the case $\gamma \geq 1$ (so $w \geq \sqrt{d}$ and $\min(k, w) = k$) and then substitute the result in Eq. (8.3).

Since we are interested in the lower bound, we can simplify the expression by discarding the terms $c, c' = g$ in the sum

$$\text{tr} \left[\Pi^{(n)} \Pi^{(n')} \right] = \sum_{c=0}^{g_n-1} \sum_{c'=0}^{g_{n'}-1} \left| \langle P_0; c'k + n' \mid P_0; ck + n \rangle \right|^2 \geq \sum_{c, c'=0}^{g-1} \left| \langle P_0; c'k + n' \mid P_0; ck + n \rangle \right|^2.$$

According to Eq. (7.8) we have

$$\left| \langle P_0; c'k + n' \mid P_0; ck + n \rangle \right|^2 = \left| \Delta_w (c - c' + \alpha) \right|^2$$

where we have introduced the variable $\alpha = \frac{n-n'}{k}$. We can now identify the sum

$$S(\alpha) = \sum_{c,c'=0}^{g-1} |\Delta_w(c - c' + \alpha)|^2 \leq \text{tr} [\Pi^{(n)} \Pi^{(n')}]$$

and focus on lower bounding $S(\alpha)$ for all possible α .

Since $|\Delta_w(x)|^2$ is a symmetric function of x we have

$$|\Delta_w(c - c' + \alpha)|^2 = |\Delta_w(-c + c' - \alpha)|^2$$

and since the values of c and c' are interchangeable in the sum, we conclude that $S(\alpha)$ is a symmetric function of α . Therefore, we only need to consider positive $\alpha = \frac{n-n'}{k}$, and since $n, n' = 0, \dots, k-1$, it takes the values $\alpha = 0, \frac{1}{k}, \dots, \frac{k-1}{k} \in [0, 1]$.

Since the summand in $S(\alpha)$ only depends on the differences $l = c - c'$, we can simplify the sum

$$S(\alpha) = \sum_{l=-g+1}^{g-1} (g - |l|) |\Delta_w(l + \alpha)|^2 = \sum_{l=-g+1}^{g-1} \frac{(g - |l|)}{w^2} \frac{\sin^2(\pi(l + \alpha))}{\sin^2(\pi(l + \alpha)/w)}$$

where in the last step we substituted the explicit form of Δ_w . Note that $\sin^2(\pi(l + \alpha)) = \sin^2(\pi\alpha)$ for integer l and also $\sin^{-2}\left(\frac{\pi(l+\alpha)}{w}\right) \geq \left(\frac{\pi(l+\alpha)}{w}\right)^{-2}$ so we get

$$S(\alpha) \geq \frac{\sin^2(\pi\alpha)}{\pi^2} \sum_{l=-g+1}^{g-1} \frac{g - |l|}{(l + \alpha)^2}. \quad (8.4)$$

We will now focus on evaluating the lower bound of the sum

$$s(\alpha) = \sum_{l=-g+1}^{g-1} \frac{g - |l|}{(l + \alpha)^2}. \quad (8.5)$$

We can rearrange the elements of this sum as follows:

$$s(\alpha) = \frac{g}{\alpha^2} + \sum_{l=1}^{g-1} \left[\frac{g-l}{(l+\alpha)^2} + \frac{g-l}{(l-\alpha)^2} \right] = \frac{g}{\alpha^2} + \sum_{l=1}^{g-1} \left[\frac{l}{(g-l+\alpha)^2} + \frac{l}{(g-l-\alpha)^2} \right]$$

where in the last step we simply reversed the order of the elements in the sum. Now we

can introduce the auxiliary variables $\beta_{\pm} = g \pm \alpha$, so

$$\begin{aligned} s(\alpha) &= \frac{g}{\alpha^2} + \sum_{l=1}^{g-1} \left[\frac{l}{(l-\beta_+)^2} + \frac{l}{(l-\beta_-)^2} \right] = \frac{g}{\alpha^2} + \sum_{l=1}^{g-1} \left[\frac{\beta_+}{(l-\beta_+)^2} + \frac{1}{(l-\beta_+)} + \frac{\beta_-}{(l-\beta_-)^2} + \frac{1}{(l-\beta_-)} \right] \\ &= \frac{g}{\alpha^2} + s_1(\alpha) + s_2(\alpha) \end{aligned} \quad (8.6)$$

where we have identified the sums of harmonic-like series

$$s_1(\alpha) = \sum_{l=1}^{g-1} \left[\frac{1}{(l-\beta_-)} + \frac{1}{(l-\beta_+)} \right] \quad s_2(\alpha) = \sum_{l=1}^{g-1} \left[\frac{\beta_-}{(l-\beta_-)^2} + \frac{\beta_+}{(l-\beta_+)^2} \right].$$

Such sums can be evaluated using the polygamma functions [1]

$$\psi^{(j)}(x) := \frac{d^j}{dx^j} \ln \Gamma(x)$$

where Γ is the gamma function that interpolates the factorial for all real (and complex) values. The two key properties of the polygamma functions that we will need are the recursion and reflection relations

$$\psi^{(j)}(1+x) = \psi^{(j)}(x) + (-1)^j \frac{j!}{x^{j+1}} \quad (8.7)$$

$$\psi^{(j)}(1-x) = (-1)^j \psi^{(j)}(x) + (-1)^j \pi \frac{d^j}{dx^j} \cot(\pi x). \quad (8.8)$$

For integer g we can expand $\psi^{(j)}(g-x)$ for $j = 0, 1$ using the recursion relation (8.7) to get

$$\begin{aligned} \psi^{(0)}(g-x) &= \psi^{(0)}(1-x) + \sum_{l=1}^{g-1} \frac{1}{l-x} \\ \psi^{(1)}(g-x) &= \psi^{(1)}(1-x) - \sum_{l=1}^{g-1} \frac{1}{(l-x)^2}. \end{aligned}$$

Applying the reflection relation (8.8) and rearranging yields

$$\sum_{l=1}^{g-1} \frac{1}{l-x} = \psi^{(0)}(g-x) - \psi^{(0)}(x) - \pi \cot(\pi x) \quad (8.9)$$

$$\sum_{l=1}^{g-1} \frac{1}{(l-x)^2} = -\psi^{(1)}(g-x) - \psi^{(1)}(x) + \frac{\pi^2}{\sin^2(\pi x)}. \quad (8.10)$$

Now, using (8.9) and recalling that $g - \beta_{\pm} = \mp \alpha$ we can express $s_1(\alpha)$ as

$$s_1(\alpha) = \psi^{(0)}(\alpha) - \psi^{(0)}(\beta_-) + \psi^{(0)}(-\alpha) - \psi^{(0)}(\beta_+)$$

where the trigonometric terms cancel each other out as they are anti-symmetric and periodic with integer g . We can re-express $\psi^{(0)}(\alpha)$ and $\psi^{(0)}(-\alpha)$ as $\psi^{(0)}(\alpha+1)$ using the recursion (8.7) and reflection relations (8.8) respectively:

$$\psi^{(0)}(\alpha) + \psi^{(0)}(-\alpha) = 2\psi^{(0)}(\alpha+1) + \pi \cot(\pi\alpha) - \frac{1}{\alpha}.$$

We can replace $2\psi^{(0)}(\alpha+1)$ with its lower bound $2\psi^{(0)}(1)$ on the interval $0 \leq \alpha < 1$ as the function $\psi^{(0)}(x)$ is monotonically increasing for $0 \leq x$. For the same reason we can also use the bound $\psi^{(0)}(\beta_{\pm}) \leq \psi^{(0)}(g+1)$ so we end up with the overall lower bound on the sum

$$s_1(\alpha) \geq 2\psi^{(0)}(1) - 2\psi^{(0)}(g+1) + \pi \cot(\pi\alpha) - \frac{1}{\alpha}. \quad (8.11)$$

Similarly, using (8.10) we can express $s_2(\alpha)$ as

$$s_2(\alpha) = -\left[\beta_- \psi^{(1)}(\alpha) + \beta_+ \psi^{(1)}(-\alpha)\right] - \left[\beta_- \psi^{(1)}(\beta_-) + \beta_+ \psi^{(1)}(\beta_+)\right] + \frac{\beta_- \pi^2}{\sin^2(\pi\beta_-)} + \frac{\beta_+ \pi^2}{\sin^2(\pi\beta_+)}.$$

Using the recursion (8.7) and reflection (8.8) relations, we express

$$-\left[\beta_- \psi^{(1)}(\alpha) + \beta_+ \psi^{(1)}(-\alpha)\right] = 2\alpha\psi^{(1)}(\alpha+1) - \frac{\beta_-}{\alpha^2} - \frac{\beta_+ \pi^2}{\sin^2(\pi\alpha)} \geq -\frac{\beta_-}{\alpha^2} - \frac{\beta_+ \pi^2}{\sin^2(\pi\alpha)}$$

where in the last step we have replaced $2\alpha\psi^{(1)}(\alpha+1)$ with its lower bound 0 at $\alpha = 0$. Since $\psi^{(1)}(x)$ is monotonically decreasing for $0 \leq x$ we also use the lower bound

$$-\left[\beta_- \psi^{(1)}(\beta_-) + \beta_+ \psi^{(1)}(\beta_+)\right] \geq -2g\psi^{(1)}(g-1).$$

Thus, the overall lower bound for $s_2(\alpha)$ is

$$\begin{aligned} s_2(\alpha) &\geq -\frac{\beta_-}{\alpha^2} - \frac{\beta_+ \pi^2}{\sin^2(\pi\alpha)} - 2g\psi^{(1)}(g-1) + \frac{\beta_- \pi^2}{\sin^2(\pi\beta_-)} + \frac{\beta_+ \pi^2}{\sin^2(\pi\beta_+)} \\ &= -\frac{\beta_-}{\alpha^2} - 2g\psi^{(1)}(g-1) + \frac{\beta_- \pi^2}{\sin^2(\pi\alpha)}. \end{aligned} \quad (8.12)$$

where in the last step we have used the fact that $\sin^2(\pi\beta_{\pm}) = \sin^2(\pi\alpha)$.

Combining the lower bounds (8.11) and (8.12) into Eqs. (8.4), (8.5), (8.6), we get

$$S(\alpha) \geq g - \frac{2\sin^2(\pi\alpha)}{\pi^2} \left[\psi^{(0)}(g+1) + g\psi^{(1)}(g-1) \right] - \alpha + \frac{2\sin^2(\pi\alpha)}{\pi^2} \psi^{(0)}(1) + \frac{\sin(2\pi\alpha)}{2\pi}.$$

On the interval $0 \leq \alpha < 1$, the minimum value of

$$-\alpha + \frac{2\sin^2(\pi\alpha)}{\pi^2} \psi^{(0)}(1) + \frac{\sin(2\pi\alpha)}{2\pi}$$

is given by $-\epsilon_1 \approx -1.005$ and the minimum value of the coefficient $-\frac{2 \sin^2(\pi\alpha)}{\pi^2}$ is $-\frac{2}{\pi^2}$. With that, we can get rid of the dependence on α :

$$S(\alpha) \geq S_{\min} = g - \frac{2}{\pi^2} \left(\psi^{(0)}(g+1) + g\psi^{(1)}(g-1) \right) - \epsilon_1.$$

We know that $\psi^{(0)}(x)$ is a smooth function for $x > 0$ and it is bounded by [6]

$$\ln x - \frac{1}{x} < \psi^{(0)}(x) < \ln x - \frac{1}{2x}$$

so asymptotically the function $\psi^{(0)}(x+1) \sim \ln(x+1)$ and it converges to $\ln x$ from above. Since $\psi^{(1)}(x) = d\psi^{(0)}(x)/dx$ then asymptotically $\psi^{(1)}(x) \sim \frac{1}{x}$ so the function $x\psi^{(1)}(x-1) \sim x/(x-1)$ and it converges to 1 from above. Therefore, for any $\epsilon_2 > 0$ there is a $x' > 0$ such that for all $x > x'$

$$\psi^{(0)}(x+1) + x\psi^{(1)}(x-1) \leq \ln x + 1 + \epsilon_2.$$

Conveniently choosing $\epsilon_2 = \frac{\pi^2}{2}(2 - \epsilon_1) - 1$ and solving for x' results in $x' \approx 1.722$. Thus, for all $g \geq 2 > x'$ we have

$$\begin{aligned} S_{\min} &\geq g - \frac{2}{\pi^2} (\ln g + 1 + \epsilon_2) - \epsilon_1 = g - \frac{2}{\pi^2} \ln g - 2 \\ &\geq \gamma - \frac{2}{\pi^2} \ln \gamma - 3 \end{aligned}$$

where the last inequality follows from $g = \lfloor \gamma \rfloor \geq \gamma - 1$ and $\ln g \leq \ln \gamma$.

Recalling that $\text{tr} [\Pi^{(n)} \Pi^{(n')}] \geq S(\alpha) \geq S_{\min}$ and $\gamma = w/k = w^2/d$, we return to the Eq. (8.3) and get the result

$$\begin{aligned} \langle \mathbf{p}_{\text{agree}} \rangle &= \frac{1}{d} \sum_{n,n'=0}^{k-1} \text{tr} [\Pi^{(n)} \Pi^{(n')}] \geq \frac{k^2}{d} S_{\min} \geq \frac{1}{w^2/d} \left[w^2/d - \frac{2}{\pi^2} \ln(w^2/d) - 3 \right] \\ &= 1 - \frac{2}{\pi^2} \frac{\ln(w^2/d) + 3\pi^2/2}{w^2/d}. \end{aligned}$$